



## Durham E-Theses

---

### *Isolation and characterization of the KNAT6 homeobox gene in Arabidopsis thaliana*

Dean, Gillian Hazel

#### How to cite:

---

Dean, Gillian Hazel (2003) *Isolation and characterization of the KNAT6 homeobox gene in Arabidopsis thaliana*, Durham theses, Durham University. Available at Durham E-Theses Online:  
<http://etheses.dur.ac.uk/4039/>

#### Use policy

---

The full-text may be used and/or reproduced, and given to third parties in any format or medium, without prior permission or charge, for personal research or study, educational, or not-for-profit purposes provided that:

- a full bibliographic reference is made to the original source
- a [link](#) is made to the metadata record in Durham E-Theses
- the full-text is not changed in any way

The full-text must not be sold in any format or medium without the formal permission of the copyright holders.

Please consult the [full Durham E-Theses policy](#) for further details.

---

Academic Support Office, Durham University, University Office, Old Elvet, Durham DH1 3HP  
e-mail: [e-theses.admin@dur.ac.uk](mailto:e-theses.admin@dur.ac.uk) Tel: +44 0191 334 6107  
<http://etheses.dur.ac.uk>

**Isolation and Characterisation  
of the *KNAT6* Homeobox Gene  
in *Arabidopsis thaliana***

**Thesis submitted for the degree of  
Doctor of Philosophy  
at the University of Durham**

**Gillian Hazel Dean B.Sc.  
Department of Biological and Biomedical Sciences  
University of Durham**

**March 2003**

**A copyright of this thesis rests  
with the author. No quotation  
from it should be published  
without his prior written consent  
and information derived from it  
should be acknowledged.**



**1 2 MAR 2004**

## Abstract

Class 1 *KNOX* genes have been demonstrated to play roles in the maintenance of the shoot apical meristem in a variety of plant species. Although the shoot and root systems differ in the way in which lateral organs are initiated, it was proposed that *KNOX* genes may also function in some aspect of the regulation of the root apical or lateral root meristems.

This work describes the isolation and characterisation of *KNAT6*, a member of this family in the model plant *Arabidopsis thaliana*. *KNAT6* cDNA was isolated from NAA-treated root tissue. Two isoforms were identified, which differ by two amino acids in the conserved MEINOX domain of the predicted protein.

The *KNAT6* transcript is detectable in seedlings between 3 and 12 days after germination. The *KNAT6* promoter is active in the phloem poles of the main root in *Arabidopsis*, especially at the bases of newly emerged lateral roots. Promoter activity is downregulated by cytokinin and the pattern of expression alters on treatment with the synthetic auxin analogue NAA.

Overexpression studies revealed that the shorter and more abundant *KNAT6* cDNA isoform causes a lobed leaf phenotype when it is overexpressed, a phenotype similar to that seen on overexpression of other class 1 *KNOX* genes in *Arabidopsis*. The longer and less abundant cDNA isoform does not cause this phenotype, indicating that there is a functional difference between the two predicted proteins. Preliminary analysis of plants carrying RNAi constructs indicates that lateral roots are initiated closer to the root tip than in wild type plants.

Taken together, and in the context of the literature, these results suggest that *KNAT6* may be involved in control of lateral root development and root architecture in *Arabidopsis*.

## **Declaration**

The material contained in this thesis has not been submitted for a degree in this or any other University.

## **Statement of Copyright**

The copyright of this thesis rests with the author. No quotation from it should be published without prior written consent and information derived from it should be acknowledged

## Acknowledgements

Firstly I would like to thank my supervisor, Keith Lindsey, for his help and support throughout this work. Without his advice and discussions, this work would not have been possible. I also wish to acknowledge funding from BBSRC and Shell Forestry, especially Glyn Edwards at Shell.

I would also like to thank all the members of the Lindsey lab, especially Jen, Marta, Paul, Stu, Kez, Mags, Martin and Matt for their help and support through many years in Durham. In particular, thank-you to Stu for his never-ending patience in the lab. I would also like to thank other members of the department for their help, including Paul Sidney in the Photographic Unit, Christine Richardson in the Microscopy Suite and members of the Edwards and Hussey labs for useful discussions and technical expertise.

Also thanks to all the people who have helped make my time in Durham enjoyable. To Kez, Helen, Ruth and Shaz for everything (what more can I say!), as well as everyone else who has won, lost or drawn numerous netball and hockey matches with me over the years, sat in the pub and cooked me dinner.

Finally, I would like to thank my family for their support (not just financial) as well as garage services and a supply of jam. Andy, you are my soulmate, and I will even forgive you for meaning I'll never be Dr Fozzard.

## Abbreviations

ABA	abscisic acid
ACC	1-aminocyclopropane-1-carboxylic acid
BAP	6-Benzylaminopurine
bp	base pair
BFA	brefeldin A
CaMV	Cauliflower Mosaic Virus
Col-0	<i>Arabidopsis</i> ecotype Columbia-0
CHX	cycloheximide
DAG	days after germination
2,4-D	2,4-dichlorophenoxy acetic acid
DNA	deoxyribonucleic acid
DMSO	dimethyl sulphoxide
EGFP	Enhanced Green Fluorescent Protein
ER	endoplasmic reticulum
EMS	ethylmethane sulphonate
GA	gibberellin
GFP	Green Fluorescent Protein
GUS	$\beta$ -Glucuronidase
HEPES	2-[4-(2-hydroxyethyl)-1-piperazinyl]-ethansulphonic acid
HPt	Histidine-containing phosphotransferase protein
IAA	indole-3-acetic acid
IPTG	isopropylthiogalactoside
kb	kilobase
MCS	multiple cloning site
MOPS	3-[N-morpholino]propanesulfonic acid
MW	molecular weight
NAA	$\alpha$ -naphthalene-acetic acid
NPA	1-N-naphthylphthalamic acid
ORF	open reading frame
PEG	polyethylene glycol
PIPES	piperazine-N,N'-bis[2-ethansulphonic acid]
PTGS	post transcriptional gene silencing
QC	quiescent centre

RNA	ribonucleic acid
RNAi	double stranded RNA interference
RR	response regulator protein
RT-PCR	Reverse Transcriptase-mediated Polymerase Chain Reaction
SAM	shoot apical meristem
SDS	sodium dodecylsulphate
TIBA	2,3,5-triiodobenzoic acid
T-DNA	Transferred DNA
UTR	untranslated region
var.	variety
Ws	<i>Arabidopsis</i> ecotype Wassilewskija
X-Gal	5-bromo-4-chloro-3-indolyl $\beta$ -D-galactopyranoside
X-Gluc	5-bromo-4-chloro-3-indolyl $\beta$ -glucuronide

## Contents

<b>Chapter 1 Introduction</b>	<b>1</b>
<b>1.1 <i>Arabidopsis thaliana</i> as a model system for the study of plant development</b>	<b>1</b>
1.1.1 Characteristics of <i>Arabidopsis thaliana</i>	1
1.1.2 The <i>Arabidopsis</i> genome	2
1.1.3 Differential splicing in plants	3
1.1.4 Analysis of gene expression using transgenic approaches	4
1.1.5 Analysis of gene function using transgenic approaches	5
1.1.6 Summary	9
<b>1.2 Plant hormones</b>	<b>9</b>
1.2.1 Auxin	10
1.2.1.1 Auxin biosynthesis	10
1.2.1.2 Auxin transport	11
1.2.1.3 Auxin perception	15
1.2.2 Cytokinin	17
1.2.2.1 Cytokinin biosynthesis and transport	18
1.2.2.2 Cytokinin perception	18
1.2.3 Ethylene	20
1.2.3.1 Ethylene biosynthesis and transport	20
1.2.3.2 Ethylene perception	20
1.2.4 Gibberellin	22
1.2.4.1 Gibberellin biosynthesis and transport	22
1.2.4.2 Gibberellin perception	24
1.2.5 Summary	26
<b>1.3 Development in <i>Arabidopsis thaliana</i></b>	<b>26</b>
1.3.1 Embryogenesis, an overview	27
1.3.2 Embryogenesis defective mutants	27
1.3.3 Vascular development defective mutants	29
1.3.4 Post-embryonic development of the root	33
1.3.4.1 Organisation of the <i>Arabidopsis</i> root	33
1.3.4.2 Development of lateral roots	34
1.3.4.3 Control of lateral root development	38
1.3.5 Summary	40

<b>1.4 Homeobox genes and plant development</b>	<b>41</b>
1.4.1 Homeobox genes	41
1.4.2 Plant homeobox genes	42
1.4.2.1 The KNOX family of homeobox genes in <i>Arabidopsis</i>	42
1.4.2.2 Conserved domains in the KNOX family	44
1.4.2.3 Control of transcription by KNOX proteins	48
1.4.2.4 Intercellular trafficking of KNOX transcripts and protein	50
1.4.2.5 KNOX genes are required to maintain the shoot apical meristem	51
1.4.3 Summary	56
<b>1.5 Aims and objectives</b>	<b>57</b>
<b>Chapter 2 Materials and Methods</b>	<b>58</b>
<b>2.1 Materials</b>	<b>58</b>
2.1.1 Chemicals	58
2.1.2 Radiochemicals	58
2.1.3 Enzymes	58
2.1.4 Kits	59
2.1.5 Bacterial strains	60
2.1.6 Plasmids	61
2.1.7 Bacterial culture media	61
2.1.8 Plant material	61
2.1.9 Plant culture media	61
2.1.10 Plant growth regulators	62
2.1.11 Antibiotics	62
<b>2.2 Plant growth, transformation and crossing</b>	<b>63</b>
2.2.1 Seed sterilisation and tissue culture	63
2.2.2 Plant growth in soil	63
2.2.3 Introduction of binary vectors into <i>Agrobacterium tumefaciens</i>	64
2.2.4 <i>Arabidopsis</i> transformation: the dipping method	65
2.2.5 Crossing	65
<b>2.3 Analysis of expression patterns and root morphology</b>	<b>67</b>
2.3.1 Examination of root tips	67
2.3.2 Histochemical GUS analysis	67
2.3.3 Paraffin embedding and sectioning of GUS stained samples	68

2.3.4 Historesin embedding and sectioning of GUS stained samples	70
2.3.5 Laser Scanning Confocal Microscopy (LSCM)	71
<b>2.4 Extraction and purification of nucleic acids</b>	<b>72</b>
2.4.1 Miniprep of plasmid DNA using theSigma GenElute™ plasmid miniprep kit	72
2.4.2 Midipreps of plasmid DNA using the Qiagen Midi Prep kit	72
2.4.3 Plant DNA extraction using the Phytopure kit	73
2.4.4 Quick DNA extraction method for PCR	75
2.4.5 RNA extractions using guanidine hydrochloride	75
2.4.6 RNA extractions using Qiagen RNeasy kit	76
2.4.7 Purification of DNA from agarose gels using the QIAquick® Gel Extraction kit	77
2.4.8 Purification of DNA using the High Pure PCR Product Purification kit	78
2.4.9 Purification of mRNA from total RNA using the PolyAtract® mRNA isolation system	78
2.4.10 Spectrophotometric analysis of RNA	79
2.4.11 Digestion of genomic DNA with restriction endonucleases	80
<b>2.5 Electrophoresis</b>	<b>80</b>
2.5.1 DNA agarose gel electrophoresis	80
2.5.2 RNA formaldehyde gel electrophoresis	81
2.5.3 Staining of RNA formaldehyde gels	82
<b>2.6 Nucleic acid hybridisation</b>	<b>82</b>
2.6.1 Southern blotting	82
2.6.2 Northern blotting	83
2.6.3 Colony lifts	84
2.6.4 Radio-labelling of probes with [ <sup>32</sup> P]α-dCTP	84
2.6.5 Pre-hybridisation and hybridisation of Southern blots using the Church system	85
2.6.6 Pre-hybridisation and hybridisation of Southern blots using the Denhardt's system	86
2.6.7 Prehybridisation and hybridisation of Northern blots using the Denhardt's system	87
2.6.8 Washing conditions for Church system	87

2.6.9 Washing conditions for Denhardt's systems	88
2.6.10 Autoradiography	89
2.6.11 Probe stripping	89
<b>2.7 DNA cloning into plasmid vectors and DNA sequencing</b>	<b>89</b>
2.7.1 Preparation of vector and inserts by digestion with restriction endonucleases	89
2.7.2 Dephosphorylation of vector DNA	89
2.7.3 Ligation of DNA fragments	89
2.7.4 Ligation of PCR fragments into pCR®2.1-TOPO	90
2.7.5 GATEWAY™ cloning: the LR and BP reactions	90
2.7.6 Transformation of chemically competent <i>E. coli</i> with plasmid DNA	91
2.7.7 Transformation of TOP10 One Shot™ competent cells	92
2.7.8 DNA sequencing	93
<b>2.8 Polymerase Chain Reaction (PCR)</b>	<b>93</b>
2.8.1 Standard PCR	93
2.8.2 PCR using Expand™ High Fidelity PCR system	94
2.8.3 PCR using Ex-Taq polymerase for screening the <i>Arabidopsis</i> Knockout Facility collection	95
<b>2.9 cDNA synthesis and purification</b>	<b>95</b>
2.9.1 cDNA synthesis	96
2.9.2 cDNA purification	96
<b>2.10 3' RACE</b>	<b>96</b>
2.10.1 Isolation of the KNAT6 3' region by 3' RACE	97
<b>2.11 5' RACE</b>	<b>98</b>
2.11.1 Synthesis and tailing of cDNA	98
2.11.2 Isolation of the KNAT6 5' region by 5' RACE	99
<b>2.12 Semi-quantitative RT-PCR</b>	<b>100</b>
<b>Chapter 3 Isolation of <i>KNAT6</i></b>	<b>102</b>
<b>3.1 Growth of tissue for RNA extraction</b>	<b>102</b>
<b>3.2 Primer design for use in 3' RACE</b>	<b>103</b>
<b>3.3 Synthesis of cDNA for use in 3' RACE</b>	<b>104</b>
<b>3.4 3' RACE strategy for isolation of novel homeobox genes</b>	<b>104</b>

from root	
<b>3.5 Analysis of preliminary 3' RACE products</b>	<b>106</b>
<b>3.6 Modification of the 3' RACE strategy</b>	<b>109</b>
<b>3.7 Analysis of modified 3' RACE products and isolation of a novel homeobox gene 3' fragment</b>	<b>110</b>
<b>3.8 Identification of the coding region of <i>KNAT6</i></b>	<b>111</b>
<b>3.9 Isolation of the 5' end of <i>KNAT6</i> by 5' RACE</b>	<b>113</b>
<b>3.10 Isolation of the <i>KNAT6</i> genomic sequence</b>	<b>115</b>
<b>3.11 Summary</b>	<b>116</b>
<b>Chapter 4 Sequence analysis of <i>KNAT6</i></b>	<b>118</b>
<b>4.1 Analysis of the <i>KNAT6</i> genomic sequence to confirm the complete <i>KNAT6</i> coding sequence was isolated</b>	<b>118</b>
4.1.1 Prediction of the <i>KNAT6</i> ATG	118
4.1.2 Analysis of the region upstream of the <i>KNAT6</i> ATG	119
<b>4.2 Positions of <i>KNAT6</i> introns and exons</b>	<b>120</b>
<b>4.3 The <i>KNAT6</i> predicted protein sequence shows conservation with other KNOX family members</b>	<b>120</b>
<b>4.4 Phylogenetic analysis of the <i>KNAT6</i> predicted protein sequence confirms it is a member of the KNOX class 1 subfamily</b>	<b>121</b>
<b>4.5 The experimentally determined 5' UTR of <i>KNAT6</i> may be truncated</b>	<b>121</b>
<b>4.6 Two isoforms of the <i>KNAT6</i> transcript have been isolated from NAA-treated <i>Arabidopsis</i> root</b>	<b>122</b>
<b>4.7 A single copy of <i>KNAT6</i> is present in the <i>Arabidopsis</i> genome</b>	<b>124</b>
<b>4.8 Summary</b>	<b>126</b>
<b>Chapter 5 Expression analysis of <i>KNAT6</i></b>	<b>127</b>
<b>5.1 Developmental and hormonal regulation of the <i>KNAT6</i> promoter</b>	<b>127</b>
5.1.1 Cloning of the <i>KNAT6</i> putative promoter and production of p <i>KNAT6</i> ::GUS <i>Arabidopsis</i>	127
5.1.2 Isolation and characterisation of p <i>KNAT6</i> ::GUS expressing <i>Arabidopsis</i>	130

5.1.3 Developmental expression of GUS under the <i>KNAT6</i> promoter in seedling roots and hypocotyl	134
5.1.4 Response of the <i>KNAT6</i> promoter to plant growth regulators	135
<b>5.2 The <i>KNAT6</i> promoter is expressed in the phloem poles of the <i>Arabidopsis</i> root</b>	<b>138</b>
5.2.1 Construction of the promoter::GFP vector pEGFP <sub>er</sub>	138
5.2.2 Production and isolation of pKNAT6::GFP <i>Arabidopsis</i>	139
5.2.3 Confocal imaging of pKNAT6::GFP <i>Arabidopsis</i> roots	143
5.2.4 Sectioning of pKNAT6::GUS <i>Arabidopsis</i> roots	143
5.2.5 Expression of pKNAT6::GUS in the <i>wol</i> mutant background	144
<b>5.3 Analysis of <i>KNAT6</i> transcript levels</b>	<b>145</b>
5.3.1 Northern analysis of the <i>KNAT6</i> transcript in different tissues	145
5.3.2 RT-PCR analysis of the <i>KNAT6</i> transcript in seedlings	147
<b>5.4 Localisation of <i>KNAT6</i> protein using GFP::KNAT6 protein fusions</b>	<b>149</b>
5.4.1 Production of plants expressing a C terminal KNAT6::GFP fusion protein	150
5.4.2 Production of plants expressing an N terminal alcohol-inducible GFP::KNAT6 fusion protein	152
<b>5.5 Summary</b>	<b>155</b>
<b>Chapter 6 Functional Analysis of <i>KNAT6</i> using transgenics</b>	<b>157</b>
<b>6.1 Overexpression and antisense of <i>KNAT6</i></b>	<b>157</b>
6.1.1 Production of <i>KNAT6</i> overexpression and antisense plants	157
6.1.2 Isolation of <i>KNAT6</i> overexpressing lines	160
6.1.3 Screening of T2 <i>KNAT6</i> overexpressing lines for a root phenotype	162
6.1.4 Analysis of aerial parts in T3 <i>KNAT6</i> overexpressing lines	165
6.1.5 Analysis of roots in T3 <i>KNAT6</i> overexpressing lines	168
6.1.6 Isolation of <i>KNAT6</i> antisense lines	169
6.1.7 Screening of T2 <i>KNAT6</i> antisense lines for a root phenotype	170
<b>6.2 RNAi <i>KNAT6</i> lines</b>	<b>171</b>
6.2.1 Production of 35S::KNAT6 RNAi plants	172
6.2.2 Production of pKNAT6::KNAT6 RNAi plants	174
6.2.3 Isolation of homozygous <i>KNAT6</i> RNAi lines	176

6.2.4 Analysis of homozygous <i>KNAT6</i> RNAi lines	178
<b>6.3 Summary</b>	<b>180</b>
<b>Chapter 7 Identification of <i>KNAT6</i> insertion mutants</b>	<b>182</b>
<b>7.1 Screening the <i>Arabidopsis</i> Knockout Facility collection</b>	<b>182</b>
<b>7.2 Isolation of SALK lines containing an insertion in <i>KNAT6</i></b>	<b>186</b>
<b>7.3 Other sequenced <i>Arabidopsis</i> insertion mutant libraries</b>	<b>192</b>
<b>7.4 Summary</b>	<b>193</b>
<b>Chapter 8 Discussion</b>	<b>194</b>
<b>8.1 Isolation of a novel homeobox gene from <i>Arabidopsis</i> root using 3' RACE</b>	<b>194</b>
<b>8.2 Sequence analysis</b>	<b>195</b>
8.2.1 Prediction of the <i>KNAT6</i> ATG	195
8.2.2 Analysis of the <i>KNAT6</i> transcript	196
8.2.3 <i>KNAT6</i> is a Class 1 KNOX gene	197
<b>8.3 Expression analysis</b>	<b>198</b>
8.3.1 Identification of conserved motifs in the <i>KNAT6</i> promoter	199
8.3.2 GUS expression level is variable in p <i>KNAT6</i> ::GUS lines	200
8.3.3 <i>KNAT6</i> promoter activity is localised to the phloem poles of the mature root	200
8.3.4 Analysis of <i>KNAT6</i> transcript levels	202
8.3.5 Regulation of the <i>KNAT6</i> promoter by plant hormones	203
<b>8.4 Functional analysis</b>	<b>207</b>
8.4.1 Overexpression of <i>KNAT6</i>	207
8.4.2 Downregulation of <i>KNAT6</i>	209
8.4.3 <i>KNAT6</i> may be partially redundant	210
<b>8.5 Roles of <i>KNAT6</i> in plant development</b>	<b>212</b>
8.5.1 <i>KNAT6</i> may play a similar role to other class 1 <i>KNOX</i> genes in the shoot	212
8.5.2 <i>KNAT6</i> may be involved in vascular development	214
8.5.3 <i>KNAT6</i> may be a regulator of lateral root initiation	216
8.5.4 <i>KNAT6</i> may play a role in control of root architecture	220
<b>8.6 Conclusions</b>	<b>221</b>

**References**  
**Appendices**

## List of figures

**Figure 1.2.1a** Proposed positions of auxin influx and efflux carrier proteins within the cell

**Figure 1.2.2.2a** The phosphorelay cascade from a hybrid kinase to a response regulator

**Figure 1.2.3.2a** The proposed ethylene signalling pathway in *Arabidopsis*

**Figure 1.3.1a** Embryogenesis in *Arabidopsis*

**Figure 1.3.4.1a** Organisation of the *Arabidopsis* root and root apical meristem

**Figure 1.4.2.5a** Organisation of the *Arabidopsis* shoot apical meristem (SAM)

**Figure 3a** 3' RACE strategy

**Figure 3.1a** Effect of the synthetic auxin analogue NAA root growth in wild type *Arabidopsis* var. Col-0

**Figure 3.2a** Clustal alignment of all homeobox sequences used for primer design

**Figure 3.5a** Analysis of preliminary 3' RACE products

**Figure 3.5b** Analysis of preliminary 3' RACE products

**Figure 3.5c** Reamplification of purified PCR products

**Figure 3.6a** Typical primary and secondary PCR products obtained using modified PCR conditions

**Figure 3.7a** Reamplification of secondary PCR products containing a band which hybridised to *STM*

**Figure 3.8a** Position of cloned *KNAT6* fragment within the GenBank predicted genomic region

**Figure 3.8b** Positions of primers used to isolate the *KNAT6* coding region

**Figure 3.8c** Amplification of *KNAT6* coding region by PCR

**Figure 3.8d** Predicted vs experimental coding sequences

**Figure 3.9a** Primer positions and 5' RACE strategy

**Figure 3.9b** Primary 5' RACE PCR reaction products

**Figure 3.9c** Secondary 5' RACE PCR reaction products

**Figure 3.9d** Colony PCR to identify specific 5' RACE Products

**Figure 3.10a** PCR amplification of the complete *KNAT6* genomic sequence

**Figure 3.10b** PCR amplification to confirm *KNAT6* genomic region amplification

**Figure 3.10c** Digestion of cloned *KNAT6* genomic fragment with EcoR1

confirms the correct sequence has been cloned

**Figure 4.1.1a** Experimentally determined *KNAT6* mRNA with predicted ATG

**Figure 4.1.2a** ORFs upstream of the *KNAT6* ATG

**Figure 4.2a** Positions of exons in *KNAT6* genomic sequence

**Figure 4.3a** KNOX Class 1 family protein domains

**Figure 4.4a** Phylogenetic tree

**Figure 4.5a** Positions of likely TATA boxes

**Figure 4.5b** Positions of promoter motifs within 2 kb of the *KNAT6* ATG

**Figure 4.6a** Site of alternative splicing in the *KNAT6* transcript

**Figure 4.6b** Addition of two amino acids to the *KNAT6* predicted protein by alternative splicing

**Figure 4.7a** Southern analysis to investigate *KNAT6* gene copy number

**Figure 5.1.1a** p*KNAT6*::GUS construct cloning strategy

**Figure 5.1.1b** Promoter fragment used for production of p*KNAT6*::GUS *Arabidopsis*

**Figure 5.1.1c** 2.1 kb promoter fragment amplified from Col-0 genomic DNA

**Figure 5.1.1d** 2.1 kb promoter fragment released from 3.9 kb pCR®2.1-TOPO vector by digestion with HindIII/XbaI

**Figure 5.1.1e** 4.5 kb pGUS-1 vector linearised with HindIII/XbaI

**Figure 5.1.1f** Release of p*KNAT6*::GUS cassette from pGUS-1 and linearisation of pCIRCE

**Figure 5.1.3a** GUS expression in p*KNAT6*::GUS Line 3.1

**Figure 5.1.4a** Response of the *KNAT6* promoter to plant growth regulators

**Figure 5.2.1a** Cloning strategy for the production of pEGFPper and p*KNAT6*::GFP

**Figure 5.2.1b** Amplification of 35S terminator and GFP cassette from the pKAR6-GFP vector

**Figure 5.2.1c** Release of 35S terminator and GFP cassette from the pCR®2.1-TOPO vector

**Figure 5.2.1d** 2.7 kb pUC19 linearised with SacI/EcoRI

**Figure 5.2.1e** 2.95 kb pUC19::35S terminator linearised with SmaI/SacI

**Figure 5.2.2a** Release of the 2.1 kb promoter fragment from pCR®2.1-TOPO by digestion with HindIII/XbaI

**Figure 5.2.2b** Linearisation of the 3.9 kb pEGFPer vector by digestion with HindIII/XbaI

**Figure 5.2.2c** Release of the 3.5 kb pKNAT6::GFP cassette from pEGFPer by digestion with EcoRI/HindIII

**Figure 5.2.2d** 11.4 kb pCIRCE linearised with EcoRI/HindIII

**Figure 5.2.3a** Orientation of root samples for LSCM

**Figure 5.2.3b** GFP expression in pKNAT6::GFP at 6 DAG

**Figure 5.2.4a** Paraffin sections from pKNAT6::GUS line 10.1

**Figure 5.2.4b** Historesin sections from pKNAT6::GUS lines

**Figure 5.2.5a** Expression of pKNAT6::GUS in the *wol* background

**Figure 5.3.1a** Northern analysis of transcripts in *Arabidopsis* tissues

**Figure 5.3.2a** Cycle quantification from amplification of *ACT1* and *KNAT6* transcripts from *Arabidopsis* RNA

**Figure 5.3.2b** Analysis of transcript levels in *Arabidopsis* seedlings

**Figure 5.4.1a** C terminal KNAT6::GFP protein fusion construct cloning strategy

**Figure 5.4.1b** KNAT6 coding region used for C terminal KNAT6::GFP protein fusions

**Figure 5.4.1c** Amplification of the 945 bp *KNAT6* coding sequence by PCR

**Figure 5.4.1d** Release of 945 bp KNAT6 coding region from the pCR®2.1-TOPO vector by digestion with SmaI

**Figure 5.4.1e** Linearisation of the 4.1 kb p35S::fusion-GFP vector by digestion with SmaI

**Figure 5.4.1f** Determination of insert orientation in recombinant p35s::KNAT6::GFP plasmids

**Figure 5.4.1g** Release of the 2.4kb KNAT6::GFP fusion cassette from the p35S::fusion-GFP vector by digestion with EcoRI

**Figure 5.4.1h** linearisation of the 11.4 kb pCIRCE vector by digestion with EcoRI

**Figure 5.4.2a** GATEWAY™ cloning strategy for the production of N terminal GFP::KNAT6 fusions

**Figure 5.4.2b** The alcohol-inducible system and N-terminal GFP::KNAT6 fusion protein construct

**Figure 5.4.2c** *KNAT6* coding region used for N terminal GFP::KNAT6 protein fusions

**Figure 5.4.2d** Amplification of the 900 bp *KNAT6* coding sequence with EcoRI linkers by PCR

**Figure 5.4.2e** Preparation of fragment for cloning the *KNAT6* coding sequence into the pENTR3C entry vector

**Figure 5.4.2f** Determination of orientation of *KNAT6* coding sequence fragments into pENTR3C

**Figure 5.4.2g** Diagnostic digests of the *KNAT6* coding sequence in the pGAT4 vector

**Figure 5.4.2h** Diagnostic digests of the *KNAT6* coding sequence in the pDONR207 vector

**Figure 5.4.2i** Diagnostic digests of the *KNAT6* coding sequence in the pBinAGRFAN vector

**Figure 6.1a** Sense and antisense construct cloning strategy

**Figure 6.1.1a** *KNAT6* fragment used for production of sense and antisense constructs

**Figure 6.1.1b** Amplification of the 1.3 kb *KNAT6* fragment with XbaI linkers by PCR

**Figure 6.1.1c** Release of the 1.3 kb *KNAT6* fragment from the pCR®2.1-TOPO

**Figure 6.1.1d** Linearisation of the 3.4 kb pDH51 vector by digestion with EcoRI

**Figure 6.1.1e** Colony PCR to determine the insert orientation of original splice *KNAT6* fragments into the pDH51 vector

**Figure 6.1.1f** Colony PCR to determine the insert orientation of alternate splice *KNAT6* fragments into the pDH51 vector

**Figure 6.1.1g** Release of 1.7 kb original splice 35S::*KNAT6* cassettes from the 3.4 kb pDH51 vector by digestion with EcoRI

**Figure 6.1.1h** Release of 1.7 kb alternate splice 35S::*KNAT6* cassettes from the 2.7 kb pDH51 vector by digestion with EcoRI

**Figure 6.1.1i** Linearisation of the 11.4 kb pCIRCE vector by digestion with EcoRI

**Figure 6.1.3a** Splitting of the main root by initiating lateral roots

**Figure 6.1.4a** Col-0 developmental series

**Figure 6.1.4b** asS16.3 developmental series

**Figure 6.1.4c** S2*d* developmental series

**Figure 6.1.4d** S7*a* developmental series

**Figure 6.1.4e** S9*c* developmental series

**Figure 6.1.4f** S10.4 developmental series

**Figure 6.1.4g** S14*b* developmental series

**Figure 6.1.4h** S15.6 developmental series

**Figure 6.1.4i** Leaf phenotype of 35S::*KNAT6* plants, 46 DAG

**Figure 6.1.5a** Length of the primary root in T3 S lines

**Figure 6.1.5b** Distance from the primary root tip to the last lateral root to emerge in T3 S lines

**Figure 6.1.5c** Number of lateral roots produced by T3 S lines

**Figure 6.1.5d** Number of anchor roots produced by T3 S lines

**Figure 6.2a** RNAi construct cloning strategy

**Figure 6.2.1a** *KNAT6* coding sequence fragments used for production of RNAi constructs

**Figure 6.2.1b** Amplification of *KNAT6* coding sequence fragments for RNAi constructs by PCR

**Figure 6.2.1c** Preparation of *KNAT6* coding sequence fragments and pRNAi vector for ligations

**Figure 6.2.1d** Linearisation of pRNAi::sense1 and pRNAi::sense2 by digestion with *SpeI/XbaI*

**Figure 6.2.1e** Preparation of pCIRCE and RNAi cassettes for ligations

**Figure 6.2.2a** Amplification of the 2.1 kb *KNAT6* promoter fragment with *NcoI/SmaI* linkers by PCR

**Figure 6.2.2b** Release of the 2.1 kb *KNAT6* promoter fragment from pCR®2.1-TOPO by digestion with *NcoI/SmaI*

**Figure 6.2.2c** Release of the 0.5 kb CaMV 35S promoter fragment from pRNAi1 and pRNAi2 by digestion with *NcoI/SmaI*

**Figure 6.2.2d** Release of RNA1+P and RNAi2+P cassettes from pRNAi1+P and pRNAi2+P plasmids by digestion with *EcoRI*

**Figure 6.2.4a** Length of primary root in homozygous RNAi1 plants

**Figure 6.2.4b** Length of primary root in homozygous RNAi2 plants

**Figure 6.2.4c** Length of primary root in homozygous RNAi1+P plants

**Figure 6.2.4d** Length of primary root in homozygous RNAi2+P plants

**Figure 6.2.4e** Distance from the primary root tip to the last lateral

root primordium to emerge in homozygous RNAi1 plants

**Figure 6.2.4f** Distance from the primary root tip to the last lateral root primordium to emerge in homozygous RNAi2 plants

**Figure 6.2.4g** Distance from the primary root tip to the last lateral root primordium to emerge in homozygous RNAi1+P plants

**Figure 6.2.4h** Distance from the primary root tip to the last lateral root primordium to emerge in homozygous RNAi2+P plants

**Figure 6.2.4i** Number of lateral roots produced by homozygous RNAi1 plants

**Figure 6.2.4j** Number of lateral roots produced by homozygous RNAi2 plants

**Figure 6.2.4k** Number of lateral roots produced by homozygous RNAi1+P plants

**Figure 6.2.4l** Number of lateral roots produced by homozygous RNAi2+P plants

**Figure 6.2.4m** Number of anchor roots produced by homozygous RNAi1 plants

**Figure 6.2.4n** Number of anchor roots produced by homozygous RNAi2 plants

**Figure 6.2.4o** Number of anchor roots produced by homozygous RNAi1+P plants

**Figure 6.2.4p** Number of anchor roots produced by homozygous RNAi2+P plants

**Figure 6.2.4q** Range of putative phenotypes in RNAi plants

**Figure 7.1a** Pooling and screening strategy for KO facility Alpha collection

**Figure 7.1b** Compatibility of *ATKO For1* and *ATKO Rev1* primers used to screen to *Arabidopsis* KO facility collection

**Figure 7.1c** Analysis of primary PCR products using *ATKO For1* and *ATKO Rev1* primers by gel electrophoresis

**Figure 7.1d** Hybridisation of primary PCR products obtained using the *ATKO For1* and *ATKO Rev1* primers to the complete *KNAT6* genomic sequence

**Figure 7.1e** Compatibility of *ATKO For1* and *ATKO Rev4* primers used to screen to *Arabidopsis* KO facility collection

**Figure 7.1f** Analysis of primary PCR products using *ATKO For1* and *ATKO Rev4* primers by gel electrophoresis

**Figure 7.1g** Hybridisation of primary PCR products obtained using the *ATKO*

*For1* and *ATKO Rev4* primers to the complete *KNAT6* genomic sequence

**Figure 7.2a** Positions of insertion in SALK\_047931 and SALK\_054482

**Figure 7.2b** Primer positions around the SALK\_47931 insertion

**Figure 7.2c** Identification of plants carrying an insertion in *KNAT6* corresponding to SALK\_47931

**Figure 7.2d** Primer positions around the SALK\_54482 insertion

**Figure 7.2e** Identification of plants carrying an insertion in *KNAT6* corresponding to SALK\_54482

**Figure 7.2f** Primer positions around the revised SALK\_54482 insertion

## List of tables

**Table 3.4a** Expected size of homeobox 3' RACE products

**Table 3.5a** PCR reaction and bands cloned into pCR®2.1-TOPO

**Table 3.5b** Sequencing of preliminary PCR products

**Table 3.8a** Expected product sizes using 3' UTR and exon primers

**Table 3.9a** Secondary 5' RACE PCR reactions

**Table 3.10a** PCR to check the *KNAT6* genomic fragment

**Table 4.7a** Enzymes selected for Southern analysis

**Table 5.1.2a** Segregation ratios and T-DNA loci numbers

**Table 5.1.2b** Number of T-DNA loci in pKNAT6::GUS lines

**Table 5.1.2c** Summary of root expression patterns in 15 independent T2 pKNAT6::GUS transgenic lines

**Table 5.1.2d** Summary of expression patterns in aerial parts of 15 independent T2 pKNAT6::GUS transgenic lines

**Table 5.1.4a** Plant growth regulators used to examine promoter activity

**Table 5.2.2a** Number of T-DNA loci in pKNAT6::GFP lines

**Table 5.2.2b** Root expression patterns in pKNAT6::GFP lines

**Table 5.3.2a** Sizes of PCR products from cDNA and genomic DNA templates

**Table 5.4.1a** PCR reactions to determine *KNAT6* orientation in the p35S::fusion-GFP vector

**Table 5.4.2a** Determination of *KNAT6* coding sequence orientation in pENTR3C by PCR

**Table 6.1.1a** Colonies containing *KNAT6* sense and antisense cassettes

**Table 6.1.2a** Segregation ratios and T-DNA loci numbers

**Table 6.1.2b** Number of T-DNA loci present in p35S::KNAT6 original splice (S) lines

**Table 6.1.2c** Number of T-DNA loci present in p35S::KNAT6 alternative splice (asS) lines

**Table 6.1.3a** Genotype of T2 S seedlings showing a putative phenotype on vertical plates

**Table 6.1.3b** Genotype of T2 asS seedlings showing a putative phenotype on

vertical plates

**Table 6.1.4a** Genotypes of Kan<sup>R</sup> S and asS plants used for aerial analysis

**Table 6.1.4b** Summary of phenotypes in plants expressing original splice (S) *KNAT6*

**Table 6.1.6a** Number of T-DNA loci present in antisense p35S::KNAT6 original splice (AS) lines

**Table 6.1.7a** T2 AS seedlings showing a putative phenotype on vertical plates

**Table 6.2.1a** Primer pairs for amplification of *KNAT6* coding sequence fragments for use in RNAi constructs

**Table 6.2.3a** Number of T-DNA loci present in RNAi lines

**Table 6.2.3b** T3 homozygous RNAi lines

**Table 6.2.4a** Range of putative phenotypes seen in T3 homozygous RNAi lines

**Table 7.1a** Reactions performed to test primers for KO facility screening

**Table 7.1b** Putative positives in DNA pools

**Table 7.2a** PCR to confirm presence of T-DNA inserts in T3 SALK\_047931 individuals

**Table 7.2b** PCR to confirm presence of T-DNA inserts in T3 SALK\_054482 individuals

## Chapter 1 Introduction

### 1.1 *Arabidopsis thaliana* as a model system for the study of plant development

With the advent of high throughput genomic sequencing in recent years, vast amounts of sequence data on a range of organisms ranging from bacteria and fungi to higher plants and animals have been generated. There are now several species from across all kingdoms for which a complete genome sequence is available. The challenge now lies in the annotation of this sequence data, and the elucidation of the function of the genes within those genomes.

In the plant kingdom there are three major model species: *Arabidopsis thaliana* (also known as Thale Cress), maize (*Zea mays*) and snapdragon (*Antirrhinum majus*). With particular reference to this project, *Arabidopsis thaliana* is an attractive species for the investigation of developmental processes for a variety of reasons as detailed in the sections below.

#### 1.1.1 Characteristics of *Arabidopsis thaliana*

*Arabidopsis thaliana* is a small crucifer that is found growing wild in many temperate zones of the world including Europe, North America and Asia. There are several morphological variants in the species, with the most common variations involving responses to day length, vernalisation and dormancy as well as differences in hairiness, chromosome number (tetraploidy) and other minor morphological and physical attributes. Four original ecotypes (Graz, Limburg, Estland and Landsberg) were selected as possible candidates for genetic studies in the 1950s. Landsberg was found to be the most vigorous and was selected as the ecotype to be used for further studies. Landsberg was subsequently found to be a non-isogenic population, and was further subdivided into two ecotypes named *Landsberg erecta* and Columbia (Col-0) (Koncz *et al.*, 1992).

*Arabidopsis* has a short life cycle (approximately 2 months) with fast development combined with easy cultivation and high seed yield. It has a tendency to self fertilise but is also easy to cross and generate hybrids. Of particular importance to this project, root development in *Arabidopsis* is



extremely well characterised and the study of root growth *in vitro* is simple and reliable. The development of the *Arabidopsis* root is discussed more in section 1.3.

*Arabidopsis thaliana* is also amenable to *Agrobacterium tumefaciens*-mediated transformation. *A. tumefaciens* is a soil-borne plant pathogen that is capable of modifying the plant's cellular mechanisms to produce metabolites which it alone can use (Zupan and Zambryski, 1995). This is achieved by the transfer of a section of DNA, known as the Transferred or T-DNA, into the plant genome. This natural genetic engineering system has been modified to allow the insertion of genes of interest into the plant genome (Bevan, 1984). This, along with the development of simplified transformation protocols such as the floral dip method (Clough and Bent, 1998), has meant that transgenic manipulation is now a central tool in understanding gene function in *Arabidopsis*.

Several transposon systems such as the maize *Ac/Ds* transposon system have also been successfully introduced into *Arabidopsis* by *Agrobacterium*-mediated transfer (Topping and Lindsey, 1995).

### **1.1.2 The *Arabidopsis* genome**

The *Arabidopsis* genome is one of the smallest among the angiosperms (1 x 10<sup>8</sup> basepairs) and there is a low fraction of redundant DNA in the genome (Meyerowitz, 1987).

The complete *Arabidopsis* genome (var. Col-0) has also been sequenced. Analysis has revealed that there are approximately 26,000 genes present in the genome, although differential splicing will lead to an increase in the number of gene products. 69% of the genes in the genome can be assigned a putative function based on sequence similarity to characterised genes (in any organism) but only 9% of *Arabidopsis* genes currently have experimental data available. This leaves 30% of the genes in the *Arabidopsis* genome that cannot be assigned to a functional category, although many of these genes have similarity to genes of unknown function in other organisms (The Arabidopsis Genome Initiative, 2000).

There is extensive segmental duplication and tandem arrays of genes in the genome. As these duplications are present as duplicated but not triplicated segments, either duplication of the entire genome or several independent segmental duplication events have occurred during the evolution of the *Arabidopsis* genome. It has been hypothesised that the *Arabidopsis* genome underwent duplication in the region of 112 million years ago. After duplication, the genes could be lost from the duplicated genome, and/or further duplications could occur to give the present day genome. The degree of conservation between the duplicated regions may be the result of divergence from an ancestral autotetraploid ancestor, or may reflect the differences present in an allotetraploid ancestor. The presence of these gene duplications indicates that there is potential for a significant level of redundancy in the *Arabidopsis* genome, or that duplicated genes may have diverged in function to play new roles in the plant. These two possibilities should be considered when determining gene function in *Arabidopsis* (The Arabidopsis Genome Initiative, 2000).

### **1.1.3 Differential splicing in plants**

As mentioned in section 1.1.2, the number of gene products in the *Arabidopsis* transcriptome will be greater than the number of genes that have been identified in the genome due to differential splicing. In animal systems, the importance of the differential splicing of genes to give more than one mRNA has long been known and more recently this phenomenon has been discovered in plants (for review see Lorkovic *et al.*, 2000). Most plant mRNAs are synthesised as pre-mRNAs that contain introns. The removal of introns and ligation of exons to produce translationally competent mRNA is mediated by the spliceosome, a large ribonucleoprotein complex.

Alternative splicing events may be constitutive, with similar levels of each mRNA variant, or they may be regulated in a tissue specific or developmental manner. For example, alternative splicing of the hydroxypyruvate reductase (HRP) gene in pumpkin produces two different proteins with distinct subcellular localisations. The HPR1 protein contains a signal for targeting to peroxisomes, whereas the cytosolic HRP2 protein does not. In the dark, equal proportions of HPR1 and HPR2 mRNA are produced, but treatment with light enhances the production of HRP2 mRNA (Mano *et al.*, 1999).

Rarely, alternative splicing may give two entirely different proteins, such as the production of ribosomal protein S14 and succinate dehydrogenase from a single gene in rice (Kubo *et al.*, 1999).

Retention of an unspliced intron in a fraction of transcripts is also common in plants and is thought to represent inefficient splicing rather than a regulated process that has a biological significance in the majority of cases. However, the presence of an inefficiently spliced intron may also play a regulatory role. Overexpression of the flowering time gene *FCA* leads to an acceleration of flowering time, thought to be mediated by a small increase in a fully spliced *FCA* transcript. However, the levels of a short transcript which is polyadenylated in intron 3 increases more than 100-fold during this overexpression, suggesting that this polyadenylation event controls the formation of *FCA* to keep flowering time constant (MacKnight *et al.*, 1997).

#### **1.1.4 Analysis of gene expression using transgenic approaches**

One of the most widely used methods for the prediction of expression pattern of a gene of interest is the use of promoter::reporter gene fusions to examine the localisation of promoter activity. The analysis of promoter activity using a transgenic approach is dependent on the use of reporter genes that can be used to visualise the cellular location of promoter activity. Two reporter genes that are of relevance to this work are those encoding  $\beta$ -glucuronidase (GUS) (Jefferson *et al.*, 1987) from *E. coli* and green fluorescent protein (GFP) (Chalfie *et al.*, 1994) from the jellyfish *Aequorea victoria*.

GUS is one of the most commonly used reporter genes (Jefferson, 1989). The  $\beta$ -glucuronidase enzyme catalyses the hydrolysis of a wide range of glucuronide molecules, including the artificial substrate 5-bromo-4-chloro-3-indolyl  $\beta$ -glucuronide (X-GLUC) that produces a bright blue insoluble dye after enzymatic hydrolysis and atmospheric oxidation.

The use of GFP is particularly attractive as the assay is non-destructive. However, wild type GFP from *A. victoria* is not expressed properly in higher plants due to low solubility and the presence of a cryptic intron in the coding

sequence that leads to mis-splicing of the transcript and the subsequent removal of 83 nucleotides from the coding sequence. Wild type GFP has been modified by a number of groups to allow use as a reporter gene. Two different GFP variants, EGFP-1 and smGFP, were used as part of this work.

EGFP-1 (Enhanced GFP, Clontech) encodes the GFPmut1 variant (Cormack *et al.*, 1996). This GFP has two amino acid substitutions that increase solubility and alter the excitation maxima to allow efficient excitation at 488 nm. The coding sequence has also been modified to include silent base changes that correspond to human coding-usage preferences (Hass *et al.*, 1996). This GFP variant gives strong expression in plant cells.

smGFP was produced by mutagenesis of modified GFP4 (mGFP4) (Haseloff *et al.*, 1997). mGFP4 was produced by removal of the cryptic intron by mutagenesis from wild type GFP. mGFP4 was then mutagenised to give soluble modified GFP (smGFP) (Davis and Vierstra, 1998). This GFP variant also gives strong expression in plant cells.

The generation of plants containing a promoter::reporter transcriptional fusion is a widely used technique which has been used to obtain a large amount of data on promoter activities. However, sequences that control gene expression are not necessarily solely located in the upstream untranscribed region of a gene, but may also be present within the transcribed region of the gene. For example, *cis*-acting elements in the intragenic sequence of the *AGAMOUS* (*AG*) gene of *Arabidopsis* are required for repression of *AG* in vegetative tissues as well as correct spatial and temporal regulation of *AG* in early flower development (Sieburth and Meyerowitz, 1997). Therefore, care should be taken when using promoter::reporter gene fusion to analyse gene expression patterns, and data should be backed up by another method of expression analysis such as in situ hybridisation, northern analysis or semi-quantitative RT-PCR.

### **1.1.5 Analysis of gene function using transgenic approaches**

Mutants have long been used to aid our understanding of gene function, but in the past this has been in a forward genetic manner (i.e. isolation and

characterisation of a mutant of interest followed by cloning of the disrupted gene).

However, with the completion of the *Arabidopsis* genome sequencing project, reverse genetics (i.e. the identification of a gene followed by the determination of its function) has become increasingly important to allow function to be assigned to the large proportion of uncharacterised genes in the genome.

Transgenic approaches are central to reverse genetic approaches and their use can be divided into two broad areas: the use of transgenic techniques to investigate the function of single genes by manipulation of their expression, and the production of large libraries of insertion mutants which can be screened for insertions in the gene of interest.

#### **[A] manipulation of the expression of single genes**

The manipulation of the expression of single genes can be divided into two areas: the overexpression and/or mis-expression of a gene of interest using a promoter which directs expression of the gene of interest at a higher level and/or in a different cell type than the native promoter as well as the downregulation of gene expression.

One promoter that is commonly used to direct gene expression in these types of construct is the 35S RNA gene promoter from Cauliflower Mosaic Virus (35S CaMV). Although this promoter is nominally referred to as constitutive, there is some evidence to show that it is not expressed in all plant tissues equally (Topping *et al.*, 1991).

This promoter is often used in the generation of overexpressing constructs (sometimes referred to as sense constructs) as it directs a high level of gene expression in a wide range of tissues and therefore leads to overexpression and misexpression of the gene of interest.

The downregulation of gene expression using transgenics can be achieved by several techniques including antisense suppression and double stranded RNA interference (RNAi).

Antisense suppression has been used for many years to downregulate gene expression in plants although there is wide variation in the extent of the downregulation in a population of antisense transformants. RNAi constructs on the other hand appear to give much more efficient and reliable downregulation of the target gene.

The mechanisms that lie behind gene silencing were poorly understood until recent advances began to shed light on the processes by which these might occur (Carthew, 2001, Matzke *et al.*, 2001).

Silencing was first observed in transgenic tobacco plants where an increase in copy number of the transgene often led to a decrease in the transgene expression level (Matzke *et al.*, 1989). Silencing can be produced both by genes which are duplicated at a single genomic locus, or which are dispersed throughout the genome, and can occur either transcriptionally by changes in methylation (Matzke *et al.*, 1989) or post-transcriptionally by degradation of mRNA (Van Blokland *et al.*, 1994).

In plants, post transcriptional gene silencing (PTGS) is a common cellular response to viral infection. Virus resistance and gene silencing has been induced in tobacco by the simultaneous expression of sense and antisense protease RNA from Potato virus Y (PVY) (Waterhouse *et al.*, 1998). It is thought that this occurs via a viral defence mechanism by which the plant recognises double stranded RNA (dsRNA) and degrades it, hence providing immunity to the plant. It is hypothesised that in this system the response is elicited as the sense and antisense transcripts form a duplex and initiate degradation of the transgene transcripts. This model can be extended to the silencing of endogenous genes by activation of this pathway upon the expression of homologous transgenes.

A requirement for successful PTGS appears to be the presence of a double stranded RNA (dsRNA) species that is homologous to the silenced gene (Carthew, 2001). The simplest way of achieving gene suppression using RNAi is to design constructs where the gene of interest (under control of a single

promoter) is present in the sense and the antisense orientations and is separated by a linker that allows the production of an mRNA molecule that can form a hairpin loop.

The use of RNAi technology has made the generation of plants which show reduced expression in the gene of interest much more reliable (Chuang and Meyerowitz, 2000). Comparison of the number of mutants generated using antisense or RNAi constructs for several genes (*AGAMOUS*, *CLAVATA3*, *APETALA1* and *PERIANTHIA*) showed that RNAi constructs led to 87-99% of transformants exhibiting the knockout mutant phenotype, whereas antisense suppression led to 0-55% of transformants exhibiting the mutant phenotype.

RNAi technology is useful in generating plants with downregulated expression of the gene of interest where no knockout mutation is available, or where the phenotypic equivalent of an allelic series is desired.

### **[B] generation of mutant libraries**

As mentioned above, transgenics have been used to produce large libraries of insertional mutants that can then be screened for insertions in a gene of interest. There is a growing number of insertional mutant libraries which are available for screening. These are produced by the insertion of either T-DNAs or transposons by *Agrobacterium*-mediated transformation followed by isolation of transformants.

This approach is viable as the generation of mutants using either T-DNA or transposon insertions provides a tag of known sequence which can then be used to identify the insertion site and hence the disrupted gene. This allows mutant libraries that were created in this way to be screened in a reverse genetic manner as opposed to the screening of traditional EMS mutant populations that can only be screened in a forward genetic approach.

There are two types of library that are currently available: those that can be screened by PCR, or those for which the junction between the plant DNA and the inserted DNA has been isolated and sequenced and which can be screened by a BLAST search.

Libraries that are screened by PCR rely on some kind of pooling system to allow a large number of individual transformants to be screened in a single PCR reaction. There are several libraries that are available for screening in this way. These include the *Arabidopsis* Knockout Facility collection at the University of Wisconsin Biotechnology Centre (<http://www.biotech.wisc.edu/Arabidopsis>) as well as the Feldmann and Thomas Jack lines that are available through NASC (<http://nasc.nott.ac.uk/home.html>). The *Arabidopsis* Knockout Facility collection was screened as part of this work and further details are given about the collection in Chapter 7.

Numerous libraries for which sequence databases are being produced are also available. These include collections at the Salk Institute (<http://www.tmri.org>), the Cold Spring Harbor Laboratory (<http://genetrap.cshl.org>) as well as the *Arabidopsis thaliana* Insertion Database (AtIDB, <http://atidb.cshl.org>) that combines data from several insertion mutant libraries. These databases were all searched as part of this work, and more details are provided in Chapter 7.

### **1.1.6 Summary**

In conclusion, *Arabidopsis thaliana* is an attractive model for the investigation of developmental biology as it has various characteristics which make it easy and convenient to work with, such as easy cultivation and tissue culture protocols, as well as a relatively small genome with low levels of repetitive DNA for which the complete sequence is available. The ease of transformation of *Arabidopsis* also makes generation of transgenics to investigate promoter activity (by promoter::reporter gene fusions) and gene function (using sense, antisense and RNAi) comparatively straightforward. Reverse genetic approaches to the elucidation of gene function in *Arabidopsis* are also simplified by the availability of libraries of insertional mutants that can be screened for gene knockouts.

## **1.2 Plant hormones**

Plant development is co-ordinated by hormones. These are naturally occurring organic substances that can influence plant physiology at low concentrations. They differ from mammalian hormones in that they are not synthesised in a specialised tissue (e.g. an endocrine gland) and then transported to their site of

action, but are synthesised in a wide range of tissues and may act at the site of synthesis or be transported. The term plant growth regulator is used to encompass all compounds, whether synthetic or natural, which can influence plant physiology.

The three plant hormones that are of most relevance to this work are auxin, cytokinin and ethylene. A brief overview of the synthesis, transport and perception of each of these hormones is given in the following sections.

### **1.2.1 Auxin**

Auxin regulates a diverse array of cellular responses and developmental processes in plants ranging from cell division, expansion and differentiation to patterning of embryos and vasculature as well as roles in regulating the primary and lateral root and shoot meristems (Davies, 1995).

#### **1.2.1.1 Auxin biosynthesis**

The majority of work into the role of auxin in the plant has focused on the main endogenous form, indole-3-acetic acid (IAA). The bioactive form of IAA is believed to be free IAA (Taiz and Zeiger, 1991). Free IAA can be inactivated reversibly or irreversibly by conjugation or can be inactivated irreversibly by oxidation.

There are multiple pathways for the synthesis, inactivation and catabolism of auxin within the plant and there are multiple genes encoding the enzymes involved in each pathway (Normanly and Bartel, 1999). Auxin may be synthesised from the amino acid tryptophan, or may be synthesised from a tryptophan precursor. These pathways allow the plant several ways in which to control the amount of auxin which is available in an active form.

The *ROOTY (RTY)* gene in *Arabidopsis* encodes an aminotransferase that is thought to be involved in auxin biosynthesis. The recessive *rti* mutant has higher levels of free and conjugated IAA than wild type plants and shows an enormous increase in the number of adventitious and lateral roots that are produced as well as small epinastic cotyledons and an elongated hypocotyl

(King *et al.*, 1995). *rtv* is allelic to *superroot1* (Boerjan *et al.*, 1995) and *alf1-1* (Celenza *et al.*, 1995).

### 1.2.1.2 Auxin transport

The development of a gas chromatography/mass spectrometry (GS-MS) method for the quantitative analysis of auxin in small amounts of plant tissue has allowed the determination of auxin levels in the *Arabidopsis* seedling (Kowalczyk and Sandberg, 2001).

After germination, the cotyledons are the major source of auxin, either as conjugated auxin is activated or de novo synthesis occurs. Actively dividing young leaves show the highest concentration of auxins. At 5-6 days after germination (DAG), when the first leaves start to develop, there is an increase in free auxin levels, with the largest increase associated with the areas of highest cell division (Bhalerao *et al.*, 2002). As the cells in the leaf switch from division to expansion the auxin levels drop. Although young leaves have the highest capacity for the synthesis of auxin, all tissues in young *Arabidopsis* seedlings, including the roots, are capable of auxin synthesis (Ljung *et al.*, 2001).

Analysis of the levels of auxin within the *Arabidopsis* root has revealed that the root is subjected to a transient pulse of auxin at 5-7 DAG that reaches the root tip at 7-8 DAG (Bhalerao *et al.*, 2002). This pulse of auxin is produced during the development of the first two true leaves, and is not repeated during development of subsequent leaves.

Examination of the auxin level along the length of the root indicates that the production of auxin in the aerial parts establishes an auxin gradient in the root between 5-8 DAG. Auxin from the aerial parts accumulates at the root/hypocotyl junction and a gradient is formed with the highest concentration at the hypocotyl (Bhalerao *et al.*, 2002).

In addition, at 3-6 DAG, a gradient of auxin is established in the root tip, with the highest levels in the most apical 1 mm. As this is before the initiation of the first leaves, it is thought that the cotyledons are the source of this auxin. At 7 DAG,

there is a further increase in the level of auxin at the root tip as the pulse of shoot-derived auxin reaches it (Bhalerao *et al.*, 2002). The root system gains increased competence to synthesise auxin between 3 and 10 DAG and becomes less reliant on shoot derived auxin.

Auxin can be transported in the vascular system in either the xylem or the phloem. Transport in the vasculature can occur by simple mass flow down a concentration gradient, and both inactive and active forms of IAA may be transported (Lomax *et al.*, 1995). In contrast, polar auxin transport is specific for free auxin and is an active process that occurs between specific cells.

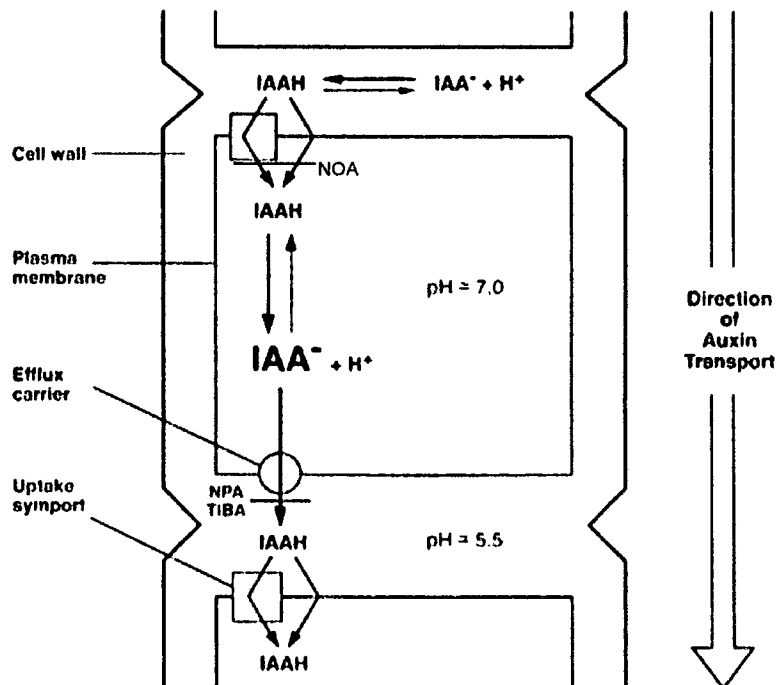
Auxin is transported basipetally through the aerial parts of the plant to the root/hypocotyl junction where it is then transported acropetally to the root tip. Here, the auxin is unloaded from the vascular tissues before a second auxin stream in the epidermal and cortical cells moves the auxin away from the root tip in a basipetal manner.

It appears unlikely that auxin is delivered to the root purely by polar auxin transport as it has been shown that treatment of plants with the auxin transport inhibitor 1-N-naphthylphthalamic acid (NPA) fails to block the export of IAA from young leaves (Ljung *et al.*, 2001) or prevent IAA accumulation in the root tip (Casimiro *et al.*, 2001).

The protein carriers that are thought to mediate polar auxin transport are the putative auxin influx and efflux carriers. These integral membrane proteins are thought to have specific locations on different sides of cells to allow the directed movement of auxin (Lomax *et al.*, 1995) (Figure 1.2.1a). The proposed influx carriers are the *AUX1* gene family and the proposed efflux carriers are the *PIN* gene family. It should also be noted that free auxin can diffuse across the membrane as shown in Figure 1.2.1a.

Currently *AUX1* has only been shown to be the influx carrier by indirect methods. The *AUX1* gene was cloned by virtue of a T-DNA tagged mutant allele, *aux1-100*, and encodes a protein that has 11 transmembrane domains and shares similarity with plant amino acid permeases (Bennett *et al.*, 1996). This

**Figure 1.2.1a** Proposed positions of auxin influx and efflux carrier proteins within the cell



From Lomax, 1995 p513

The positions of the auxin influx and efflux carriers allow the movement of auxin in the direction indicated.

Several inhibitors of auxin transport (NOA, NPA and TIBA) have been isolated and are also marked on the scheme.

Free IAA can diffuse over the membrane in its protonated form. The neutral pH inside the cell causes deprotonation. This deprotonated IAA cannot diffuse back out of the cell and must rely on the efflux carrier.

indicates a role as a transmembrane transporter of an amino acid based compound such as tryptophan-based auxin. *aux1* mutants are agravitropic and show an increase in root length (Pickett *et al.*, 1990). The *aux1* mutant shows an auxin resistant phenotype when treated with IAA, or the synthetic auxin analogue 2,4-D that requires the influx carrier to enter the cell. However, *aux1* is sensitive to the synthetic auxin analogue NAA that can enter the cell by diffusion (Marchant *et al.*, 1999). In addition, wild type plants that are treated with the influx carrier inhibitor 1-naphthoxyacetic acid (1-NOA) phenocopy the *aux1* mutant (Parry *et al.*, 2001a).

*AUX1* is expressed in the columella and protophloem poles of the stele but is not expressed in mature phloem cells. As *aux1* mutants do not show IAA accumulation at the root apex, *AUX1* appears to function in unloading of auxin from the phloem (Swarup *et al.*, 2001). *AUX1* is also expressed in the lateral root cap and elongating epidermal cells, suggesting that *AUX1* may also play a role in basipetal auxin transport away from the root tip. It has been demonstrated that the auxin responsive reporter construct pIAA2::GUS is not expressed in the lateral root cap and elongating epidermal cells in *aux1*, indicating that basipetal auxin transport is impaired (Swarup *et al.*, 2001).

Three other genes that have similarity to *AUX1* have been identified in the *Arabidopsis* genome by homology searches, and have been designated *LIKE AUX1 (LAX)* genes (Parry *et al.*, 2001b). *LAX3* is expressed in the mature vasculature of the root (M. Bennett, unpublished, pers. comm.). The *lax3* mutant is not agravitropic and has only 50-60% of the lateral roots seen in a wild type plant. *lax3/aux1* doubles show a further decrease in the number of lateral roots produced. *LAX3* appears to function in delivering auxin to the developing lateral root primordia. *LAX1* is also expressed in the laterals, explaining why some laterals are still seen in *lax3/aux1* doubles. Expression of the *LAX* proteins under control of the *AUX1* promoter cannot rescue the *aux1* phenotype, indicating that there must be some signal, possibly in the protein itself that directs it to the correct part of the membrane.

The *PIN* gene family has been shown indirectly to be the putative efflux carriers. *PIN1* was identified due to the phenotype of the *pin-formed1 (pin1)* mutant

whose inflorescence lacks any lateral organs and instead forms a pin-like structure, and which shows a reduction in basipetal auxin transport (Okada *et al.*, 1991). This phenotype can be phenocopied by the compound 1-N-naphthylphthalamic acid (NPA). Cloning of the *PIN1* gene has revealed that it is a transmembrane protein with homology to bacterial transporter proteins (Galweiler *et al.*, 1998). In the root, *PIN1* is localised on the lower (acropetal) side of stele cells (Friml, 2003) where it functions in delivery of auxin to the root tip.

Other genes have since been identified by homology with *PIN1*. The other three *PIN* genes which have been characterised to date, *PIN2*, *PIN3* and *PIN4* are localised on sides of cells in the root apex to allow acropetal auxin transport to the root tip and basipetal transport towards the shoot apex (Friml and Palme, 2002). The *pin2* mutant has also been shown to be allelic to *ethylene insensitive root1* (*eir1*), indicating that there is crosstalk between different hormone pathways.

However, recent work in the field has begun to indicate that the auxin carriers do not function to transport auxin across the plasma membrane, but that the polar transport of auxin is achieved by endo- and exocytosis via vesicles.

There are several pieces of experimental evidence that support this model. It has been shown that auxin efflux carrier inhibitors such as TIBA and NPA actually affect *PIN1* localisation by disrupting vesicle trafficking (Geldner *et al.*, 2001) and that membrane localisation of *AUX1* is inhibited by the vesicle trafficking inhibitor brefeldin A (BFA) (Grebe *et al.*, 2002).

In addition, the *GNOM* gene, whose product is involved in vesicle trafficking, is required for correct localisation of the *PIN1* protein and polar auxin transport is affected in the *gnom* mutant (Steinmann *et al.*, 1999). It has recently been shown that *GNOM* is BFA sensitive, as is correct *PIN1* localisation (Geldner *et al.*, 2003). *PIN1* localisation is BFA resistant in plants that carry a BFA resistant, fully functional form of *GNOM*, which indicates that *GNOM* is required for recycling of auxin transport system components.

### 1.2.1.3 Auxin perception

Over the past few years, analysis of auxin response mutants has led to the development of a model in which auxin signalling is mediated by regulated protein degradation (Leyser, 2001, Gray and Estelle, 2000). This is mediated by the SCF<sup>TIR1</sup> ubiquitin ligase complex which ubiquitinates target proteins and targets them to the proteasome where they are degraded. Two *Arabidopsis* mutants that are defective in components of this system are *axr1* (del Pozo and Estelle, 1999, del Pozo *et al.*, 1998) and *tir1* (Ruegger *et al.*, 1997, Gray *et al.*, 1999). These two mutants show morphological phenotypes that reflect reduced sensitivity to auxin.

It is thought that the SCF<sup>TIR1</sup> complex mediates auxin response by degrading members of the Aux/IAA protein family. *Aux/IAA* genes are rapidly induced in response to auxin and the proteins they encode share four conserved domains, denoted I, II, III and IV. In addition, they contain nuclear localisation signals (Reed, 2001).

Domains III and IV are required for homo- and heterodimerisation between different Aux/IAA proteins, and also allow interaction with the related auxin response factor (ARF) family, which contain domains III and IV in their structure (Reed, 2001).

Genes in the ARF family have a highly conserved DNA binding domain that binds to auxin response elements (AuxREs) of the sequence TGTCTC in the promoters of primary/early auxin response genes (Ulmasov, 1999). ARFs may function as activators or repressors of transcription.

Aux/IAA proteins have extremely high turnover in the plant, and this instability is required for normal auxin signalling (Worley *et al.*, 2000). For example, mutations in domain II of the *AXR3/IAA17* gene (*axr3-1*) show increased levels of the AXR3 protein in the cell (Ouellet *et al.*, 2001). In addition, overexpression of Aux/IAA proteins can block auxin inducible transcription from an auxin activated promoter (Ulmasov *et al.*, 1997), probably because dimerisation with an Aux/IAA protein prevents dimerisation with a second ARF protein.

Hence, Aux/IAA proteins are central in mediating downstream auxin responses through interaction with ARFs. The current model (Tiwari *et al.*, 2001) proposes that a low auxin level within a cell allows the transcription of *Aux/IAA* genes. The Aux/IAA proteins then form heterodimers with ARFs, which prevents the ARFs initiating transcription of auxin responsive genes that contain an AuxRE. When the cellular level of auxin increases, Aux/IAA proteins are targeted for degradation by the SCF<sup>TIR1</sup> complex. Dissociation of the Aux/IAA proteins from the ARFs allows ARF dimerisation and the transcription of target genes containing an AuxRE. If the auxin level then drops, Aux/IAA proteins are not degraded by the ubiquitination pathway, but cause a downregulation in transcription of auxin responsive genes by interaction with ARFs.

The ubiquitin binding site in Aux/IAA proteins is located in domain II (Tiwari *et al.*, 2001). Therefore, mutations in this binding site prevent ubiquitination and degradation of the Aux/IAA protein, which causes an increase in protein stability. Therefore, in these mutant backgrounds, an increase in cellular auxin levels does not lead to the lifting of transcriptional repression and expression of auxin responsive genes, but causes the cell to be auxin insensitive.

The *bodenlos* (*bdl*) mutant (Hamann *et al.*, 1999) disrupts domain II of the *Aux/IAA* gene *IAA12*, leading to a gain-of-function mutant with increased stability (Hamann *et al.*, 2003). The *bld* mutant is resistant to the auxin 2,4-D, which is consistent with a mutation that prevents breakdown of the protein on an increase in auxin level. The *bdl* seedling phenotype is characterised by a deletion of the basal organs of the seedling such as the root and the hypocotyl, and decreased vasculature in the cotyledons (Hamann *et al.*, 1999).

The *arf5/monopteros* (*mp*) mutation disrupts an ARF transcription factor (Hardtke and Berleth, 1998). The *mp* mutant was isolated during a screen for *Arabidopsis* pattern mutants and is characterised by seedlings where the basal elements (root and hypocotyl) were deleted (Berleth and Jürgens, 1993). The *mp* seedling phenotype is similar to that described for *bdl* above. The vascular system of *mp* mutants does not develop properly, and auxin transport capacity is impaired (Przemeck *et al.*, 1996). These observations support the proposed

role of MP as an ARF transcription factor involved in the sensing of auxin and control of auxin dependent pathways such as vascular development.

It is also thought that the *PIN* family of auxin efflux carriers could be targets for auxin-regulated degradation. Accumulation of *PIN2* protein is increased in the *axr1* mutant background, indicating that it may be a target for degradation by the SCF<sup>TIR1</sup> complex (Sieberer *et al.*, 2000). This would provide a link between auxin signalling and auxin transport.

The model provides an explanation for how a single molecule such as auxin can induce a diverse array of effects in plant tissues. The specificity of the auxin response is not contained within the auxin molecule itself, but is determined by the available targets for degradation, which are determined by cell type (Leyser, 2001).

Currently, little is known about how auxin influences the degradative machinery. It may be that auxin can change the activity of, or regulate the recruitment of target proteins to, the SCF<sup>TIR1</sup> complex. Phosphorylation of target proteins is a mechanism that is used in other SCF systems to recruit proteins for degradation (Craig and Tyers, 1999), and in *Arabidopsis*, the *PINOID* (*PID*) serine/threonine kinase is required for correct auxin responses (Christensen *et al.*, 2000). The site of auxin perception also remains elusive. The best candidate auxin receptor is *AUXIN BINDING PROTEIN1* (*ABP1*) that shows an ability to bind auxin specifically (Napier *et al.*, 2002).

### **1.2.2 Cytokinin**

The cytokinins consist of a group of compounds that have been described as “substances which, in the presence of auxin, stimulate cell division and which interact with auxin in determining the direction in which differentiation of cells takes” (Whitty and Hall, 1974). Cytokinins have been implicated in many aspects of plant development including roles in control of the cell cycle and the shoot apical meristem (D'Agostino and Keiber, 1999).

### 1.2.2.1 Cytokinin biosynthesis and transport

There are various natural plant cytokinins, almost all of which have a purine-based structure (McGaw and Burch, 1995). In general, a given plant tissue will normally contain several different cytokinins, with the distribution of various types of cytokinin differing between plant species. No mutants that have altered levels of specific cytokinins have been discovered, making it impossible to assign roles to different cytokinin types (Harberer and Keiber, 2002).

The root tip has been identified as a major source of cytokinin biosynthesis. It is assumed that, as cytokinins have been identified in the xylem sap, transport of cytokinin to the shoot occurs via this mechanism (Harberer and Keiber, 2002). Both immunolocalisation and direct measurements of cytokinin levels have indicated that high levels accumulate in areas of cell division such as the shoot meristem (Dewitte *et al.*, 1999).

### 1.2.2.2 Cytokinin perception

The *cytokinin response 1-1 (cre1)* mutation was isolated in a screen to identify mutants with altered cytokinin sensitivity. Cloning of the *CRE1* gene revealed that it encoded a type of histidine kinase known as a hybrid kinase (Inoue *et al.*, 2001). Cytokinin recognition by the *CRE1* protein has been demonstrated in several heterologous bacterial and yeast systems to confirm that *CRE1* is the cytokinin receptor in *Arabidopsis* (Schmulling, 2001). *CRE1* is allelic to *WOODENLEG (WOL)* (Mähönen *et al.*, 2000) and *AHK4* (Yamada *et al.*, 2001).

The *cytokinin independent1 (cki1)* mutant was isolated from a population of activation-tagged plants designed to identify constitutive cytokinin responses in the absence of cytokinin (Kakimoto, 1996). The *CKI1* gene also encodes a histidine kinase, which is probably involved in some aspect of cytokinin perception and signalling. In addition, two *Arabidopsis CRE1* homologues, *AHK2* and *AHK3*, have been identified (Suzuki *et al.*, 2001).

Information on the downstream signalling cascade that occurs after binding of cytokinin to the *CRE1* receptor is also emerging. The predicted protein structure of *CRE1* indicates that it consists of two N terminal membrane spanning domains that allow the formation of an extracellular input domain. The *CRE1*

protein also has three intracellular domains consisting of a histidine kinase transmitter domain followed by two receiver domains (Inoue *et al.*, 2001). Cytokinin binding causes phosphorylation of a histidine residue in the transmitter domain. This phosphate is then transferred to an aspartate residue in the receiver domain before being transferred to the histidine residue of a Histidine-containing phosphotransferase protein (HPT). Finally, the phosphate is transferred to the aspartate residue of a response regulator (RR) protein (Figure 1.2.2.2a) (Lohrmann and Harter, 2002) that alters the transcription of target genes and causes a response.

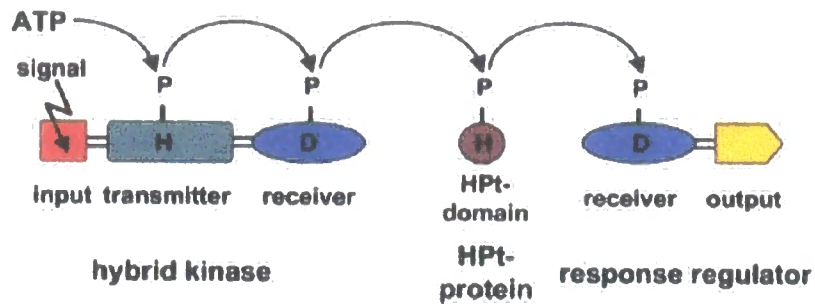
This model is supported by experimental evidence where mutation of His<sub>459</sub> in the *CRE1* His-kinase transmitter domain, or of Asp<sub>973</sub> in the receiver domain, abolishes *CRE1* activity (Inoue *et al.*, 2001). In addition, when *CRE1* is expressed in *E. coli* or yeast strains that do not have functional HPT or RR genes, no response is elicited on treatment with cytokinin (Suzuki *et al.*, 2001). This indicates that *CRE1* mediates cytokinin responses via a His-Asp phosphorelay cascade involving HPT and RR proteins in a manner typical of two-component histidine kinases.

In *Arabidopsis* there are five genes encoding HPT proteins, *AHP1-5*, and it has been shown that several of these purified proteins can be phosphorylated in an *E. coli* system (Suzuki *et al.*, 1998). In support of the role of AHP proteins in cytokinin perception, it has been demonstrated that overexpression of *AHP2* leads to cytokinin hypersensitivity (Suzuki *et al.*, 2002).

There are approximately 20 response regulator (*ARR*) genes in *Arabidopsis*. The sequences of the *ARR* genes have homology to bacterial response regulator genes which act downstream of sensory histidine kinases. The *ARR* genes fall into two classes, type A and type B, based upon the domains they contain (Imamura *et al.*, 1999).

The presence of both HPT and *ARR* proteins in *Arabidopsis* indicates that responses may be elicited by a change in transcription of target genes brought about by a phosphotransfer cascade in the same way as in bacterial systems.

**Figure 1.2.2a** The phosphorelay cascade from a hybrid kinase to a response regulator



From Lohrmann and Harter, 2002

The phosphorelay works by transfer of a phosphate group from ATP to the hybrid kinase, which can then autophosphorylate. This phosphate is then transferred to the response regulator via the HPT protein.

Conserved residues are phosphorylated in these proteins (H = histidine, D = aspartic acid)

### 1.2.3 Ethylene

The gas ethylene (C<sub>2</sub>H<sub>4</sub>) has long been known to be involved in several aspects of plant development such as fruit ripening, leaf senescence, abscission and germination (Reid, 1995). In addition, it is also involved in a number of stress responses such as flooding, wounding and pathogen attack (Davies, 1995). Ethylene also mediates the seedling triple response where treatment with ethylene in the dark leads to inhibited elongation of the hypocotyl and root, an increase in hypocotyl girth and failure of the apical hook to open (Reid and Howell, 1995). Various ethylene-insensitive mutants have been isolated by their failure to show the triple response under these conditions.

#### 1.2.3.1 Ethylene biosynthesis and transport

Ethylene can be synthesised by most cell types and is produced from a methionine precursor that is converted to S-adenosyl-methionine by the enzyme methionine adenosyl transferase. S-adenosyl-methionine is then converted to 1-aminocyclopropane-1-carboxylic acid (ACC) by the *ACC SYNTHASE (ACS)* gene products, a multienzyme family which consists of five members (Liang *et al.*, 1995). ACC can then be converted into ethylene by the enzyme ACC oxidase (McKeon *et al.*, 1995).

Ethylene moves by diffusion from the site of synthesis to local sites of action. However, the ethylene precursor ACC has also been shown to be transported, which may account for ethylene responses at positions removed from the ethylene production stimulus (Reid, 1995). As treatment of plants with ethylene directly can be technically difficult, addition of ACC to plant growth medium is often used to examine the effect of ethylene upregulation.

#### 1.2.3.2 Ethylene perception

As in the case of cytokinin, ethylene is perceived by membrane bound histidine kinases receptors that elicit a response via a phosphorelay cascade. Binding of ethylene to the receptor changes its conformation and causes inactivation that leads to the ethylene response (Hua and Meyerowitz, 1998).

The first *Arabidopsis* ethylene-response mutant to be identified was *ethylene resistant 1-1 (etr1)* (Bleeker *et al.*, 1988). Cloning of the *ETR1* gene revealed

that it encodes a protein that has similarity to bacterial receptor histidine kinases (Chang *et al.*, 1993) and it has been demonstrated that the ETR1 protein binds ethylene reversibly (Schaller and Bleeker, 1995). Subsequently, another four related genes, *ERS1*, *ERS2*, *ETR2* and *EIN4*, have been discovered in *Arabidopsis*, and ethylene perception is thought to involve all five receptors.

Downstream of ETR1 and the other receptors, the response is mediated by CONSTITUTIVE TRIPLE RESPONSE1 (CTR1). The *ctr1* mutant shows the triple response in the absence of ethylene i.e. it has the phenotype of an ethylene overproducer, indicating that *CTR1* is a negative regulator of downstream responses. Cloning of the *CTR1* gene revealed that it encodes a member of the Raf family protein kinases (Kieber *et al.*, 1993) which are involved in signal transduction via a phosphorylation cascade. The CTR1 protein has also been shown to interact directly with ETR1 and ERS1 (Clark *et al.*, 1998).

It is currently proposed that the receptors are negative regulators of the ethylene signalling pathway (Chang and Stadler, 2001). Therefore, when ethylene is bound to the receptor, the receptor is inactive. If the receptor is inactive, it cannot phosphorylate the negative regulator CTR1 and activate it, which allows ethylene responses to occur. When ethylene dissociates from the receptor, it is activated and can activate CTR1, which then represses ethylene responses.

Downstream of CTR1 and presumably linked by a MAP kinase cascade, is ETHYLENE INSENSITIVE2 (EIN2). The *ein2* mutant shows ethylene insensitivity (Guzman and Ecker, 1990). The EIN2 protein has membrane-spanning domains, may be localised in the nuclear membrane and is an ethylene-response activator (Alonso *et al.*, 1999).

Two types of ethylene-responsive transcriptional activators have been discovered: the ETHYLENE INSENSITIVE3 (EIN3) and EIN3-LIKE (EIL) proteins and the ETHYLENE RESPONSE ELEMENT-BINDING PROTEINS (EREBPs). Several members of the EIN3/EIL family have been shown to bind to the promoter of the EREBP gene *ETHYLENE RESPONSE FACTOR1* (*ERF1*)

and activate its transcription (Solano *et al.*, 1998). ERF1 is thought to be a transcriptional activator as overexpression leads to activation of many ethylene responses (Stepanova and Ecker, 2000). Figure 1.2.3.2a shows a scheme of the ethylene signalling pathway.

#### **1.2.4 Gibberellin**

The gibberellins (GAs) are responsible for a variety of processes in the plant including stem elongation, leaf expansion, trichome, fruit and flower development and the promotion of germination (Davies, 1995).

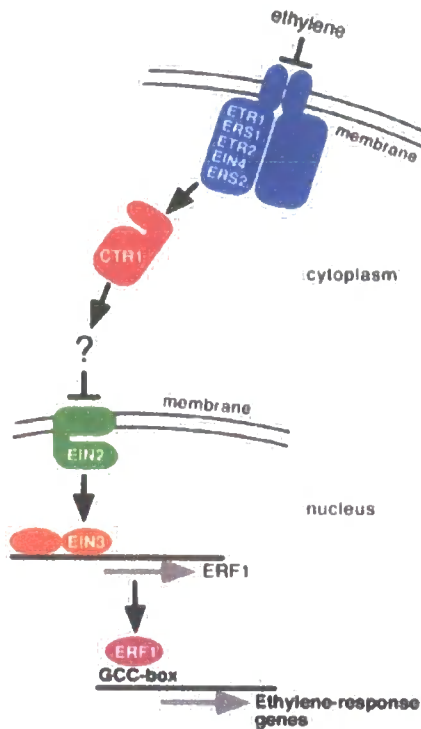
##### **1.2.4.1 Gibberellin biosynthesis and transport**

GAs are tetracyclic diterpenoid acids with either 19 or 20 carbon atoms in the ring structure (Sponsel, 1995). Many structural modifications can be made to the ring structure and hence there are a large number of naturally occurring GAs. Naturally occurring GAs which have been characterised are allocated a number, giving the GA<sub>n</sub> nomenclature. GAs may be inactivated (reversible or irreversibly) by conjugation to another molecule such as glucose. GA responses are mediated by alterations in GA concentration and/or the sensitivity of the plant to GA (Davies, 1995).

Not all of the GAs which have been isolated have high biological activity (Sponsel, 1995). One of the most important bioactive GAs in many plant species is GA<sub>1</sub>, and many of the other GAs are precursors to, or deactivation products of, GA<sub>1</sub>. In *Arabidopsis* it appears that GA<sub>1</sub> and GA<sub>4</sub> are the most bioactive forms.

GAs are synthesised in rapidly growing tissues such as shoot apices and root tips, developing anthers and seeds, expanding leaves and elongating stems. Recently, most of genes encoding enzymes involved in GA biosynthesis have been cloned and characterised (for review see Olszewski *et al.*, 2003). Synthesis of the basic ring structure occurs in the proplastids before it is modified in the ER and then in the cytoplasm. It is in the cytoplasm that the precursors GA<sub>20</sub> and GA<sub>9</sub> are synthesised by the GA<sub>20</sub>-oxidases before they are converted by the GA<sub>3</sub>-oxidases to bioactive GA<sub>1</sub> and GA<sub>4</sub> respectively. In *Arabidopsis*, the GA<sub>20</sub>-oxidases and the GA<sub>3</sub>-oxidases are encoded by small

**Figure 1.2.3.2a** The proposed ethylene signalling pathway in *Arabidopsis*



From Chang and Stadler, 2001

When the ethylene receptors binds ethylene they are switched off and no longer activate the negative regulator CTR1. This allows EIN2 to activate transcription of ethylene responsive target genes via EIN3 and ERF1.

Conversely, when ethylene dissociates from the receptors, they are activated and can activate CTR1 which then represses ethylene responses.

gene families that consist of several members with tissue specific expression patterns.

In general, it appears that GA biosynthesis is controlled by feedback mechanisms. Many of the *GA20ox* and *GA3ox* genes, whose products catalyze the formation of bioactive GA<sub>1</sub> and GA<sub>4</sub>, are downregulated by applied GA (reviewed by Hedden and Phillips, 2000; Yamaguchi and Kamiya, 2000). In contrast, the genes encoding 2-oxidases, that convert active GAs to inactive catabolites, are upregulated by GA treatment (Thomas *et al.*, 1999; Elliott *et al.*, 2001).

GA biosynthesis is developmentally regulated as well as being influenced by interactions with other hormones and by light. In *Arabidopsis* seed, the primary role of GA appears to be in breakage of the seed coat. Mechanical damage of the seed coat of *ga1-3* mutants, which have a mutation in a GA biosynthetic gene, allows the seeds to germinate (Silverstone *et al.*, 1997; Telfer *et al.*, 1997), indicating that it is a failure of seed coat breakage that normally prevents germination in these mutants. This is supported by *in situ* hybridization that revealed the presence of GA biosynthetic enzyme transcripts in the embryo (Yamaguchi, *et al.*, 2001).

Interactions with hormones including auxin have also been demonstrated. In pea and tobacco, GA<sub>1</sub> content in the stem is reduced by the removal of apical tissues or by the application of auxin transport inhibitors (Ross, 1998; Wolbang and Ross, 2001) and is accompanied by a decrease in GA biosynthetic enzyme transcripts (Ross *et al.*, 2000).

It is also now apparent that red light promotes seed germination by increasing GA biosynthesis (For review see Kamiya and García-Martínez, 1999; Yamaguchi and Kamiya, 2000) and by affecting tissue responsiveness to GA (Hilhorst and Karssen, 1988).

It is thought that GAs are probably transported in the xylem and phloem and that short range cell to cell transport also occurs in specific tissues (Olszewski *et al.*, 2003).

#### 1.2.4.2 Gibberellin perception

Gibberellin responses are mediated both by changes in the amount of bioactive GA which is present, and also by the responsiveness of the tissue to the available GA. Information on the pathways by which GA is perceived and elicits a response has been gathered by the analysis of mutants, some of which are described below.

Several MYB transcription factors have been implicated in GA responses. The expression of *AtMYB33* is induced in the shoot apex by GA. The *AtMYB33* protein then binds to a GA responsive element in the *LEAFY* promoter to promote gene expression and the induction of flowering (Gocal *et al.*, 2001). In addition, the trichomeless phenotype of the *glabra1* mutant can be rescued by the application of GA (Chien and Sussex, 1996; Telfer *et al.*, 1997; Perazza *et al.*, 1998). In addition, it has been shown that the *ga1* mutant has decreased levels of *GLABRA1* (*GL1*) mRNA, and that the *GL1* promoter is induced by GA, indicating that GA is required for production of *GL1* transcript and subsequent trichome development in *Arabidopsis*.

*Arabidopsis* loss-of-function *pkl* mutants are GA-insensitive dwarfs that have increased amounts of GAs. Embryonic characteristics such as accumulation of lipids and the expression of storage protein genes in the swollen tip of the primary root persist in *pkl* after germination (Ogas *et al.*, 1997). These embryonic phenotypes are not fully penetrant, and treatment with GA biosynthesis inhibitors increases the penetrance of the phenotypes, whereas treatment with GA reduces the penetrance. Cloning of the *PICKLE* (*PKL*) gene revealed that it is a CH3 chromatin-remodeling factor (Ogas *et al.*, 1999). These proteins are part of a large complex that inhibits transcription, and therefore it has been proposed that *pkl* phenotypes may be caused by ectopic gene expression. The *PKL* gene has also been implicated in *Arabidopsis* *KNOX* gene pathways (section 1.4.2.5.).

Many of the mutations that modify GA sensitivity affect genes encoding members of the RGA/GAI family, such as the *rga* and *gai* mutations in *Arabidopsis* (Peng *et al.*, 1997; Silverstone *et al.*, 1998). *RGA* was identified in a screen for mutations suppressing the vegetative dwarfism of the GA-deficient

*ga1* mutant (Silverstone *et al.*, 1997). Loss-of-function *rga* alleles partially suppress most of the phenotypes of *ga1* plants, including delayed abaxial trichome initiation, dwarfed rosette leaves, delayed flowering, dwarfism of the internodes of the floral shoot, and reduced apical dominance. In contrast, the *gai-t6* loss-of-function allele suppresses *ga1* only weakly. However, double mutants between *rga* and *gai-t6* rescue the vegetative and delayed flowering phenotypes of *ga1* completely and may even produce GA overexpression (Dill and Sun, 2001; King *et al.*, 2001).

It is believed that active GA signaling inhibits the repressor action of the GAI/RGA proteins by destabilizing them (Silverstone *et al.*, 2001). The molecular mechanism by which GA affects the stability of the RGA/GAI proteins is not clear, but ubiquitin-mediated proteolysis has been proposed to be involved (Dill *et al.*, 2001; Itoh *et al.*, 2002).

*SPINDLY* (*SPY*) is another negative regulator of GA signaling that was identified during a screen for mutants where both germination and the dwarfing effects of the GA biosynthesis inhibitor paclobutrazol were inhibited (Jacobsen and Olszewski, 1993; Jacobsen *et al.*, 1996). *spy* mutants have a phenotype similar to that seen when plants are treated with GA, such as more erect rosette leaves with a pale green color, early flowering, and reduced seed set. Overexpression of *SPY* produces phenotypes consistent with reduced GA activity (Swain *et al.*, 2001). The *SPY* gene encodes a protein that has homology to UDP-GlcNAc transferase (OGT) from animal systems, and it has been shown to have OGT activity (Thornton *et al.*, 1999). Animal OGT transfers GlcNAc to serine and threonine residues and thereby modulates their activity. The proteins that are the target of *SPY* have not been identified but the RGA/GAI proteins have been proposed as possible targets (Silverstone *et al.*, 1998). Like *PKL*, the *SPY* gene has also been implicated in *Arabidopsis KNOX* gene pathways (section 1.4.2.5.).

Although the GA receptor has not yet been identified, it has been established that it is located in the plasmamembrane of aleurone cells of cereal species (Gilroy and Jones, 1994; Hooley, *et al.*, 1991). The role of heterotrimeric G proteins in the GA response in cereal aleurone cells has also been suggested.

Aleurone cells from the rice dwarf mutant *d1*, which is defective in the  $\alpha$  subunit of a heterotrimeric G protein (Ashikari *et al.*, 1999; Fujisawa *et al.*, 1999), have reduced sensitivity to GA compared with the wild type (Ueguchi-Tanaka *et al.*, 2000). However, it should be noted that in *Arabidopsis*, loss-of-function mutations affecting G $\alpha$  proteins do not cause the dwarf phenotype that is typical of mutants with defective GA responses although they do affect other signaling pathways (Ullah *et al.*, 2001; Wang *et al.*, 2001). Therefore, the relative importance of the G protein in GA responses may vary between species.

### **1.2.5 Summary**

This section describes the basics of the biosynthesis, transport and perception of four major plant hormones. The pathways by which these hormones elicit a response from the plant cell are gradually being dissected, and molecular genetics have played an important role in this.

### **1.3 Development in *Arabidopsis thaliana***

The development of plants and animals is fundamentally different in that animal embryos resemble a miniature version of the adult whereas most of the organs of the mature plant develop post-embryonically. This process is dependent on the activity of the meristems. These tissues represent pools of undifferentiated cells that divide to provide new cells for the growth and differentiation of organs.

The development of the shoot meristem during plant embryogenesis is crucial as it provides a reservoir of undifferentiated cells from which the aerial parts of the plant subsequently arise.

The root apical meristem is also formed during embryogenesis and provides cells that contribute to the length of the root during the lifetime of the plant. The lateral organs of the root system (namely the lateral roots) are not produced by the root apical meristem but are formed from pericycle cells. Hence, the function of the root and shoot meristems differs in the provision of cells for lateral organs.

The following sections describe some aspects of *Arabidopsis* development that are of particular relevance to this work.

### **1.3.1 Embryogenesis, an overview**

The development of the *Arabidopsis* embryo involves the generation of shape (morphogenesis), the spatial organisation of cells (pattern formation) and the generation of cellular diversity (cytodifferentiation) (Lindsey *et al.*, 1996).

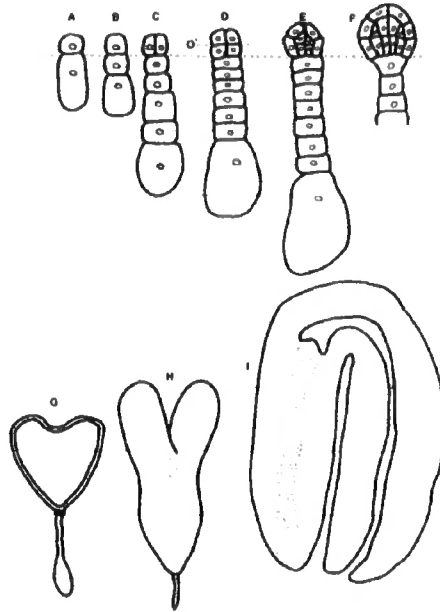
Fertilisation of the egg cell by a sperm cell forms a zygote that undergoes highly regulated cell divisions to form the embryo (Jürgens *et al.*, 1991, Scheres *et al.*, 1994). The initial zygotic division is asymmetric and results in a smaller apical cell which will form the embryo proper and a larger basal cell which forms the suspensor, which supplies nutrients to the embryo; and the hypophysis, which forms the quiescent centre of the root meristem and the columella root cap. This two-cell embryo then undergoes further, highly regulated cell divisions. At the octant stage, the cells of the embryo proper are organised into two cell layers separated by the O' boundary. The upper tier is destined to become the cotyledons and the shoot apex while the bottom tier will become the hypocotyl and embryonic root. Cotyledons develop as the embryo enters the heart stage before it grows and differentiates through the torpedo and curled cotyledon stages until it reaches maturity. By the heart stage, the epidermis, the ground tissue (endodermis and cortex) and the vascular tissue have been established, albeit in an undifferentiated form, and the cotyledons are evident. Figure 1.3.1a shows a summary of this developmental process.

Aspects of pattern formation include the apical-basal polarity which is established by the first symmetric division of the zygote, radial patterning which is evident by the heart stage when layers of different tissues in the stem, hypocotyl and root can be identified, and bilateral symmetry established at the heart stage by the formation of cotyledons. Therefore, the plant has laid down its basic body plan, consisting of apical meristems, ground tissues and vasculature, and subsequent development simply alters the size and shape of these zones (Lindsey and Topping, 1998).

### **1.3.2 Embryogenesis defective mutants**

There is an increasing amount of evidence that apical-basal pattern formation is regulated independently of correct cell morphogenesis and division. The *tangled-1* mutation of maize is defective in the planes of cell division in the leaf

**Figure 1.3.1a Embryogenesis in *Arabidopsis***



From Lindsey and Topping, 1993

A: first asymmetric division of the zygote

B-C: proembryonic stages

D: octant stage with the O' boundary marked

E-F: globular stage

G: heart stage

H: torpedo stage

I: cotyledonary stage

but the shape of the leaf is unaffected (Smith *et al.*, 1996) and the *Arabidopsis hydra* and *fass* mutants show pleiotropic defects in cellular organisation but still display correct apical-basal polarity (Topping *et al.*, 1997, Torres-Ruiz and Jürgens, 1994).

In the *fass* mutant, there is a failure of pre-prophase band formation and a corresponding defect in the control of cell shape from early in embryogenesis (Torres-Ruiz and Jürgens, 1994). Therefore, morphogenesis is defective, but cell differentiation and apical-basal patterning still occurs. *fass* seedlings are compressed in the apical-basal axis, and are also radially swollen, especially in the hypocotyl. The *fass* mutant is characterised by an increase in cell layers in the root, which leads to an enlarged vascular cylinder and multiple cortical cell layers (Scheres *et al.*, 1995). The *fass* mutation affects cell elongation and orientation of the cell wall, but does not interfere with polarity of the cells (i.e. they still have apical-basal polarity).

The *fass* mutant is allelic to *tonneau2 (ton2)* (Mayer *et al.*, 1991, Camilleri *et al.*, 2002). Cloning of *fass* has revealed that it has similarity to a protein phosphatase 2A regulatory subunit (Camilleri *et al.*, 2002) and is required for control of the cytoskeleton.

The *hydra1* mutant was isolated in a screen for seedling defective mutants (Topping *et al.*, 1997) and is defective in the control of cell shape in embryos and seedlings. *hydra1* mutants are normal up to the octant stage of development but by the globular stage, there is a lack of organised cellular arrangement in the upper and lower tiers. This is exaggerated in the heart stage, and there appears to be no clearly defined vasculature or embryonic root. Torpedo and early cotyledonary stage embryos lack bilateral symmetry and the embryonic shoot apex has many primordia which give rise to cotyledon-like structures.

Three markers have been used to assess the cellular organisation of *hydra1* (Topping and Lindsey, 1997). *COLUMELLA* marks the seedling root cap, *EXORDIUM* is expressed constitutively from the octant stage onwards and then in the seedling shoot and root meristems and *POLARIS* marks the basal part of

the embryo from the heart stage, and the seedling root tip. Crosses between *hydra1* and these markers show that *EXORDIUM* and *POLARIS* are expressed in *hydra1* embryos and seedling in essentially the same patterns as in wild type, and that *COLUMELLA* is expressed in the least abnormal of the *hydra1* roots. This indicates that, although *hydra1* shows defective morphogenesis, some shoot and root meristem genes are active. This, along with the expression of *COLUMELLA*, show that apical-basal patterning still occurs in *hydra1* despite a lack of bilateral symmetry and radial patterning.

The *hydra2* mutant of *Arabidopsis* has a similar phenotype to *hydra1*. Both genes have been cloned and sequenced and have been shown to encode a  $\Delta 8$ - $\Delta 7$  sterol isomerase (*HYDRA1*) and a sterol C14 reductase (*HYDRA2*) (Souter *et al.*, 2002). It is proposed that correct sterol biosynthesis is required for regulated auxin and ethylene signalling through effects on membrane function.

The *mp* mutation is evident from the globular stage of embryogenesis when the lower tier fails to undergo orientated expansions and divisions which allow the production of the hypocotyl and root (Berleth and Jürgens, 1993) This leads to a deletion in the basal parts of the embryo such as the hypocotyl and root meristem. The *bd1* mutation is also evident from early embryogenesis, when the apical daughter cell of the zygote divides horizontally rather than vertically (Hamann *et al.*, 1999). This leads to abnormal divisions in the basal daughter cell and a failure to generate the quiescent centre of the root meristem and the central root cap. These two mutants will be discussed further in section 1.3.3 below.

### **1.3.3 Vascular development defective mutants**

The transport of auxin from the shoot to the root has been implicated in controlling differentiation along the axis of the plant (Nelson, 1998), and in controlling the development of lateral organs along this axis.

Apical-basal transport of auxin is required during embryogenesis where it functions in establishment of bilateral symmetry. Treatment of *Brassica juncea* embryos with auxin transport inhibitors causes defects in the establishment of lateral organs such as cotyledons. This phenotype is similar to that seen in

*Arabidopsis pin* and *gnom* embryos where auxin transport is impaired (Liu *et al.*, 1993).

Auxins have been implicated as pathfinding signals in vascular strand development. This has been demonstrated by observing that auxin application leads to the development of a vascular strand basal to the point of application (Berleth and Mattsson, 2000). This process is dependent on auxin transport, and it may be that flow of auxin may set up coarse patterns that are further refined by induction of specific genes that fine-tune the developmental response.

Treatment of *Arabidopsis* with auxin transport inhibitors such as NPA and TIBA leads to an increase in the number of vascular strands that are produced, although these strands are not properly aligned (Mattsson *et al.*, 1999). Analysis of the *pin1* mutation indicates that it has a vascular phenotype that is similar to that of wild type plants that have been treated with an auxin transport inhibitor (Galweiler *et al.*, 1998). Therefore, as defective auxin transport leads to an increase in the number of vascular strands, it appears that the auxin signal is required to limit the development of vascular strands to a narrow strand, as well as for vascular tissue continuity.

The *mp* mutant (introduced in sections 1.2.1.3 and 1.3.2) was isolated as an embryo pattern mutant that lacks basal structures in the embryo axis such as the hypocotyl and root meristem (Berleth and Jürgens, 1993).

Occasionally, *mp* plants can be induced to form roots and this has allowed the study of postembryonic development. In *mp* seedlings, one or two cotyledons that show reduced vasculature are present. The vascular system of *mp* mutant plants does not develop properly as the vascular cells do not align and interconnect properly (Przemeck *et al.*, 1996).

Cloning of the *MP* gene has revealed that it is a member of the ARF transcription factor family (Hardtke and Berleth, 1998) that is involved in auxin response pathways. *MP* mRNA is detected in all subepidermal cells in globular stage embryos and is gradually restricted to provascular domains in later embryos. A similar pattern of broad expression that becomes restricted to

vascular tissues was seen in developing aerial parts. In the mature root, the *MP* transcript is detected in the stele. This localisation of expression to the developing vasculature is consistent with a role in vascular development. As both xylem and phloem cells are present in *mp* mutants, *MP* appears to mediate integration of vascular cell files rather than to promote particular events during vascular differentiation. The reduced auxin transport in *mp* has been proposed to be a result of distorted cellular continuity in the vascular strands combined with a reduction in vasculature, rather than a decrease in the capacity of individual cells for auxin transport (Mattsson *et al.*, 1999).

As mentioned in section 1.2.1.3, the *bdl* mutant phenotype is caused by a disruption in the *AUX/IAA* gene *IAA12* (Hamann *et al.*, 2003). The *bdl* mutant has a similar phenotype to *mp* with a deletion of the basal organs of the seedling such as the root and the hypocotyl, and decreased vasculature in the cotyledons (Hamann *et al.*, 1999). Although *bdl* seedlings do not have a primary root, they readily form secondary roots and give rise to fertile, adult plants. They also have reduced vasculature in the same way as *mp* mutant plants. The *bdl* mutation is semi-dominant.

It has recently been demonstrated that the BDL protein can interact directly with the MP protein in a yeast two-hybrid system (Hamann *et al.*, 2003), and that *BDL* mRNA is coexpressed with *MP* mRNA during embryogenesis, with expression becoming restricted to the vascular precursor cells. Although the *bdl* mutation resembles the *mp* mutation, *MP* is expressed in *bdl* embryos, indicating that transcription of *MP* is not abolished.

As an increase in the stability of the BDL protein in the *bdl* mutant has a similar phenotype to loss of function of the MP protein in the *mp* mutant, these results indicate that BDL is required to repress the activity of MP, and that MP is an activator of auxin responsive genes.

Serial radial sectioning of wild type *Arabidopsis* roots has revealed that xylem lineages are specified early (i.e. close to the QC) whereas phloem and procambium are specified by initial cells that flank the xylem pole (Mähönen *et al.*, 2000).

The structure of the wild type xylem pole consists of two outer protoxylem poles that have a ring-like pattern of lignification, with a central metaxylem pole which has more uniform lignification.

The *woodenleg* (*wol*) mutation was first identified as a radial pattern mutant that has fewer cells in the vascular system in comparison with the wild type, and where all of these cells differentiate to form xylem elements (Scheres *et al.*, 1995). Cloning of the *WOL* gene (Mähönen *et al.*, 2000) revealed that it is allelic to the cytokinin receptor *CRE1* (see section 1.2.2.2).

The *wol* mutant has fewer cells in the vascular initials as the final divisions that complete the stele initials during embryogenesis do not occur. This reduction in the number of stele initial cells in *wol* seedlings means that the divisions which normally occur next to the xylem poles and produce cells destined to become phloem and procambium do not occur. All of the available stele cells differentiate into xylem (Mähönen *et al.*, 2000).

In addition, the *wol* vascular system consists entirely of protoxylem with no metaxylem (Mähönen *et al.*, 2000). It is the decrease in cell numbers in the *wol* vasculature that affects phloem and metaxylem differentiation, rather than a requirement for the *WOL* gene product. This has been indicated by the presence of phloem and metaxylem in *fass/wol* double mutants, where *fass* supernumerary cell layers function to replace cells that are missing in *wol*. It therefore appears that *WOL* is required to control the number of cells in the stele, which has an indirect effect on xylem and phloem differentiation. As the *WOL* gene product has been shown to be a cytokinin receptor (Inoue *et al.*, 2001), this indicates a requirement for cytokinin in regulating vascular bundle development during embryogenesis.

The *gollum* (*glm*) mutant was isolated in the same screen as *wol* (Scheres *et al.*, 1995) and is also defective in radial patterning. The root of the *glm* mutant is characterised by disorganised vascular tissues and an incomplete pericycle layer. The *glm* mutant phenotype is visible in mature embryos where the stele cells appear disorganised.

### **1.3.4 Post-embryonic development of the root**

As described in the sections below, the basic pattern of the main root is established during embryogenesis by precise cell divisions. Post-embryonically, the main root continues to grow as cells are generated by the root apical meristem. In addition, root architecture is also elaborated by the development of lateral roots.

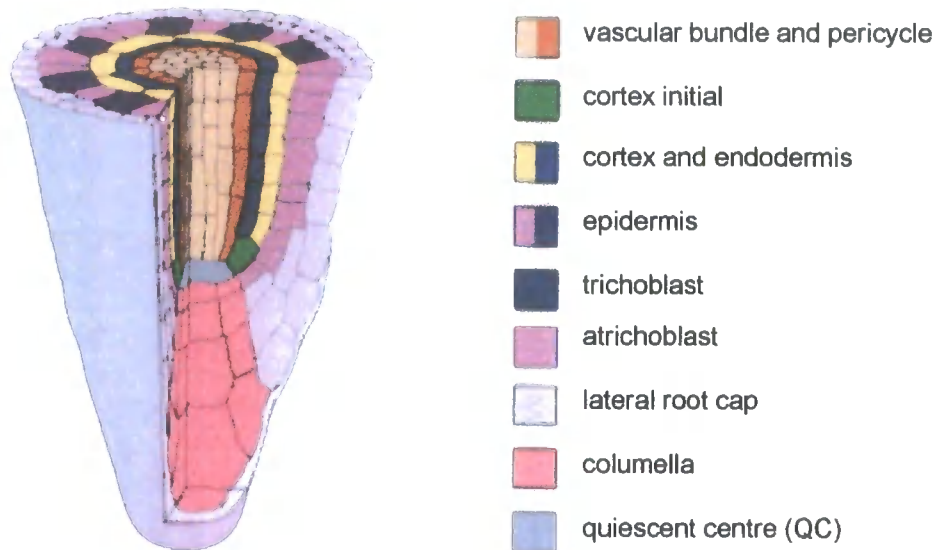
#### **1.3.4.1 Organisation of the *Arabidopsis* root**

The root meristem functions to provide new cells with are added to pre-existing cell files that extend back into the main root. The root meristem is contained within the distal 250  $\mu\text{m}$  of the root, and is characterised by small cells that are overlaid by the root cap. Proximal to this zone is the elongation zone, which also spans approximately 250  $\mu\text{m}$ . The next zone is the differentiation zone, where elongated cells in different files mature into different cell types. Epidermal cells that are beginning to produce root hairs mark the end of this zone (Dolan *et al.*, 1993).

The organisation of the root tip is shown in Figure 1.3.4.1a. In the centre of the root meristem are the cells of the quiescent centre (QC). On the distal side (i.e. towards the root apex) of the QC lie initial cells for the columella and lateral root caps as well as the epidermis. The lateral root cap and the epidermis appear to originate from the same initials. The tier of cells on the proximal (shoot) side of the QC consists of the initials for the vascular tissues (xylem and phloem, also referred to as the stele) and the pericycle. Positioned radially around the QC are the initials that provide cells to the endodermal and cortical layers (collectively known as the ground tissues). The initial cells for each file divide less frequently than their daughter cells, which divide rapidly to produce new root cells, with the exception of the columella daughter cells that appear to endoreduplicate rather than divide (Dolan *et al.*, 1993).

Examination of transverse sections of the mature *Arabidopsis* root reveal that these different cell layers are arranged in concentric layers with the stele in the centre of the root followed by single layers of pericycle, endodermal, cortical and finally epidermal cells (Figure 1.3.4.1a). The number of cells in the cortex and endodermis is invariant, with eight cells in each of these layers.

**Figure 1.3.4.1a** Organisation of the *Arabidopsis* root and root apical meristem



From the Root Development Group, University of Utrecht  
[www.bio.uu.nl/~mcbroots/anatmap.htm](http://www.bio.uu.nl/~mcbroots/anatmap.htm)

The *Arabidopsis* root is organised into concentric circles of different cell types, with a single layer of each cell type.

Only the cortex initial cells are marked on this map, but there are initial cells for the columella, the lateral root cap and the epidermal cells below the QC, as well as pericycle and vascular cell initials above the QC.

The vascular bundle consists of xylem and phloem and is also referred to as the stele.

The importance of position effects can be seen in several cell types in the root. For example, epidermal cells can either form trichoblasts (which develop a root hair) or atrichoblasts (which do not develop a root hair). The trichoblasts are found only in cell files that are touching more than one underlying cortical cell (Figure 1.3.4.1a). Similarly, only pericycle cells that are adjacent to an underlying xylem pole can initiate divisions in the mature pericycle to form a lateral root. Those pericycle cells that are adjacent to a phloem pole are not activated to form lateral roots (see section 1.3.4.2 and 1.3.4.3).

It has been demonstrated that it is position effect, rather than cell lineage, which determines cell fate. Laser ablation of specific cells in the root caused division of a neighbouring cell from a different cell layer, with the position of the dead cell being filled by one of the daughter cells (van den Berg *et al.*, 1995). For example, the ablation of cortical/endodermal initials caused the asymmetric division of neighbouring pericycle cells to produce new cortical and endodermal initials, and ablation of epidermal/lateral root cap initials caused cortical cells to divide and then acquire the identity of these initials.

It is thought that one role of the QC is to prevent the adjacent initial cells from differentiating and therefore maintain their undifferentiated state. A series of laser ablation studies on the QC and initial cells revealed that removal of a QC cell allowed the differentiation of the adjacent initial cell (van den Berg *et al.*, 1997).

#### **1.3.4.2 Development of lateral roots**

As described in section 1.3.4.1, the apical meristem of the main root contributes cells to the primary root to allow growth during the life of the plant. In addition, root architecture is elaborated by the initiation and growth of lateral roots in an acropetal sequence along the root. As mentioned in section 1.3, there is a fundamental difference in the elaboration of the architecture of the aerial parts of the plant compared to that of the root system. In the aerial part of the plant, lateral organs such as leaves originate from the shoot apical meristem. However, in the root system, lateral organs in the form of lateral roots arise from the pericycle cells of the primary root.

Lateral root primordia are initiated by divisions in pericycle cells that are in contact with the underlying protoxylem cells of the xylem pole (Dubrovsky *et al.*, 2001). Those pericycle cells that are adjacent to the phloem poles do not divide. Initiation of lateral roots occurs behind the root tip in the zone of differentiation, where the pericycle cells are not actively dividing (Malamy and Benfey, 1997).

The overall tissue patterning in the lateral roots is similar to that in the main root, with single layers of epidermis, cortex, endodermis and pericycle surrounding the stele, although radial organisation is less stereotyped. This is thought to be due to variation in the number of founder pericycle cells that are recruited in the pericycle to form the new lateral (Dolan *et al.*, 1993).

Pericycle cells in files that are adjacent to phloem poles or xylem poles are anatomically different, with those adjacent to a phloem pole being approximately twice the length of those adjacent to a xylem pole (Laskowski *et al.*, 1995).

It is thought that pericycle cells do not leave the cell cycle like other differentiated cell types (Beeckman *et al.*, 2001). In the main root, pericycle cells in files adjacent to xylem poles or phloem poles can be distinguished not only by their length, but also by their cell cycle status. Those that are adjacent to phloem poles reach maturation after fewer cell divisions and remain in the G1 phase. Those that are adjacent to the xylem poles undergo more divisions in the meristem and then progress through the cell cycle to the G2 phase. It may be that xylem pole pericycle cells are more susceptible to lateral root initiation as they have already completed DNA synthesis (S phase) and are arrested immediately prior to the mitotic (M) whereas phloem pole pericycle cells are arrested prior to the S phase.

The formation of a lateral root begins with anticlinal divisions that increase the number of cells in the pericycle file (Laskowski *et al.*, 1995). These cells then divide periclinally to form the lateral root primordia. When the developing lateral root contains approximately eight cell layers, the cells become organised into a pattern that is characteristic of the primary root meristem. Several distinct cell

layers are formed at the root apex and these continue to divide periclinally to form the root cap, in which starch cells can be visualised. Divisions behind this apex also produce long slender cells that are characteristic of procambium.

When the lateral root emerges from the primary root it has 8-10 cell layers. The emergence step occurs primarily by expansion of the cells in the primordia, rather than by further cell divisions. After emergence, cell division starts in the newly formed lateral root meristem, and the number of cells in the lateral root increases (Malamy and Benfey, 1997).

Excision of segments of primary root which contain a lateral root primordia consisting of only two cell layers fail to form a lateral root in culture whereas excision of primordia with at least six cell layers develop into morphologically normal roots (Laskowski *et al.*, 1995). The development of lateral roots from primordia with between three and five cell layers gave variable results, indicating that a functional lateral root meristem may be formed during this period.

The point at which the developing lateral root primordia undergoes a developmental transition which allows it to independently form a lateral root appears to be just before the change in root architecture described above. The presence of a developmental transition is supported by the observation that treatment of roots with auxin causes all of the cells in the pericycle adjacent to the xylem poles to divide, but only a subset form a lateral root meristem (Laskowski *et al.*, 1995).

The exact point at which a functional meristem is formed is difficult to pinpoint. The excision of primordia and their ability to form a meristem does not necessarily mean that a true meristem has been established, but that the primordia is sufficiently developed to direct formation of the meristem (Malamy and Benfey, 1997).

Further evidence to support a model where lateral root development occurs in distinct stages is provided by the *rootmeristemless1* (*rml1*) and *aberrant lateral root formation3-1* mutants (*alf3-1*).

The *rml1* mutant (Cheng *et al.*, 1995) is characterised by normal embryonic development of the primary root followed by failure of the meristem to divide after germination. Lateral roots can be initiated but arrest just after emergence. Therefore, it appears that the lateral root phenotype is due to the lack of a functional lateral root meristem.

A similar situation occurs in the *alf3-1* mutant (Celenza *et al.*, 1995), which forms a primary root that is covered in arrested lateral root primordia, where the primordium cells are dead. The *alf3-1* lateral roots develop in the same way as *ALF3-1* lateral roots but then arrest just after emergence. The mutant primordia appear similar to wild type primordia in their overall shape, but lack cellular differentiation. The *alf3-1* mutant also initiates more lateral root primordia when compared with *ALF3-1* plants, with new primordia initiating adjacent to, or on top of, arrested primordia. In addition, the primary root meristem also arrests by 8 days after germination.

Growth of the *alf3-1* plants with the IAA precursor indole allows newly initiated lateral root primordia to develop into mature lateral roots. As the *alf3-1* mutant can be rescued by growth on indole, it is thought that the role of the *ALF3-1* gene product is maintain auxin levels in the primordium at a level which is required to keep the cells viable. This could either be by *de novo* synthesis of auxin in the primordium, or by auxin transport to the primordium.

The analysis of these two mutants supports the model proposed by Malamy (Malamy and Benfey, 1997), where there are four key stages in lateral root formation:

- (1) stimulation and dedifferentiation of pericycle cells
- (2) ordered cell divisions and cell differentiation to generate an organised lateral root primordia which may include a group of cells which function as a meristem
- (3) emergence by cell expansion
- (4) activation of the lateral root meristem to allow continued growth of the organised lateral root by cell division

#### 1.3.4.3 Control of lateral root development

The application of auxin leads to initiation of lateral roots along the entire length of the primary root (as is also seen in the auxin overproducing mutant *rt<sub>y</sub>*), indicating a role for auxin in lateral root initiation.

The polar auxin transport inhibitor NPA has been shown to block lateral root development (Reed *et al.*, 1998). Application of NPA to the shoot/root junction caused a decrease in the number and density of lateral roots that were produced, and also decreased the free IAA and transport of IAA to the root. Application of NPA in the middle of the root inhibited lateral root formation at positions apical to the application, and this could be rescued by the application of IAA apical to the NPA application. Similarly, growth of plants in the dark, or excision of the shoot also caused inhibition of lateral root development that was reversible by application of IAA. This indicates a requirement for shoot derived auxin in lateral root development.

A closer analysis of the effect of NPA on lateral root development (Casimiro *et al.*, 2001) has indicated that NPA blocks the first anticlinal divisions of the xylem pole pericycle cells.

NPA does not act to respecify the fate of xylem pole pericycle founder cells, as demonstrated by the continued expression of a specific marker for xylem pole pericycle cells in the presence of the inhibitor (Casimiro *et al.*, 2001). In addition, as the inhibitory effects of NPA can be reversed by transfer of plants from medium containing NPA to medium containing NPA and NAA, this indicates that transport inhibitor-treated roots are still competent to respond to auxin. Therefore, it appears the NPA causes endogenous root IAA to be reduced to a level that is suboptimal for lateral root development.

NPA inhibits both basipetal and acropetal auxin transport (Rashotte *et al.*, 2000), and causes IAA to accumulate in the root tip. Studies using marker lines for auxin accumulation (DR5::GUS) and cell division (*cycB1-1::GUS*) indicate that the site of auxin accumulation in the root is spatially distinct from the site of lateral root initiation by pericycle cells (Casimiro *et al.*, 2001). This implies that the zone of lateral root initiation is at a position basal to the root apex.

Between 5 and 7 days after germination (DAG), a transient pulse of auxin travels from the shoot to the root tip, and this is correlated with the emergence of the first lateral roots (Bhalerao *et al.*, 2002). Removal of aerial tissues at 4 DAG leads to a decrease in the number of lateral roots, whereas removal of aerial parts at 7 DAG did not affect the number of lateral roots. The number of lateral roots in 4 day-old excised seedlings could be restored by exogenous application of auxin to the cut surface. This indicates that shoot derived IAA is important for lateral root emergence during the early stages of seedling development. The decrease in dependency on shoot derived auxin for emergence of lateral root primordia between 3 and 10 DAG is due to increased IAA synthesis in the root itself.

The *shootmeristemless (stm)* mutant (Barton and Poethig, 1993) cannot produce aerial tissues, and therefore has reduced auxin transport from the shoot to the root. However, auxin distribution and sensitivity is normal in the root. *stm* mutant plants produce a wild type number of lateral root primordia, although they do not emerge in acropetal sequence, and elongation can be erratic (Casimiro *et al.*, 2001). Therefore, it appears that the lack of coordinated lateral root emergence in *stm* mutants is due to the lack of a pulse of shoot derived auxin between 5 and 7 DAG, supporting the finding that shoot derived IAA is required for lateral root emergence early in seedling development.

Several authors have proposed a two step model for lateral root formation where auxin is required at both stages, first for the initiation of the primordia by promoting initial cell divisions in the pericycle and then for maintenance of cell division to ensure formation of a viable lateral root primordium (Bhalerao *et al.*, 2002, Casimiro *et al.*, 2001, Celenza *et al.*, 1995).

*aux1* mutants have decreased auxin levels at the root tip and blocked basipetal transport, which can be rescued by the addition of NAA, indicating that the decrease in lateral roots in *aux1* is caused by a decrease in auxin levels in the root.

*AUX1* is expressed in lateral root primordia after the first anticlinal division of the xylem pole pericycle cells (Marchant *et al.*, 2002). It is then required to import

IAA into newly developing lateral root primordia to allow their continued development. Consistent with this model, lateral root primordia in *aux1* mutants are delayed at the transition from anticlinal to periclinal divisions (i.e. from initiation to emergence).

It has been proposed that basipetal auxin transport is required for lateral root initiation and acropetal auxin transport is required for emergence. However, it has been noted that mutants that selectively disrupt basipetal auxin transport such as *pin2* do not cause reduction in the number of lateral root primordia. In addition, growth of the *aux1* mutant on NAA does not correct gravitropism and basipetal transport but does restore lateral root primordia development to wild type levels (Marchant *et al.*, 2002). In addition, it has been observed that at 1-3 DAG, seedlings accumulate auxin in their root apex (Bhalerao *et al.*, 2002) and that this coincides with the initiation of lateral root primordia (Casimiro *et al.*, 2001).

It is has been hypothesised that a threshold level of auxin is required in the root apex to allow xylem pole pericycle cells to undergo increased cell division, and that unloading of IAA from the phloem pole by *AUX1* is required for this (Marchant *et al.*, 2002). Suboptimal auxin levels at the root tip may alter the mitotic activity of these cells and influence their ability to divide at later stages. Therefore, *AUX1* functions at both stages in lateral root development by promoting IAA accumulation in the root tip which influences lateral root primordia initiation, and then facilitating lateral root emergence by supplying IAA to the developing primordium.

### **1.3.5 Summary**

This section has provided an overview of the developmental processes that are of particular relevance to this work.

Development of the *Arabidopsis* embryo and root are highly ordered processes that are mediated by highly ordered cell divisions. This leads to the formation of invariant structures that simplifies the analysis of mutants in these systems.

Lateral root formation in *Arabidopsis* involves the activation of specific pericycle cells in the primary root that are competent to divide and form root primordia. These root primordia go on to form fully functional autonomous meristems. An important mediator in this process appears to be the plant hormone auxin, although the exact mechanisms by which this is achieved are currently unknown.

#### **1.4 Homeobox genes and plant development**

The spatial and temporal expression of specific genes during development is essential in the production of a fully functional mature plant. The perception of plant hormones and the regulatory cascades that follow cause changes in gene expression that elicit hormone responses. These changes in gene expression are controlled by transcription factors.

Although there are many groups of transcription factors, only the homeobox family will be discussed here.

##### **1.4.1 Homeobox genes**

The effects of disrupting homeobox genes were first observed when mutations that cause disturbance of body plan in the fruitfly *Drosophila melanogaster* were identified. For example, the *antennapedia* mutation causes legs to develop from the head of the fly in place of antennae, and the *bithorax* mutation causes the partial formation of extra wing pairs. Hence, these mutations cause the transformation of certain body parts into other structures found elsewhere in the fly. Homeotic genes play a central role in the patterning of the body parts of *Drosophila* by specifying differences between body segments along the head to rear axis, i.e. they provide positional information to cells (Alberts *et al.*, 1994).

Homeobox genes have since been found in a huge diversity of animals including earthworms and nematodes, beetles, molluscs, sea urchins, fish, frogs and mammals where they are also involved in body plan organisation and patterning. In addition, homeobox genes have also been discovered in fungi and plants. In plants, the role of the homeobox genes is less clear-cut than in animals and they appear to have roles in other developmental and response processes as well as in patterning of the plant.

The homeodomain proteins that are encoded by homeobox genes are transcription factors that regulate gene expression and control developmental processes. All homeodomain proteins contain a highly conserved homeobox sequence that encodes a DNA binding domain of 60 amino acids. The homeodomain consists of three helices with the best conserved being the third helix at the C terminal end. This third helix sits in the major groove of DNA and, along with the N terminal arm of the protein, regulates transcription of the target gene (Lewin, 1995).

#### **1.4.2 Plant homeobox genes**

Homeobox genes have been isolated using various techniques from a large number of different species including maize, rice, soybean, rape, barley, tomato and *Arabidopsis*. The homeobox genes isolated so far from plants can be divided into seven families based on the sequence of the homeobox itself and of other conserved domains. These families are HD-*KN1*, HD-ZIP I, HD-ZIP II, HD-ZIP III, HD-*GL2*, HD-*BEL* and HD-*PHD*. The HD-*KN1* family have also been referred to as *KNOTTED-1* like homeobox genes (*KNOX*).

##### **1.4.2.1 The *KNOX* family of homeobox genes in *Arabidopsis***

As mentioned above, typical homeobox proteins contain a conserved DNA binding domain of 60 amino acids, which forms three alpha helices. However, there are particular subsets of homeobox genes that show deviations in the number of amino acids that are present. It has been shown that the extra amino acids are either located between helices 1 and 2, or between helices 2 and 3. One group of atypical homeobox genes that has been identified is characterised by the addition of three amino acids between helix 1 and helix 2. This group has been named the TALE superfamily (three amino acid loop extension) (Bertolino *et al.*, 1995). Members of this group include groups from yeast, human and fly systems as well as the HD-*KN1* and HD-*BEL* families from plants

The first plant homeobox gene to be discovered was the maize *KNOX* gene *KNOTTED1* (*KN1*) (Vollbrecht *et al.*, 1991). The *Kn1* locus was first identified as a transposon-tagged gain-of-function mutant that alters leaf development. *Kn1* is normally expressed in the shoot apical meristem but ectopic expression in the leaf veins of mutant plants causes localised zones of extra cell division that

results in outgrowths or knots. It is proposed that the *Kn1* gene product is involved in maintaining the indeterminate structure of the plant meristem and that its down-regulation leads to the formation of determinate lateral organs such as leaves or flowers and it has been shown that loss of function mutations are defective in shoot meristem maintenance (Kerstetter *et al.*, 1997).

The members of the *KNOX* family are related to the maize *Kn1* gene and were isolated in *Arabidopsis* by homology to *Kn1*. The *KNOX* family in *Arabidopsis* consist of the *SHOOTMERISTEMLESS* (*STM*) gene as well as seven *KNAT* genes (*KNOTTED*-like *Arabidopsis*). These genes share various conserved domains, which are also conserved in *KNOX* family members from other species.

Southern analysis in maize reveals that there are twelve sequences with similarity to *Kn1* in maize (Kerstetter *et al.*, 1994), and cDNAs were isolated for these genes. These genes were then divided into two subfamilies, Class 1 and Class 2, based upon the sequence of the homeobox region. Each *KNOX* gene has an intron in a conserved position within the homeobox region, near the N-terminal end of the second helix. In addition, the Class 2 genes share another small intron upstream of the homeobox. Investigation of the expression pattern of these *KNOX* genes showed that the Class 1 genes were expressed in meristematic tissues such as inflorescence primordia and the shoot apical meristem. The Class 2 genes showed greater diversity in their expression pattern, and were not confined to expression in meristem tissues. Therefore there is a functional division between the Class 1 and Class 2 genes as well as divergence in sequence.

*KNOX* genes that have been isolated from other plant species also fall into these two subfamilies.

In *Arabidopsis*, Class 1 genes include the genes *KNAT1*, *KNAT2* and *STM*. *KNAT1* (Lincoln *et al.*, 1994) is expressed in the shoot apical meristem and overexpression of this gene induces lobed leaves with ectopic meristems (Chuck *et al.*, 1996). *KNAT2* (Lincoln *et al.*, 1994) has also been isolated as *ATK1* (Dockx *et al.*, 1995) and is expressed in the shoot apex of seedlings. The

overexpression phenotype of *KNAT2* is similar to that of *KNAT1* (Pautot *et al.*, 2001).

The *shootmeristemless* (*stm*) mutant was first isolated as an ethylmethane sulphonate (EMS) mutant where the initiation of the shoot apical meristem (SAM) is blocked completely (Barton and Poethig, 1993). The *Merihb1* cDNA was isolated from a cauliflower meristem cDNA library using the *Kn1* sequence as a probe. The corresponding clone from *Arabidopsis* was then isolated using this sequence (Granger *et al.*, 1996). It was also demonstrated that the *Merihb1* locus was the same as the *stm* locus (Long *et al.*, 1996). The *STM* transcript is detected in a similar pattern to the *Kn1* transcript, with expression in meristematic tissues such as the vegetative, axillary, inflorescence and floral meristems but not in more determinate tissues such as leaves (Long *et al.*, 1996). It has been proposed that *STM* is the *Arabidopsis* homologue of *Kn1*, based on the analysis of the sequences of *Kn1* and *RS1* from maize, *SBH1* from soybean and *KNAT1*, *KNAT2* and *STM* from *Arabidopsis* (Granger *et al.*, 1996). However, a more detailed phylogenetic analysis of a wider range of sequences did not support this hypothesis (Bharathan *et al.*, 1999). In addition, the overexpression of *STM* does not lead to a phenotype that is the same as that of *Kn1* or *KNAT1* overexpression in *Arabidopsis*. The *STM* overexpression phenotype consists of severely stunted plants with a highly disorganised SAM (Williams, 1998).

*Arabidopsis* Class 2 genes include *KNAT3*, *KNAT4* and *KNAT5*. There are no mutant phenotypes associated with these genes and their functions are unknown as yet. They are all expressed in all tissues examined, albeit at different levels. *KNAT3* and *KNAT4* show reduced expression in etiolated seedlings, which indicates that they are light regulated (Serikawa *et al.*, 1996). Overexpression of *KNAT3* in *Arabidopsis* does not result in a clearly visible phenotype, and plants remain wild type in appearance (Serikawa *et al.*, 1997, Serikawa and Zambryski, 1997).

#### **1.4.2.2 Conserved domains in *KNOX* family genes**

As mentioned above, the key feature of these genes is the homeobox region which functions to bind DNA. This region is located at the extreme 3' of the

coding sequence in the *KNOX* genes. Although the *KNOX* homeobox region is very similar to that found in the *BEL* family of homeobox transcription factors (another TALE superfamily member), the *KNOX* family are distinct from the *BEL* family by the presence of several other well-conserved domains as detailed below.

Immediately upstream of the homeobox lies the ELK domain, named as three conserved amino acids in this region in several family members are E (glutamic acid), L (leucine) and K (lysine). This region has been shown to contain a nuclear localisation signal (Meisel and Lam, 1996). The ELK domain has also been proposed to function in protein-protein interactions as it contains regularly spaced residues which are reminiscent of the leucine zipper motif which is known to be involved such interactions (Kerstetter *et al.*, 1994).

The MEIS class of animal TALE homeobox genes contain a conserved domain that is also found in the *KNOX* family of plant homeobox genes (Bürglin, 1997). This domain, referred to as the MEIS domain in the MEIS family, and the *KNOX* domain in the *KNOX* family, is collectively known as the MEINOX domain, and is located at 5' end of the gene, upstream of the homeobox and the ELK domains. The secondary structure of the MEINOX domain has been proposed to include  $\alpha$ -helical domains which have been proposed to function in protein-protein interactions (Mushegian and Koonin, 1996, Bürglin, 1997).

One further conserved domain that has also been identified is the GSE box. This small domain is found between the *KNOX* domain and the ELK domain and is less highly conserved. The GSE box has been identified in Class 1 genes (Bürglin, 1997) but is not easily identifiable in Class 2 genes by simple alignment. Deletion of the GSE domain causes an increase in the number of plants displaying the most severe phenotype observed in rice plants overexpressing the rice homeobox gene *OSH15* (Nagasaki *et al.*, 2001). The GSE domain is enriched with proline (P), serine (S) and glutamate (E) residues. Sequences that are enriched for these residues as well as threonine (T) are referred to as PEST sequences, and have been implicated as signals for rapid protein degradation (Rogers *et al.*, 1986). Therefore, removal of this sequence from the *OSH15* protein may increase the half-life of the protein and increase

the number of plants displaying the severe overexpression. A further PEST sequence has also been identified at the extreme C-terminal of the *KNOX* proteins, downstream of the homeodomain.

The lack of a mutant phenotype when *KNAT3* is overexpressed has allowed the analysis of domains in the *KNAT1* protein that confer the overexpression phenotype (Serikawa and Zambryski, 1997). As mentioned previously, the overexpression of *KNAT1* leads to a deeply lobed leaf phenotype. In addition, the flowers of *KNAT1* overexpressing plants are deformed and show reduced fertility (Lincoln *et al.*, 1994). Expression of a construct consisting of the N-terminus of *KNAT3* and the C-terminus of *KNAT1* (including the ELK and homeodomains) leads to a leaf phenotype that is less severe than the *KNAT1* overexpression phenotype, and where flower development is normal. This indicates that *KNAT1* specificity is mediated largely by sequences within the homeobox and ELK domains, but that sequences N-terminal to these two domains (which includes the MEINOX domain) are required for complete specificity of the *KNAT1* protein.

In support of this, domain change experiments in tobacco and rice have also indicated that the MEINOX domain is required for mediating specificity of these proteins (Sakamoto *et al.*, 1999, Nagasaki *et al.*, 2001).

The overexpression of three tobacco *KNOX* genes, *NTH15*, *NTH1*, and *NTH23* results in severe, mild and no morphological alterations respectively (Sakamoto *et al.*, 1999). *NTH15* and *NTH1* are Class 1 genes, whereas *NTH23* is a Class 2 gene. Domain exchanges between these three proteins revealed that the severity of the abnormal phenotype is dependent on the synergistic action of both the MEINOX and ELK domains.

Overexpression of the complete *NTH15* protein gave a severe phenotype. Overexpression of *NTH1::NTH15* and *NTH23::NTH15* gave a mild phenotype, indicating that the N-terminus of *NTH15* is important in generation of the overexpression phenotype. Overexpression of *NTH15::NTH1* resulted in a severe phenotype.

Overexpression of the complete NTH1 protein gave a mild phenotype as did overexpression of NTH23::NTH1. Overexpression of the complete NTH23 protein resulted in a wild type phenotype as did overexpression of NTH1::NTH23. Overexpression of NTH15::NTH23 resulted in a mild phenotype. Therefore, these results also support the hypothesis that it is the N-terminal of the NTH15 protein that is required for induction of the overexpression phenotype.

However, the C-terminal is also required for generation of the complete overexpression phenotype as indicated by alterations in phenotypic severity when the C-terminal domains are exchanged. For example, overexpression of the complete NTH15 protein has a more severe phenotype than overexpression of NTH15::NTH1 and overexpression of NTH1::NTH15 has a more severe phenotype than overexpression of the complete NTH1.

Overexpression of the rice class 1 *KNOX* protein OSH15 leads to a multiple shoot phenotype in the majority of transgenic plants (Nagasaki *et al.*, 2001). Overexpression of the OSH15 protein where domains have been deleted, or conserved residues mutated, has allowed further dissection of the roles of the various conserved domains in *KNOX* protein.

The MEINOX domain can be divided into two subdomains, *KNOX1* and *KNOX2* (Nagasaki *et al.*, 2001). Overexpression of proteins where either the *KNOX2* domain or both of these domains have been deleted does not induce the OSH15 overexpression phenotype. Deletion of the *KNOX1* domain alone resulted in a mild phenotypic perturbation of the boundary between the leaf sheath and blade. This suggests that *KNOX1* is important for, and *KNOX2* is essential for, induction of altered leaf morphology. It has been demonstrated that OSH15 can form homodimers with itself as well as heterodimers with other rice *KNOX* genes (Nagasaki *et al.*, 2001). The results presented above correlate with yeast two-hybrid results where the mutant proteins that could not induce a phenotype were also incapable of homodimerisation.

In addition, mutation of highly conserved residues in the homeodomain itself such as the three amino acid loop extension (PYP) between helices 1 and 2

also result in a lack of abnormal phenotype on overexpression of the mutant protein. It has been demonstrated that these proteins cannot bind their target DNA sequence, and they cannot form homodimers (Nagasaki *et al.*, 2001).

Therefore dimerisation of the OSH15 protein as well as its interaction with target DNA sequences appears to play a role in induction of the mutant phenotype in OSH15 overexpressing plants.

In both the experiments from tobacco and rice, analysis of protein levels revealed that these were similar, therefore the phenotypic effects were due to differences in the protein domains rather than the expression level of the different proteins.

The yeast two-hybrid system has also been used to demonstrate that the *Arabidopsis* BEL1 protein can selectively heterodimerise with specific KNAT homeodomain proteins, and that this interaction is mediated by the MEINOX domain of the KNAT proteins (Bellaoui *et al.*, 2001). It may be that the differences in the severity of altered leaf morphology caused by overexpression of these tobacco *KNOX* proteins is mediated by interactions with different accessory proteins, and it is these proteins which determine the phenotypic severity.

Taken together, these results indicate that the function of homeodomain proteins is mediated by a number of conserved domains. The ability of regulatory proteins to form homo- and heterodimeric interactions may help explain why a large number of cell-specific responses can be mediated by a relatively small number of proteins.

#### **1.4.2.3 Control of transcription by *KNOX* proteins**

The data discussed above indicates some of the possible roles of the conserved domains in the *KNOX* family of proteins. The induction of abnormal leaf development appears to be controlled by a number of factors such as DNA binding and homo- and heterodimerisation of *KNOX* and other TALE family proteins.

Expression of the complete OSH15 protein in yeast one-hybrid experiments reveals that this protein interacts with a specific DNA sequence (TGTCAC) to transactivate a LacZ reporter gene. Removal of either the *KNOX1* or the ELK domain result in an increase in transactivational activity of the rice OSH15 protein in yeast one-hybrid assays (Nagasaki *et al.*, 2001), indicating that these domains play a role in suppression of transactivating activity of the protein. Removal of the complete MEINOX domain (i.e. removal of *KNOX1* and *KNOX2* domains) gives a transactivation level similar to that of the complete protein. Therefore, it appears that the OSH15 protein may be able to function both as a transcriptional activator and repressor, depending on its cellular context. This dual function has been reported in animal systems, where a complex between the TALE superfamily member PBX1 and the HOX1 typical homeodomain proteins can be converted from a transcriptional repressor to a transcriptional activator by association with corepressors or coactivators (Saleh *et al.*, 2000).

In support of the role of class 1 *KNOX* genes in transcriptional repression, overexpression of the tobacco *NTH15* gene leads to a decrease in the expression of the gibberellin biosynthesis gene GA 20-oxidase which catalyses the final steps in GA<sub>1</sub> biosynthesis (section 1.2.4.1 and Tanaka-Ueguchi *et al.*, 1998). As expected, there is a corresponding decrease in the amount of bioactive gibberellin GA<sub>1</sub>. The leaf phenotype can be largely rescued by application of GA<sub>1</sub>, which is consistent with the major effect on phenotype being caused by downregulation of the GA 20-oxidase enzyme, rather than an inability to respond to GA.

The expression patterns of these two genes are exclusive, with GA 20-oxidase expression in leaf primordia and cells surrounding the procambium, and *NTH15* expression in the procambium as well as the tunica and corpus of the meristem. Therefore, these expression patterns support the antagonistic functions of these two genes.

Subsequently, it has been shown that the NTH15 protein (Sakamoto *et al.*, 2001) directly suppresses GA 20-oxidase expression in the shoot apical meristem. The inducible glucocorticoid receptor (GR) system was used to examine the effect of *NTH15* gene overexpression in transgenic plants. Induction of *NTH15*

expression by the addition of dexamethazone (DEX) caused a decrease in the expression of GA 20-oxidase mRNA and a corresponding decrease in the level of GA<sub>1</sub>. Inhibition of protein synthesis by cycloheximide (CHX) still allowed a decrease in GA 20-oxidase mRNA, indicating that the NTH15 protein interacts directly with its target gene rather than by initiating production of another regulatory protein. A sequence that binds NTH15 has been identified in a GA 20-oxidase intron sequence.

A set of similar experiments has also been carried out in *Arabidopsis* (Hay *et al.*, 2002). Again, plants carrying an inducible fusion between *Kn1* and a glucocorticoid receptor (35S::KN1-GR) exhibit the lobed leaf phenotype typically of *KNOX* gene overexpression on induction with DEX. Induction with DEX and GA suppresses this phenotype and indicates that *Kn1* misexpression represses GA biosynthesis rather than GA signalling. In addition, misexpression of *KNOX* protein in 35S::KNAT1 and 35S::KN1-GR plants led to a decrease in the amount of *AtGA20ox1* mRNA. The *AtGA20ox1* gene encodes a GA 20-oxidase that is responsible for the final steps in GA biosynthesis. Repression of transcription occurs within 30 minutes of induction of the 35S::KN1-GR plants, indicating that repression of GA synthesis is an early response. These results are therefore in agreement with those presented for tobacco above.

#### **1.4.2.4 Intercellular trafficking of *KNOX* transcripts and protein**

It has been reported that although the expression pattern of *Kn1* mRNA is similar to that of *Kn1* protein i.e. expressed in the shoot apical meristem but not in developing leaves, the *Kn1* protein is detected in all layers of the meristem whereas the *Kn1* mRNA is not (Jackson *et al.*, 1996). This suggests that *Kn1* can move from cell to cell.

A series of experiments where the *Kn1* transcript or the *Kn1* protein were labelled (with the nucleotide-specific probe TOTO-1 or with fluorescein isothiocyanate, FITC, respectively) demonstrated that the *Kn1* transcript and protein is trafficked through plasmodesmata in tobacco leaf mesophyll cells (Lucas *et al.*, 1995). Subsequently, further work has indicated that a *Kn1*::GFP fusion protein can be specifically trafficked between leaf cells as well as between cells in the SAM of *Arabidopsis* (Kim *et al.*, 2002). The trafficked

*Kn1::GFP* fusion also localised to the nucleus, indicating that this trafficking may be functionally significant. The presence of a phenotype similar to that obtained when other *KNOX* genes are overexpressed in *Arabidopsis* also indicated that this fusion was biologically active.

#### **1.4.2.5 *KNOX* genes are required to maintain the shoot apical meristem**

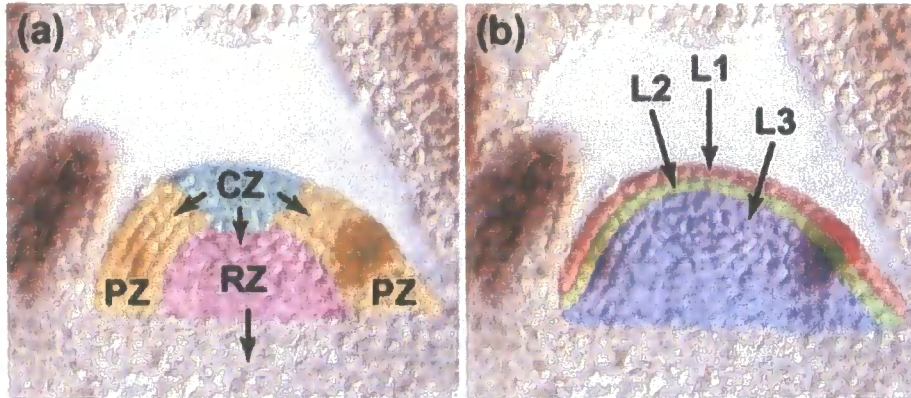
As mentioned in the sections above, *KNOX* class 1 genes appear to play a role in the maintenance of the SAM. This has been demonstrated in *Arabidopsis* by the formation of lobed leaves and ectopic meristems when *KNAT1* and *KNAT2* are misexpressed (Chuck *et al.*, 1996, Pautot *et al.*, 2001) and the failure of shoot apical meristem formation when *STM* activity is abolished (Barton and Poethig, 1993).

As well as expression in the SAM, *KNAT1* and *STM* are also expressed in the stem of the plant. Expression of *STM* in the stem is absent from cells around the vascular strands (Long *et al.*, 1996). *KNAT1* is expressed in cells that are adjacent to the developing vasculature in the stem (Lincoln *et al.*, 1994).

The *brevipedicellus* (*bp*) mutant phenotype has recently been shown to be a disruption in the *KNAT1* gene (Venglat *et al.*, 2002). The pedicels and internodes in *bp* plants are compacted due to the occurrence of fewer cell divisions than in wild type plants, and defects are seen in cortical and epidermal cell elongation and differentiation. The effect of the *bp* mutation is asymmetric, with cell differentiation, elongation and growth being affected more on the abaxial side of the pedicel, leading to downward-pointing flowers. Hence, the *bp* mutant is characterised by compacted inflorescence architecture and downward-pointing flowers.

The *Arabidopsis* SAM consists of three zones (Figure 1.4.2.5a). Cells are recruited from the peripheral zone (PZ) to produce lateral organs and the outer layers of the stem and from the rib zone (RZ) to produce the stem. The central zone acts as a reservoir of stem cells which replenishes the peripheral and rib zones, as well as maintaining its own integrity. The CZ can then be subdivided into several clonally distinct layers. The outermost epidermal layer (L1) and the

**Figure 1.4.2.5a** Organisation of the *Arabidopsis* shoot apical meristem (SAM)



From Bowman and Eshed, 2000

Panel (a) shows the division of the meristem into the central zone (CZ), the peripheral zone (PZ) and the rib zone (RZ).

Panel (b) shows the three layers which make up the SAM. Single layers of cells form the L1 and L2 layers which cover the inner L3 layer.

subepidermal layer (L2) are collectively referred to as the tunica. Cells on the inside of L2 form the corpus (L3) (Bowman and Eshed, 2000).

*STM* and *KNAT1/2* are expressed in different areas of the SAM. *STM* mRNA is detected throughout the meristem in the central, peripheral and rib zones (Long *et al.*, 1996) and is downregulated in the cells that will produce the next leaf (Hake and Ori, 2002). *KNAT1* is expressed in the peripheral and rib zones but not in the central zone (Lincoln *et al.*, 1994). Expression of *KNAT1* is seen in two stripes in the peripheral zone, and appears to mark the boundary between the cells of the meristem, and the cells which will form the next leaves (Hake and Ori, 2002). It has been hypothesised that *STM* is required for formation of the SAM and the maintenance of a pool of stem cells, whereas *KNAT1* is involved in maintaining cells of the meristem in an undifferentiated state. In addition, *KNAT1* appears to play a role in controlling organ initiation as plants overexpressing *KNAT1* show defects in spiral phyllotaxy (Ori *et al.*, 2000).

Based on its similar expression pattern in the shoot apex (Dockx *et al.*, 1995) and overexpression phenotype (Pautot *et al.*, 2001), it appears likely that *KNAT2* plays a similar role to *KNAT1*. There does appear to be some functional redundancy between *KNAT1* and another gene(s) in the vegetative SAM as the *bp* mutation does not lead to any defects in plant development until the transition from the vegetative to the reproductive stage (Venglat *et al.*, 2002), indicating that the vegetative SAM is fully functional. It has also been reported that *KNAT2* knockout plants do not have a phenotype (O. Hamant, personal communication). The production of *knat1/knat2* double mutants may help to define the role of these genes in SAM maintenance.

In addition, *STM* and *KNAT1* are expressed during development of the floral organs (Lincoln *et al.*, 1994, Long *et al.*, 1996). For example, *bp* mutants display defects in cell differentiation and radial growth of the style (Venglat *et al.*, 2002), which is consistent with expression of *KNAT1* in the fourth whorl during flower development in wild type plants (Lincoln *et al.*, 1994). *KNAT2* has also been implicated in carpel development (Pautot *et al.*, 2001).

A number of other proteins that are involved in the same pathways as the *KNOX* genes in the shoot apical meristem have been discovered in the last few years, and these are allowing the role of *KNOX* genes in meristem maintenance to be elucidated.

The *asymmetric leaves1* and *asymmetric leaves2* (*as1* and *as2*) mutants are characterised by rumpled rosette leaves that may also exhibit occasional lobes near the leaf base (Byrne *et al.*, 2000; Ori *et al.*, 2000). The *as1/as2* double mutant phenotype is the same as the *as2* single mutant, indicating that *as2* is epistatic. This indicates that these two genes act in a common pathway. *AS1* encodes a myb transcription factor and is expressed in lateral organ primordia (Byrne *et al.*, 2000). *AS2* encodes a member of a novel protein family which is characterised by cysteine repeats and a leucine zipper (Iwakawa *et al.*, 2002) and is expressed in high levels in the shoot apex as well as in various vegetative tissues such as leaves.

Analysis of *as1/stm* double mutants (Byrne *et al.*, 2000) has revealed that *as1* suppresses the *stm* mutation, and double mutants have an *as1* phenotype. In addition, in *stm* embryos, *AS1* is expressed in a wider domain than in wild type plants. These results indicate that *STM* normally functions to prevent *AS1* expression in the SAM. *AS2* is also negatively regulated by *STM* and may interact with *AS1* (Byrne *et al.*, 2002).

In order to identify genes which negatively regulate *KNOX* gene expression, mutants that show phenotypes similar to 35S::*KNAT1* were examined (Ori *et al.*, 2000). In addition to the *as1* and *as2* mutants described above, the *serrate* (*se*) mutant was also examined. *se* has more pronounced serration of the leaves than the wild type, and also exhibits phyllotaxy defects in the same way as 35S::*KNAT1* plants (Ori *et al.*, 2000, Clarke *et al.*, 1999). The inability to find single mutants which phenocopy 35S::*KNAT1* plants completely indicates that multiple factors control homeobox gene expression and function. In support of this, the generation of *as1/se* and *as2/se* double mutants causes a deeply lobed phenotype which is similar to that of 35S::*KNAT1* (Ori *et al.*, 2000).

pKNAT1::GUS and pKNAT2::GUS promoter fusions have been used to examine the expression of *KNAT1* and *KNAT2* in these mutant backgrounds (Ori *et al.*, 2000). pKNAT1::GUS is expressed in the leaves of *as1* and *as2* mutants, whereas expression is normal in *se* mutants. pKNAT1::GUS is also expressed in the leaves of *as1/se* and *as2/se* double mutants. pKNAT2::GUS is expressed in a similar pattern to pKNAT1::GUS in these backgrounds.

In situ hybridisation also revealed that *KNAT1* mRNA in the SAM was expressed in a similar pattern in wild type plants and in all of these mutant backgrounds. This suggests that *AS1* and *AS2* are not required for down-regulation of *KNAT1* during leaf initiation (or are redundant), but are required for keeping *KNAT1* gene expression off in leaves after initiation (Ori *et al.*, 2000).

The *PICKLE* (*PKL*) gene (section 1.2.4.2) is a chromatin remodelling factor which has been implicated in restricting the expression of meristematic genes. The apical parts of *pk1* mutants are similar to that of wild type plants, although they are slow growing and organ differentiation is delayed (Eshed *et al.*, 1999). *as1/pk1* and *as2/pk1* mutants are similar to *as/se* double mutants and 35S::*KNAT1* plants. The expression pattern of pKNAT1::GUS in *pk1* mutants was identical to that in a wild type background, whereas pKNAT1::GUS expression in *as1/pk1* was similar to that in *as1/se*. Similar results were obtained using the pKNAT2::GUS reporter.

The *se* and *pk1* mutations enhance the *as* mutant phenotype, but cannot cause *KNAT1* or *KNAT2* misexpression on their own. It has been proposed that *SE* negatively regulates downstream targets of *KNOX* genes which may explain why the *se* mutation enhances the *as* phenotype (Ori *et al.*, 2000). *SE* encodes a transcription factor that is a member of a family that regulates gene activity by the modification of chromatin structure, and it may therefore function to keep genes in an inactive state (Prigge and Wagner, 2001).

As mentioned above, one of the consequences of *KNOX* gene expression in the SAM is the downregulation of genes involved in GA biosynthesis. It has recently been reported that the 35S::*KNAT1* phenotype is reduced in plants which are also homozygous for the *spindly* (*spy*) mutation which confers constitutive GA

signalling (section 1.2.4.2 and Hay *et al.*, 2002). Therefore, exogenous GA and elevated GA signalling suppress the effects of *KNOX* misexpression because *KNOX* cannot downregulate GA synthesis in areas where it is required such as the leaves under these circumstances. As mentioned above, the *AS1* locus encodes a transcription factor that negatively regulates *KNAT1* and *KNAT2*. Blocking GA signalling leads to further enhancement of the *as1* mutation. These findings are consistent with the hypothesis that repression of GA biosynthesis is instrumental to *KNOX* gene function.

Misexpression of *KNOX* protein in 35S::*KNAT1* and 35S::*KN1-GR* plants lead to a decrease in the amount of *AtGA20ox1* mRNA (Hay *et al.*, 2002). The *AtGA20ox1* transcript is also reduced in both *as1* and *pk1* mutants. The reduction seen in *as1* mutants suggests that repression of *AtGA20ox1* in the leaf is caused by misexpression of *KNOX* genes. Although *pk1* mutants do not show misexpression of *KNOX* genes in the leaf, *pk1* does enhance the *as1* phenotype. The reduction of *AtGA20ox1* in *pk1* therefore suggests that *PKL* normally acts to promote expression *AtGA20ox1* and GA synthesis. Therefore it appears that control of GA biosynthesis represents a point of convergence between *KNOX* and *PKL* proteins in the control of meristem activity. It is possible that *PKL* acts in a similar way to *SE* (Ori *et al.*, 2000).

The weak *stm-2* allele, which does not form an embryonic SAM but can form a shoot postembryonically, is enhanced by constitutive GA signalling conferred by a *spy* mutant background (Hay *et al.*, 2002). This indicates that constitutive GA signalling is detrimental to meristem function. This is consistent with the proposed role of GA in promoting, and *KNOX* genes in repressing, cellular differentiation. In the *stm* mutant, *AtGA20ox1* is expressed in the shoot apex, a region from where it is normally excluded.

It is also likely that other hormones are involved in the *KNOX* gene pathways in *Arabidopsis*. Isolation of mutant *Arabidopsis* lines which can grow in vitro as callus and produce shoots without exogenous hormones have increased levels of *KNAT1* and *STM* transcripts (Frank *et al.*, 2000).

*Arabidopsis* plants that express the cytokinin-synthesising gene *ipt* from *Agrobacterium tumefaciens* show a phenotype that is characterised by serrated leaf margins and a decrease in apical dominance (as determined by the release of axillary buds from dormancy) as well as increased steady state mRNA levels of *STM* and *KNAT1* (Rupp *et al.*, 1999). This indicates that cytokinin upregulates *KNAT1* and *STM*.

Alternatively, it has been proposed that *KNOX* genes upregulate levels of cytokinin (Hay *et al.*, 2002). For example, ectopic expression of *Kn1* in transgenic tobacco leads to an increase in cytokinin levels (Ori *et al.*, 1999) and overexpression of *KNAT1* leads to accumulation of cytokinin in lettuce (Frugis *et al.*, 2001).

*ROUGH SHEATH2* is the maize homologue of the *Arabidopsis* *KNOX* negative regulator *AS1* (Timmermans *et al.*, 1999). It has been shown that *rs2* mutants have decreased polar auxin transport in the shoot (Tsiantis *et al.*, 1999). However, although germination of wild-type maize seedlings on auxin transport inhibitors mimics some aspects of the *rs2* mutant phenotype, this phenotype is not correlated with ectopic *KNOX* protein accumulation. Therefore, it appears that changes in auxin homeostasis do not alter *KNOX* gene expression, but that genes involved in auxin function may be among the *KNOX* gene targets. Alternatively, the link between ectopic *KNOX* gene expression in the *rs2* background and alterations in auxin transport may be indirect. For example, if alterations in cellular identity occur as a result of ectopic *KNOX* gene expression, this may disrupt normal auxin transport and cause a reduction in polar auxin transport as a secondary effect.

### 1.4.3 Summary

The *KNOX* family of homeobox genes form part of the TALE superfamily that is characterised by an atypical homeodomain and is conserved between plants and animals. The *KNOX* genes can be divided into two subfamilies, Class 1 and Class 2, based on their sequences and functions in the plant. The Class 1 genes are involved in the maintenance of meristematic tissues in an undifferentiated form in the plant. The function of Class 2 genes has not been so well characterised as the Class 1 genes, but based on their wide expression

pattern in diverse plant organs it seems that they may have more general functions in plant development.

There are a number of conserved domains in class 1 proteins that act in concert to allow the function of the protein. It is thought that these proteins act as homo- or heterodimers, and that they may interact with a variety of corepressors or coactivators in a cell type-specific manner to exert a variety of different effects. These proteins are also trafficked between different cell types. This may allow them to elicit a response in cell types other than where they are transcribed.

Finally, several other genes that are involved in *KNOX* pathways have recently been identified including *AS1* and *AS2* that negatively regulate *KNAT1* and *KNAT2* as well as several chromatin remodelling factors (*SE* and *PKL*). The *SE* and *PKL* gene products do not interact directly with *KNOX* genes, but they affect the transcription of the downstream targets of *KNOX* genes.

### **1.5 Aims and objectives**

It is well known that *KNOX* homeobox genes are expressed in the shoot apical meristem of plants including *Arabidopsis*, and that they play a role in regulation of SAM activity. The shoot and the root systems differ in the way in which lateral organs are initiated. Lateral organs in the shoot (such as leaves) arise directly from the SAM, whereas the lateral organs of the root (namely the lateral roots) arise by *de novo* meristem formation. However, despite this difference it originally hypothesised that *KNOX* genes may play roles similar to those in the shoot in the initiation and/or maintenance of the root system meristems. Roles for *KNOX* genes in the root could involve regulation of either the primary root meristem or the lateral root meristems, although no genes with these functions had been identified at the time.

The aim of the project was to isolate a novel *KNOX* gene that was expressed in the *Arabidopsis thaliana* root using a PCR based strategy. Following isolation, the sequence of the gene was characterised, as well as its expression pattern and function.

## Chapter 2 Materials and Methods

Described in this chapter are the materials and methods that were used to obtain the results described in the following chapters.

### 2.1 Materials

#### 2.1.1 Chemicals

The chemicals used for this research were obtained from Sigma Chemical Company Ltd. (Poole, UK), Fisher Scientific (Loughborough, UK), ICN Pharmaceuticals Ltd (Basingstoke, UK), Merck Ltd. (Poole, UK), Fisons Scientific Equipment (Loughborough, UK), Promega (Southampton, UK) or Bio-Rad Laboratories (Hemel Hempstead, UK) unless otherwise stated.

Oligodeoxynucleotide primers used in PCR reactions were obtained from MWG-Biotech (Ebersberg, Germany). X-Gluc and IPTG were from Melford Laboratories (Suffolk, UK). X-Gal was from Bioline (London, UK). The sequence of all oligodeoxynucleotide primers that were used in this work are given in Appendix 1.

#### 2.1.2 Radiochemicals

Radiolabelled nucleotides were obtained from ICN Pharmaceuticals Ltd. [ $^{32}\text{P}$ ] $\alpha$ -dCTP was supplied at a concentration of 10 mCi/mL and a specific activity of 3000 Ci/mmol.

#### 2.1.3 Enzymes

Restriction endonucleases, T4 DNA ligase, RQ1 RNase-free DNase, AMV reverse transcriptase, M-MLV reverse transcriptase, terminal transferase, RNasin ribonuclease inhibitor and polynucleotide kinase were obtained from Promega Ltd (Southampton, UK). *Taq* DNA polymerase was from Bioline. The Expand™ High Fidelity PCR system was from Roche Diagnostics (Mannheim, Germany). Shrimp alkaline phosphatase was obtained from Sigma Chemical Company Ltd, Poole, UK. TaKaRa EX-*Taq* polymerase was obtained from Bio-Whittaker UK Ltd (Wokingham, Berks, UK).

#### 2.1.4 Kits

The PolyAtract® mRNA isolation system and the Access RT-PCR System were from Promega Ltd (Southampton, UK). The High Pure PCR Clean-Up kit was from Roche Diagnostics (Mannheim, Germany). The Prime-It® II random primer labelling kit was from Stratagene Ltd (La Jolla, California, USA). The Topo-TA cloning kit and the GATEWAY™ Cloning System kits were from Invitrogen (Paisley, UK). The RNeasy Plant RNA extraction kit, Plasmid Midi kit and QIAquick® Gel Extraction kit were from Qiagen Ltd. (Surrey, UK). The Phytopure plant DNA extraction kit was from Nucleon Biosciences (Lanarkshire, UK). The GenElute™ Plasmid Mini prep kit was from Sigma (Poole, UK).

#### 2.1.5 Bacterial strains

The *E. coli* strains used were XL1-blue MRF' (Jerpseth, 1992), TOP10 (Grant *et al.*, 1990) and DB3.1 (Bernard *et al.*, 1993). XL1-blue MRF' was used to prepare competent cells and as a plasmid host. The TOP10 strain was a host for pCR®2.1-TOPO. DB3.1 cells are used for the propagation of GATEWAY™ Entry and Destination Vectors that carry the cytotoxic *ccdB* gene. Cultures were grown in LB liquid or on LB plates (section 2.1.7) at a temperature of 37°C.

*Agrobacterium tumefaciens* C58C3 (Dale *et al.*, 1989) was used for plant transformations. This strain has been disabled so that it does not cause crown-gall disease but still has the virulence factors required for T-DNA transfer and insertion into the plant genomic DNA. C58C3 has a streptomycin resistance marker located chromosomally allowing selection with the presence of 100 µg/mL streptomycin. The virulence helper plasmid confers nalidixic acid resistance allowing selection with 20 µg/mL nalidixic acid. Cultures were grown in LB liquid or on LB plates (section 2.1.7) at a temperature of 28-30°C.

For long-term storage of bacterial strains, glycerol stocks were made by adding 0.5 mL of an overnight liquid culture to 0.5 mL of sterilized 50% v/v glycerol and storing at -20°C (*E. coli*) or snap freezing in liquid nitrogen and storing at -80°C (*A. tumefaciens*).

### 2.1.6 Plasmids

The following plasmids were used during this project: pCR<sup>®</sup>2.1 TOPO (Invitrogen, Paisley, UK), pUC19 (Yanish-Perron *et al.*, 1985), pGUS-1 (Topping *et al.*, 1991), pDH51 (Pietrzak *et al.*, 1986), pRNAi and p35S::fusion-GFP (kindly donated by Dr S. Casson, University of Durham, UK), pKar6-GFP (kindly donated by Dr P. Gallois, University of Manchester, UK), pCR<sup>®</sup>2.1::STM (kindly provided by Dr P. Chilley, University of Durham, UK), pCR<sup>®</sup>2.1::ACT (kindly provided by Dr J. Topping, University of Durham, UK) and pCIRCE (a derivative of pBIN19, (Bevan, 1984)).

In addition, the following GATEWAY<sup>™</sup> compatible vectors were used: pENTR3c and pDONR207 (Invitrogen, Paisley, UK), pGAT4 (kindly donated by Dr T. Ketelaar, University of Durham, UK) and pBinAGRFAN (kindly donated by Dr R. Anthony, Royal Holloway, University of London, UK).

pCR<sup>®</sup>2.1 TOPO is used for cloning DNA fragments generated by PCR. pDH51 contains the CaMV 35S promoter and terminator and was used to produce overexpressor and antisense constructs. pGUS-1 was used in the construction of promoter-GUS constructs and contains the  $\beta$ -Glucuronidase gene followed by the NOS terminator. pRNAi was used in the production of RNAi constructs and contains the CaMV 35S promoter and terminator as well as an ampicillin-based hinge region. p35S::fusion-GFP was used in the production of a C terminal KNAT6-GFP fusion and contains the CaMV 35S promoter and terminator as well as smGFP (Davis and Vierstra, 1998). pKar6-GFP contains EGFP with a translational enhancer, a signal peptide to allow entry to the ER and a KDEL sequence for ER retention and was used as a PCR template. pCR<sup>®</sup>2.1::STM contains the homeobox region from the *Arabidopsis* homeobox gene *SHOOTMERISTEMLESS* (*STM*) and was also used as a template for PCR. pCIRCE is a wide host range binary cloning vector for *Agrobacterium* - mediated gene transfer into plant cells.

pENTR3c was used to make a GATEWAY<sup>™</sup> compatible entry vector by restriction endonuclease digestion and ligation. pGAT4 is a destination vector and was used to make an intermediate expression clone by reaction with

pENTR3c. pDONR207 is a donor vector which was used in conjunction with pGAT4 to make an intermediate entry clone which was suitable for reaction with pBinAGRFAN. pBinAGRFAN is a wide host range binary cloning vector for *Agrobacterium* - mediated gene transfer into plant cells which allows alcohol inducible expression of a protein::GFP fusion.

All plasmid maps are shown in Appendix 2.

### **2.1.7 Bacterial culture media**

All bacterial culture media were sterilized by autoclaving at 121°C for 20 minutes.

- LB: 10 g/L bacto-tryptone, 5 g/L bacto-yeast extract, 5g/l NaCl.
- LB agar: prepared by adding 15 g bacto-agar to one litre of LB prior to autoclaving.

### **2.1.8 Plant material**

Wild type *Arabidopsis thaliana* var. Columbia (Col-0), C24 and Wassilewskija (Ws) were obtained from Lehle Seeds, Texas, USA.

In addition, a number of *Arabidopsis* mutants were used in crossing experiments: *hydra1* (Topping *et al.*, 1997), *hydra2* (Souter and Lindsey, 2000), *fass* (Torres-Ruiz and Jürgens, 1994), *aux1-100* (Bennett *et al.*, 1996), *alf3.1* (Celenza *et al.*, 1995), *rooty* (King *et al.*, 1995), *lax3*, (Parry *et al.*, 2001) *woodenleg* and *gollum* (Scheres *et al.*, 1995), *bodenlos* (Hamann *et al.*, 1999) and *monopteros* (Berleth and Jürgens, 1993).

### **2.1.9 Plant culture media**

½MS10: Half strength Murashige and Skoog medium (Sigma M5519), 10 g/L sucrose, pH 5.7 adjusted with 1 M KOH, 8 g/L agar (hard set) or 6 g/L agar (soft set), autoclaved at 121°C for 20 minutes. If required, filter sterilised antibiotic or plant growth regulator solutions were added to the autoclaved medium after it had been cooled to 50°C.

### 2.1.10 Plant growth regulators

The following plant growth regulators were used in this study. All stocks were made up fresh and filter sterilised using 0.2  $\mu\text{m}$  pore Acrodiscs™ (Gelman, Northampton, UK) before addition to plant growth medium.

- ACC (1-aminocyclopropane-1-carboxylic acid, Sigma): ethylene precursor. A 1000x stock was prepared in distilled water.
- BAP (6-Benzylaminopurine, Sigma): cytokinin analogue. A 1000x stock was prepared by dissolving in a small volume of dilute HCl before making up to volume with distilled water.
- 1-NAA ( $\alpha$ -naphthalene-acetic acid, Sigma): auxin analogue that enters cell by diffusion. A 1000x stock was prepared in 70% v/v ethanol.
- NPA (1-N-naphthylphthalamic acid, Greyhound Chromatography and Allied Chemicals, Birkenhead, UK): auxin transport inhibitor that inhibits the efflux carrier. A 1000x stock was prepared in 70% v/v ethanol.
- TIBA (2,3,5-triodobenzoic acid, Sigma): auxin transport inhibitor that inhibits the efflux carrier. A 1000x stock was prepared in 50% v/v DMSO.

### 2.1.11 Antibiotics

The following antibiotics were used in this study. Antibiotics were dissolved in distilled water and filter sterilised using 0.2  $\mu\text{m}$  pore Acrodiscs™ (Gelman, Northampton, UK) before addition to plant or bacterial growth media.

- Kanamycin sulphate (Sigma): made as 1000x stock and stored  $-20^{\circ}\text{C}$ . Used for selection of transformed plants and for selection of bacterial plasmids.
- Augmentin (Beecham Research, UK): made fresh as 1000x stock. Used for removal of *Agrobacterium tumefaciens* after transformation
- Streptomycin sulphate (Sigma): made as 1000x stock and stored  $-20^{\circ}\text{C}$ . Used for selection of bacterial plasmids.
- Nalidixic acid (Sigma): made as 1000x stock and stored  $-20^{\circ}\text{C}$ . Used for selection of bacterial plasmids.
- Methicillin (Sigma): made as 1000x stock and stored  $-20^{\circ}\text{C}$ . Used for selection of bacterial plasmids.
- Ampicillin (Sigma): made as 1000x stock and stored  $-20^{\circ}\text{C}$ . Used for selection of bacterial plasmids.

## **2.2 Plant growth, transformation and crossing**

### **2.2.1 Seed sterilisation and tissue culture**

*Arabidopsis* seeds were surface sterilised by treatment with 70% v/v ethanol for 1-2 minutes followed by 20% v/v hypochlorite/0.05% v/v Tween 20 for 20 minutes then washed in sterile distilled water three times. Following seed transfer to sterile media, Petri dishes were sealed with micropore tape (Industriacare Ltd., Shepshed, UK) and vernalised in the dark at 4°C for seven days. The plates were then transferred to a growth room with conditions consisting of a 16 hour photoperiod ( $150 \mu\text{mol m}^{-2} \text{s}^{-2}$  PAR) with a temperature of 22°C in the light and 16°C in the dark.

For root growth assays and GUS histochemical staining, plants were transferred to sterile media in square Petri dishes 3-5 days after germination and grown vertically. Roots were examined while on the plates using an Olympus SZH10 research stereo microscope (Olympus Optical Company UK Ltd, London, UK), numbers of laterals were counted and lengths were measured using a graph paper "ruler".

### **2.2.2. Plant growth in soil**

Plants in soil were grown in Levingtons multipurpose compost mixed 6:1 with silver sand (soil and sand from Klondyke Garden Centre, Chester-Le-Street, UK). If seeds were sown, the sand and soil mixture was autoclaved at 121°C for 20 minutes before use. Prior to use, soil was treated with the insecticide Intercept (Levington Horticulture Ltd., UK) at a concentration of 64 mg per 24 well seed tray. Greenhouse and environment room conditions consisted of  $150 \mu\text{mol m}^{-2} \text{s}^{-2}$  PAR over a 16 hour photoperiod, light temperature 22°C and dark temperature 16°C. In the greenhouse, Aracons (Betatech, Belgium) were used to facilitate seed collection.

## 2.2.3 Introduction of binary vectors into *Agrobacterium tumefaciens* by electroporation

### Solutions and media

- 1 mM HEPES/KOH, pH 7.0, filter sterilised
- 20% v/v glycerol, filter sterilised
- liquid LB
- LB selective plates

### Method

*A. tumefaciens* strain C58C3 was used for the preparation of electrocompetent cells. A single colony of C58C3 from a fresh LB selective plate was inoculated into 5 mL of selective LB media and grown for 48 hours with shaking. 1/1000<sup>th</sup> volume of this culture was then used to inoculate 200 mL of selective LB medium that was grown for 16 hours with shaking. The culture was then pelleted at 3,700xg for 10 minutes at 4°C. The supernatant was discarded and the resulting pellet was resuspended in 1/3 of the initial culture volume of ice cold 1 mM HEPES/KOH before the centrifugation step was repeated. These resuspension and centrifugation steps were repeated a further three times, giving a total of four washes in ice cold HEPES/KOH. After the final centrifugation, the pellet was resuspended in 1/75<sup>th</sup> the initial culture volume of ice cold 20% v/v glycerol. The cells were kept on ice throughout the procedure. The bacteria were stored as 100 µL aliquots by flash freezing in liquid nitrogen and storing at -80°C.

For electroporation, a 100 µL aliquot of cells was thawed on ice, and pipetted into an ice cold electroporation cuvette (0.2 cm electrode gap, Bio-Rad). 2 µL of supercoiled plasmid DNA was added and mixed with a pipette tip. The electroporation was carried out using Gene Pulser and Pulser Controller apparatus from Bio-Rad (Hercules, CA, USA). The Gene Pulser was set to 2.5 KV and 25 µFD and the Pulser Controller to 400 Ω. Immediately after electroporation, 1 mL of LB medium was added and the cells were transferred to an Eppendorf tube. Following incubation at 30°C for 5-6 hours with gentle shaking, 500 µL of the cells were spread onto LB plates supplemented with 100 mg/L streptomycin, 20 mg/L nalidixic acid and 50 mg/L kanamycin sulphate and grown for 48 hours at 30°C. Colonies were checked for the correct insert by colony PCR.

## 2.2.4 *Arabidopsis* transformation: the dipping method

(Clough and Bent, 1998)

### Solutions and media

- 5% w/v sucrose with 0.05% v/v Silwett L-77 (Lehle Seeds, Texas, USA).
- ½ MS10 soft set (½ MS10 SS), supplemented with 35 mg/L kanamycin sulphate and 200 mg/L augmentin (Beecham Research, UK)

### Method

*Arabidopsis thaliana* var. Columbia were grown in soil in 3.5" pots (10-15 plants per pot) with a plastic mesh placed over the soil. Plants were grown for 3-4 weeks until they were approximately 10-15 cm tall and displaying a number of immature, unopened flower buds. 2-3 days prior to dipping, open flowers and any young siliques were removed. *Agrobacterium tumefaciens* strain C58C3 was used for all binary vector constructs. The *Agrobacterium* was grown for 48 hours at 30°C in 200 mL LB supplemented with 100 mg/L streptomycin, 20 mg/L nalidixic acid and 50 mg/L kanamycin sulphate. The culture was transferred to sterile 50 mL Falcon centrifuge tubes and pelleted by centrifugation at 2500xg for 15 minutes at 4°C before being resuspended in 1 litre of a freshly made solution of 5% w/v sucrose with 0.05% v/v Silwet. Plants were then dipped fully into the solution and gently agitated for 10-15 seconds before removal. Dipped plants were placed in transparent bags to maintain humidity and placed in the greenhouse in a shaded position overnight. A second dipping was repeated 7 days after the first. Plants were then allowed to set seed and dry out in the greenhouse. Seed was collected from individual pots of plants and allowed to dry for 2 weeks at room temperature. Seed was surface sterilised and germinated on ½MS10 SS supplemented with 35 mg/mL kanamycin (to select for transformants) and 200 mg/L augmentin (to remove *Agrobacterium*). Kanamycin resistant plants were transferred to soil and seed from these plants was tested for segregation on selective plates.

## 2.2.5 Crossing

*Arabidopsis* plants will self fertilise if left unattended, therefore it is necessary to cross-pollinate by hand if hybrid progeny are required. Homozygous plants were used for crossing wherever possible. In the case of seedling lethal mutations that show an embryo phenotype, plants were screened to identify heterozygotes. In the case of seedling lethal mutations that do not show an embryo phenotype,

at least 6 plants were used for crossing to ensure that some progeny carrying the mutation were obtained.

## **Solutions**

- 0.5 M KOH

## **Method**

To screen for an embryo phenotype, mature siliques were removed from putative heterozygous parents and cut open using fine forceps and a dissecting needle. The developing seeds were removed from the siliques and mounted on a microscope slide in a drop of 0.5 M KOH. A coverslip was placed over the sample, and the slide was viewed using an Olympus SZH10 research stereo microscope (Olympus Optical Company UK Ltd, London, UK). By gently applying pressure to the coverslip, the embryos can be popped out of the developing seeds and examined for the mutant phenotype.

To carry out the cross, the recipient (female) was prepared as follows. Large buds with no visible petals were chosen. Any open flowers and developing siliques on the same stem were removed. The stem was taped carefully to the Olympus microscope stage using micropore tape (Industriacare Ltd., Shepshed, UK), and the inflorescence meristem was removed, along with any buds that were too small for crossing. The remaining buds were then opened using watchmakers forceps, and the anthers removed. Newly opened flowers with fresh fluffy yellow pollen and no silique from the donor (male) were selected. The anthers were removed and pollen was dabbed onto the exposed stigma of the female recipient. The flower bud was then closed and the stem labelled with a micropore tape tag. A second dusting of pollen was applied two days after the first. Plants were grown on in the environment room and siliques with hybrid seeds were collected after they had begun to dry out. F1 seeds from crosses were not surface sterilised but were sown in Petri dishes of autoclaved Silvaperl Perlite (J. Arthur Bowers, Lincoln, UK) moistened with sterile B5 salts (Sigma) before being transferred to soil.

## 2.3 Analysis of expression patterns and root morphology

### 2.3.1 Examination of root tips

#### Solutions

- 50% v/v glycerol

#### Method

14 day old seedlings were mounted on microscope slides in 50% v/v glycerol. Whole seedlings were viewed under an Olympus SZH10 research stereo microscope (Olympus Optical Company UK Ltd, London, UK) fitted with an Olympus SC35 type 12 camera containing Ektachrome 160 tungsten-balanced film (Kodak Ltd, Hemel Hempstead, Herts, UK). The meristem was examined on a Zeiss Axioskop microscope (Carl Zeiss Ltd., Welwyn Garden City, Herts, UK) fitted with a Nikon FX-35 camera (Nikon UK Ltd, Kingston-upon-Thames, Surrey, UK) containing Ektachrome 160 tungsten-balanced film (Kodak Ltd, Hemel Hempstead, Herts, UK).

### 2.3.2 Histochemical GUS analysis

(Stomp, 1990)

#### Solutions

- X-Gluc stock: 20 mM X-Gluc (5-Bromo-4-Chloro-3-Indolyl- $\beta$ -D-Glucuronide) in N,N-dimethylformamide, stored at -20°C.
- X-Gluc buffer: 100 mM NaH<sub>2</sub>PO<sub>4</sub>, 10 mM EDTA, 0.1% v/v Triton X-100, 0.5 mM potassium ferricyanide (K<sub>3</sub>[Fe(CN)<sub>6</sub>]) and 0.5 mM potassium ferrocyanide (K<sub>4</sub>[Fe(CN)<sub>6</sub>]), pH 7.0.
- X-Gluc staining solution: prepared by mixing 1 volume of X-Gluc stock with 19 volumes of X-Gluc buffer to give a final concentration of 1 mM X-Gluc.

#### Method

Localisation of GUS enzyme activity was determined by staining seedlings for 3-16 hours in 1 mM X-Gluc staining solution at 37°C. Specimens were then cleared of chlorophyll using 70% v/v ethanol before being mounted in 50% v/v glycerol on microscope slides. Slides were examined on a Leica MZ12 stereo microscope (Leica Instruments, Heidelberg, Germany) and photographs were taken using Photometrics COOLSNAP™*cf* (Roper Scientific Inc, Trenton, New

Jersey, USA) colour digital camera using OpenLab3.1.1 software. Slides were then sealed with clear nail polish to allow long term storage.

### **2.3.3 Paraffin embedding and sectioning of GUS stained samples**

#### **Solutions**

- 90% v/v acetone
- X-Gluc stock: 20 mM X-Gluc (5-Bromo-4-Chloro-3-Indolyl- $\beta$ -D-Glucuronide) in N,N-dimethylformamide, stored at -20°C
- X-Gluc buffer: 100 mM NaH<sub>2</sub>PO<sub>4</sub>, 10 mM EDTA, 0.1% v/v Triton X-100, 0.5 mM potassium ferricyanide (K<sub>3</sub>[Fe(CN)<sub>6</sub>]) and 0.5 mM potassium ferrocyanide (K<sub>4</sub>[Fe(CN)<sub>6</sub>]), pH 7.0
- X-Gluc staining solution: prepared by mixing 1 volume of X-Gluc stock with 19 volumes of X-Gluc buffer to give a final concentration of 1 mM X-Gluc
- Ethanol series consisting of 10%, 25% 30%, 50%, 70% 80% and 90% v/v ethanol in distilled water
- Dry ethanol: 95% ethanol stored with Molecular Sieves type 4A (Sigma)
- Dry ethanol/0.1% w/v Safranin O (Sigma)
- 1:1 v/v dry ethanol/xylene
- 0.02% w/v Ruthenium Red (Sigma) in distilled water

#### **Method**

Whole seedlings were fixed on ice in 90% v/v acetone for 15-20 minutes in 7 mL snap top vials (Laboratory Sales UK Ltd., Rochdale, UK) and then rinsed once in GUS buffer before incubation in X-gluc staining solution for 16 hours at 37°C. Samples were then dehydrated in an ethanol series consisting of 1 hour in each of the following solutions in this order: 10% v/v ethanol, 30% v/v ethanol, 50% v/v ethanol, 70% v/v ethanol. The 70% v/v ethanol was then replaced with 90% v/v ethanol and the samples left overnight. Samples were then stained for 2 hours in dry ethanol/0.1% w/v Safranin O to allow the samples to be visualised in the embedding medium before being destained overnight in dry ethanol. Two further 1 hour dry ethanol washes were then carried out to ensure all the excess Safranin O had been removed. After dehydration, samples were cleared by incubation for 1 hour in 1:1 v/v dry ethanol/xylene followed by three 1 hour incubations with xylene only. While

these incubations were being performed, paraplast embedding medium (Sigma) was melted in an oven at 50°C. Next, the samples were incubated at 50°C in 1:1 v/v xylene/embedding medium for 3 hours before this solution was replaced with embedding medium only and incubated overnight at 50°C. Two further 3 hour incubations in embedding medium at 50°C were then carried out. Samples were then oriented in embedding medium in Peelaway Disposable Embedding Moulds (Agar Scientific, Stansted, UK).

The embedding medium was then allowed to cool and set, before the embedding mould was peeled off. As the samples had been stained with Safranin O before embedding, they could be visualised to allow the embedding medium to be trimmed. The samples were then mounted onto wooden blocks before 10 micron sections were cut using a Leitz microtome fitted with disposable metal blades. The sections were then placed onto microscope slides which had been prepared by applying a thin layer of albumin and a drop of water. The slides were placed on a hot plate at 45°C and left overnight.

Sections were then deparaffinised by carrying out three 1 minute washes in xylene and before being rehydrated in an ethanol series consisting of 1 minute in each of the following solutions in this order: absolute ethanol (x2), 95% v/v ethanol, 80% v/v ethanol, 70% v/v ethanol, 50% v/v ethanol, 25% v/v ethanol and finally distilled water. The sections were then counterstained by immersion in 0.02% w/v Ruthenium Red (Sigma) solution for 10 minutes before being rinsed in distilled water and then mounted in glycerol.

The slides were then viewed using a Zeiss Axioskop microscope (Carl Zeiss Ltd., Welwyn Garden City, Herts, UK) and photographs were taken using Photometrics COOLSNAP™*cf* colour digital camera (Roper Scientific Inc, Trenton, New Jersey, USA) using OpenLab3.1.1 software. Slides were sealed with clear nail polish to allow long term storage.

### 2.3.4 Histoiresin embedding and sectioning of GUS stained samples

#### Solutions

- X-Gluc stock: 20 mM X-Gluc (5-Bromo-4-Chloro-3-Indolyl- $\beta$ -D-Glucuronide) in N,N-dimethylformamide, stored at -20°C
- X-Gluc buffer: 100 mM NaH<sub>2</sub>PO<sub>4</sub>, 10 mM EDTA, 0.1% v/v Triton X-100, 0.5 mM potassium ferricyanide (K<sub>3</sub>[Fe(CN)<sub>6</sub>]) and 0.5 mM potassium ferrocyanide (K<sub>4</sub>[Fe(CN)<sub>6</sub>]), pH 7.0
- X-Gluc staining solution: prepared by mixing 1 volume of X-Gluc stock with 19 volumes of X-Gluc buffer to give a final concentration of 1 mM X-Gluc
- Fixative solution: 1.5% w/v glutaraldehyde, 0.3% w/v paraformaldehyde in 25 mM PIPES
- Ethanol series consisting of 10%, 30%, 50%, 70% and 90% v/v ethanol in distilled water
- Histoiresin Embedding kit (Leica Instruments, Heidelberg, Germany)
- DPX mounting medium (Sigma, UK)

#### Method

Whole seedlings were stained in X-Gluc staining solution for 16 hours at 37°C, rinsed in X-Gluc buffer and then incubated overnight at 4°C in fixative solution. Samples were then dehydrated in an ethanol series by incubation for 1 hour in each of the following solutions in the following order: 10% v/v ethanol, 30% v/v ethanol, 50% v/v ethanol, 70% v/v ethanol. The 70% v/v ethanol was replaced with 90% v/v ethanol and the samples left overnight. Samples were then embedded using the Histoiresin Embedding kit (Leica Instruments, Heidelberg, Germany). Infiltration solution was prepared by mixing 50 mL of Basic Resin liquid with 1 packet (0.5 g) of Activator. Each sample was then incubated in the following solutions in the following order at 4°C: 5 hours in 3:1 v/v ethanol/Infiltration solution, overnight in 1:1 v/v ethanol/Infiltration solution, 5 hours in 1:3 v/v ethanol/Infiltration solution and finally overnight in Infiltration solution. The first 30 minutes of each incubation was carried out under vacuum at room temperature. Embedding Medium was then prepared by mixing 15 mL of Infiltration solution with 1 mL of Hardener. The Embedding Medium was used immediately as it hardened within a few minutes. Flat Bottom Embedding Capsules (Agar Scientific, Stansted, UK) were filled with Embedding Medium

then the samples were added and oriented using forceps. The caps were closed on the Embedding Capsules and the resin was left to harden overnight. The caps were then cut from the hardened resin containing the seedlings using a scalpel. 50 micron sections were cut from the samples with a glass knife using a Reichert ultramicrotome and floated in water on microscope slides. The water was then allowed to evaporate from the slide before the sections were mounted in DPX mounting medium (Fisons Scientific Equipment, Loughborough, UK) and examined using DIC optics on a Nikon Optiphot 2 microscope (Nikon UK Ltd, Kingston-upon-Thames, Surrey, UK). Photographs were taken using a Nikon Coolpix digital camera.

### **2.3.5 Laser Scanning Confocal Microscopy (LSCM)**

Laser scanning confocal microscopy was used to examine promoter-GFP expression patterns and GFP-protein fusion localisation in roots as well as the cellular organisation of roots in *KNAT6* overexpressing plants. Images are obtained by exciting fluorochromes in a tissue sample using a laser light source. An image of the tissue is obtained by scanning a laser beam over the specimen. Crucially, only light which is emitted from the section that is in focus is detected. This reduces background fluorescence and allows the tissue to be sectioned optically (e.g. (White and Amos, 1987); (White *et al.*, 1987)).

#### **Solutions**

- 50% v/v glycerol
- 10 µg/mL propidium iodide (Sigma) in water

#### **Method**

Promoter-GFP and *KNAT6* overexpressing plants were grown under sterile tissue culture conditions as detailed in 2.2.1. To prepare seedlings for confocal microscopy, they were counterstained by immersion in 10 µg/mL propidium iodide solution and vacuum infiltrated for 1 hour. Seedlings were then rinsed in distilled water to remove any excess propidium iodide before being mounted on microscope slides in 50% v/v glycerol. Coverslips of thickness 1 were used. Slides were then viewed using a Zeiss Axioskop microscope (Carl Zeiss Ltd., Welwyn Garden City, Herts, UK) fitted with a Bio-Rad Radiance 2000 laser scanning system. Red and green channels were acquired sequentially using a green HeNe laser with an HQ 590/70 filter for the red channel and an Argon laser with a HQ 530/60 filter for the green channel. The excitation wavelength

for propidium iodide is 536 nm and the emission wavelength is 617 nm. The excitation wavelength for GFP is 489 nm and the emission wavelength is 508 nm.

## **2.4 Extraction and purification of nucleic acids**

### **2.4.1 Miniprep of plasmid DNA using the Sigma GenElute™ Plasmid miniprep kit**

The Sigma GenElute™ Plasmid Miniprep kit was used for the extraction of high copy number plasmid DNA from small (1-5 mL) culture volumes. The resulting DNA was suitable for sequencing, PCR and all cloning purposes. All centrifugation was carried out at 13,000 rpm in a microcentrifuge. Bacteria containing the plasmid of interest were grown overnight at 37°C with vigorous shaking in selective LB liquid media. 1.5 mL of culture was transferred to an Eppendorf tube and the cells pelleted by centrifugation for 2 minutes. The supernatant was removed and a further 1.5 mL of culture was added to the tube and it was centrifuged as above. 200 µL of resuspension solution was added and the cells resuspended by vortex mixing. 200 µL of lysis solution was then added and mixed by inversion and the solution was incubated at room temperature for no more than 5 minutes. 350 µL of neutralisation solution was added and mixed by inversion before the tube was centrifuged for 10 minutes to pellet the cell debris. The cleared supernatant was then applied to a Mini Spin Column in a collection tube and centrifuged for 1 minute. The flow-through was discarded and 750 µL of wash solution was added to the spin column before centrifugation as above. Again, the flow through was discarded before the column was centrifuged for 5 minutes to dry the membrane. To elute the plasmid DNA, the column was transferred to a new collection tube and 50 µL of sterile distilled water was applied and left to stand for 2 minutes before centrifugation for 2 minutes. The DNA was stored at -20°C.

### **2.4.2 Midipreps of plasmid DNA using the Qiagen Midi Prep kit**

The Qiagen Midi Prep kit was used for the preparation of low copy number plasmids such as pCIRCE from large culture volumes (100-200 mL). The resulting DNA was suitable for PCR, DNA sequencing and all cloning purposes.

Bacteria containing the plasmid of interest were grown overnight in 100 mL selective liquid LB medium with vigorous shaking. The culture was transferred to sterile 50 mL Falcon centrifuge tubes, and the cells were pelleted by centrifugation at 6,000xg for 15 minutes at 4°C. The supernatant was discarded and the cells were resuspended in 4 mL of Buffer P1. 4ml of Buffer P2 was then added and mixed thoroughly by inversion before incubation at room temperature for 5 minutes. 4 mL of chilled Buffer P3 was added and mixed by inversion before incubation on ice for 15 minutes. The resulting mixture was then centrifuged at 20,000xg for 30 minutes at 4°C and the supernatant removed to a new tube before centrifugation for a further 15 minutes at 20,000xg at 4°C. During these centrifugation steps, a QIAGEN-tip 100 was equilibrated by adding 4 mL of Buffer QBT to the column and allowing it to drain by gravity flow. The cleared supernatant containing the plasmid DNA was applied promptly to the column and allowed to drain as before. The QIAGEN tip 100 was then washed with 2 x 10 mL of Buffer QC before the DNA was eluted into a sterile 15 mL Falcon tube with 5 mL of Buffer QF. The DNA was precipitated by adding 3.5 mL (0.7 volumes) of room temperature isopropanol, mixing and then transferring to Eppendorfs before centrifuging at 15,000xg for 30 minutes at 4°C. The resulting DNA pellet was washed with room temperature 70% v/v ethanol and centrifuged at 15,000xg for 15 minutes at 4°C. The supernatant was removed and the pellet left to air dry until all visible droplets of liquid had disappeared. The DNA was resuspended in 100 µL of sterile, distilled water and stored at -20°C.

### **2.4.3 Plant DNA extraction using the Phytopure kit**

#### **Additional solutions**

- 3 M sodium acetate, pH 5.5
- absolute ethanol
- 70% v/v ethanol

#### **Method**

The Phytopure kit was from Nucleon Biosciences and was used to prepare plant genomic DNA for Southern blotting analysis and PCR amplification.

1 gram (fresh weight) of plant tissue was ground to a fine powder in liquid nitrogen using a mortar and pestle and transferred to a 50 mL polypropylene

tube. 4.6 mL of reagent 1 was added and mixed by inversion. DNase-free RNase was added to a concentration of 400  $\mu\text{g}/\text{mL}$  to digest cellular RNA. The mixture was placed in a shaking water bath at 65°C for 10 minutes then placed on ice for 20 minutes. 2 mL of ice cold chloroform was added and mixed by inversion. 200  $\mu\text{L}$  of Nucleon Phytopure DNA extraction resin suspension (which binds polysaccharides and other impurities) was added and the mixture was shaken gently for 10 minutes at room temperature. The mixture was centrifuged at 1300xg for 10 minutes at 4°C and the DNA-containing upper phase was removed to a new tube. One volume of -20°C isopropanol was added and mixed by inversion. The solution was centrifuged for 5 minutes at 4000xg at 4°C to pellet the DNA. The DNA pellet was washed with 70% v/v ethanol and centrifuged for 5 minutes at 4000xg at 4°C. The ethanol was removed and the pellet allowed to air dry. The DNA-containing pellet was then resuspended in 500  $\mu\text{l}$  of sterile, distilled water and left at room temperature overnight to allow the DNA to resuspend completely. The solution was transferred to an Eppendorf tube and centrifuged at 14000 rpm for 1 minute in a benchtop microfuge to remove any undissolved contaminating material. The supernatant was removed to a new tube, and the DNA precipitated by the addition of 50  $\mu\text{L}$  of 3 M sodium acetate (pH 5.5) and 1 mL of ethanol. The DNA was spun down at 14000 rpm in a benchtop microfuge for 10 minutes before being washed twice with 70% v/v ethanol. After the pellet had been allowed to air dry, it was resuspended in 300  $\mu\text{l}$  of sterile distilled water. Again, the DNA was left overnight at room temperature to allow complete resuspension before any undissolved contaminating material was spun out as before. The supernatant containing the DNA was transferred to a new tube and stored at -20°C.

#### **2.4.4 Quick DNA extraction method for PCR**

(Edwards *et al.*, 1991)

##### **Solutions**

- Extraction buffer: 200 mM Tris-HCl pH 7.5, 250 mM NaCl, 25 mM EDTA, 0.5% w/v SDS.

##### **Method**

All centrifugation steps were carried out at 14000 rpm in a benchtop microfuge. A small leaf or leaf disk was placed in an Eppendorf along with a small amount (approximately 30  $\mu$ L) of quartz sand and 400  $\mu$ L of extraction buffer. The tissue was macerated with a hand held grinder for approximately 15 seconds and then vigorously vortex mixed. The sample was centrifuged for 5 minutes to pellet cell debris. The cleared supernatant was removed to a new Eppendorf and DNA precipitated with an equal volume of isopropanol. Following centrifugation for 5 minutes, the DNA pellet was washed with 70% v/v ethanol and centrifuged for 2 minutes. The DNA pellet was allowed to dry until no drops of liquid were visible and then resuspended in 100  $\mu$ L sterile distilled water. 1-2  $\mu$ L of this DNA prep was used in subsequent 50  $\mu$ L PCR reactions. If required, tissue was placed in Eppendorfs with the quartz sand, frozen in liquid nitrogen and stored at -80°C until required.

#### **2.4.5 RNA extractions using Guanidine hydrochloride**

(Logeman *et al.*, 1987)

##### **Solutions**

- Extraction buffer: 8 M Guanidine hydrochloride, 20 mM EDTA, 20 mM MES, 50 mM  $\beta$ -Mercaptoethanol.
- Sterile, distilled water treated with 0.1% v/v DEPC (diethylpyrocarbonate). Briefly, DEPC was added and stirred overnight at room temperature before autoclaving for 25 minutes to remove traces of DEPC.
- 3 M Sodium acetate pH 5.2 (DEPC treated).
- 1 M acetic acid.

##### **Method**

This method was used to isolate RNA from medium to large amounts of tissue or from tissue with high polysaccharide, especially siliques. Prior to RNA extraction, plant tissue was quick frozen in liquid nitrogen and then stored at -

80°C. 0.5-10 g (fresh weight) of tissue was ground in liquid nitrogen using a mortar and pestle. More liquid nitrogen was added before 2 volumes of extraction buffer were added and ground in with the sample. The powder was transferred to a 50 mL tube and allowed to thaw on ice. The sample was further disrupted by homogenisation with a polytron homogeniser. Cell debris was pelleted by centrifugation at 9200xg for 10 minutes at 4°C and the resulting supernatant was filtered through Miracloth (Calbiochem, La Jolla, CA, USA). An equal volume of 25:24:1 phenol:chloroform:isoamylalcohol was added and mixed thoroughly by inversion several times before being incubated on ice for 5 minutes. Following centrifugation at 9200xg for 30 minutes at 4°C, the RNA-containing upper phase was removed to a new tube. 0.2 volumes of ice cold 1 M acetic acid was added and mixed by inversion before the addition of 0.7 volumes of ice cold absolute ethanol. The RNA was allowed to precipitate overnight at -20°C before pelleting by centrifugation at 9200xg at 4°C. The RNA pellet was washed twice with 10 mL 3M sodium acetate pH 5.2 by centrifugation at 9200xg for 10 minutes at room temperature to remove contaminating polysaccharides. Finally, the RNA pellet was washed with 70% v/v ethanol, dried and then resuspended in 100 µL of DEPC treated water. RNA was quantified by spectrophotometric analysis (section 2.4.10) and was stored at -80°C.

#### **2.4.6 RNA extractions using Qiagen RNeasy kit**

The RNeasy kit from Qiagen was used to prepare total RNA from small amounts of tissue (50-100 mg). All centrifugation steps were carried out at 14000 rpm in a benchtop microfuge. Prior to RNA extraction, plant tissue was quick frozen in liquid nitrogen and then stored at -80°C. Samples were ground to a fine powder in liquid nitrogen using a mortar and pestle and then transferred to an Eppendorf containing 450 µL of buffer RLT with 4.5 µL of β-mercaptoethanol and vigorously vortex mixed. The sample was transferred to the QIAshredder spin column sitting in a 2 mL collection tube and centrifuged for 2 minutes. The flow-through was removed to a new Eppendorf and 0.5 volumes of ethanol were added and mixed by pipetting. The sample was transferred to an RNeasy mini spin column sitting in a 2 mL collection tube and centrifuged for 15 seconds. The flow-through was discarded and 700 µl of buffer

RW1 was added to the column and the tube centrifuged for 15 seconds. The flow-through was discarded and the column placed in a new 2 mL collection tube. Two washes were performed with 500  $\mu$ L buffer RPE per wash by centrifugation for 15 seconds and then 2 minutes. The column was transferred to an Eppendorf and 50  $\mu$ L of RNase-free water was applied to the column followed by centrifugation for 1 minute to elute the RNA. This elution step was repeated once more into the same tube. RNA was quantified by spectrophotometric analysis (section 2.4.10) and was stored at  $-80^{\circ}\text{C}$ .

## **2.4.7 Purification of DNA from agarose gels using the QIAquick® Gel Extraction kit**

### **Additional solutions**

- 3M Sodium acetate pH 5.0
- Isopropanol

### **Method**

The Qiagen QIAquick® Gel Extraction kit was used for the purification of DNA from agarose gels following restriction enzyme digestion or PCR. The resulting DNA was suitable for all cloning purposes, as a PCR template and as a template for the synthesis of radiolabelled probes. All centrifugation steps were carried out at 14000 rpm in a benchtop microfuge. DNA fragments were separated on 0.7-1.5% w/v agarose gels in TAE buffer. The gel slice containing the band of interest was excised using a clean sharp scalpel, weighed and placed in a Eppendorf. Three volumes of Buffer QG were then added before incubation at  $55^{\circ}\text{C}$  for 10 minutes until the gel slice had dissolved completely. The dissolving process was aided by vortex mixing every 2-3 minutes during the incubation. Buffer QG1 contained a pH indicator that indicated optimum pH by remaining yellow after the gel had been dissolved. If the solution turned orange or purple, 10  $\mu$ L of 3M sodium acetate was added to regain optimum pH. If the DNA fragment being purified was less than 500 bp or more than 4 kb in length, then 1 gel volume of room temperature isopropanol was added. A QIAquick spin column was inserted into a 2 mL collection tube and the sample was applied to the column. After centrifugation for 1 minute, the flow-through was discarded and 0.5 mL of Buffer QG was added to the column before it was centrifuged as above. Again, the flow-through was discarded, and 0.75 mL of

Buffer PE was added to the column. After centrifugation for 1 minute, the flow through was discarded before the column was centrifuged for 5 minutes to ensure that it was completely dry. The QIAquick column was then placed into a clean 1.5 mL Eppendorf and 50  $\mu$ L of sterile distilled water was added to elute the DNA. If a more concentrated DNA sample was required (e.g. for cloning), then 30  $\mu$ L of sterile distilled water was added and the column was left to stand for 5 minutes. The DNA containing solution was then collected by centrifugation for 5 minutes and stored at  $-20^{\circ}\text{C}$

#### **2.4.8 Purification of DNA using the High Pure PCR Product Purification kit**

The *High Pure* PCR Product Purification kit was obtained from Roche Diagnostics and was used to purify DNA and cDNA from various enzymatic reactions e.g. PCR reactions, restriction enzyme digests and reverse transcription. It was also used to remove oligonucleotide primers (less than 100 bp) from DNA. All centrifugation steps were carried out at 14000 rpm in a benchtop microfuge. The DNA containing solution was mixed with binding buffer (100  $\mu$ L buffer per 20  $\mu$ L DNA solution) and applied to a *High Pure* filter tube in a 2 mL collection tube and centrifuged for 30 seconds. The flow-through was discarded and 500  $\mu$ L wash buffer added to the filter tube before centrifugation for 30 seconds. The wash step was then repeated with 200  $\mu$ L of wash buffer. The filter tube was placed in a clean Eppendorf and 50  $\mu$ L of elution buffer (or 10 mM Tris-HCl pH 8.2 for certain applications) was added before DNA was eluted by centrifugation for 30 seconds. The DNA was stored at  $-20^{\circ}\text{C}$

#### **2.4.9 Purification of mRNA from total RNA using the PolyAtract® mRNA isolation system**

##### **Solutions**

- 20x SSC: 3 M NaCl, 0.3 M trisodium citrate, pH 7.0

##### **Method**

The polyadenylated (poly(A)<sup>+</sup>) fraction of RNA was purified from plant total RNA using the PolyAtract® system from Promega. Up to 1 mg of total RNA was made up to a volume of 500  $\mu$ L in sterile, DEPC treated water in an Eppendorf and heated at  $65^{\circ}\text{C}$  for 10 minutes to disrupt RNA secondary structure. 3  $\mu$ L of biotinylated-Oligo (dT) probe and 13  $\mu$ L of 20x SSC was added to the RNA and

mixed before the tube was allowed to cool slowly to room temperature (approximately 10 minutes) This allows annealing of the biotinylated-Oligo (dT) probe to the poly(A) tail of mRNA. An aliquot of Streptavidin-Paramagnetic particles (SA-PMP) were washed 3 times with 300  $\mu$ L of 0.5x SSC and captured using a magnetic stand. After the final wash the SA-PMP were resuspended in 100  $\mu$ L of 0.5x SSC. The annealing reaction mix was then added to the washed SA-PMP and incubated for 10 minutes at room temperature allowing streptavidin binding to the biotin. The SA-PMP were captured using the magnetic stand and the supernatant removed. The SA-PMP were then washed 4 times with 300  $\mu$ L of 0.1x SSC by resuspension and then capture of the SA-PMP. After the final wash all the supernatant was removed and the SA-PMP were resuspended in 100  $\mu$ L of sterile, RNase free water. The SA-PMP were captured using the magnetic stand and the mRNA containing supernatant was removed to another tube. The elution step was repeated with 150  $\mu$ L of sterile, RNase free water. To concentrate the mRNA, 1/10 volume of 3 M sodium acetate pH 5.2 and 1  $\mu$ L of 10 mg/mL glycogen (Roche) was added and mixed followed by 2.5 volumes of ethanol. After overnight incubation at -20°C, the precipitate was pelleted by centrifugation at 18000xg for 20 minutes at 4°C. After washing with 70% v/v ethanol the pellet was dried and resuspended in 10-20  $\mu$ L sterile, RNase free water.

#### **2.4.10 Spectrophotometric analysis of RNA**

RNA in solution was analysed and quantified using a UniCam UV2 UV/Vis spectrophotometer (ATI, Cambridge, UK). A 1/100 dilution was made of RNA samples in sterile distilled water, and water was used as a blank. The absorbance of the sample was scanned from 200 nm to 300 nm. If good quality RNA has been obtained, there should be a peak at 260 nm on the trace. The absorbance at 260 nm and 280 nm was then recorded and the 260:280 ratio calculated. To indicate that good quality RNA has been obtained, this ratio should be at least 1.7. The concentration of RNA in the sample can then be calculated using the following formula:

$$A_{260} \times \text{dilution factor} \times 40 = \text{RNA concentration } (\mu\text{g/mL})$$

## 2.4.11 Digestion of genomic DNA with restriction endonucleases

### Solutions

- **Spermidine:** 10 mM spermidine (Sigma, UK) in sterile distilled water

### Method

Restriction enzymes and 10x reaction buffers were obtained from Promega Ltd., and reactions were carried out according to the manufacturers instructions. Digestion reactions were performed by mixing 500 ng of genomic DNA with 2.2  $\mu$ L of 10x reaction buffer in an Eppendorf tube. The volume was made up to 17.6  $\mu$ L with sterile distilled water before incubation on ice for 1 hour. The mixture was then warmed to room temperature before 2.2  $\mu$ L of restriction enzyme and 2.2  $\mu$ L of 10 mM spermidine was added. The reaction was then incubated at 37°C for 5 hours.

## 2.5 Electrophoresis

### 2.5.1 DNA agarose electrophoresis

(Sambrook *et al.*, 1989)

#### Solutions

- 1x TAE buffer: 40 mM Tris-acetate pH 8.0, 1 mM EDTA
- 10x loading buffer: purchased from Promega
- DNA markers: Hyperladder I or Hyperladder IV (Bioline) were used according to the manufacturers instructions.

#### Method

Gels of 0.7% w/v to 2% w/v agarose were prepared in 1x TAE buffer depending on the size of the DNA fragments to be separated. Gels were melted in a microwave, allowed to cool to approximately 50°C before 0.1  $\mu$ g/mL of ethidium bromide was added and mixed. The molten agarose was immediately poured into a gel tray and allowed to solidify at room temperature for 20-40 minutes. DNA samples were mixed with 1/10 volume of 10x loading buffer and loaded into gel wells by pipetting. DNA markers were run alongside sample DNA to enable quantitation and approximate sizing of fragments. Electrophoresis was performed at 5-10 V/cm in 1x TAE buffer. DNA was visualized on a UV transilluminator (Gel Doc 1000 system with Molecular Analyst version 2.1.1 software, Bio-Rad) and photographed. If a Southern blot was to be performed a

ruler was placed alongside the gel in the photograph to enable DNA fragment sizes to be determined following hybridisation.

## 2.5.2 RNA formaldehyde gel electrophoresis

Method based on that by (Sambrook *et al.*, 1989)

### Solutions

- RNA removal solution: 0.1M NaOH, 1 mM EDTA
- Sterile, distilled water treated with 0.1% v/v DEPC (diethylpyrocarbonate). Briefly, DEPC was added and stirred overnight at room temperature before autoclaving for 25 minutes to remove traces of DEPC
- 10x MOPS buffer: 0.5 M MOPS, 10 mM EDTA, pH to 7.0 with NaOH, DEPC treat as above.
- Denaturing buffer: prepared by mixing 100µl 10x MOPS buffer, 100 µl DEPC treated water, 100 µl of deionised formamide, 120 µl of 37% v/v formaldehyde, made fresh
- 10x loading buffer: purchased from Promega
- RNA markers: purchased from Promega

### Method

The gel tank, casting tray and comb were soaked in RNA removal solution overnight then rinsed in sterile distilled water before use. Gels of 1% w/v were prepared by melting an appropriate amount of agarose in DEPC treated water. After cooling to approximately 70°C, 10x MOPS buffer was added to give a final concentration of 1x, and formaldehyde (37% v/v) added to give a final 3% v/v concentration. The molten gel was immediately poured into a gel tray and left to solidify for 1-2 hours at room temperature. The gel was electrophoresed in 1x MOPS for 1 hour at 3-6 V/cm prior to loading of samples. RNA samples (up to 50 µg) in a maximum volume of 25 µl water were mixed with an equal volume of Denaturing buffer, incubated for 10 minutes at 65°C and placed immediately on ice. After the addition of 1/10 volume of loading buffer, samples were loaded onto the gel and electrophoresed as above. For northern analysis samples were run alongside 10 µl RNA markers (Promega). After electrophoresis gels were stained and photographed.

### **2.5.3 Staining of RNA formaldehyde gels**

(Ausubel *et al.*, 1994)

#### **Solutions**

- 0.5 M Ammonium acetate, DEPC treated
- 0.5 M Ammonium acetate/0.5 µg/mL ethidium bromide, DEPC treated

#### **Method**

After electrophoresis the RNA gel was placed in a container and submerged in enough 0.5 M ammonium acetate to cover it. The gel was shaken gently for 20 minutes and the solution then replaced with fresh solution for a further 20 minutes. The solution was then replaced with fresh 0.5 M ammonium acetate containing 0.5 µg/mL ethidium bromide and shaken gently for 40 minutes to stain RNA. The gel was then de-stained in fresh 0.5 M ammonium acetate for 20 minutes to 2 hours before being visualized on a UV transilluminator (Gel Doc 1000 system with Molecular Analyst version 2.1.1 software, Bio-Rad) and photographed. A ruler was placed alongside the gel in the photograph to allow the size of hybridising bands to be determined after hybridisation.

### **2.6 Nucleic acid hybridisation**

Southern and northern analyses were carried out using Zeta-Probe GT membranes (Bio-Rad) according to the manufacturer's instructions.

#### **2.6.1 Southern blotting**

##### **Solutions**

- Depurinating solution: 0.25 M HCl
- Denaturing solution: 0.5 M NaOH, 1.5 M NaCl
- Neutralising solution: 3 M NaCl, 0.5 M Tris-HCl, pH 7.4
- 10x SSC: 1.5 M NaCl, 0.15 M trisodium citrate, pH 7.0

##### **Method**

This technique involves the transfer of DNA fragments from agarose gels to a nylon membrane following which the membrane is incubated with a probe of known DNA sequence in order to detect homologous sequences. After electrophoresis, gels were treated with 2-3 volumes of depurinating solution for 15 minutes with gentle shaking. The gel was rinsed briefly in distilled water then transferred to 2-3 volumes of denaturing solution and incubated with gentle shaking for 30 minutes. The gel was rinsed briefly in distilled water then

incubated in 2-3 volumes of neutralising solution with gentle shaking for 30 minutes. The gel was rinsed briefly in sterile water and blotted in a tray containing 10x SSC as follows. A glass plate was placed across the tray to form a platform. Two pieces of Whatman 3MM paper were placed over the platform and into the reservoir of 10x SSC to act as a wick through which the solution could move. The gel was placed on the paper and a piece of Zeta-Probe GT membrane placed on the gel without trapping any air bubbles. Clingfilm was placed around the edges of the gel so that liquid movement could only occur through the membrane. Two pieces of Whatman 3MM paper were placed on top of the membrane followed by 2 layers of absorbent nappy liners on top of which was placed a tray and a small weight (250-400 grams). The DNA was allowed to transfer to the membrane by capillary action overnight. The blotting apparatus was then dismantled and the position of the wells was marked on the membrane with a soft pencil before it was rinsed briefly in 2x SSC. DNA was immobilised on the membrane by crosslinking using a Bio-Rad GS Gene Linker™ set to programme 3 (damp Southern membrane) and then baking at 80°C for 30 minutes.

## **2.6.2 Northern blotting**

### **Solutions**

- 10x SSC: 1.5 M NaCl, 0.15 M trisodium citrate, pH 7.0

### **Method**

This technique involves the transfer of RNA to a nylon membrane in order to detect a transcribed sequence using a known fragment of DNA as a probe. Following electrophoresis, RNA formaldehyde gels were gently shaken in sterile water for 2x 20 minutes to remove traces of formaldehyde that can interfere with transfer. Blotting was carried out in a tray containing 10x SSC as follows. A glass plate was placed across the tray to form a platform. Two pieces of Whatman 3MM paper were placed over the platform and into the reservoir of 10x SSC to act as a wick through which the solution could move. The gel was placed on the paper and a piece of Zeta-Probe GT membrane placed on the gel without trapping any air bubbles. Clingfilm was placed around the edges of the gel so that liquid movement could only occur through the membrane. Two pieces of Whatman 3MM paper were placed on top of the membrane followed by 2 layers of absorbent nappy liners on top of which was placed a tray and a

small weight (250-400 grams). The RNA was allowed to transfer to the membrane by capillary action overnight. The blotting apparatus was then dismantled and the position of the wells was marked on the membrane with a soft pencil before it was rinsed briefly in 2x SSC. RNA was immobilised on the membrane by crosslinking using a Bio-Rad GS Gene Linker™ set to programme 3 (damp Southern membrane) and then baking at 80°C for 30 minutes.

### **2.6.3 Colony lifts**

#### **Solutions**

- Denaturing solution: 0.5 M NaOH, 1.5 M NaCl.
- Neutralisation solution: 0.5 M Tris-HCl pH 8.0, 1.5 M NaCl.
- 2x SSC: 0.3 M NaCl, 0.03 M trisodium citrate, pH 7.0

#### **Method**

Following ligation of DNA fragments into a plasmid vector and transformation into bacteria, the bacterial plates were incubated at 4°C for 2 hours. Zeta-Probe GT membrane was cut into discs and gently lowered onto the bacterial plate. The membrane was quickly orientated by making asymmetric pin marks through the membrane and then peeled from the plate. The membrane was then placed bacterial surface up on a sheet of Whatman paper soaked in denaturing solution for 3 minutes. The membrane was then transferred to a sheet of Whatman paper soaked in neutralisation solution for 3 minutes after which it was briefly washed in 2x SSC. Nucleic acid was fixed to the membrane by vacuum drying at 80°C for 30 minutes prior to hybridisation.

### **2.6.4 Radio-labelling of probes with [<sup>32</sup>P]α-dCTP**

#### **Solutions**

- TE-8: 10 mM Tris.Cl, pH 8.0, 1 mM EDTA, pH 8.0
- Sephadex G-50 in TE-8: 8g sephadex G-50 in 200 mL TE-8, autoclaved 20 minutes at 121°C

#### **Method**

In this study, double-stranded DNA probes were used for all hybridisations. Plasmid DNA containing the DNA probe of interest was used as template for

PCR and the products were separated on an agarose gel. The DNA fragment of interest was purified from the gel using the QIAquick® Gel Extraction kit.

DNA fragments were radioactively labelled using the Prime-It® II random primer kit (Stratagene Ltd.). In an Eppendorf tube, 25 – 50 ng of DNA template was mixed with 10 µL of random oligonucleotide primers and made up to a volume of 34 µL with sterile distilled water. The mixture was denatured at 100°C for 5 minutes, centrifuged briefly and allowed to cool to room temperature. To this was added 10 µL of 5x buffer (dCTP labelling buffer), 5 µL of [<sup>32</sup>P]α-dCTP and 1 µL Exo(-) Klenow (5 U/µL) following which the mixture was incubated at 37°C for 30 minutes. The reaction was stopped by adding 2 µL of stop mix. The radio-labelled probe was separated from unincorporated [<sup>32</sup>P]α-dCTP using a column consisting of a 5 mL syringe with the plunger removed. A Miracloth (Calbiochem, La Jolla, California, USA) frit was placed at the bottom of the syringe barrel before it was filled to the 2.5 mL mark with Sephadex-G50 in TE-8. 20 µL of TE-8 was then added to the probe synthesis reaction, before it was applied carefully to the top of the column. 650 µL of TE-8 was added to the column and collected as waste. Two further 650 µL aliquots were added to the column and collected as probe. The probe was boiled for 5 minutes, snap cooled on ice and then added to the hybridisation mixture.

## **2.6.5 Pre-hybridisation and hybridisation of Southern blots using the Church system**

(Church and Gilbert, 1984)

### **Solutions**

- Church Buffer: 0.5 M Na<sub>2</sub>HPO<sub>4</sub> buffer, 7% w/v SDS, pH 7.2

### **Method**

The pre-hybridisation step is designed to block sites on the membrane to which the probe may bind non-specifically. Membranes were placed in hybridisation bottles (Techne, Cambridge, UK) with the bound nucleic acid facing inwards. 50 mL of Church buffer was added and placed inside a Techne hybridisation oven (model HB-1D) at 65°C and pre-hybridised for at least 1 hour, or overnight if convenient. Just before addition of the probe, the Church buffer was replaced with 10 mL of fresh, preheated (to 65°C) Church buffer. The radiolabelled,

denatured probe was then added to the hybridisation tube, and hybridisation was carried out at 65°C overnight.

## **2.6.6 Pre-hybridisation and hybridisation of Southern's using the Denhardt's system**

### **Solutions**

- 50x Denhardt's solution: 5 g Ficoll (type 400), 5 g polyvinylpyrrolidone, 10 g Bovine serum albumin, water to 500 mL, filter sterilise and store at -20°C
- 20x SSC: 3 M NaCl, 0.3 M trisodium citrate, pH 7.0
- Prehybridisation: 6x SSC, 5x Denhardt's solution, 0.5% w/v SDS, 2.5 mg denatured fish sperm DNA, sterile distilled water to 25 mL
- Hybridisation solution: 6x SSC, 5x Denhardt's solution, 0.5% w/v SDS, 1 mg denatured fish sperm DNA, sterile distilled water to 10 mL

### **Method**

The pre-hybridisation step is designed to block sites on the membrane to which the probe may bind non-specifically. Membranes were placed in hybridisation bottles (Techne, Cambridge, UK) with the bound nucleic acid facing inwards. 25 mL of pre-hybridisation solution, minus the fish sperm DNA was made up in a 50 mL Falcon centrifuge tube and warmed to 65°C in the hybridisation oven (Techne, model HB-1D). The fish sperm DNA was boiled for 10 minutes, snap cooled on ice and then added to the rest of the prehybridisation solution. The prehybridisation solution was then added to the hybridisation bottle with the membrane, placed in the oven and prehybridised at 65°C for 1 hour. Afterwards, the pre-hybridisation solution was replaced with 10 mL of hybridisation solution prepared as above. Radiolabelled, denatured probe was then added to the hybridisation mix and left to hybridise at 65°C for 24 hours.

## **2.6.7 Prehybridisation and hybridisation of Northernblots using the Denhardt's system**

### **Solutions**

- 50x Denhardt's solution: 5 g Ficoll (type 400), 5 g polyvinylpyrrolidone, 10 g Bovine serum albumin, water to 500 mL, filter sterilise and store at -20°C.
- 20x SSPE: 3.6 M NaCl, 0.2 M Na<sub>2</sub>HPO<sub>4</sub>·7H<sub>2</sub>O, 0.02 M EDTA.
- Pre-hybridisation solution: 50% v/v deionised formamide, 5x Denhardt's solution, 0.1% w/v SDS, 5x SSPE, 2.5 mg polyadenylic acid, 2.5 mg denatured fish sperm DNA, sterile water to 25 mL.
- Hybridisation solution: 50% v/v deionised formamide, 2x Denhardt's solution, 0.1% w/v SDS, 5x SSPE, 1 mg polyadenylic acid, 2 mg denatured fish sperm DNA, sterile distilled water to 10 mL.

### **Method**

The pre-hybridisation step is designed to block sites on the membrane to which the probe may bind non-specifically. Membranes were placed in hybridisation bottles (Techne, Cambridge, UK) with the bound nucleic acid facing inwards. 25 mL of pre-hybridisation solution, minus the fish sperm DNA was made up in a 50 mL Falcon centrifuge tube and warmed to 42°C in the hybridisation oven (Techne, model HB-1D). The fish sperm DNA was boiled for 10 minutes, snap cooled on ice and then added to the rest of the prehybridisation solution. The prehybridisation solution was added to the hybridisation bottle with the membrane, placed in the oven and prehybridised at 42°C for 4-24 hours. Afterwards, the pre-hybridisation solution was replaced with 10 mL of hybridisation solution prepared as above. Radiolabelled, denatured probe was then added to the hybridisation mix and left to hybridise at 42°C for 24 - 48 hours.

## **2.6.8 Washing conditions for Church system**

### **Solutions**

- Church Wash 1: 20 mM Na<sub>2</sub>HPO<sub>4</sub> buffer, 5% w/v SDS, pH 7.2
- Church Wash 2: 20 mM Na<sub>2</sub>HPO<sub>4</sub> buffer, 1% w/v SDS, pH 7.2

### **Method**

After hybridisation, the probe was then removed and 50 mL of prewarmed Church Wash 1 was added to the tube using a 50 mL syringe and the

membrane was washed for 20 minutes at 65°C in the hybridisation oven. This 20 minute wash was then repeated. The stringency of this wash at 65°C is approximately 70%. If required, a further two 20 minute washes were carried out using Church wash 2 at 65°C. The stringency of Church Wash 2 at 65°C is approximately 100%. The membrane was then removed from the tube, and checked with a Geiger counter. If the background appeared high, a further wash was carried out with the appropriate Church Wash. After washing was complete, the membrane was wrapped in Saran wrap (Dow Chemical Company, Midland, Michigan, USA) and exposed to autoradiography film. The membrane was not allowed to dry out during any part of the procedure.

### **2.6.9 Washing conditions for Denhardt's system**

#### **Solutions**

- Wash solution 1: 2x SSC, 0.1% w/v SDS.
- Wash solution 2: 1x SSC, 0.1% w/v SDS.
- Wash solution 3: 0.1x SSC, 0.1% w/v SDS.

#### **Method**

After hybridisation, the solution was drained off and the membrane washed twice for 20 minutes at 55°C with 50 mL wash 1 (stringency = 75%). This was followed by two washes with wash 2 for 20 minutes at 55°C with 50 mL per wash (stringency = 81%). Wash 2 was performed as before except at a temperature of 65°C, giving a stringency of 91%. Finally, wash 3 was performed as previous washes at a temperature of 65°C to give a stringency of 99%. The membrane can be exposed to autoradiography film after any of the washes, depending on the similarity between the probe and the target sequence. When the membrane had been washed to the desired stringency, it was removed from the tube, and checked with a Geiger counter. If the background appeared high, a further wash was carried out at the appropriate stringency. After washing was complete, the membrane was wrapped in Saran wrap (Dow Chemical Company) and exposed to autoradiography film. The membrane was not allowed to dry out during any part of the procedure.

### **2.6.10 Autoradiography**

Autoradiography was carried out using Amersham Hyperfilm-MP X-ray film (Amersham Pharmacia Biotech Ltd, Little Chalfont, Bucks, UK) in a cassette fitted with an intensifying screen. Cassettes were left at -80°C for periods ranging from overnight to 4 weeks depending on the abundance of the target nucleic acid in the sample. X-ray film was developed using a Compact X4 automatic developer (X-ograph imaging systems, Malmesbury, UK).

### **2.6.11 Probe stripping**

If a membrane was to be re-probed it was not allowed to dry out between hybridisations and was stripped as soon as possible after autoradiography. The membrane was washed twice in a large volume of 0.1x SSC/ 0.5% w/v SDS for 20 minutes at 95°C. The membrane was checked by exposure overnight to ensure probe had been successfully stripped prior to re-hybridisation.

## **2.7 DNA cloning into plasmid vectors and DNA sequencing**

### **2.7.1 Preparation of vector and inserts by digestion with restriction endonucleases**

Restriction enzymes and 10x reaction buffers were obtained from Promega Ltd. Reactions were carried out according to the manufacturers instructions. Typically, a digestion reaction contained 0.5-3 µg of DNA, 1 µL of 10x reaction buffer, 1 µL restriction enzyme (10 units/µL) and made up to 10 µL with sterile, distilled water. Reactions were left at the required temperature for a period of 2 - 4 hours. Following digestion reactions, vector DNA for use in ligations was dephosphorylated. All digestions were analysed by DNA agarose gel electrophoresis and fragments to be used in cloning were excised from the gel and purified using the QIAquick® Gel Extraction kit.

### **2.7.2 Dephosphorylation of vector DNA**

Following restriction digestion, vector DNA for use in ligations was treated with shrimp alkaline phosphatase (Sigma) to dephosphorylate the 5' ends and prevent re-ligation of vector ends. This was only performed if the vector DNA had been treated with just one restriction enzyme. After digestion, 1 unit of shrimp alkaline phosphatase was added to the digestion reaction. The reaction

was incubated at 37°C for 30 minutes followed by 10 minutes at 70°C to inactivate the phosphatase. Linearized vector DNA was purified from an agarose gel using the QIAquick® Gel Extraction kit.

### **2.7.3 Ligation of DNA fragments**

The enzyme T4 DNA ligase catalyses the formation of a covalent phosphodiester bond between a 5'-phosphoryl group and an adjacent 3'-hydroxyl group. Vector DNA and insert DNA were digested using the same restriction enzyme(s) to allow ligation between complementary ends. In a typical ligation reaction, 50-100 ng of vector DNA was mixed with insert DNA to give a ratio of 3 vector ends to 1 insert end in an Eppendorf tube. 1 µL of 10x ligation buffer (supplied with enzyme from Promega Ltd.) and 1 µL (3 units) of T4 DNA ligase was then added and the volume made up to 10 µL with sterile, distilled water. The contents were mixed and incubated at 4°C overnight before transformation of competent *E. coli* cells.

### **2.7.4 Ligation of PCR fragments into pCR®2.1-TOPO**

DNA fragments generated by PCR were generally cloned into the pCR®2.1-TOPO vector from Invitrogen. The vector is supplied linearized with 3' thymidine overhangs for efficient ligation of PCR products with a 5' adenine overhang. It utilises the ligation activity of the topoisomerase enzyme resulting in fast, high efficiency ligation. The vector also contains primer sites for the universal primers M13F and M13R on either side of the insertion site to allow analysis of clones by PCR and sequencing. 1-4 µL of fresh, unpurified PCR product (or gel purified PCR product in some cases) was mixed with 1 µL of the pCR®2.1-TOPO vector and made up to 5 µL with sterile distilled water. The reactants were mixed and incubated at room temperature for 5 minutes to allow ligation to proceed. The tube was then placed on ice until ready for transformation into TOP10 competent cells (Invitrogen).

## 2.7.5 GATEWAY™ cloning: the LR and BP reactions

### Solutions

- TE-8: 10 mM Tris-HCl, pH 8.0, 1 mM EDTA, pH 8.0

### Method

The GATEWAY™ Cloning System from Invitrogen uses phage lambda-based site specific recombination instead of restriction endonucleases and ligase. A cocktail of proteins mediate recombination reactions between DNA recombination sequences (*att* sites). The LR reaction is used to produce an Expression clone with *attB* sites by recombination between an Entry clone with *attL* sites and a Destination vector with *attR* sites. The BP reaction is used to produce an Entry clone with *attL* sites by recombination between an Expression clone with *attB* sites and a Donor vector with *attP* sites.

For the LR reaction, 4 µL of LR reaction buffer placed in an Eppendorf tube with 100-300 ng of Entry clone and 300 ng of Destination vector. The volume was then made up to 16 µL with TE-8. The LR CLONASE Enzyme Mix was thawed on ice for 2 minutes and then vortex mixed briefly. 4 µL of CLONASE was then added to the reaction before it was incubated at 25°C for 1 hour. 2 µL of Proteinase K was added and incubated at 37°C for 10 minutes to stop the reaction. The complete reaction was then transformed into chemically competent *E. coli*.

The BP reaction was carried out in the same way, but BP reaction buffer was used in place of LR reaction buffer, and BP CLONASE Enzyme Mix was used in place of LR CLONASE Enzyme Mix.

## 2.7.6 Transformation of chemically competent *E. coli* with plasmid DNA

(Ausubel *et al.*, 1994)

### Solutions

- TfbI buffer: 30 mM potassium acetate, 100 mM rubidium chloride, 10 mM calcium chloride, 50 mM manganese chloride, 15% v/v glycerol, pH 5.8 with dilute acetic acid, filter sterilised
- TfbII buffer: 10 mM MOPS, 75 mM calcium chloride, 10 mM rubidium chloride, 15 % v/v glycerol, pH 6.5 with NaOH, filter sterilised
- liquid LB
- LB selective plates

## Method

*E. coli* XL1-blue MRF' were used for the preparation of chemically competent cells. A single colony of XL1-blue MRF' from a fresh selective LB plate was inoculated into 100 mL of sterile selective LB media and grown overnight at 37°C with vigorous shaking. The culture was poured into sterile 50 mL Falcon centrifuge tubes and chilled on ice for 10 minutes before cells were pelleted by centrifugation at 5000xg for 5 minutes at 4°C. The supernatant was removed and the cells gently resuspended in 40 mL (0.4 volumes of the original culture volume) of TfbI buffer. The cells were stored on ice for 15 minutes before the centrifugation step was repeated and the supernatant removed. The cells were then resuspended in 4 mL (0.04 volumes of the original culture volume) of ice cold TfbII buffer and stored on ice for 15 minutes. 50 µL aliquots were pipetted into ice cold Eppendorfs and flash frozen in liquid nitrogen before being stored at -80°C until required.

For transformation, an aliquot of cells was defrosted on ice. 10 µL of ligation mix or 1 µL of supercoiled plasmid was added and mixed gently before incubation on ice for 20 minutes. The cells were then heat shocked at 42°C without shaking for 30 seconds before being placed back on ice for 2 minutes. 1 mL of liquid LB was added and the cells were incubated at 37°C with shaking for 1 hour. 30-1000 µL of the cells were spread onto LB plates containing an appropriate antibiotic for selection of recombinants and grown overnight at 37°C. If blue/white colour selection of recombinants was required, 37.5 µg/mL X-Gal and 37.5 µg/mL IPTG were added to the molten LB agar prior to pouring. Due to disruption of the *lacZ* gene, recombinants would appear white instead of blue. Recombinants were checked by colony PCR or by minipreps using the Sigma GenElute™ plasmid miniprep kit followed by diagnostic restriction endonuclease digestion.

### 2.7.7 Transformation of TOP10 One Shot™ competent cells

#### Solutions

- SOC medium: 20 g/L tryptone, 5 g/L bacto-yeast extract, 10 mM NaCl, 2.5 mM KCl, 10 mM MgCl<sub>2</sub>, 10 mM MgSO<sub>4</sub>, 20 mM glucose

## Method

TOP10 One Shot™ competent cells were supplied with the TOPO TA Cloning® kit (Invitrogen, Paisley, UK) along with the pCR®2.1-TOPO vector. Following the ligation of PCR products a tube of TOP10 One Shot™ competent cells was defrosted on ice. 2 µL of the ligation mix was added and mixed by gentle stirring with a pipette tip. The tube was incubated on ice for 30 minutes before heat shocking at 42°C for 30 seconds. The tube was returned to ice for 2 minutes following which 250 µL of SOC medium was added. The tube was then incubated for 1 hour at 37°C with gentle shaking. 50-100 µL of cells were spread onto selective LB plates containing 37.5 µg/mL X-Gal. Recombinants appeared as white colonies following overnight growth at 37°C and were checked by colony PCR.

### 2.7.8 DNA sequencing

DNA sequencing was performed by the DNA sequencing lab at the University of Durham using an ABI 373 DNA sequencer and dye terminator labelling reactions (Perkin Elmer Applied Biosystems). Samples were normally supplied as plasmids prepared using the Sigma GenElute™ plasmid miniprep kit at a concentration of 100 ng/µl. Primers for sequencing were supplied at a concentration of 3.2 pmoles/µl.

## 2.8 Polymerase Chain Reaction (PCR)

### 2.8.1 Standard PCR

For standard PCR reactions, *Taq* DNA polymerase was obtained from Bioline and was supplied with Mg<sup>++</sup>-free 10x reaction buffer and 50 mM MgCl<sub>2</sub> stock solutions. Oligodeoxynucleotide primers were obtained from MWG-Biotech as lyophilised pellets and resuspended to the desired concentration in sterile, distilled water. The template for amplification was either genomic DNA, a cloned fragment of DNA in a plasmid, or a bacterial plasmid. A standard PCR reaction contained 10-100 ng of DNA sample, 0.2 µM of each primer, 1.5 µL 50mM MgCl<sub>2</sub> (1.5 mM final concentration), 5 µL Mg<sup>++</sup>-free 10x reaction buffer, 1 µL 10 mM dNTP mix and 2.5 units of *Taq* DNA polymerase made up to 50 µL with sterile, distilled water in a 0.5 mL Eppendorf. Where bacterial colonies were the

template, the reaction mix minus the DNA was made up and aliquoted into PCR tubes before a tiny amount of colony was picked up using a sterile toothpick and swirled in the reaction mixture. Reactions were overlaid with 40  $\mu$ L of mineral oil and placed in a DNA Thermal Cycler (Perkin Elmer, Foster City, CA, USA) once the block temperature had reached 90°C. A typical amplification was carried out using the following conditions: 2 minutes denaturation at 94°C then 25 cycles (from a DNA template unless otherwise stated) or 40 cycles (from a cDNA template unless otherwise stated) of 1 minute denaturation at 94°C, 1 minute annealing at 55°C (unless otherwise stated) and an extension of 1 minute per kilobase of expected product at 72°C. A final extension of 10 minutes at 72°C was performed after the amplification steps. 10-20  $\mu$ L of the reaction was run on a 1% w/v agarose gel to check the products. Cloning of PCR fragments was carried out as described in sections 2.8.4.

### **2.8.2 PCR using Expand™ High Fidelity PCR system**

The Expand™ High Fidelity PCR system consists of a mix of *Taq* polymerase and *Pwo* DNA polymerase. Due to the 3'-5' exonuclease proofreading activity of *Pwo* DNA polymerase, the Expand™ High Fidelity PCR system results in a 3-fold increase in the fidelity of DNA synthesis ( $8.5 \times 10^{-6}$  error rate). This system was used for amplification of long products and when a high degree of sequence fidelity was required, for example, the cloning of DNA fragments for subsequent transformation into plants. The system was supplied with 10x reaction buffer containing 15 mM  $MgCl_2$ . A typical reaction contained 10-100 ng of DNA target, 0.4  $\mu$ M of each primer, 5  $\mu$ L 10x reaction buffer, 1 mM dNTP mix and 2.5 units enzyme mix made up to 50  $\mu$ L with sterile, distilled water in a 0.5 mL Eppendorf and overlaid with 40  $\mu$ L of mineral oil. The tube was placed in a pre-heated block at 90°C. A typical amplification was carried out using the following conditions: denaturation at 94°C for 2 minutes followed by 25 cycles of denaturation at 94°C for 1 minute, primer annealing at 55°C for 1 minute and extension at 72°C allowing 1 minute per kilobase of product. This was followed by a final extension at 72°C for 10 minutes. If the expected product was greater than 3 kb in length then the extension step was carried out at 68°C instead of 72°C. 5-10  $\mu$ L of product was then analysed on a 1% w/v agarose gel. If

required, cloning of PCR fragments then was carried out as described in section 2.8.4.

### 2.8.3 PCR using Ex-Taq polymerase for screening the *Arabidopsis* Knockout Facility collection

#### Oligonucleotides

- *Con-1A*: CGTCTAGGTGGTTCAGTACCTGTTGAATG
- *Con-1B*: TTTATCGAAGAAACATGTCGTTGAACCAG
- *JL-202*: CATTTTATAATAACGCTGCGGACATCTAC
- *ATKO For1*: GTTAGGAAGGCCTTATCTCGACCTATGAA
- *ATKO Rev1*: AATTCATGTGTCGTCCATGCTTCACTCTT

#### Method

TaKaRa Ex-Taq polymerase, 10x Ex-Taq buffer containing 20 mM MgCl<sub>2</sub> and dNTP mix (2.5 mM each dNTP) were obtained from Bio-Whittaker (Wokingham, Berks, UK) for use in screening the *Arabidopsis* Knockout Facility collection of T-DNA insertion lines. Stock solutions of PCR primers were prepared at a concentration of 12 pmol/μL and *Arabidopsis* genomic DNA (var. Ws) was at 0.2 ng/μL. The following components were mixed in an 0.5 mL Eppendorf and the volume made up to 40 μL with sterile distilled water: 4 μL of 10x Ex-Taq buffer, 4 μL of dNTP mix, 1 μL each primer, 2 μL of Ws DNA. The tubes were then overlaid with 40 μL of mineral oil and placed in the PCR machine at 96°C. Once the samples had heated to 96°C, 10 μL of enzyme mix consisting of 8.5 μL of sterile distilled water, 1 μL of 10x EX-Taq buffer and 0.5 μL of Ex-Taq polymerase was added. The PCR amplification was then carried out under the following conditions: 96°C until Ex-Taq was added then 36 cycles of denaturation at 94°C for 15 seconds, primer annealing at 65°C for 30 seconds and extension at 72°C for 2 minutes. A final extension of 4 minutes at 72°C was then performed. 5 μL of PCR product was then analysed by gel electrophoresis using a 1% w/v agarose gel.

### 2.9 cDNA synthesis and purification

cDNA was synthesised from total RNA from roots and aerial parts of *Arabidopsis* seedlings, and from Poly(A)<sup>+</sup> RNA from *Arabidopsis* roots during the course of this work. The method given below is the general method which

was used for cDNA synthesis. The cDNA was then used for a variety of different procedures such as 3' RACE, 5' RACE and semi-quantitative RT-PCR.

### **2.9.1 cDNA synthesis**

#### **Method**

1-2.5  $\mu\text{g}$  of RNA (either total or poly(A)<sup>+</sup>) was mixed with 1  $\mu\text{L}$  of primer (10  $\mu\text{M}$  stock) in a sterile Eppendorf tube and made up to 11  $\mu\text{L}$  with sterile distilled water. The sample was heated at 65°C for 10 minutes before being snap cooled on ice. The following components were then added in this order: 4  $\mu\text{L}$  of 5x AMV buffer (supplied with AMV reverse transcriptase, Promega Ltd.), 2  $\mu\text{L}$  dNTP mix (10 mM stock), 1  $\mu\text{L}$  RNasin (Promega Ltd.) and 2  $\mu\text{L}$  (20 units) AMV reverse transcriptase, giving a total volume of 20  $\mu\text{L}$ . After mixing and brief centrifugation, the sample was incubated at 42°C for 45 minutes and 50°C for 25 minutes. The reverse transcriptase was then heat inactivated by incubation at 95°C for 5 minutes.

### **2.9.2 cDNA purification**

The first strand cDNA was purified away from the RNA template and primer using the *High Pure* PCR Product Purification kit from Roche as described in section 2.4.8. The only modification was that 50  $\mu\text{l}$  of 10 mM Tris-HCl pH8.2 was used for the elution rather than the elution buffer supplied in the kit.

### **2.10 3' RACE**

3' RACE (Random Amplification of cDNA Ends) is used to obtain the sequence of the 3' end of a partial transcript i.e. downstream of the known region. The method utilises the polyA tail of mRNA to allow the addition of an *Adaptor* sequence to the 5' end of a cDNA (i.e. the 3' end of the transcript) during reverse transcription with an Oligo-d(T) primer. A primer to this *Adaptor* sequence can then be used in subsequent PCR reactions along with gene specific primers. In this study, degenerate primers to the highly conserved homeobox region were used in conjunction with 3' RACE to isolate the 3' end of a novel homeobox gene.

### 2.10.1 Isolation of the *KNAT6* 3' region by 3' RACE

This method was developed based on the preliminary experiments described in Chapter 3. The *KN1 1* primer is towards the 5' end of the homeobox region and was used for primary PCR. The *KN1 2* primer is located downstream of the *KN1 1* primer and was used for secondary PCR.

#### Oligonucleotides

- *Oligo d(T) Adaptor*:  
CTTATACGGATATCCTGGCAATTCGGACTTTTTTTTTTTTTTTTTT(A  
/G/C)
- *Adaptor*: CTTATACGGATATCCTGGCAATTCGGACTT
- *KN1 1*: TGGTGGI(A/G)III(T/G)CA(T/C)(T/A)(C/A)IAA(A/G)TGG
- *KN1 2*: (A/T)IAAACA(A/G)AT(C/A)AACCAATTGG
- *MHF*: AGGGAGCCTCAAGCAAGAGTTCA
- *MHRT*: GCTTCCAATGCCGTTTCCTCTGG

#### Method

Poly(A)<sup>+</sup> RNA was isolated from total root RNA (Columbia ecotype) as described in sections 2.5.5 and 2.5.9. The *Oligo d(T) Adaptor* primer was used to synthesise cDNA from 2.5 µg of Poly(A)<sup>+</sup> RNA as described in sections 2.9.1. The cDNA was then purified as described in section 2.9.2.

Primary PCR reactions were set up as detailed in section 2.8.1., with 2 µL of purified cDNA as the template and 0.2 µM *Adaptor* primer and 0.4 µM first nested HD degenerate primer. Single primer control reactions with either the *Adaptor* primer or the degenerate primer were also included. Touchdown PCR was then carried out using the following conditions: initial denaturation at 94°C for 2 minutes, followed by single cycles of 1 minute denaturation at 94°C, 1 minute annealing at 65°C down to 56°C in 1°C increments, and a 1 minute extension at 72°C. Following this, 30 cycles of 94°C for 1 minute, 55°C for 1 minute and 72°C for 1 minute were performed followed by a final extension of 10 minutes at 72°C.

15 µL of each reaction was analysed by gel electrophoresis and the DNA was transferred to membrane by Southern blotting. A 1/10 dilution of the primary reaction products was made and used for secondary PCR with the second nested HD degenerate primer. Again, single primer reactions were included. The reaction mixture and the PCR conditions were as above except that only 20

cycles at the final anneal temperature were carried out. 15  $\mu$ L of each secondary reaction was analysed by gel electrophoresis and the DNA transferred to membrane by Southern blotting.

The primary and secondary PCRs were then repeated using touchdown conditions that started 10°C above final anneal temperatures of 50°C and 45°C. All of the primary and secondary products for these reactions were also analysed by gel electrophoresis and transferred to membranes by Southern blotting.

The southern blots were then hybridised to the homeobox region of the *Arabidopsis SHOOTMERISTEMLESS (STM)* gene. Probe was prepared by PCR as detailed in section 2.6.4 using the pCR<sup>®</sup>2.1::STM plasmid and the *MHF* and *MHRT* primers. Probe was hybridised to the blots using the Church system and washed to approximately 70% stringency. The membranes were exposed to autoradiography film for 5 days.

## **2.11 5' RACE**

5' RACE (Random Amplification of cDNA Ends) is used to obtain the sequence of the 5' end of a partial transcript i.e. upstream of the known region. In this study, 5' RACE was used to clone the 5' end of the *KNAT6* transcript. This method involves the addition of an adaptor sequence to the 3' end of the cDNA (i.e. the 5' end of the transcript) following reverse transcription. A primer to this adaptor sequence can then be used in subsequent PCR reactions along with a gene specific primer.

### **2.11.1 Synthesis and tailing of cDNA**

#### **Oligonucleotides**

*5' RACE 1*: CCAAAGCAAGAAGAAGGAACAACC

#### **Method**

Poly(A)<sup>+</sup> RNA was isolated from total root RNA (Columbia ecotype) as described in sections 2.5.5 and 2.5.9. The *5' RACE 1* was used to synthesise cDNA from 2.5  $\mu$ g of Poly(A)<sup>+</sup> RNA as described in sections 2.9.1, The cDNA was then purified as described in section 2.9.2.

A homopolymeric A-tail was added to the 3' end (i.e. 5' end of transcript) of the purified cDNA using the enzyme terminal transferase (Promega Ltd.). In a sterile Eppendorf, 16.5  $\mu$ L of the purified cDNA was mixed with 5  $\mu$ L of 5x TdT

reaction buffer and 2.5  $\mu$ L of 2 mM dATP. The sample was heated at 94°C for 3 minutes to denature RNA secondary structure and snap cooled on ice. Following brief centrifugation to collect the sample, 1  $\mu$ L (10 units) of terminal transferase was added to the tube and mixed. The reaction was incubated for 30 minutes on ice followed by 10 minutes at 37°C. After the reaction, the terminal transferase was inactivated by incubation at 70°C for 10 minutes. The sample was used in PCR without further purification.

### 2.11.2 Isolation of the *KNAT6* 5' region by 5' RACE

#### Oligonucleotides

- 5' RACE 2: CCTCTAGTAAACACGCTATCTCC
- 5' RACE 3: GCTTGAAGTAAGCGAGGATACG
- *Oligo d(T) Adaptor*:  
CTTATACGGATATCCTGGCAATTCGGACTTTTTTTTTTTTTTTTTT(A  
/G/C)
- *Adaptor*: CTTATACGGATATCCTGGCAATTCGGACTT

#### Method

5  $\mu$ l of the tailed cDNA from section 2.11.1 was used in a standard PCR reaction with 0.2  $\mu$ M 5' RACE 2 and 0.2  $\mu$ M of the *Oligo d(T) Adaptor* primer. The PCR conditions consisted of an initial denaturation of 2 minutes at 94°C followed by 35 cycles of 94°C for 1 minute, 55°C for 1 minute and 72°C for 1 minute. A final extension of 72°C for 10 minutes was then performed. 15  $\mu$ L of the primary products were analysed by gel electrophoresis.

Secondary PCR was then performed using 1  $\mu$ L of a 1/20 dilution of the primary PCR products as the template with the *Adaptor* primer and 5' RACE 3. Conditions were as for the primary reaction, but with 30 cycles at an anneal temperature of 60°C instead of 35 cycles at an anneal temperature of 55°C.

15  $\mu$ L of the secondary PCR products were analysed by gel electrophoresis. A band of approximately 500 bp was seen as expected so the products were shotgun cloned into the pCR®2.1-TOPO vector as described in section 2.7.4. Plasmids containing inserts were identified by colony PCR and sequenced.

## 2.12 Semi-quantitative Reverse Transcriptase-mediated Polymerase Chain Reaction (RT-PCR)

Semi-quantitative RT-PCR is a PCR based method that allows the semi-quantitative determination of transcript levels in a set of RNA samples. The technique relies on the selection of a standard transcript e.g. a constitutively expressed actin or tubulin gene, which can act as a "loading control" with which to compare the gene of interest. Primers with similar annealing temperatures that give products of similar lengths are used to amplify the control gene and the gene of interest from a standard amount of RNA. The Access RT-PCR System from Promega was used for the RT-PCR reactions.

### Oligonucleotides

- *ACT For*: GATCCTAACCGAGCGTGGTTAC
- *ACT Rev*: GACCTGACTCGTCATACTCTGC
- *HD Exon 1*: GTTTCCTTCCGATTACCAAGC
- *HD Exon 4 Rev*: GCAACCTATCTTTGAGGTCC

### Method

RNA extractions from tissue samples using the Qiagen RNeasy kit were carried out as described in section 2.4.6. The resulting total RNA was quantified by spectrophotometric analysis according to the protocol given in section. 2.4.10.

2 µg of each RNA sample was then treated with RQ1 RNase-free DNase (Promega) as follows: 2 µL of 5x AMV/*Tfl* buffer from the Access RT-PCR System was mixed in a sterile 0.5 mL Eppendorf tube with 2 µg of RNA and 2 units of DNase in a volume of 10 µL. After incubation at room temperature for 15 minutes the reaction was stopped by the addition of 1 µL of stop solution. The DNase was then heat inactivated by incubation at 65°C for 10 minutes.

The DNased RNA was then used for RT-PCR reactions. The following components were mixed in an 0.5 mL Eppendorf and the volume made up to 50 µl with sterile distilled water: 1 µg of RNA, 1 µM of each primer, 1 µL of 10 mM dNTPs, 2 µL of 25 mM MgSO<sub>4</sub>, 5x AMV/*Tfl* buffer to give a final concentration of 1x buffer (taking into account the amount transferred from the DNase step above) 5 units of AMV reverse transcriptase and 5 units of *Tfl* DNA polymerase. Negative controls were carried out by omitting the AMV reverse transcriptase from the reactions. Reactions were then layered with mineral oil and placed in a

PCR machine on the following programme: cDNA synthesis was carried out at 48°C for 45 minutes followed by reverse transcriptase inactivation and DNA/RNA denaturation at 94°C for 2 minutes. The PCR amplification consisted of 40 cycles of denaturation at 94°C for 1 minute, primer annealing at 55°C for 1 minute and extension at 72°C for 1 minute. A final extension of 10 minutes at 72°C was then performed before the samples were held at 4°C. 10 µl of each RT-PCR was then analysed by gel electrophoresis.



## Chapter 3 Isolation of *KNAT6*

The original aim of the project was to isolate a novel homeobox gene from *Arabidopsis* root. As homeobox genes were known to be involved in a variety of developmental processes in the shoot, it was hypothesised that homeobox genes were also involved in root development. A 3' RACE strategy was adopted to isolate a novel homeobox gene family. This strategy is shown in Figure 3a.

### 3.1 Growth of tissue for RNA extraction

It was hypothesised that an experimentally induced increase in the number of lateral roots would lead to a corresponding increase in root and root meristem transcripts. cDNA obtained from this tissue would therefore be enriched for root and root meristem sequences. Previous work in this and other labs has indicated that the growth of *Arabidopsis* seedlings in the presence of the synthetic auxin analogue NAA ( $\alpha$ -naphthalene-acetic acid) leads to an increase in the number of lateral roots which are initiated (Topping and Lindsey, 1997, Laskowski *et al.*, 1995). To confirm this, Columbia ecotype *Arabidopsis* seedlings were surface sterilised and germinated on  $\frac{1}{2}$  MS10 soft set ( $\frac{1}{2}$  MS10 SS) medium. 9 days after germination (DAG), the seedlings were transferred to  $\frac{1}{2}$  MS10 SS supplemented with either 0.25  $\mu$ M NAA, 2.5  $\mu$ M NAA, 5  $\mu$ M NAA or 10  $\mu$ M NAA. After 5 days growth on the NAA containing medium, whole seedlings and the root tips were examined and photographed as described in section 2.3.1.

The addition of 0.25  $\mu$ M NAA to the medium led to an increase in the root system and an increase in number of laterals. The addition of NAA from 2.5  $\mu$ M to 10  $\mu$ M led to a large increase in the number of lateral roots that were initiated, although elongation of the primary root was inhibited and the laterals did not elongate (Figure 3.1a). Examination of seedlings under high power indicated that the lateral root meristem was still formed, as indicated by a dense area of cells at the root tip.

Following this preliminary experiment, it was concluded that treatment of seedlings on NAA led to the increased initiation of lateral roots, and that these laterals still possessed a root meristem. Seedlings as a source of RNA for use

**Figure 3a 3' RACE strategy**

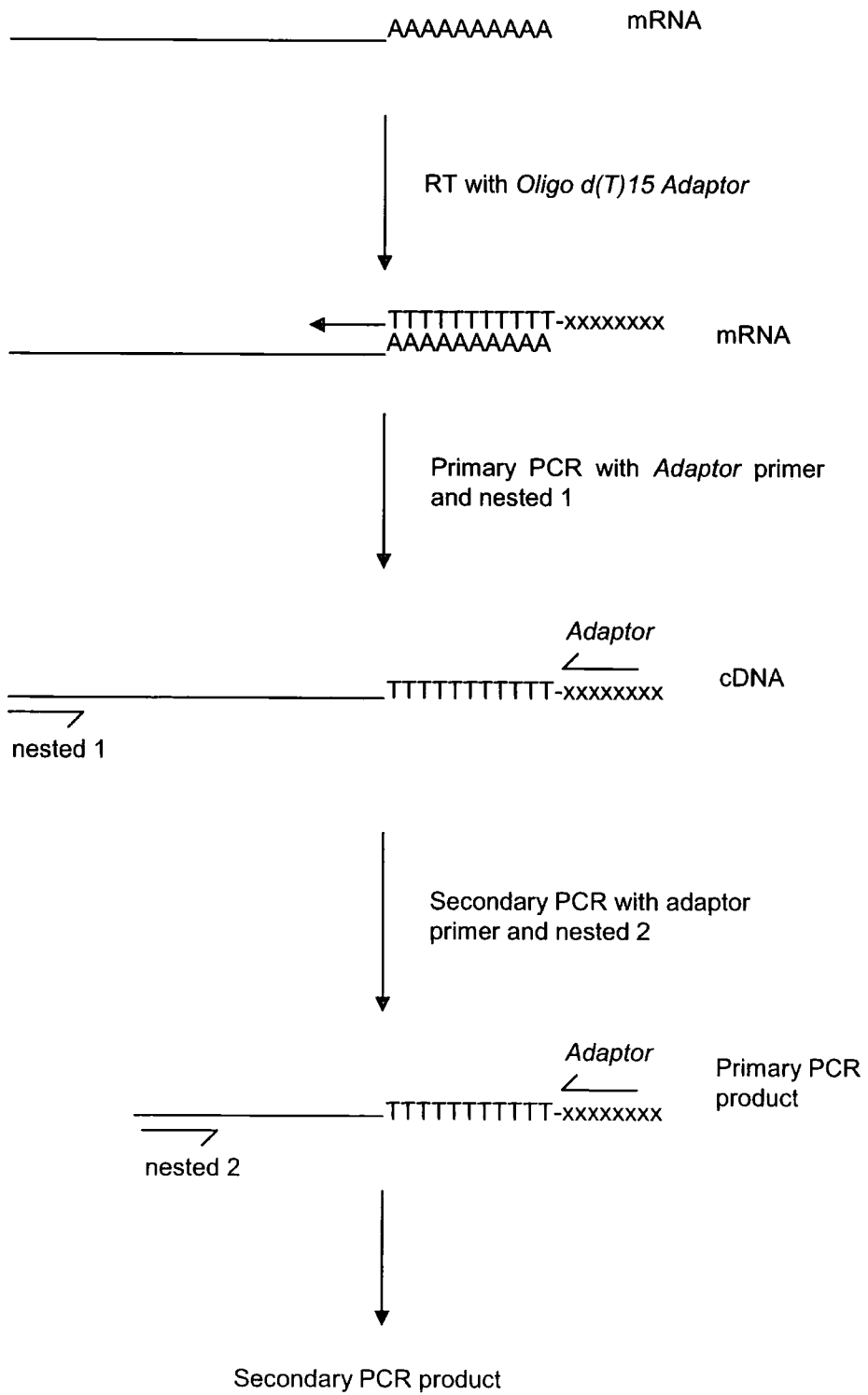
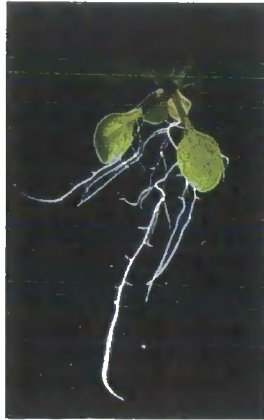


**Figure 3.1a** Effect of the synthetic auxin analogue NAA on root growth in wild type *Arabidopsis* var. Col-0



(i) 14 day old *Arabidopsis*, no treatment

(ii) 14 day old *Arabidopsis*, treated for 5 days on 10µM NAA.

in 3' RACE were grown for 9 days on ½ MS10 SS and then transferred to ½ MS10 SS supplemented with 10 µM NAA and grown for a further 5 days. 10 µM NAA was chosen as it led to the maximum increase in the number of lateral roots initiated. Roots from these 14 day old seedlings were then excised, flash frozen in liquid nitrogen and stored at -80°C until required for RNA extraction.

### **3.2 Primer design for use in 3' RACE**

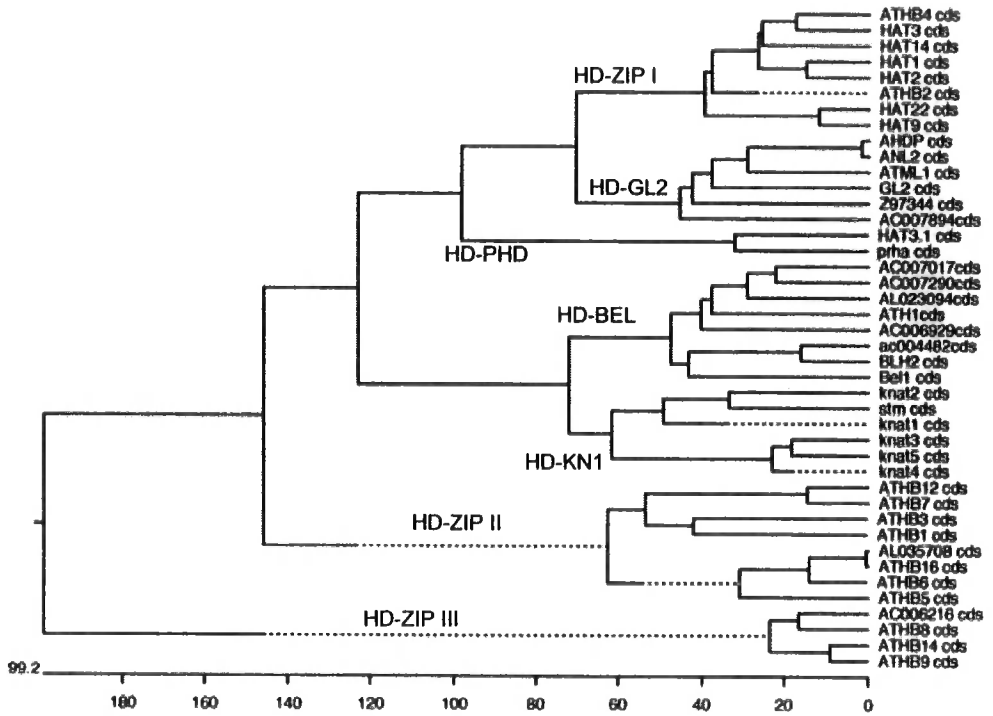
The GenBank database (<http://www.ncbi.nlm.nih.gov>) was searched using BLAST and Entrez programmes to obtain the DNA and protein sequences of *Arabidopsis* homeobox genes. The genomic homeobox sequences which were retrieved from the database fell into two categories – those which had experimental evidence available either as published data or as they matched ESTs from the EST sequencing projects, and those which are putative genes generated by analysis using GeneScan software. At the time of primer design, 41 *Arabidopsis* homeobox gene sequences were retrieved, 31 of which had published data available and 10 that were GeneScan predicted genes.

Not all of these putative homeobox genes were included in the alignments. Sequences were only used if they had some experimental evidence such as published data or an associated EST, or if they were specifically annotated as homologues of a known homeobox gene. Alignments were performed using the MegAlign programme (Clustal method) that is part of the DNASTAR suite of programmes (<http://www.dnastar.com>).

Alignment of all of these sequences (Figure 3.2a) showed that they fell into the seven families described in the literature (section 1.4.2) i.e. HD-*KN1*, HD-*BEL*, HD-PHD FINGER, HD-ZIP I, HD-ZIP II, HD-ZIP III and HD-*GL2*. Due to differences in the sequences outside the homeobox region, this alignment was not useful for primer design as the homeobox regions did not align.

For primer design, alignments were initially performed for each family using the complete coding sequence (experimental or predicted). However, for some families (HD-PHD FINGER, HD-ZIP III and HD-*GL2*) alignment of the complete coding region still did not result in the alignment of the homeobox region. For these three families, the coding region of the homeobox only was aligned.

**Figure 3.2a** Clustal alignment of all homeobox genes used for primer design



The resulting alignments were used to design nested forward primers in the homeobox region for use in 3' RACE. The longest possible primers were chosen, with primer length being at least 18 bases. To increase the stability of the interaction between the degenerate primer and the target sequence, preference was given to primers with a non-degenerate 3' end of at least 3 bases, with the final one or two nucleotides being G or C. Where the degeneracy at a given position in the alignment was greater than or equal to 3, the synthetic nucleotide inosine (I) was used (inosine will anneal to A, T, G or C). Two nested degenerate primers were designed for each family. The 1<sup>st</sup> (5') nested primer was denoted 1 and the 2<sup>nd</sup> (3') nested primer was denoted 2.

In addition, a PolydT primer with an *Adaptor* sequence, and a primer to the *Adaptor* sequence were also synthesised. These primers had been used previously in this lab (S. Casson, pers. comm.).

### **3.3 Synthesis of cDNA for use in 3' RACE**

Total RNA was prepared from the NAA-treated *Arabidopsis* root tissue (section 3.1) using the Guanidine hydrochloride method (section 2.4.5). As degenerate primers were being used for the 3' RACE, Poly(A)<sup>+</sup> was prepared as detailed in section 2.4.9 so as to remove as many non-coding RNA sequences (e.g. tRNA and rRNA) as possible in case these were amplified non-specifically during PCR.

cDNA was synthesised from the Poly(A)<sup>+</sup> using the *Oligo d(T)15 Adaptor* primer according to the protocol given in section 2.9.1. The integrity of the cDNA was checked by standard PCR (section 2.8.1) using 2 µl of cDNA and primers to the *Arabidopsis ACTIN1 (ACT1)* and *Constitutive Triple Response (CTR)* genes. PCR products of the expected sizes were obtained (700 bp for the *CTR* transcript and 600 bp for the *ACT* transcript), indicating that cDNA synthesis was successful.

### **3.4 3' RACE strategy for isolation of novel homeobox genes from root**

Primary PCR reactions were carried out using 2 µl of cDNA produced as described in section 3.3. For each homeobox family, PCR with nested degenerate primer 1 and the *Adaptor* primer was performed. Reactions using

the *ACT1* primers were included to show that the reaction conditions were viable for amplification.

To calculate the extension time for the PCR reactions, the expected product sizes for each homeobox family were estimated using the alignments produced in section 3.2 and allowing 200 bp for the 3' UTR. These sizes are shown in Table 3.4a.

**Table 3.4a** Expected size of homeobox 3' RACE products

Homeobox family	Expected product size inc. 3' UTR
<i>HD-BEL</i>	850 bp
<i>HD-KN1</i>	400 bp
<i>HD-PHD</i>	1400 bp
<i>HD-ZIP I</i>	900 bp
<i>HD-ZIP II</i>	700 bp
<i>HD-ZIP III</i>	2400 bp
<i>HD-GL2</i>	2200 bp

The PCR reactions were carried out using an extension time determined by the longest expected product i.e. that for *HD-ZIP III*, giving an extension time of 2 minutes 30 seconds. Two sets of modified PCR conditions, [A] and [B], were used for primary PCR with each HD degenerate nested primer 1 and the *Adaptor* primer as detailed below.

#### **PCR conditions**

[A] After the initial denaturation step at 94°C, amplification was carried out by 5 cycles with annealing at 42°C, 5 cycles annealing at 52°C and then 30 cycles annealing at 60°C. A final extension of 10 minutes at 72°C was then performed.

[B] After initial denaturation of 2 minutes at 94°C, amplification was carried out by 5 cycles with annealing at 72°C, 5 cycles annealing at 65°C and then 30 cycles annealing at 55°C. A final extension of 10 minutes at 72°C was then performed.

The secondary reactions were carried out using 1  $\mu$ l of a 1/20 dilution of the primary products with the nested degenerate primer 2 and the *Adaptor* primer. The conditions were as above but with only 20 cycles at the final anneal temperature.

### 3.5 Analysis of preliminary 3' RACE products

The products of these reactions were analysed by gel electrophoresis (Figure 3.5a). The reactions carried out under the [A] conditions resulted in few clear bands in either the primary or secondary reactions. The reactions carried out under the [B] conditions yielded duplicated bands of the same size in all of the reactions, regardless of the homeobox primer used. As only a few unique bands could be identified by eye, the products were analysed by hybridisation to the homeobox region of the *Arabidopsis SHOOTMERISTEMLESS (STM)* gene. PCR products from the gels were transferred to membrane by Southern blotting.

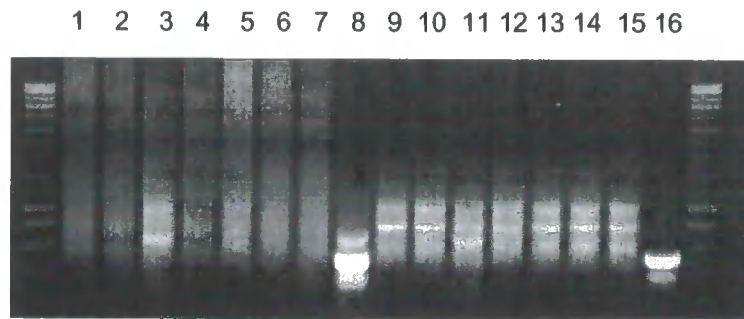
The *STM* probe was prepared by standard PCR amplification (section 2.8.1) of the *STM* homeobox region from the pCR<sup>®</sup>2.1::STM plasmid using the *MHF* and *MHRT* primers. The PCR product was purified from a gel using the QIAquick<sup>®</sup> Gel Extraction kit (section 2.4.7) and then radiolabelled with [<sup>32</sup>P] $\alpha$ -dCTP (section 2.6.4).

Prehybridisation and hybridisation was carried out using the Church method (section 2.6.5). Blots were washed to approximately 70% stringency and exposed to autoradiography film as detailed in sections 2.6.8 and 2.6.10. No hybridising bands were revealed.

To confirm that no homeobox gene fragments had been amplified by PCR, seven reaction products were selected for further analysis as follows. The *ZIP III 1* primer bands produced under [A] conditions were selected as they were the only clear unique bands obtained under these conditions with any HD degenerate primers. The *ZIP III 1* products obtained under the [B] conditions included a further unique band. The *ZIP I 1* bands were selected as an example of apparently duplicated bands in the primary and secondary reactions to test whether the nested primers were working as expected

**Figure 3.5a** Analysis of preliminary 3' RACE products

(i) Primary PCR products, [A] and [B] conditions



(ii) Secondary PCR products, [A] and [B] conditions

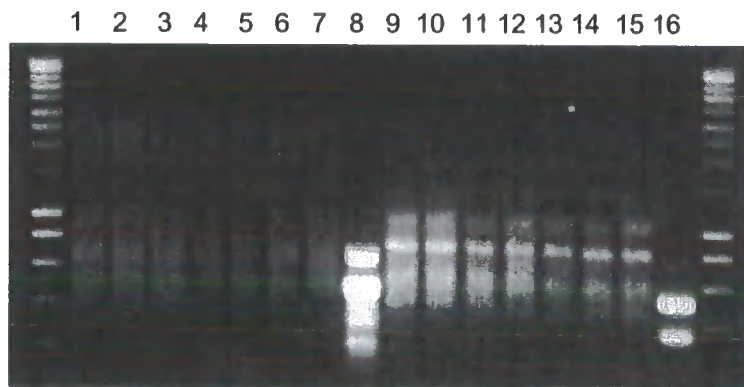
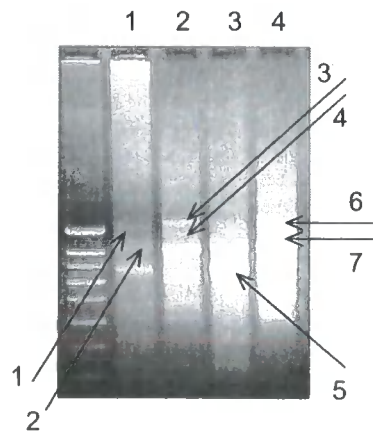


**Figure 3.5b** Analysis of preliminary 3' RACE products



20 µl of each reaction was separated by gel electrophoresis and specific bands were cut out, purified using the QIAquick® Gel Extraction kit and cloned into pCR®2.1-TOPO (sections 2.7.4 and 2.7.7). The universal primers *M13F* and *M13R* were used to check insert size by colony PCR and to sequence the plasmids.

The bands that were purified are shown in Figure 3.5b, and are detailed in Table 3.5a below.

**Table 3.5a** PCR reaction and bands cloned into pCR®2.1-TOPO

PCR reaction	HD primer	Band sizes (kb)	Arrow number in Figure 3.5b
Primary PCR, [A] conditions	ZIP III 1	1.0	1
		0.85	2
Primary PCR, [B] conditions	ZIP I 1	1.05	3
		0.8	4
Primary PCR, [B] conditions	ZIP III 1	0.65	5
Secondary PCR, [B] conditions	ZIP I 2	1.05	6
		0.8	7

Sequencing revealed that some of these products were double primed by the *Adaptor* primer (or possibly by the *Oligo d(T)15 Adaptor* primer and the *Adaptor* primer) or that the degenerate HD primers had amplified non-specific products. Table 3.5b shows the sequencing results.

The three apparently unique bands obtained using the *ZIP III 1* primer were shown to be non-specific products. Although single bands had been purified from the gel, sequencing revealed that these bands were mixtures of different products as different sequences were obtained from apparently duplicated bands in the primary and secondary reactions. This is illustrated by comparing the sequences obtained using the *ZIP I* primers: in the primary PCR reaction with *ZIP I 1*, the 0.8 kb band was an unknown protein but in the secondary PCR reaction with *ZIP I 2*, the 0.8 kb fragment was tRNA-Leu. Similarly, in the

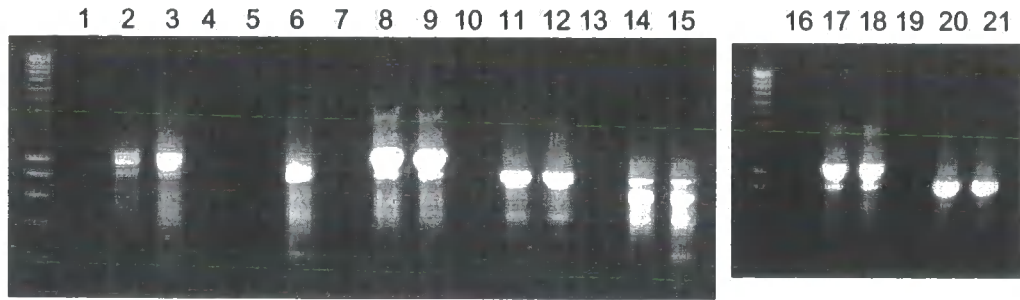
primary PCR reaction with *ZIP I 1*, the 1.05 kb band was a peroxidase but in the secondary PCR reaction with *ZIP I 2*, the 1.05 kb fragment was an unknown protein.

**Table 3.5b** Sequencing of preliminary PCR products

PCR product	Sequence and primers
[A] conditions, <i>ZIP III 1</i> , 0.85 kb band	Unknown protein <i>ZIP III 1 + Adaptor</i>
[A] conditions, <i>ZIP III 1</i> , 1.0 kb band	Peroxidase <i>ZIP III 1 + Adaptor</i>
[B] conditions, <i>ZIP I 1</i> , 0.8 kb band	Unknown protein <i>Adaptor + Adaptor</i>
[B] conditions, <i>ZIP I 1</i> , 1.05 kb band	Peroxidase <i>Adaptor + Adaptor</i>
[B] conditions, <i>ZIP III 1</i> , 0.65 kb band	Putative ribosomal protein <i>ZIP III 1 + Adaptor</i>
[B] conditions, <i>ZIP I 2</i> , 0.8 kb band	tRNA-Leu <i>Adaptor + not determined</i>
[B] conditions, <i>ZIP I 2</i> , 1.05 kb band	Unknown protein <i>Adaptor + Adaptor</i>

As mixtures of products had been cloned, but only single clones had been sequenced, PCR was carried out on the purified fragment mixtures (Table 3.5a) to ensure that no specific products had been missed. For each of the seven purified pools of fragments, PCR was carried out using the second nested degenerate primer and the *Adaptor* primer. Single primer reactions were included to allow products primed twice by the same primer to be identified. All of the reactions showed the same size product in the *Adaptor* only and the *Adaptor* + HD primer reactions apart from the reamplification of the 850 bp fragment originally obtained with the *Adaptor* and *ZIP III 1* primers under [A] conditions. The products are shown in Figure 3.5c. This product was cloned and sequenced as before but was found to be another peroxidase.

**Figure 3.5c** Reamplification of purified PCR products



Reamplification of purified PCR products using a secondary nested PCR primer.

Lane	Purified fragment	Primer 1	Primer 2
1	<i>ZIPIII 1</i> [A] 1 kb band	<i>ZIPIII 2</i>	-
2	<i>ZIPIII 1</i> [A] 1 kb band	-	<i>Adaptor</i>
3	<i>ZIPIII 1</i> [A] 1 kb band	<i>ZIPIII 2</i>	<i>Adaptor</i>
4	<i>ZIPIII 1</i> [A] 850 bp band	<i>ZIPIII 2</i>	-
5	<i>ZIPIII 1</i> [A] 850 bp band	-	<i>Adaptor</i>
6	<i>ZIPIII 1</i> [A] 850 bp band	<i>ZIPIII 2</i>	<i>Adaptor</i>
7	<i>ZIPI 1</i> [B] 1.05 kb band	<i>ZIPI 2</i>	-
8	<i>ZIPI 1</i> [B] 1.05 kb band	-	<i>Adaptor</i>
9	<i>ZIPI 1</i> [B] 1.05 kb band	<i>ZIPI 2</i>	<i>Adaptor</i>
10	<i>ZIPI 1</i> [B] 800 bp band	<i>ZIPI 2</i>	-
11	<i>ZIPI 1</i> [B] 800 bp band	-	<i>Adaptor</i>
12	<i>ZIPI 1</i> [B] 800 bp band	<i>ZIPI 2</i>	<i>Adaptor</i>
13	<i>ZIPIII 1</i> [B] 650 bp band	<i>ZIPIII2</i>	-
14	<i>ZIPIII 1</i> [B] 650 bp band	-	<i>Adaptor</i>
15	<i>ZIPIII 1</i> [B] 650 bp band	<i>ZIPIII 2</i>	<i>Adaptor</i>
16	<i>ZIPI 2</i> [B] 1.05 kb band	<i>ZIPI 2</i>	-
17	<i>ZIPI 2</i> [B] 1.05 kb band	-	<i>Adaptor</i>
18	<i>ZIPI 2</i> [B] 1.05 kb band	<i>ZIPI 2</i>	<i>Adaptor</i>
19	<i>ZIPI 2</i> [B] 800 bp band	<i>ZIPI 2</i>	-
20	<i>ZIPI 2</i> [B] 800 bp band	-	<i>Adaptor</i>
21	<i>ZIPI 2</i> [B] 800 bp band	<i>ZIPI 2</i>	<i>Adaptor</i>

Although unsuccessful in isolating a novel homeobox gene, this preliminary experiment gave useful information that led to the development of the PCR conditions that did allow the amplification of a novel homeobox gene.

### 3.6 Modification of the 3' RACE strategy

It was thought possible that the presence of the *Oligo d(T)15 Adaptor* primer which was used for cDNA synthesis may be interfering with the 3' RACE reactions. Therefore, cDNA was prepared as detailed in section 3.3 and then purified away from this primer using High Pure PCR Product Purification kit as detailed in section 2.9.2. The amount of degenerate primer in each reaction was also increased from 0.2  $\mu$ M to 0.4  $\mu$ M with the amount of *Adaptor* primer being kept at 0.2  $\mu$ M. To help identify double primed products single primer reactions were included.

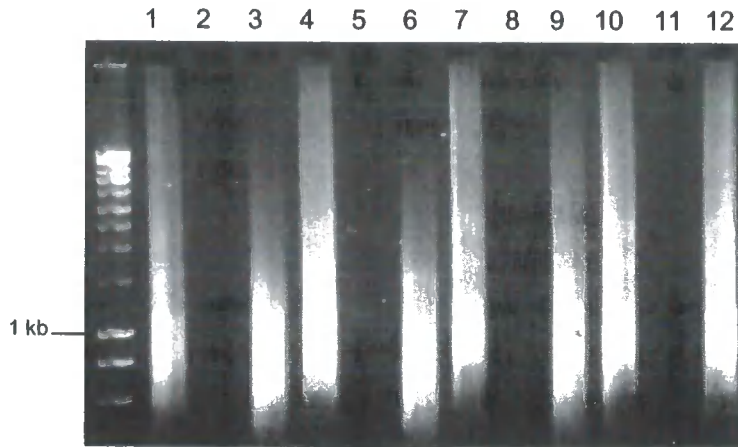
It was decided not to use the ZIP III primers as they consistently amplified peroxidase sequences. The remaining sets of primers were then divided into two groups depending on expected size of the product and were used under separate reaction conditions. *HD-BEL*, *HD-KN1*, *HD-ZIP I* and *HD-ZIP II* primers were used with an extension time of 1 minute and *HD-PHD* and *HD-GL2* primers were used with an extension time of 2 minutes 30 seconds (refer to Table 3.4a).

As the [A] PCR conditions did not give many clear bands in the reaction products, it was decided to use the [B] conditions. These were further modified and separate PCR reactions were carried out at three final anneal temperatures (see section 2.10.1).

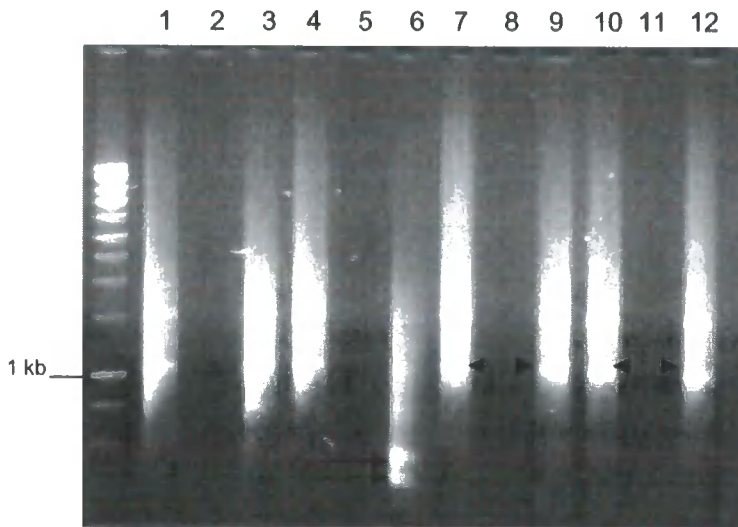
The primary and secondary PCR products that were obtained were analysed by gel electrophoresis. An example of these products (obtained using *BEL*, *KN1*, *ZIP I* and *ZIP II* primers with annealing at 50°C) is shown in Figure 3.6a. In these reactions, duplicate bands can be seen in reactions using the *Adaptor* primer only and reactions using the *Adaptor* and degenerate primers (examples of duplicate bands indicated by arrowheads on Figure 3.6a part (ii)). However, some unique bands can also be identified, most notably in the secondary PCR

**Figure 3.6a** Typical primary and secondary PCR products obtained using modified PCR conditions

(i) Primary PCR products



(ii) Secondary PCR products



products obtained using the *Adaptor* primer in combination with the *KN1 2* primer (arrows on Figure 3.6a part (ii)).

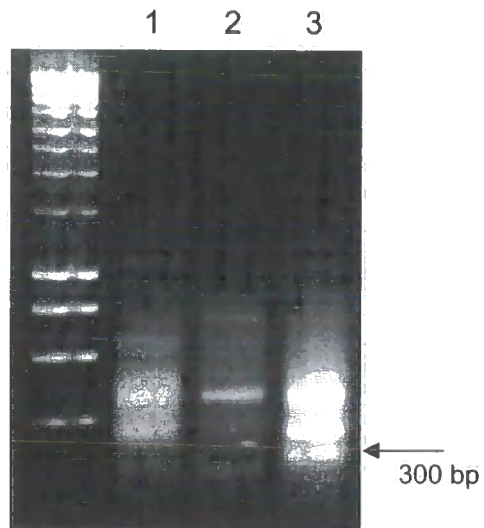
These PCR products were transferred to membranes and hybridised to the *STM* probe as before. Again, membranes were washed to approximately 70% stringency before being exposed to autoradiography film.

### **3.7 Analysis of modified 3' RACE products and isolation of a novel homeobox gene 3' fragment**

One putative positive was identified by Southern hybridisation. A band of approximately 300 bp was identified in the secondary reaction using the *KN1* second nested degenerate primer (*KN1 2*) and the *Adaptor* primer when annealing was carried out at 50°C. 20 µl of this secondary PCR reaction as well as the single primer controls were separated by gel electrophoresis and examined. The block containing the band of interest was cut out and purified using the QIAquick® Gel Extraction kit. Re-amplification of the positive from this pool of fragments was attempted using the secondary PCR conditions described in section 2.10.1 using the *KN1 2* and the *Adaptor* primers. Single primer reactions were included.

After reamplification, the reaction products were examined (Figure 3.7a) but although there was a product of approximately the right size (300 bp) in the reaction using both the *KN1 2* and the *Adaptor* primers (and this band did not appear in the single primed reactions), the band was not clean. Therefore, the PCR reaction products obtained with both the *KN1 2* and the *Adaptor* primers were shotgun cloned into pCR®2.1 TOPO. A positive colony was identified by colony hybridisation (section 2.6.3) using the *STM* probe with hybridisation and wash conditions as described in section 3.5. Plasmid DNA was prepared from the positive colony and sequenced with the universal primer *M13F*. Sequencing revealed that the hybridising band was the 3' end of a novel *Arabidopsis* homeobox gene.

**Figure 3.7a** Reamplification of secondary PCR products containing a band which hybridised to *STM*



Lane 1: Adaptor primer only

Lane 2: KN1 2 primer only

Lane 3: Adaptor and KN1 2 primers

The arrow indicates the putative hybridising band

### 3.8 Identification of the coding region of *KNAT6*

The fragment hybridising to the *STM* probe identified in section 3.7 is part of the last exon and 3' UTR of a novel homeobox gene and was assigned to a predicted GeneScan gene on chromosome 1 (GenBank Accession numbers AC007945 and AC005292, available at <http://www.ncbi.nlm.nih.gov>). These two chromosomal sequences were aligned and shown to overlapping, indicating that there was a single copy of this region rather than a duplicated gene on different parts of the chromosome. The predicted gene was annotated as a homologue of the homeobox gene *ATK1* (Dockx *et al.*, 1995). *ATK1* (also isolated as *KNAT2*, (Lincoln *et al.*, 1994)) is a class 1 KNOX gene (section 1.4.2). There were no ESTs available for this gene at the time of identification. The position of the homeobox gene fragment, designated *KNAT6* within the GenBank predicted gene is shown in Figure 3.8a.

The predicted coding region of the gene was used to design PCR primers to amplify the rest of the *KNAT6* coding sequence (Figure 3.8b). One forward primer was designed to each exon (*HD Exon 1* to *HD Exon 5*) and two reverse primers were designed to the 3' UTR (*3' UTR-51* and *3' UTR-116*). As the predicted *KNAT6* coding sequence was most similar to the *ATK1/KNAT2* coding sequence, alignment to *ATK1/KNAT2* was used for primer design to ensure that the primers were as specific for *KNAT6* as possible.

Expected product sizes using these primers were determined and are shown in Table 3.8a.

**Figure 3.8a** Position of cloned *KNAT6* fragment within the GenBank predicted genomic region

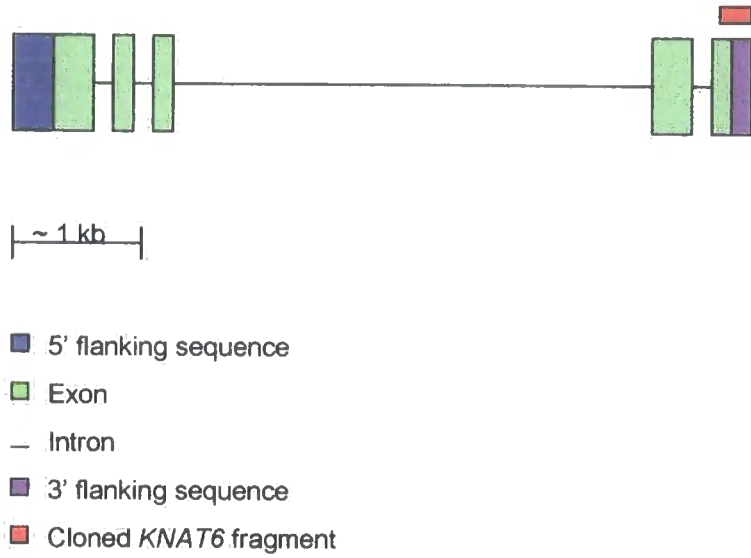


**Figure 3.8b** Positions of primers used to isolate the *KNAT6* coding region

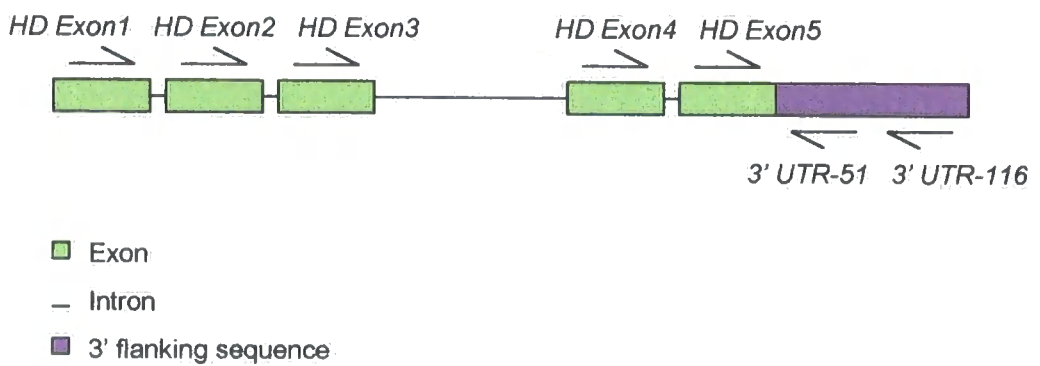


**Table 3.8a** Expected product sizes using 3' UTR and exon primers

Primer combination	Product size with cDNA template (bp)	Product size with genomic DNA template (bp)
<i>HD Exon 1 + 3' UTR-51</i>	1091	4991
<i>HD Exon 2 + 3' UTR-51</i>	817	4573
<i>HD Exon 3 + 3' UTR-51</i>	665	4337
<i>HD Exon 4 + 3' UTR-51</i>	490	579
<i>HD Exon 5 + 3' UTR-51</i>	221	221
<i>HD Exon 1 + 3' UTR-116</i>	1155	5055
<i>HD Exon 2 + 3' UTR-116</i>	881	4637
<i>HD Exon 3 + 3' UTR-116</i>	729	4401
<i>HD Exon 4 + 3' UTR-116</i>	554	643
<i>HD Exon 5 + 3' UTR-116</i>	285	285

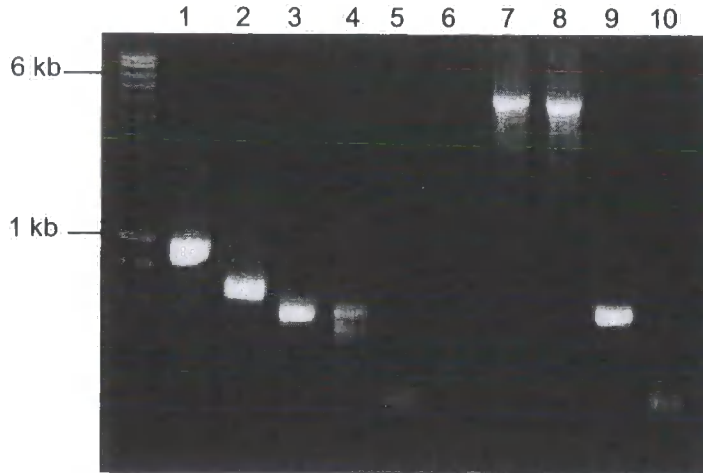
PCR was carried out using both purified cDNA (from section 3.6) and genomic DNA (ecotype C24, prepared using Phytapure kit, section 2.4.3) as a template. Reactions with each exon primer and the 3' UTR-51 primer and with each exon primer and the 3' UTR-116 primer were carried out under standard PCR conditions.

The reaction products are shown in Figure 3.8c. In most cases, the expected product sizes were obtained. The amplification of the gene from genomic DNA did not work with the 3' UTR-116 primer and the *HD Exon 1*, *HD Exon 2* or *HD Exon 3* primers, or with the 3' UTR-51 and the *HD Exon 1* primers. The amplification of the largest fragment (with the *HD Exon 1* primer and a 3' UTR primer) may have failed as the *Taq* Polymerase may not be able to efficiently amplify such a large fragment and it appears that the 3' UTR-116 primer did not work with the *HD Exon 2* or *HD Exon 3* primers. Furthermore, the reactions with the *HD Exon 4* primer and either of the 3' UTR primers resulted in a doublet rather than a single product when cDNA was used as the template.

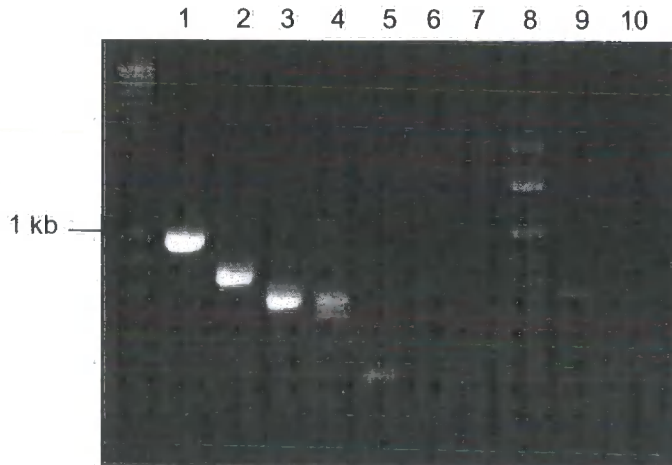
The products from the 3' UTR-116 primer and either the *HD Exon 1*, 2 or 3 primers using the cDNA template were shotgun cloned using the TOPO-TA PCR II cloning kit (section 2.7.4). Inserts were checked by colony PCR (section

**Figure 3.8c** Amplification of *KNAT6* coding region by PCR

(i) Amplification using the *5' UTR-51* primer



(ii) Amplification using the *5' UTR-116* primer



2.8.1) using the 3' *UTR-51* primer and the corresponding HD exon primer. Bacterial colonies containing inserts of the expected size were used to prepare plasmid. The plasmid containing the insert using the *HD Exon 1* primer was sequenced with the universal primers *M13F* and *M13R*. The plasmids containing inserts using the *HD Exon 2* and 3 primers were sequenced with the universal primer *M13F*.

The sequencing indicated that the cloned fragments were longer fragments of the *KNAT6* coding region. Sequencing errors were corrected to the GenBank genomic sequence, and the sequences were assembled to make a contig of the coding region. Alignment of the contig produced by experimental evidence with the GenBank sequence (Accession AC007945) revealed that the splice sites predicted by GeneScan were incorrect. The experimental and predicted coding sequences are shown in Figure 3.8d.

The *HD Exon 4* primer site was located over an intron/exon boundary and may explain why a doublet rather than a single band was seen where PCR was performed on cDNA using this primer. The two bands that were obtained using cDNA as a template corresponded to the expected bands for cDNA and genomic templates. Therefore, it was likely that the larger band was produced by amplification of contaminating genomic DNA, and the smaller band was produced by inefficient amplification of the cDNA template by the *HD Exon 4* primer as only 3' end of primer matches cDNA sequence.

### **3.9 Isolation of the 5' end of *KNAT6* by 5' RACE**

Having isolated the majority of the coding region by PCR, the extreme 5' end of the *KNAT6* transcript was identified using 5' RACE (Random Amplification of cDNA Ends). The 5' RACE method is detailed in section 2.11. Primers for use in 5' RACE were designed with reference to the *ATK1/KNAT2* sequence to ensure that they were as specific as possible for the *KNAT6* transcript. Based on the position of the predicted ATG in the database, and allowing 200 bp for the 5' UTR, a product of approximately 300-500 bp was expected from the 5' RACE reactions. Figure 3.9a shows the positions of the primers used for 5' RACE as well as a schematic of the process.

**Figure 3.8d Predicted vs experimental coding sequences**

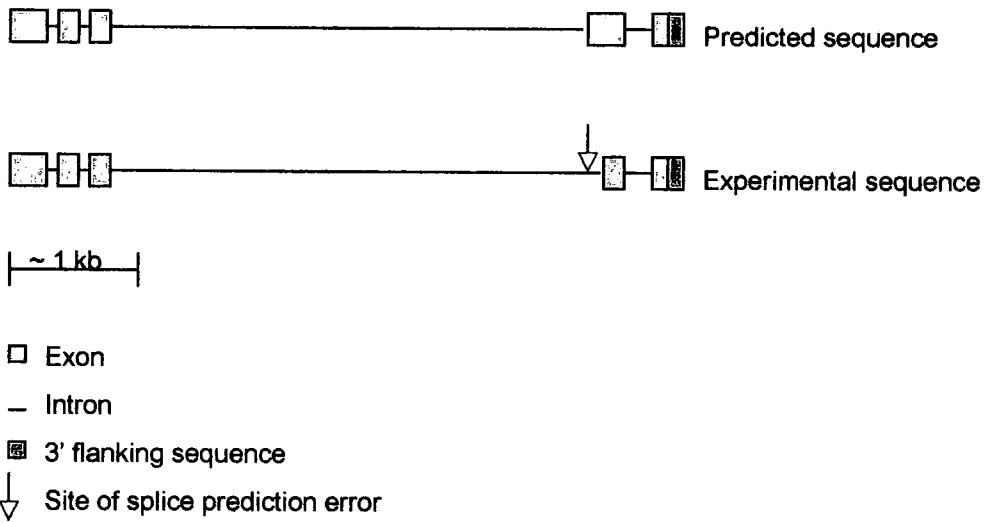
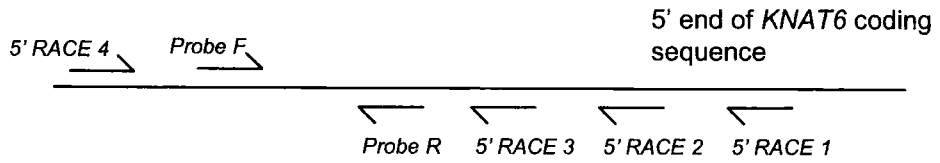
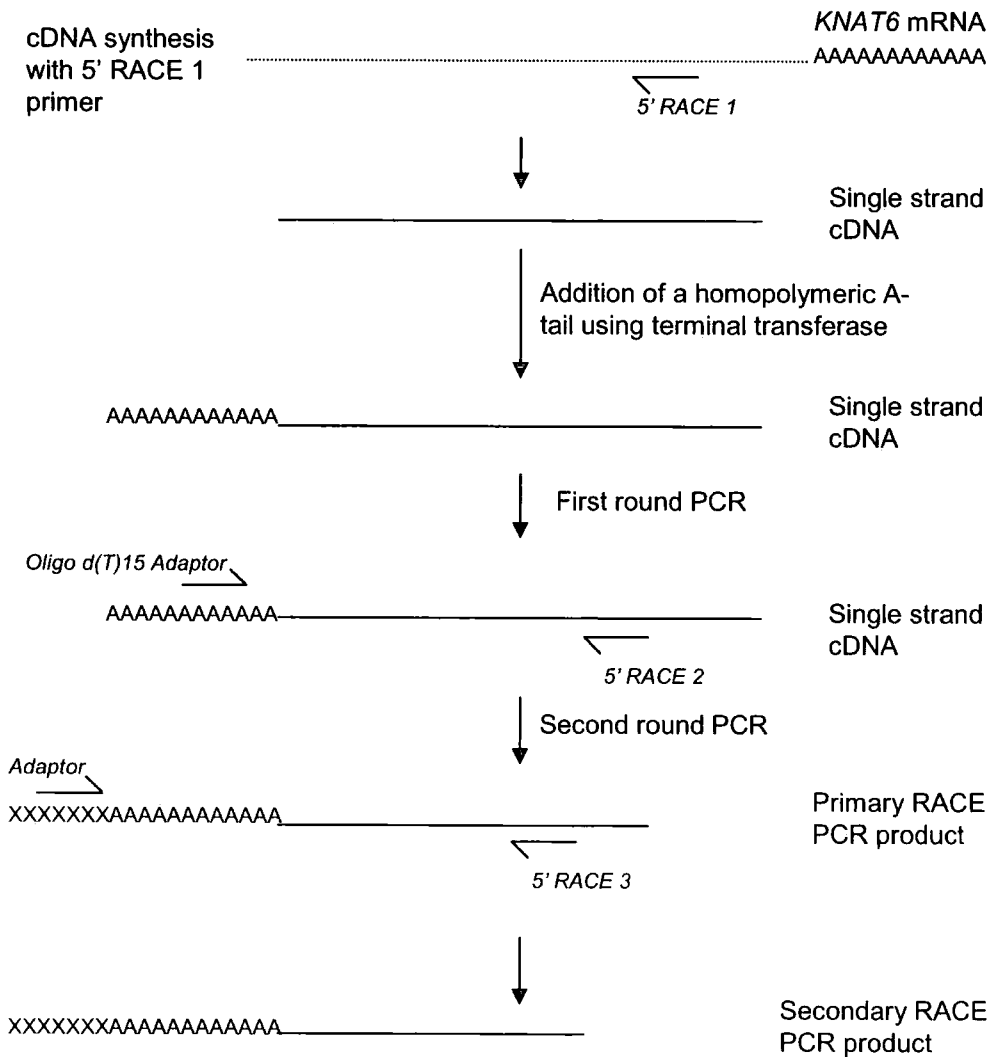


**Figure 3.9a** Primer positions and 5' RACE strategy

(i) Primer positions



(ii) 5' RACE strategy



Poly(A)<sup>+</sup> RNA from roots treated with 10  $\mu$ M NAA (prepared as in sections 2.4.5 and 2.4.9) was used as the template for cDNA synthesis using the *5' RACE 1* primer. The cDNA was then purified and a homopolymeric A-tail was added to the 3' end (i.e. the 5' end of the transcript). Primary PCR was carried out using the *5' RACE 2* primer and the *Oligo d(T)15 Adaptor* primer. Control reactions using the *5' RACE 4* primer with either *5' RACE 1* or *5' RACE 2* were included. The PCR products were examined by gel electrophoresis and are shown in Figure 3.9b. A smear can be seen in the *5' RACE* reaction as expected. However, the controls did not give the expected products (a band of 263 bp was expected with the *5' RACE 1* primer, and a band of 205 bp was expected with the *5' RACE 2* primer).

Despite the failure of the control reactions, secondary *5' RACE* PCR was performed using 1  $\mu$ l of a 1/20 dilution of the primary PCR products as the template with the *Adaptor* primer and *5' RACE 3* primer. Various control reactions using both the primary *5' RACE* PCR product and Col-0 genomic DNA were also included as detailed in Table 3.9a.

**Table 3.9a** Secondary *5' RACE* PCR reactions

Tube	Primer 1	Primer 2	Template	Product size, bp
1	<i>Adaptor</i>	<i>5' RACE 3</i>	Primary PCR products	300-500
2	<i>5' RACE 2</i>	<i>5' RACE 4</i>	Primary PCR products	205
3	<i>5' RACE 1</i>	<i>5' RACE 4</i>	Genomic DNA	407
4	<i>5' RACE 2</i>	<i>5' RACE 4</i>	Genomic DNA	350
5	<i>5' RACE 3</i>	<i>5' RACE 4</i>	Genomic DNA	150
6	<i>Probe F</i>	<i>Probe R</i>	Genomic DNA	152
7	<i>5' RACE 3</i>	<i>5' RACE 4</i>	Primary PCR products	263

Reaction products are shown in Figure 3.9c. The secondary *5' RACE* reaction (Lane 1) has a band of approximately the correct size. Although the positive controls reactions 2-5 and 7 did not give the expected products, the control reaction 6 gave a band of the correct size, indicating that the *5' RACE 4* primer was not useful.

**Figure 3.9b** Primary 5' RACE PCR reaction products

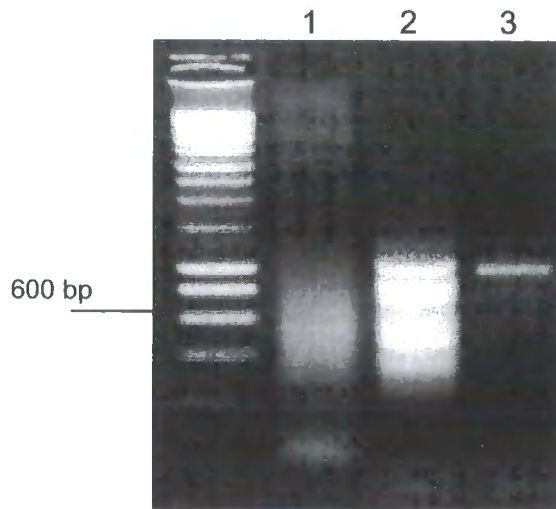
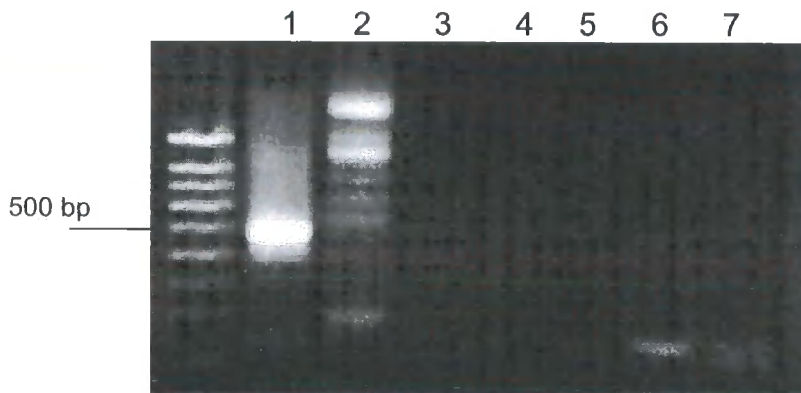


**Figure 3.9c** Secondary 5' RACE PCR reaction products



Although a band of the expected size was produced in the secondary 5' RACE reaction products, other PCR products were also present so the reaction was shotgun cloned into the pCR®2.1-TOPO vector (section 2.7.4). Colonies were analysed by colony PCR using *M13F* and *M13R* primers to identify the longest 5' UTR clone and using *Probe F* and *Probe R* primers to check that the inserts were specific. Figure 3.9d shows the results of the colony PCR. The expected sizes were approximately 700 bp using *M13F* and *M13R*, and 152 bp using the *Probe F* and *Probe R* primers. The four longest clones (1, 2, 13, and 16) were selected and sequenced with *M13F* and *M13R*. All four sequences overlap with the *KNAT6* contig obtained in section 3.8, with clone 13 being the longest.

As this sequence obtained using 5' RACE included the ATG that was predicted in GenBank, it was expected that the complete *KNAT6* coding sequence had been isolated. The 5' RACE experiment also indicated that the 5' UTR of the *KNAT6* transcript was at least 364 bp long (based on the sequence of the longest fragment, clone 13).

### **3.10 Isolation of the *KNAT6* genomic sequence**

A forward primer (5' UTR+51) was designed in the 5' UTR of *KNAT6* based on the experimentally determined *KNAT6* sequence. This was used in conjunction with the 3' UTR-116 primer to amplify the 5.4 kb of the complete gene sequence from wild type Columbia DNA using the Expand™ High Fidelity PCR system (section 2.8.2). Although the reaction product appeared to be of the correct size (Figure 3.10a), PCR was carried out with various *KNAT6* specific primers on a 1/20 dilution of the PCR product to confirm that it was specific. Table 3.10a shows the primers used and the expected product sizes.

**Figure 3.9d** Colony PCR to identify specific 5' RACE products

Colony PCR on colonies 1-20 using either *M13F* and *M13R* (1a-20a, expected size approx. 700 bp) or *Probe F* and *Probe R* (1b-20b, expected size 152 bp).

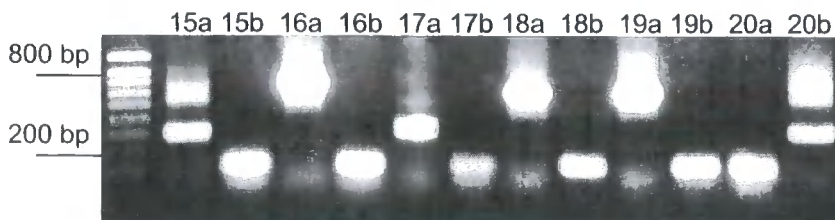
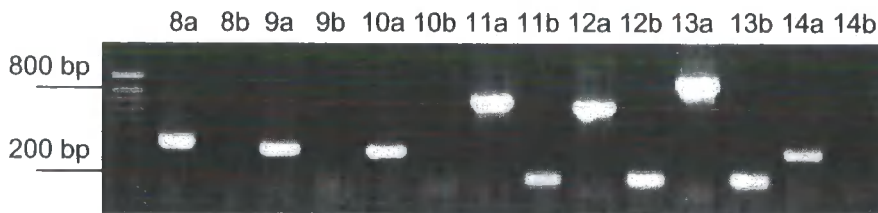
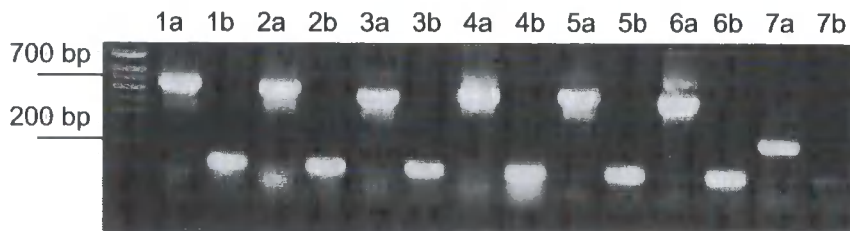
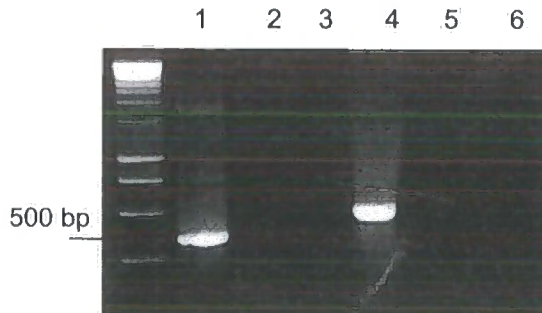


**Figure 3.10a** PCR amplification of the complete *KNAT6* genomic sequence



Amplification of the *KNAT6* genomic sequence with the 5' *UTR*+51 and 3' *UTR*-116 primers resulted in a 5.4 kb band as expected

**Figure 3.10b** PCR amplification to confirm *KNAT6* genomic region amplification



PCR indicated that the *KNAT6* genomic region had been amplified.

Lane	Primer 1	Primer 2	Size
1	<i>Probe F</i>	5' <i>RACE1</i>	479 bp
2	<i>Probe F</i>	-	-
3	-	5' <i>RACE1</i>	-
4	<i>HD Exon 4</i>	3' <i>UTR</i> -116	579 bp
5	<i>HD Exon 4</i>	-	-
6	-	3' <i>UTR</i> -116	-

**Table 3.10a** PCR to check the *KNAT6* genomic fragment

Tube	Primer 1	Primer 2	Expected size, bp
1	<i>Probe F</i>	<i>5' RACE 1</i>	479
2	<i>Probe F</i>	-	-
3	-	<i>5' RACE 1</i>	-
4	<i>HD Exon 4</i>	<i>3' UTR-51</i>	579
5	<i>HD Exon 4</i>	-	-
6	-	<i>3' UTR-51</i>	-

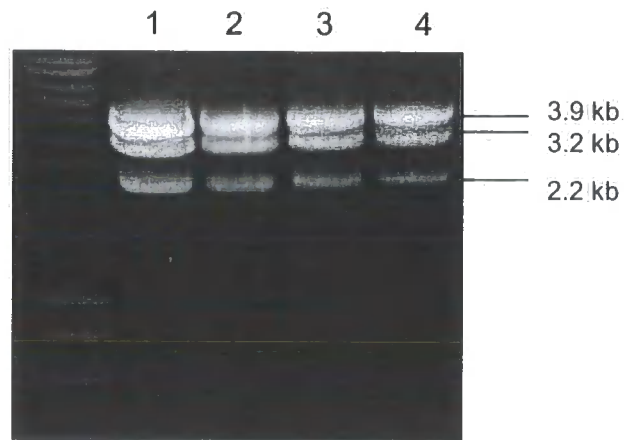
The products obtained by PCR were of the expected sizes (Figure 3.10b), indicating that the *KNAT6* genomic fragment had been amplified.

The 5.4kb product was then cloned directly into the pCR®2.1-TOPO vector (section 2.7.4). Inserts were checked by colony PCR using the *HD Exon 4* and *3' UTR-51* primers and several putative positive colonies were used to prepare plasmids containing the *KNAT6* genomic insert. These plasmids were digested with the restriction enzyme *EcoRI* that cleaves the pCR®2.1-TOPO vector just outwith the cloning site to allow release of the inserted DNA fragment. The *KNAT6* genomic sequence was found to have an internal *EcoRI* site, giving fragments of 2.2 kb and a 3.2 kb fragment on digestion. The size of the pCR®2.1-TOPO vector is 3.9 kb. Figure 3.10c shows that the expected fragment sizes were obtained on digestion with *EcoRI*, indicating that the *KNAT6* genomic sequence had been cloned.

### 3.11 Summary

This chapter describes the development of a 3' RACE strategy that allowed the isolation of a novel homeobox fragment from NAA-treated *Arabidopsis* roots. This novel homeobox gene was found to be a member of the *KN1* family of homeobox genes and has been designated *KNAT6*. Having isolated this fragment, the availability of the complete *Arabidopsis* genome allowed the amplification of the majority of the *KNAT6* coding region by PCR. The extreme 5' end of the transcript was then isolated by 5' RACE. Finally, the complete genomic fragment was amplified from *Arabidopsis* genomic DNA and cloned.

**Figure 3.10c** Digestion of cloned *KNAT6* genomic fragment with EcoR1 confirms the correct sequence has been cloned



Plasmid DNA from four colonies containing the *KNAT6* genomic locus was digested with EcoRI. Two bands (of 2.2kb and 3.2 kb were expected, as well as a 3.9kb band corresponding to the pCR®2.1-TOPO vector

Future chapters will deal with analysis of the *KNAT6* sequence as well as expression and functional analysis.

## Chapter 4 Sequence Analysis of *KNAT6*

This chapter describes the analysis of the *KNAT6* genomic, coding and putative protein sequences as well as the identification of two isoforms of the *KNAT6* transcript that arise from a single genomic locus.

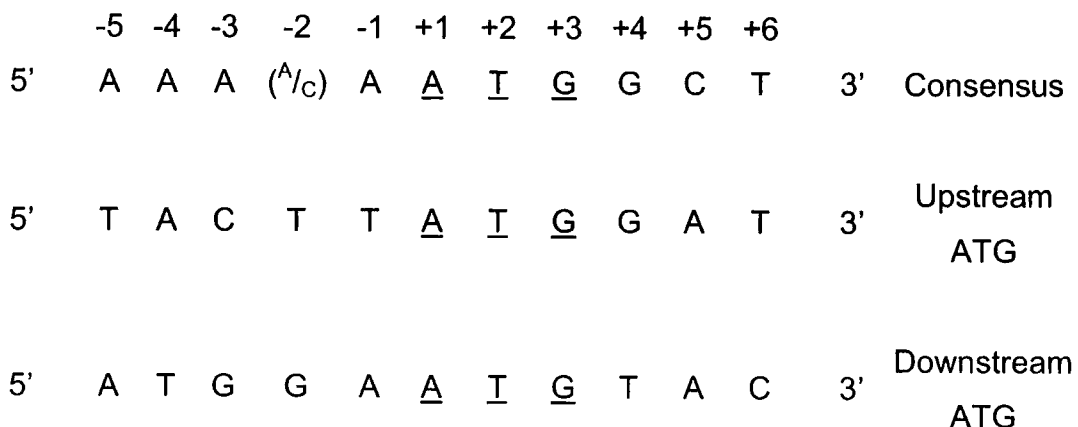
### 4.1 Analysis of the *KNAT6* genomic sequence to confirm that the complete *KNAT6* coding sequence had been isolated

Although the ATG predicted by GenBank was present in the 5' RACE products obtained in section 3.9 indicated that the complete *KNAT6* coding region had been isolated, further analysis on the *KNAT6* genomic region was performed in order to confirm this.

#### 4.1.1 Prediction of the *KNAT6* ATG

Examination of the sequence adjacent to the ATG predicted by GenBank revealed a second in-frame ATG 9 bases upstream. To determine which of these two ATGs was more likely to be the true ATG used for translation of the *KNAT6* protein, the Kozak Scanning Hypothesis (Kozak, 1981) was used to predict which ATG was in the best context for translation initiation.

The consensus sequence for translation initiation has been determined for dicotyledonous plants (Joshi *et al.*, 1997). This consensus sequence was compared with the nucleotide sequences around the two possible *KNAT6* ATGs, with the ATG underlined in each case.



The highest degree of conservation is seen at the -3 and the +4 positions. Although neither sequence fits the consensus exactly, the upstream ATG shares the highly conserved G (67% of examined sequences) at the +4 position, whereas the downstream ATG has a T (12% of examined sequences) at this position. At the -3 position, the upstream sequence contains a C (8% of examined sequences) whereas the downstream sequence contains a G (22% of sequences). Therefore, it is likely that the upstream ATG is the ATG used for translation initiation of the KNAT6 protein.

Figure 4.1.1a shows the complete *KNAT6* mRNA as determined experimentally. The coding sequence has been predicted based on the position of the ATG that is most likely to be used for translation of the KNAT6 protein. The position of the downstream ATG predicted by GenBank (Accession numbers AC007945 and AC005292) as being the likely ATG for translation is also indicated.

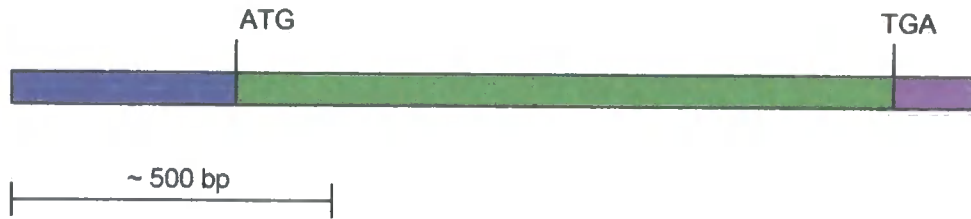
#### **4.1.2 Analysis of the region upstream of the *KNAT6* ATG**

Examination of 1 kb of genomic sequence upstream of the predicted *KNAT6* ATG revealed the presence of five small open reading frames (ORFs) which began with an ATG (Figure 4.1.2a). However, analysis of 4 kb of sequence upstream of the predicted ATG using the NetPlantGene server (<http://www.cbs.dtu.dk/services/NetPGene>, (Hebsgaard *et al.*, 1996)) which predicts splice sites (and therefore intron and exon positions) did not reveal any further likely upstream exons. It is possible that these upstream ORFs play a role in regulation of translation of the KNAT6 protein. This is discussed more in section 8.2.2.

It was concluded that the complete *KNAT6* coding region had been isolated from NAA-treated *Arabidopsis* root.

Recently, a cDNA clone for *KNAT6*, RAFL 14-89-I21 (GenBank Accession BT002930) was isolated. The sequence was available at GenBank (<http://www.ncbi.nlm.nih.gov>). The coding region of this clone supported the *KNAT6* coding sequence isolated in this work. Note that the cDNA clone RAFL19-60-J07 (GenBank Accession AK118326) that was annotated as *KNAT6* at the time of writing was actually the *KNAT7* cDNA.

**Figure 4.1.1a** Experimentally determined KNAT6 mRNA with predicted ATG



- 5' UTR, 364 bp
- Coding sequence based on predicted ATG, 974 bp
- 3' UTR, 137 bp

The ATG predicted by GenBank is underlined

```

ATAACACAGCCTTGGACCTTTCTTAGATATATATGTTAGGAAGGCCTTAT
CTCGACCTATGAAGCCTGAAGCTCCATTGAGCCTTTTAGCATATGTCCT
TTTTCGTAATTATCATTTTATTTTCTTCTCCGTTAACTTTCATATCTTTT
TCTTCCAAAAGAAAATAAATTAAGATCCCTCGAGCCTCTCTCTCTCTA
CACACTCCCATAGAAATAAATATTTTCAAGAACC AAAAAGTTTGTTATAA
GCGGTTTCATATTATTCTTCTTCATCGATTCTTGATTTTGCAAGAAGACA
ATTCAAGAAAGCGATTTAGAAGACGGAGGAGTTCCTACCGGAGATCTTA
TACTTATGGATGGAATGTACAATTTCCATTCCGCCGGTGATTATTCAGA
TAAGTCGGTTCTGATGATGTCACCGGAGAGTCTCATGTTTCCCTCCGAT
TACCAAGCTTTGCTATGTTCCCTCCGCCGGTAAAATCGTGTCTCTGATG
TTTTCGGATCCGACGAGCTACTCTCAGTAGCCGTCTCCGCTTTGTCGTC
GGAGGCGGCTTCGATCGCTCCGGAGATCCGAAGAAATGATGATAACGT
TTCTCTAACTGTCATCAAAGCTAAAATCGCTTGTCATCCTTCGTATCCTC
GCTTACTTCAAGCTTACATCGATTGCCAAAAGGTCGGAGCACCACCGG
AGATAGCGTGTTTACTAGAGGAGATTCAACGGGAGAGTGATGTTTATAA
GCAAGAGGTTGTTCTTCTTCTTGCTTTGGAGCTGATCCTGAGCTTGAT
GAATTTATGGAAACGTA CTGCGATATATTAGTGAAATACAAATCGGATCT
AGCAAGACCGTTTGACGAGGCAACGTGTTTCTTGAACAAGATTGAGATG
CAGCTACGGAACCTATGTA CTGGTGTGAGTCTGCCAGGGGAGTTTCT
GAGGATGGTGTAAATATCATCTGACGAGGAACTGAGTGGAGGTGATCAT
GAGGTAGCAGAGGATGGGAGACAAAGATGTGAAGACCGGGACCTCAA
AGATAGGTTGCTACGCAAATTTGGAAGCCGTATTAGTACTTTAAAGCTT
GAGTTCTCAAAGAAGAAGAAGAAAGGAAAGTTACCAAGAGAAGCAAGA
CAAGCTCTTCTTGATTGGTGGAATCTCCATTATAAGTGGCCTTACCCTA
CTGAAGGAGATAAGATAGCATTAGCTGATGCAACGGGGTTAGACCAA
AACAAATCAACAATTGTTTATAAACCAAAGGAAACGTCATTGGAAGCC
ATCAGAGAATATGCCTTTCGCTATGATGGATGATTCTAGTGGATCATT
TTTACCGAGGAATGAATTTATTTATGGTACTTATTTAACGTTGATTA
GATGGATGTATAATTCTGCCTTGCTTTGCCGACAAAGGAAAAAAGAAA
GAAAGAGTGAAGCATGGACGACACATGAAATGGATCTTACACTCACTCA
CATG
    
```

**Figure 4.1.2a** ORFs upstream of the *KNAT6* ATG

The *KNAT6* ATG is shown in red

The five ORFs which begin with an ATG are shown in blue or underlined

TAATATCTATTTCTAATTGACTCGATTCAATATCATTAGTACT  
ATATTATCTTCTGATATGCGACTTCATTTGTTTTCTTTCTTCT  
GTTCCGTTTTCCACTTGTTGTTAACATTTTCACCTTGTTTCA  
CTATTTGCAATCAAATAAACGATTTATGTAGGTGTATCTATAT  
ATGTTCTTAGGATCATAATAAAAATATATTTTCTACAAAGTTT  
TTCGAAAATATATACATTGGGGATTATTTTTTTAACTGTCT  
ACAGCTCACACATGCATATTATCATATTTGAATGAAGATAAC  
GATACAATGCCGATACTGATACAAATCATTATGTTAGATGCT  
CAATTTGTTTCTATAGGTCCTATAATATACATCAAGTCATC  
AACTATACTTTTTGAAAAGAAAATTACACAGAGCTTTCAAATA  
AGTTGCGTGTAGTTTAGTGGTTATATGACTAGTAGTTATGT  
TACCATCTAAGTGTATTGTCGATGAGAAAAAAGAGTTCAA  
ATAAACTGACATAGTATGCTGGTAAATAATCACACTTTTTCC  
GTTTTTCCATTTTCGTTTTCAATAATATATAATTTTGTTTCTC  
GCCATGTTTCATTGATATTAATAATCTCATGATCATGCAAATT  
CTATCATAACACAGCCTTGGACCTTCTTAGATATATATGTT  
AGGAAGGCCTTATCTCGACCTATGAAGCCTGAAGCTCCATT  
GAGCCTTTTAGCATATGTCCTTTTTTCGTAATTATCATTTTATT  
TTTTCTTCTCCGTTAACTTTCATATCTTTTTTCTTCCAAAAGAA  
AATAAATTAAGATCCCTCGAGCCTCTCTCTCTCTACACAC  
TCCCATAGAAATAAATATTTTCAAGAACCAAAAAGTTTGTTAT  
AAGCGGTTTCATATTATTCTTCTTCATCGATTCTTGATTTTGC  
AAGAAGACAATTCAAGAAAGCGATTTAGAAGACGGAGGAGT  
TCTTACCGGAGATCTTATACTT**ATG**

## 4.2 Positions of *KNAT6* introns and exons

The positions of the exons in the *KNAT6* genomic sequence were determined by alignment with the experimental coding sequence obtained in sections 3.8 and 3.9. The exact intron/exon boundaries were then assigned based on the splice site consensus as follows.

In dicotyledonous plants, the sequence of the 5' and 3' splice sites are conserved and have the following consensus (Croy, 1993):

5' splice site            **AAG:GTAAGT**.....**GCAG:GT**            3' splice site

Bold type indicates the exon bases, standard type indicates the intron bases and the colons indicate the intron/exon boundaries. The GT at the 5' of the intron and the AG at the 3' end of the intron are the most highly conserved positions in the consensus sequence. The genomic sequence for *KNAT6* with the intron and exon positions marked is shown in Figure 4.2a.

NetPlantGene analysis was also carried out using the complete genomic sequence for *KNAT6* including 2 kb of upstream sequence. This confirmed the intron and exon positions shown in Figure 4.2a.

The positions of introns in *KNAT6* are as expected for a Class 1 KNOX gene (see section 1.4.2.1).

## 4.3 The *KNAT6* predicted protein sequence shows conservation with other KNOX family members

The identification of the complete coding sequence for *KNAT6* allowed the protein sequence of this gene to be predicted. Various domains were conserved between this gene and other family members. The *KNAT6* predicted protein sequence contained all of the protein domains previously identified in Class 1 KNOX genes (Figure 4.3a). The roles of these domains were discussed in section 1.4.2.2. The three additional amino acids in the *KNAT6* homeodomain that are characteristic of all the TALE superfamily genes are also indicated on the *KNAT6* predicted protein sequence in Figure 4.3a.

**Figure 4.2a** Positions of exons in KNAT6 genomic sequence

Exons are in red

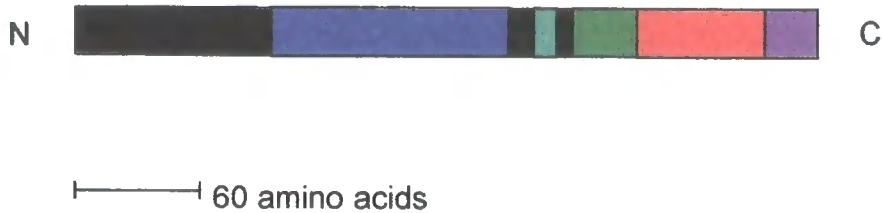
Introns are in black

```
ATGGATGGAATGTACAAATTCATTCCGGCCGGTGATTATTCAGATAAGTC
GGTTCTGATGATGTCAACCGGAGAGTCTCATGTTTCCCTCCGATTACCAAGC
TTTGCTATGTTCCCTCCGCCGGTGAAAATCGTGTCTCTGATGTTTTCCGGATC
CGACGAGCTACTCTCAGTAGCCGTCTCCGCTTTGTCGTCGGAGGCGGCTTC
GATCGCTCCGGAGATCCGAAGAAATGATGATAACGTTTCTCTAACTGTCA
TCAAAGCTAAAATCGCTTGTATCCTTCGTATCCTCGCTTACTTCAAGCTT
ACATCGATTGCCAAAAGGTGATCGTTAACTCTTTCTTTTTTATCACTTAG
ATAAAATCTAGGTTTTACTTTTTAAAGATAAAGATAAAGATTGAGAAGCTT
TGATATTTGATTGTTTTTTTTATAATTTTATGGTTTAACAATTCATAATTT
AGAAACAGGTCGGAGCACCACCGGAGATAGCGTGTTTACTAGAGGAGAT
TCAACGGGAGAGTGATGTTTATAAGCAAGAGGTTGTTCCCTTCTTCTTGCTT
TGGAGCTGATCCTGAGCTTGATGAATTTATGGTCTCTCTTTTTTTCCCTC
GATTTTTTTTCCGATTTTTATTTTTGTTAAAATATTTTTTTTTGGAAATTTTT
GTACTTAAGAAGATAATTTATTATCAGGAAACGTA CTGCGATATATTAGT
GAAATACAAATCGGATCTAGCAAGACCGTTTGACGAGGCAACGTGTTTCT
TGAACAAGATTGAGATGCAGCTACGGAACCTATGTACTGGTGTGAGTCT
GCCAGGGGAGTTTCTGGTATGTCTTAAATTATCCCTCTCTGGTTCGGTCTT
TTAGTGGTCTATTTTGTGGTAGTTCTGAATGATTTCTTTTGATCTTTTTCC
GTGGTTTTTTCATTAATAATATCCTTTCCCTCGATATTTCCATAGGGTTTTGAT
TCATATGACCAGTTTCTGAAAATGATTGGTAGCTTGTGATAGAATAAC
CCTAGGCTTTTGAAGTGATCAGAAAGCAAAATAGATAAAAAATGAAAAA
AAAGAAGATAAACCCCTAGCTACAAGTTTCATTTCCATAGCTATTTTTCCCT
TGATGGGTTTTGTTTTGTGTGTGCTTTTCTTTGGGCACGTTGAAACTCTGG
AGACAAAGATCTGTTTAAAGGTGTTGTGCAATTTTTACTCGTTCATTTAA
TGTTTTAGCCATGGGATTAGGGTGTGGAGTGTGGTGGGATTTCCCTCTC
TTCTTGTGTTGATCTTTGTGCTAATCATACAAATTTACTTTATATCTTTT
TCTCTTCTTCTCTGTGCAAGAAAATGGTGTAGAAAGCAATAAACTTTT
GTGGTAGAGATTCTGATTTTGACGTTTCAGAGGCTTGTGCGTACTGAATG
TTTTTTCAACTTGTTGCTTTTTTCTAGTGAAAAACCAATTGACAGAAAAAC
CTAGTCATAACTTTTTAAACAATATGTGTAGTTGATTTTTCATGAGCTTCTTT
TGCTTCACTTCTCGTTTAAACAATAAGTAAGTATAAGTACTAGTCATAACTC
ATAAGTCGCTTCACTCTTGTTTATGGGTAACAACCTTATTAGGTTACCAGT
TTTTCTAAGACTTCAACTTCTTTTTGGTCAGATGATTATTAATAACCAATAA
GCCATAAGAGTTATTAGCTGTAATTCCTCTTTAAGCTCATTACAGATTCT
CTGGATCGGAATTAATAAGCGTGTTAGATAATTTACGATTAATTTCTG
TTATATCTTAATAACACACCATATAATTTTTCTATCTAATTAATAGGTTA
AAACAATAAAGTTAAAATTGATTTTAAATTTAATATAGAAGTCTACAAA
ACGACATTCTTTGTGAAATAAAAAATTAATCCTGAATTCGACATTTATTAT
GAAGAACGTAACCTTTGGTCTATTTCAAGTTTCAATGATCTGAGAACAAGA
GTAGGGAGATTTTTGTTGATCATCGGAAATAGTATCATTGCCAAGTGGCC
ACTCTTATCTGCATGTTCTTGTGGAGTCTTGTGGACTTATATGTAAGTA
ATAAACCAAAACTGACTCAATTTTGAAGCGATTTAAAAGTCTAGGTTTTA
TGCTTATACATGA
```

ATGAAATGCTTCAAATAAGTGACTTTCTTTGTGGTTTACTGATATTATCTCTT  
TAGACCACATATTGTA CTACA ACTAGCAAAAACATTTGTGGCCATAACAAATC  
AACCGATCAGGTTAGCTAGAAATACTGATCCTTAGGAGTTTTTTTTTAATAC  
AATAAAATAGAAGAAAACTCCAGCTGAAAAGAGTTAGCTGTAAAGAAATGA  
AACTCCATAGATTGGTAGACTTTTTTTCAGCTTTGCAGGAGTTTTCCATTATC  
GTGGTTCGATCTCAAATGCAGGTTCCACTTGTACTTTGGTAATATTGTTTATTG  
GGGAAAAAAGCTGCTGATATATAAAAACATATCAGCTTATCTTTATAAACTA  
ATCGAGAGTTAGCATAGAGTATCAACTGGAAAAGTTGAAAATAGATCGATG  
CAGGTTTTCCATAATGGACGAATGTTTATGATTAATAATTTTAAAATTTGTTC  
AAAGTACAACCTTGCCTTTTGAATGATCTCATCTGTTTTTTTTTTCTTTGGTTG  
TGTGCTTTATTTAACCATCTTTTTCTTTCACCTGAATGAAATCATAACTAAT  
AAAGAAAAAAGAAGCTTACAATTGTTAGACAATATTACATGGGATGCGAT  
GTTATCTACTAGTTTCTCAGTTCAATCATATGCTTGGTTTCTTTCATGTTGATC  
TGATTTAGTAATAACAAGTTGATCACATAGACTTTTGATTTCTCACTTCTTGGT  
TGTTGTGATACGGTAATGCAACTTAGCGAAAGCCCTTCTTTGGACTAGCTAA  
AAAAGCAACACATTTCTTTCTTCTAATGCGTGGTTATCTTGCTACTTAGAGTG  
GATGGTCTCTTATTGACTTTTATAGTCAACATTTGTCTTGTGTCATGCAATAT  
CATCAATGTTACATGTTTGCATATTTGATCTAGAAGATAAGAATACTGCAAC  
GAGAAGAATAGGAACATAGTGCATGATTAGCTTGAATTAGAGGTTCTTTTGG  
TTTTTGTATATAAAGTAAAAGGTGGAAAAGTCACATGGGACTCCCGTGGATTC  
CGCTAATGACCCCACTTTCTCTCTAAGATTTTATTTTTGATTTGGTTAT  
TAAAAAAAAGGAGACATAGGGTCTCTACACACCACAATCAAATCATCT  
ATAAGACTGCGACTATGCTTCTTCTATCTTTCTCAACTCTTTGCCATGCC  
TCTGGTTGCGTTGTTCCCTTGGTGGGTGCTATTATGTCTCTCTGAGGCACGCT  
ACTAGCACGTGTCTACTTGCATGTTACCTTCTTCAGTGAACCCCTATTTTCAA  
GCAGTCAATGCATTGCTGAAAATGTAATAATAATCCCAACCATACAAATA  
TCGTTTTTTGCCATTAACCTGTTACCCTAACTACTCATATGTGTGTAATGTGA  
ACGTAATGGTCTCTATAATATATGATCAGTTCATGTTTTATGCATTTTAGTAT  
ATTTTTATTGGCCTATTTAACATCTCTATTTCCCTCATAATTA CTGTGGCTGCT  
GTAGAAATCTTTTAACTTTTATAATATGTTTATAAACTGACTGAATTGCGTG  
AATTATAAATTGACTGAAATTACCTTGGCTGTTGTAGAAATCTTTTAACTTTT  
TTTAATATATGTTTATAAACTGACTGAAATTGCGTGTATATATTATGTAGTCC  
AGTATTTTGTGTGACTGACTAAATATTTTGACTAAGCACGGTTGCTTGGTCCG  
ACTATATATTCTGTACATAGGCAAACTATTGTA AAAATCAGGTAATGTTCT  
TGAATCGTCTTTGGGTTGAGTTTTGGTGTGTCAGAGAAGCTGGGTAAGTGGGTC  
AGTAGAGTCGTTGGGGCATATATAAATGTCCAAATACATTAAGAAAGA  
GAGAGAGAAAAGGAAATTGAGTTTTGGGGTATCGTGGAGAACATAAATGAG  
AGGTGTAGCGTTATTTCCGGGGGTTACACAACCTCTAAATGGTATTTACAC  
GTGTCATATTGAGATTGGGTAATTAGTAGGCCTAAGGGGGGATGTCTCCTCA  
TGGGGACAAGACTATTAGTCTCTCCTGACAAATGACAATGGAGGTA ACTAT  
TCACTGCGGCGTTTTTTGACTGCTGCACTCAATCGTGTGCGTCTCGATATT  
CTCTACCCCTTACCACTCTTTCTTCTTTCCCTTTTTTGCCTCTTTAGCCACTTA  
GCCGTTTTAGCCGAGAAAGCCCATTTAACTTTTTCATGGTAGTGAATAGTG  
ATAATTCTGTTACATTTACTTGTCTATAACCTATAACCATCTCTGTCTTTGATG  
TCTTTGTATAGTGATAATTCTTGTGAATTTGGTGTAAACAGAGGATGGTGTAA  
TATCATCTGACGAGGAACTGAGTGGAGGTGATCATGAGGTAGCAGAGGATG  
GGAGACAAAGATGTGAAGACCGGGACCTCAAAGATAGGTTGCTACGCAAAT  
TTGGAAGCCGTATTAGTACTTTAAAGCTTGA GTTCTCAAAGAAGAAGAAGAA  
AGGAAAGTTACCAAGAGAAGCAAGACAAGCTCTTCTTGATTGGTGGAACTCT  
CCATTATAAGTGGCCTTACCCTACTGTAAGCAAAAAGCAACACTTGCATGTTT  
TCCGACATAACTAACCCTACACTTATATATAAATGGGTGGTATGAATGTGT  
GTGTACACAGGAAGGAGATAAGATAGCATTAGCTGATGCAACGGGGTTAGA  
CCAAAAACAAATCAACAATTGGTTTATAAACCAAAGGAAACGTCATTGGAA  
GCCATCAGAGAATATGCCTTTCGCTATGATGGATGATTCTAGTGGATCATTCT  
TTTACCGAGGAATGA

### Figure 4.3a KNOX Class 1 family protein domains

#### (i) Protein domains in KNOX Class 1 proteins



**MEINOX** domain (protein-protein interactions)

**GSE** box (for rapid intracellular degradation)

**ELK** domain (nuclear localisation signal)

**homeodomain** (DNA binding domain)

**PEST** sequence (for rapid intracellular degradation)

#### (ii) *KNAT6* predicted protein domains

The key is as in (i) above. The three extra amino acids between loops 1 and 2 on the homeodomain are underlined.

```
MDGMYNFHSAGDYSDKSVLMMSPESLMFPSDYQALL
CSSAGENRVSDVFGSDELLSVAVSALSSEAAASIAPEIR
RNDDNVSLTVIKAKIACHPSYPRLQAYIDCQKVGAPP
EIACLLLEEIQRESVYKQEVVPSSCFGADPELDEFMET
YCDILVKYKSDLARPFDEATCFLNKIEMQLRNLCTGVE
SARGVSEDGVISSDEELSGGDHEVAEDGRQCEDRD
LKDRLLRKFGSRISTLKLEFSKKKKKGKLPREARQALLD
WWNLHYKWPYPTEGDKIALADATGLDQKQINNWFINQ
RKRHWKPSENMPFAMMDDSSGSFFTEE
```

#### **4.4 Phylogenetic analysis of the *KNAT6* predicted protein sequence confirms it is a member of the KNOX class 1 subfamily**

Although the results presented in the previous sections in this chapter indicated that *KNAT6* was a member of the KNOX Class 1 subfamily, phylogenetic analysis using the PHYLIP package of programmes (Felsenstein, 1989) was performed to confirm this.

The GenBank database was used to obtain sequences for those homeobox genes which had an experimentally determined coding sequence. Homeobox genes from all families were included, giving a total of 48 coding sequences. The coding sequences were translated into protein sequence before being aligned using the Clustal programme. The Clustal alignment was then analysed using the PHYLIP suite of programmes (PROTDIST was used to calculate the evolutionary distance between each pair before NEIGHBOUR was used to produce a tree using neighbour-joining) and bootstrap analysis was performed using 100 datasets to give the degree of confidence in each branchpoint.

Figure 4.4a shows the phylogenetic tree and the bootstrap value for the branchpoint between *KNAT2* and *KNAT6* (97). This analysis confirmed that *KNAT6* was a member of the KNOX Class 1 subfamily of homeobox genes and that it was most closely related to *KNAT2*. The other homeobox genes that were included in this analysis were also shown to be in families as expected from previously published phylogenetic analysis (Kerstetter *et al.*, 1994).

#### **4.5 The experimentally determined 5' UTR of *KNAT6* may be truncated**

Although the evidence presented above indicated that the complete *KNAT6* coding region had been identified, there was still the possibility that the experimentally determined 5' UTR was truncated.

To identify putative TATA boxes (consensus sequence TATA<sup>A</sup>/TA<sup>A</sup>/T), the sequence immediately upstream of the experimentally determined 5' UTR was examined. A good candidate TATA box was identified 50 bp upstream of the start of the longest 5' RACE product (Figure 4.5a). As the TATA box would be expected to be approximately 35 bp upstream of the transcription start, it was concluded that the 5' UTR of the *KNAT6* transcript was slightly truncated.



Analysis of 2 kb of genomic sequence upstream of the *KNAT6* ATG using the Softberry (<http://www.softberry.com/berry.phtml?topic=promoter>) promoter prediction website did not select this TATA box, but gives the most likely TATA box as being much further upstream (Figure 4.5a), indicating that the 5' UTR may be even more truncated.

The cDNA clone for *KNAT6*, RAFL14-89-I21 (GenBank Accession BT002930), which was mentioned in section 4.1.2 has a shorter 5' UTR than the 5' UTR determined in this work (Figure 4.5a), and therefore did not help with identification of the complete *KNAT6* 5' UTR.

Despite the possibility that the 5' UTR may be truncated, no further work was carried out to address this as enough 5' UTR had been determined for the purposes of this work (see section 8.2.2).

Analysis of the promoter region was also carried out using the PLACE database ([www.dna.affrc.go.jp/htdocs/PLACE](http://www.dna.affrc.go.jp/htdocs/PLACE), (Higo *et al.*, 1999)), which is a collection of cis-acting regulatory DNA elements from vascular plants. Analysis of 2 kb upstream of the *KNAT6* ATG revealed that there were motifs for a variety of promoter activities in this promoter region (Figure 4.5b).

Two auxin response elements at positions 309 and 1736 (Xu *et al.*, 1997) were identified as well as an ethylene response element (ERE) at position 294 (Montgomery *et al.*, 1993). The 2 kb upstream sequence was also searched for the TGTCTC motif, which is known to direct high auxin inducibility in several species including *Arabidopsis* (Ulmasov *et al.*, 1995, Ulmasov *et al.*, 1997) but this motif was not found in the *KNAT6* promoter. There are also eleven copies of a root motif (Elmayan and Tepfer, 1995) spread over the entire 2 kb region.

#### **4.6 Two isoforms of the *KNAT6* transcript were isolated from NAA-treated *Arabidopsis* root**

During amplification of the complete *KNAT6* coding sequence for use in overexpressing (sense) and antisense constructs (see section 6.1.1 for details of the cloning of the complete *KNAT6* coding region), two different isoforms of the *KNAT6* transcript were isolated from NAA-treated *Arabidopsis* roots.

**Figure 4.5a** Positions of likely TATA boxes

The TATA box identified by eye is shown in **red**

The TATA box selected by Softberry is shown in **orange**

The 5' UTR as determined experimentally is in **blue**

The *KNAT6* ATG is in **green**

The 5' UTR of RAFL14-89-I21 in underlined

TAATATCTATTTCTAATTGACTCGATTCAATATCATTAGTACT  
ATATTATCTTCTGATATGCGACTTCATTTGTTTTCTTTCTTCT  
GTTTCGGTTTTCCAATTGTTGTTAACATTTTCACCTTGTTTCA  
CTATTTGCAATCAAATAAACGATTTATGTAGGTGTATCTATAT  
ATGTTCTTAGGATCATAATAAAAAATATATTTTCTACAAAGTTT  
TTCGAAAA**TATATAT**ACATTGGGGATTATTTTTTTAACTGTCT  
ACAGCTCACACATGCATATTATCATATTTGAATGAAGATAAC  
GATACAATGCCGATACTGATACAAATCATTATGTTAGATGCT  
CAATTTGTTTCTATAGGTCCTATAATATATACATCAAGTCATC  
AACTATACTTTTTGAAAAGAAAATTACACAGAGCTTTCAAATA  
AGTTGCGTGTAGTTTAGTGGTTATATGTAAGTAGTATGT  
TACCATCTAAGTGTATTGTTCGATGAGAAAAAAAAAGAGTTCAA  
ATAAACTGACATAGTATGCTGGTAAATAATCACACTTTTTCC  
GTTTTTTCCATTTTCGTTTTCAATAA**TATATAA**TTTTGTTTCTC  
GCCATGTTTCATTGATATTAATAATCTCATGATCATGCAAATT  
CTATCATAACACAGCCTTGGACCTTTCTTAGATATATATGTT  
AGGAAGGCCTTATCTCGACCTATGAAGCCTGAAGCTCCATT  
GAGCCTTTTAGCATATGTCCTTTTTTCGTAATTATCATTTTATT  
TTTCTTCTCCGTTAACTTTCATATCTTTTTTTCTTCCAAAAGAA  
AATAAATTAAGATCCCTCGAGCCTCTCTCTCTCTACACAC  
TCCCATAGAAATAAATATTTTCAAGAACC AAAAGTTTGTTAT  
AAGCGGTTTCATATTATCTTCTTCATCGATTCTTGATTTTGC  
AAGAAGACAATTCAAGAAAGCGATTTAGAAGACGGAGGAGT  
TCTTACCGGAGATCTTATACTTATG

**Figure 4.5b** Positions of promoter motifs within 2 kb of the *KNAT6* ATG

The auxin response elements at bp 309 and 1736 are shown in blue

The ethylene response element at bp 284 is shown in green

The root boxes are shown in orange

The *KNAT6* ATG is shown in red

```
TACGTTAGGTGATTTAGAGCAACCAATAGTTTGCAAGTACCTTTAAGATGAAA
ATGACTTTCTCTAGTCTTTGAGAAAAAATAAAAAACAGAAACAAAGTTTATAT
TAAAGTAGTATGAAAGAACATGCCACTTTCTTGATTGAAAATTATATGATAGAC
GTA AAAAGCTGTGACAAAAC TAAAAGAATAGTTCCATTTCGAAATATTATAGA
TGCTCTCGTTCTATTTTCTTTTTGGTTAAAGTGCTCGTTTTTTTTCTTGATACTC
TCTTTAAATTACGGCCAATTCATAATTTCAAACCTTAATACATATGTAAAATCAT
TAAATATACCAAATTATGCTTATGTCTATTTTTGTGAATAAATTACATAGTTCAT
TTTCATAAGCTAAAGTCATCATGAATATCAGCATCATCAATTTGGCATAAATT
TCATAAATCATAAATTAGCTAAGACCATTGATTTTGCAGCTCCTATACGCCTA
GACCAGCGTTTATTTTATTCTTAGTTTTATCCACAAACTTGCTTTATACAGAAC
TATTCTAAAGTAAACACTAGCTGATACTATATACTAATTTAATCTTAATTAGAC
GATTTTCCATTAGGGCCTTCTTATCTACTATCTAGGAACGGACCTTCGCTTCT
CGAAACCCATTTTATCCCGTACAATCGAAGTGCCAACATCCGAGTTGGTAA
AAAATTTCTTACTACGTAGTAGTACTAAGAATCACTTATCATATCCATATATT
CTTCACATTTGATTTATTTTACATACCATCATTTGAATATATATGTGTTGATTATCA
TTTTGTTAGTAGTCGTGTTGATAATTTTGTCTGTATCTAGCAACAAATTTAC
AGTGACAAGTATTAATAAATAACCGCTCTTAACTATATATATGTATGTATCAG
CTCACTAGTTGTTTGAACCAGTTCTTGTTTTTCCAGTTTGATATATTTCGATTC
AACATACCCAAAACATCTCTCATATACTGAACTAATATCTATTTCTAATTGACT
CGATTCAATATCATTAGTACTATATTCTTCTGATATGCGACTTCATTTGTTT
TCTTTCTTCTGTTTCGGTTTTCCACTTGTGTTTAAACATTTTACCTTGTTTCAC
TATTTGCAATCAAATAAACGATTTATGTAGGTGTATCTATATATGTTCTTAGGA
TCATAATAAAAATATATTCTACAAAAGTTTTTTCGAAAATATATATACATTGGG
GATTATTTTTTTAACTGTCTACAGCTCACACATGCATATTATCATATTGAAATG
AAGATAACGATACAATGCCGATACTGATACAAATCATTATGTTAGATGCTCAA
TTTGTTTCTATAGGTCCTATAATATATACATCAAGTCATCAACTATACTTTTTG
AAAAGAAAATTACACAGAGCTTTCAAATAAGTTGCGTGTAGTTTGTGGTTAT
ATGTA TAGTAGTTATGTTACCATCTAAGTGTATTGTGCGATGAGAAAAAAG
AGTTCAAATAAACTGACATAGTATGCTGGTAAATAATCACACTTTTTCCGTTTT
TTCCATTTTCGTTTTCAATAATATATAATTTTGTCTCGCCATGTTTCATTGATA
TTAAAATCTCATGATCATGCAAATCTATCATAACACAGCCTTGACCTTTCT
TAGATATATATGTTAGGAAGGCCTTATCTCGACCTATGAAGCCTGAAGCTCCA
TTGAGCCTTTTAGCATATGTCCTTTTTCGTAATTATCATTTTATTTTTCTTCTCC
GTTAACTTTTATATCTTTTTTCTTCCAAAAGAAAATAAATTAAGATCCCTCGAG
CCTCTCTCTCTCTACACACTCCCATAGAAATAAATATTTC AAGAACCAAAA
AGTTTGTATAAGCGGTTTCAATTTATTCTTCTTCATCGATTCTTGATTTTGCA
AGAAGACAATTCAAGAAAGCGATTTAGAAGACGGAGGAGTTCTTACCGGAGA
TCTTATACTATG
```

Sequencing of a number of clones revealed that two different cDNAs had been isolated from NAA-treated root mRNA. The shorter cDNA was designated “original splice” as it corresponded to the GenBank predicted coding sequence (AC007945 and AC005292). The longer cDNA, designated “alternate splice”, contained the extra 6 bases that led to the insertion of 2 amino acids at the start of exon 2. In total, 12 of the shorter original splice isoform and 3 of the longer alternate splice isoform were isolated. As the alternate splice isoform was isolated on more than one occasion, it was concluded that this probably was a true isoform rather than a chance PCR or sequencing error. The number of times each isoform has been isolated by PCR also indicated that the original isoform is more abundant in NAA-treated root tissue.

The cDNA clone for *KNAT6*, RAFL14-89-I21 (GenBank Accession BT002930), mentioned in section 4.1.2 was the shorter, original splice isoform.

Comparison of these two sequences with the GenBank database showed that they both mapped to the single region of chromosome 1 which was assigned to the *KNAT6* gene in section 3.8, rather than mapping to different parts of the genome. In addition, the six extra bases in the alternate coding sequence formed part of the genomic sequence for the *KNAT6*. This indicated that the two isoforms were likely to be alternative transcription products from the same gene rather than products from two different genes. Figure 4.6a shows the site of alternate splicing.

The differential splicing in the *KNAT6* transcript was observed at the 3' splice site, and had the following sequences (refer to section 4.2 for splice site consensus):

3' splice site consensus	<b>GCAG:GT</b>
[a] original isoform 3' splice site	<b>ACAG:GT</b>
[b] alternate isoform 3' splice site	<b>TTAG:AA</b>

The splice site for the shorter original isoform matched the consensus more closely and may help to explain why this isoform appeared to be more abundant

**Figure 4.6a** Site of alternative splicing in the *KNAT6* transcript

(i) Scheme of original and alternative spliced isoforms

Exons are shown in red

Introns are indicated by a solid line

The extra bases in the alternative isoform are shown in blue

Original isoform



Alternative isoform



(ii) Sequence of the alternative splice site at  
the intron 1/exon 2 junction

Key as in part (i) above

```
ATGGATGGAATGTACAATTTCCATTCGGCCGGTGATTATTC
AGATAAGTCGTTTCTGATGATGTCACCGGAGAGTCTCATG
TTTCCTTCCGATTACCAAGCTTTGCTATGTTCCCTCCGCCGG
TGAAAATCGTGTCTCTGATGTTTTCCGGATCCGACGAGCTAC
TCTCAGTAGCCGTCTCCGCTTTGTCGTCGGAGGCCGGCTTC
GATCGCTCCGGAGATCCGAAGAAATGATGATAACGTTTCT
CTAACTGTCATCAAAGCTAAAATCGCTTGTCATCCTTCGTA
TCCTCGCTTACTTCAAGCTTACATCGATTGCCAAAAGGTGA
TCGTTAACTCTTTCTTTTTTATCACTTAGATAAAATCTAGG
TTTTACTTTTTAAAGATAAAGATAAGATTGAGAAGCTTTGAT
ATTTGATTGTTTTTTTATAATTTTATGGTTTAAACAATTTTCA
AATTTAGAAACAGBGTCCGGAGCACCACCGGAGATAGCGTGT
TACTAGAGGAGATTCAACGGGAGAGTGATGTTTATAAGC
AAGAGGTTGTTCTTCTTCTTGCTTTGGAGCTGATCCTGAG
CTTGATGAATTTATGGTCTCTCTTTTTTTCCCTCGATTTT
TTTTCGGATTTTTATTTTGTAAATATTTTTTTTTTGAAAT
TTTTGTACTIONAAGAAGATAATTTATTATCAG
```

(based on the number of times each isoform was isolated) in NAA-treated *Arabidopsis* root.

In support of this, analysis of splice sites in the *KNAT6* genomic sequence using the NetPlantGene server (<http://www.cbs.dtu.dk/services/NetPGene>) indicated that the two alternate spliced products were both likely to occur but that the splice site for the alternate isoform had a lower confidence value (0.95 for the alternative isoform and 0.96 for the original isoform).

The addition of these six bases leads to the addition of a lysine residue followed by a glutamine (Figure 4.6b). These two amino acids are added in the MEINOX domain of the *KNAT6* protein, and therefore may affect the function of this domain (see section 8.4.1).

The evidence presented above indicated that the two cDNAs were produced by differential splicing of the same gene. However, as the *Arabidopsis* genome sequencing project was not completed at the time of this work, it still remained possible that there were two genomic copies of *KNAT6*. To determine the number of copies experimentally, Southern analysis was performed as detailed in section 4.7 below.

Recently, these two isoforms have been submitted to the GenBank database (Semiarti *et al.*, 2001) and are annotated as *KNAT6S* for the original splice isoform (Accession AB072361) and *KNAT6L* for the alternative splice isoform (Accession AB072362).

#### **4.7 A single copy of *KNAT6* is present in the *Arabidopsis* genome**

Comparison of the experimentally determined *KNAT6* sequence with the GenBank database indicated that *KNAT6* was present as a single copy gene in the *Arabidopsis* genome. However, the isolation of two isoforms of *KNAT6* from NAA-treated root mRNA raised the possibility that there may have been a second copy of *KNAT6*. To clarify this, the number of copies of *KNAT6* was determined by Southern analysis.

**Figure 4.6b** Addition of two amino acids to the *KNAT6* predicted protein by alternative splicing

MDGMYNFHSAGDYSKSVLMMSPESLMFPSDYQALL  
CSSAGENRVSDVFGSDELLSVAVSALSSEAASIAPEIR  
RNDDNVSLTVIKAKIACHPSYPRLQAYIDCQK**KQ**VGA  
PPEIACLLLEEQRESVYKQEVVPSSCFGADPELDEFM  
ETYCDILVKYKSDLARPFDEATCFLNKIEMQLRNLCTG  
VESARGVSEDGVISSDEELSGGDHEVAEDGRQRCE  
RDLKDRLLRKFGSRISTLKLEFS**KKKKKGKLPREARQA**  
**LLDWWNLHYKWPYPTEGDKIALADATGLDQKQINNWF**  
**INQRKRHWKPSENMPFAMMDDSSGSFFTEE**

MEINOX domain (unknown function)

GSE box (unknown function)

ELK domain (nuclear localisation signal)

**homeodomain** (DNA binding domain)

PEST sequence (for rapid intracellular degradation)

The additional two bases are shown in **orange**

The probe used for Southern analysis was designed to be as specific for *KNAT6* as possible. As described in the previous sections in this chapter, *KNAT6* shares a high degree of sequence similarity with *KNAT2*. For this reason, the extreme 5' end of the *KNAT6* coding region consisting of part of the 5' UTR and exon 1 was selected as a probe. This region had 42% similarity with *KNAT2*.

The 422 bp probe fragment was amplified using the *Cds For* and *Probe R* primers under standard PCR conditions (section 2.8.1) with the template being the cloned full length cDNA from section 4.6. The resulting product was analysed by gel electrophoresis, and the probe fragment was cut out and purified using the QIAquick® Gel Extraction kit (section 2.4.7).

Restriction endonuclease analysis was performed on the *KNAT6* genomic sequence (including experimentally determined 5' and 3' UTRs) to identify enzymes that cut at various points in relation to the probe. Enzymes that cut outwith the probe should give single bands per copy and enzymes that cut within the probe should give two bands per copy. The enzymes selected are shown in Table 4.7a

**Table 4.7a** Enzymes selected for Southern analysis

Enzyme	Location	Number of bands per copy
Bgl II	within probe	2
Xho I	outwith probe	1
EcoRI	outwith probe	1
Xba I	outwith probe	1
Pst I	outwith genomic sequence, does not cut in promoter	1
Sac I	outwith genomic sequence, cuts in promoter	1

Genomic DNA was extracted from wild type *Arabidopsis* (var. Col-0) using the Phytopure plant DNA extraction kit (section 2.4.3). 500 ng of genomic DNA was digested with each of the enzymes shown in Table 4.7a as described in section

2.4.11. The resulting fragments were separated by gel electrophoresis and transferred to membrane by Southern blotting (section 2.6.1).

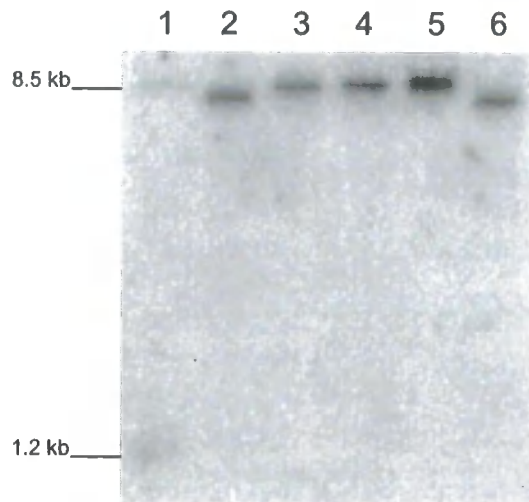
The probe fragment was then radiolabelled with [<sup>32</sup>P]α-dCTP as described in section 2.6.4 and hybridised to the Southern according to the Denhardt's method (section 2.6.6). The membrane was washed to 80% stringency and then exposed to autoradiography film for 18 days (sections 2.6.9 and 2.6.10).

Examination of the autoradiogram (Figure 4.7a) revealed two bands in the lane where BgIII was the restriction enzyme and a single band in each of the other lanes. This is as expected for a single copy gene, and it was concluded that *KNAT6* was present in the *Arabidopsis* genome as a single copy gene and that two isoforms are produced by differential splicing of the *KNAT6* transcript.

#### **4.8 Summary**

The analysis presented in the chapter confirmed that the complete *KNAT6* coding region had been isolated by PCR as described in Chapter 3. This coding sequence was then used to assign the *KNAT6* ATG and exons to the genomic sequence. Several putative TATA boxes were identified in the region upstream of the experimentally determined 5' UTR, and this indicated that the 5' UTR may be slightly truncated. Promoter analysis was also carried out and several motifs for promoter activities were identified. The *KNAT6* predicted protein sequence was also analysed, and this showed that *KNAT6* contains the same domains as other Class 1 KNOX genes. Phylogenetic analysis confirmed that *KNAT6* is a member of this family. Finally, two alternatively spliced isoforms of *KNAT6* have been isolated from *Arabidopsis* NAA-treated root and southern analysis demonstrated that *KNAT6* is a single copy gene.

**Figure 4.7a** Southern analysis to investigate *KNAT6* gene copy number



Lane 1: *Bgl*III, cuts within probe

Lane 2: *Xho*I, outside probe but within *KNAT6* genomic sequence

Lane 3: *Eco*RI, outside probe but within *KNAT6* genomic sequence

Lane 4: *Xba*I outside probe but within *KNAT6* genomic sequence.

Lane 5: *Pst*I outside *KNAT6* genomic sequence

Lane 6: *Sac*I outside *KNAT6* genomic sequence

## Chapter 5 Expression Analysis of *KNAT6*

Expression analysis of the *KNAT6* gene was carried out using northern blot analysis and semi-quantitative RT-PCR to determine the abundance of the *KNAT6* transcript, and reporter gene fusion analysis to determine the activity of the *KNAT6* 5' flanking region.

The putative *KNAT6* promoter was used for the production of p*KNAT6*::GUS and p*KNAT6*::GFP expressing plants. A 2 kb fragment of the *KNAT6* 5' flanking sequence, predicted to contain the promoter, was isolated from Col-0 plants and used to drive the expression of the GUS ( $\beta$ -glucuronidase) and EGFP (Enhanced Green Fluorescent Protein) reporter genes. This allowed the spatial and temporal activity of the putative *KNAT6* promoter to be investigated.

Northern blot analysis and semi-quantitative RT-PCR analysis of the *KNAT6* transcript was carried out in wild type *Arabidopsis* Col-0 plants.

The *KNAT6* coding region was also used to produce protein fusions with the GFP reporter gene under the control of both the Cauliflower Mosaic Virus 35S (CaMV 35S) RNA gene promoter and an alcohol-inducible system to allow the subcellular localisation of the *KNAT6* protein to be investigated.

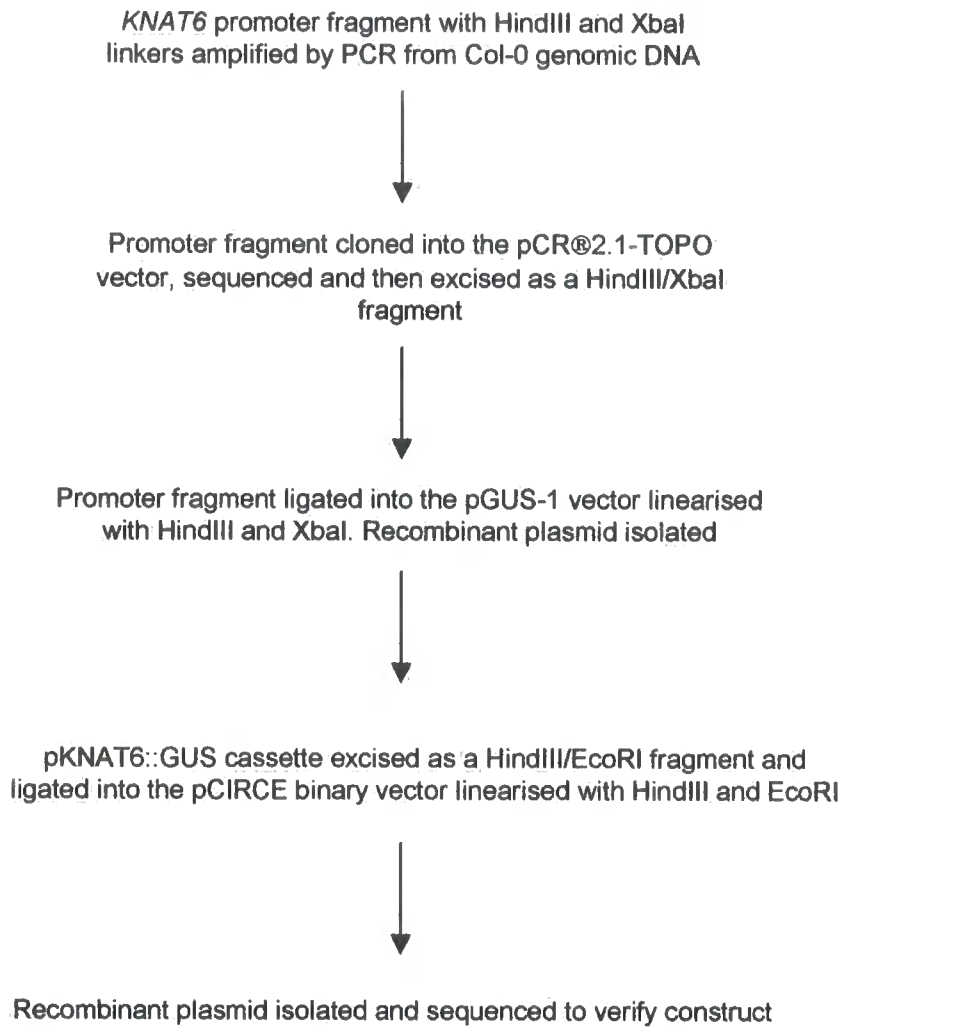
### 5.1 Developmental and hormonal regulation of the *KNAT6* promoter

To investigate the temporal expression of the *KNAT6* promoter in *Arabidopsis* seedling roots, p*KNAT6*::GUS constructs were made. Plants expressing this construct were isolated and GUS activity was examined during seedling development. These plants were then used to examine the promoter activity in response to various exogenous plant hormones.

#### 5.1.1 Cloning of the *KNAT6* putative promoter and production of p*KNAT6*::GUS *Arabidopsis*

p*KNAT6*::GUS constructs were made using the pGUS-1 vector which contained the pUC19 multiple cloning site (MCS) for the insertion of the promoter fragment followed by the GUS coding sequence and the *nos* terminator. The cloning strategy is shown in Figure 5.1.1a. Approximately two kilobases (kb) of

**Figure 5.1.1a** pKNAT6::GUS construct cloning strategy



sequence upstream of the ATG of *KNAT6* were selected as the putative promoter to be used in this work. As most regulatory elements are usually found within 1 kb upstream of the ATG of a gene, many of the cis acting elements which affect *KNAT6* transcription were expected to have been included in this sequence. A large proportion of the 5' UTR was included in the promoter fragment as this may also play a role in the regulation of *KNAT6* transcription (Sieburth and Meyerowitz, 1997). Two primers were designed to amplify the promoter fragment (Figure 5.1.1b). The *Promoter For* primer includes a HindIII site and *Promoter Rev* contains an XbaI site to allow the promoter fragment to be directionally cloned into the pGUS-1 MCS. In addition, two internal primers, *Prom Seq For* and *Prom Seq Rev*, were designed to allow the sequencing of the promoter fragment.

The promoter fragment was amplified from Col-0 genomic DNA prepared using the Phytopure DNA extraction kit (section 2.4.3) using the Expand High Fidelity PCR system (section 2.8.2). The PCR product was analysed by gel electrophoresis (section 2.5.1) and a band of 2.1 kb was obtained as expected (Figure 5.1.1c). The PCR product was cloned directly into the pCR®2.1-TOPO vector (section 2.7.4) and introduced into chemically competent *E. coli*. Putative positive white colonies were checked by colony PCR (section 2.8.1) using the *M13F* and *M13R* primers and a colony containing an insert of the correct size was used to prepare plasmid DNA (section 2.4.1). Plasmid DNA was then sequenced using the universal primers *M13F* and *M13R* as well as the *Prom Seq For* and *Prom Seq Rev* primers mentioned above.

Sequencing revealed that two point mutations had been introduced into the promoter sequence during the PCR amplification. However, as they were both more than 1 kb away from the ATG, it was considered unlikely that they would influence promoter activity greatly, and this cloned promoter region was used. The promoter fragment was released from the pCR®2.1-TOPO vector by digestion with HindIII and XbaI (section 2.7.1). The pGUS-1 vector was also digested with these restriction endonucleases before being dephosphorylated (section 2.7.2) to prevent religation during subsequent ligation steps. Both digests were analysed by gel electrophoresis (Figure 5.1.1d and e). The bands corresponding to the *KNAT6* promoter and the digested pGUS-1 vector were

**Figure 5.1.1b** Promoter fragment used for production of pKNAT6::GUS *Arabidopsis*

The *KNAT6* ATG is shown in red

The *Promoter For* and *Promoter Rev* primer positions are shown in blue

The *KNAT6* 5' UTR is underlined

GTGGCGCATCGCATGGATAACCAGAGAAAGAAAATATTGAACATTTTGATT  
GTGTCTCCAGAAAAATTTGTATTGTTTTTCTCACCAAGAATATGCATATG  
TGAACAAATAATATGTTAAATAAATAAACATATTTTCGTCTGATCTTTGC  
CAATAATAAGAAGGCAAACCTGTTTGTGATATATATATTGTTTTCGCTTTTG  
TGACTTCATATTTATCTAATTTCAAGTCTCCTTTCTTTAACTTAATTTCCCTG  
TGATTATTTATGATACGTTAGGTGATTTAGAGCAACCAATAGTTTGCAAGTA  
CCTTTAAGATGAAAATGACTTTCTCTAGTCTTTGAGAAAAAAAATAAAAACA  
GAAACAAAGTTTATATTAAGTAGTATGAAAGAACATGCCACTTTCTTGATT  
GAAAATTATATGATAGACGTAAAAAGCTGTCGACAAAACATAAAGAATAGT  
TCCATTCGAAATATTATAGATGCTCTCGTTCTATTTTCTTTTTGGTTAAAGT  
GCTCGTTTTTTTTCTTGATACTCTCTTTAAATTACGGCCAATTTCATAATTTCA  
AACTTAATACATATGAAAATCATTAAATATACCAAATTATGCTTATGTCTAT  
TTTTGTGAATAAATTACATAGTTCATTTTCATAAGCTAAAGTCATCATGAATA  
TCAGCATCATCAATTTTGGCATAAATTTCATAAATCATAAATTAGCTAAGAC  
CATTGATTTTGCAGCTCCTATACGCCTAGACCAGCGTTTATTTTATTCTTAG  
TTTTATCCACAAACTTGCTTTATACAGAACTATTCTAAAGTAAACACTAGCT  
GATACTATATACTAATTTAATCTTAATTAGACGATTTTCCATTAGGGCCTTC  
TTATCTACTATCTAGGAACGGACCTTCGCTTCTCGAAACCCATTTTCATCCC  
GTACAATCGAAGTGTCCAACATCCGAGTTGGTAAAAAATTTCTTACTACGT  
AGTAGGTAAGAATCACTTATCATATCCATATATTCTTCACATTTGATTT  
ATTTCATACCATCATTGAATATATATGTGTTGATTATCATTTTGTTAGTAGT  
CGTGTTGATAAATTTGTTCTGTATCTAGCAACAAATTTACAGTGACAAGTA  
TTAAAATAATACCGCTCTTTAACTATATATATGTATGTATCAGCTCACTAGT  
TGTTTGTAACCGATTCTTGTTTTCCAGTTTGATATATTCGATTCAACATAC  
CCAAAACATCTCTCATATACTGAACTAATATCTATTTCTAATTGACTCGATT  
CAATATCATTAGTACTATATTATCTTCTGATATGCGACTTCATTTGTTTTCTT  
TCTTCTGTTCCGTTTTTCCACTTGTTGTTTAAACATTTTACCTTGTTTCACTAT  
TTGCAATCAAATAAACGATTTATGTAGGTGTATCTATATATGTTCTTAGGAT  
CATAATAAAAATATATTTTCTACAAAGTTTTTTCGAAAATATATACATTGGG  
GATTATTTTTTTAACTGTCTACAGCTCACACATGCATATTATCATATTTGAAT  
GAAGATAACGATACAATGCCGATACTGATACAAATCATTATGTTAGATGCT  
CAATTTGTTTCTATAGGTCCTATAATATATACATCAAGTCATCAACTATACTT  
TTGAAAAGAAAATTACACAGAGCTTTCAAATAAGTTGCGTGATGTTAGTG  
GTTATATGACTAGTAGTTATGTTACCATCTAAGTGATTGTGCGATGAGAAA  
AAAAAGAGTTCAAATAAACTGACATAGTATGCTGGTAAATAATCACACTTTT  
TCCGTTTTTCCATTTCTGTTTTCAATAATATAATTTTGTCTCGCCATGT  
TTCATTGATATTAATAAATCTCATGATCATGCAAATCTATCATAACACAGCC  
TTGGACCTTTCTTAGATATATATGTTAGGAAGGCCTTATCTCGACCTATGA  
AGCCTGAAGCTCCATTGAGCCTTTTAGCATATGTCCTTTTTTCGTAATTATCA  
TTTTATTTTTCTTCTCCGTTAACTTTCATATCTTTTTTCTTCCAAAAGAAAAT  
AAATTAAGATCCCTCGAGCCTCTCTCTCTCTACACACTCCCATAGAAAT  
AAATATTTTCAAGAACC AAAAAGTTTGTTATAAGCGGTTTCATATTATTCTT  
CTTCATCGATTCTTGATTTTGCAAGAAGACAATTCAGAAAGCGATTTAGA  
AGACGGAGGAGTTCTTACCGGAGATCTTATACTT**ATG**

**Figure 5.1.1c** 2.1 kb promoter fragment amplified from Col-0 genomic DNA

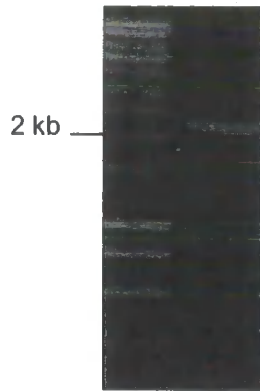


**Figure 5.1.1d** 2.1 kb promoter fragment released from 3.9 kb pCR®2.1-TOPO vector by digestion with HindIII/XbaI

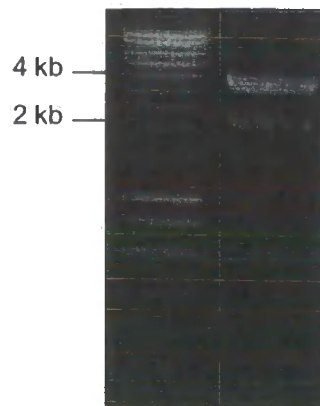
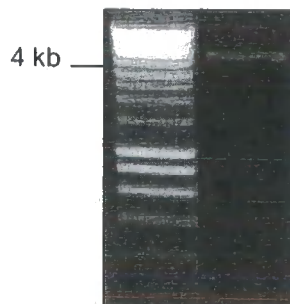


**Figure 5.1.1e** 4.5 kb pGUS-1 vector linearised with HindIII/XbaI

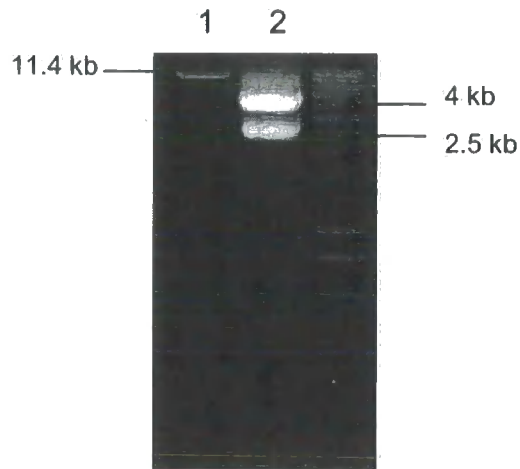


cut out of the gel and purified using the QIAquick® Gel Extraction kit (section 2.4.7). The promoter fragment was then ligated into the pGUS-1 vector (section 2.7.3) and introduced into chemically competent *E. coli* (section 2.7.6). Putative positive colonies were checked by colony PCR using the *Promoter For* and *Promoter Rev* primers (section 2.8.1) and a colony containing an insert of the correct size was used to prepare plasmid DNA (section 2.4.1).

The cassette consisting of the promoter fragment linked to the GUS coding sequence and *nos* terminator was released from the pGUS-1 vector backbone by digestion with HindIII and EcoRI in the same way as above. The pCIRCE binary vector was also digested with these enzymes and dephosphorylated in the same way as pGUS-1. Both digests were analysed by gel electrophoresis (Figure 5.1.1f). Again, the bands corresponding to the 4.1 kb promoter::GUS cassette and the 11.4 kb digested pCIRCE vector were cut out, purified from the gel and the ligated as above. The ligation mix was transformed into chemically competent *E. coli*, and putative positive white colonies were checked by colony PCR using the *Prom Seq For* primer and a primer to the GUS coding sequence, *GUS nested 1*. Positive colonies were used to prepare plasmid DNA (section 2.4.2) that was sequenced with *M13F* and *M13R* primers to confirm that the construct was correct.

The pKNAT6::GUS construct in pCIRCE was introduced into electrocompetent *Agrobacterium tumefaciens* strain C58C3 by electroporation (section 2.2.3) and putative positive colonies were checked using the *Prom Seq For* and *GUS nested 1* primers as above. A single positive colony was selected and used for introduction of the constructs to *Arabidopsis* var. Col-0 by the dipping method (section 2.2.4). Seed from the dipped plants was sown on ½ MS10 SS medium supplemented with 35 mg/L kanamycin sulphate and 200 mg/L augmentin. Kanamycin-resistant seedlings remained green while sensitive seedlings became bleached 7-10 days after germination (DAG) on the selective medium. Kanamycin-resistant transformed (T1) plants were identified and transferred to soil. T2 seed was collected from these plants as individual lines.

**Figure 5.1.1f** Release of pKNAT6::GUS cassette from pGUS-1 and linearisation of pCIRCE



Lane 1 shows the 11.4 kbpCIRCE binary vector linearised with HindIII/EcoRI

Lane 2 shows the release of the 4.1 kb pKNAT6::GUS cassette from the 2.5 kb pGUS-1 vector backbone by digestion with HindIII/EcoRI

### 5.1.2 Isolation and characterisation of pKNAT6::GUS expressing *Arabidopsis*

The number of unlinked T-DNA loci in a hemizygous line can be estimated by the ratio of kanamycin-resistant (Kan<sup>R</sup>) seedlings to kanamycin-sensitive (Kan<sup>S</sup>) seedlings (Table 5.1.2a).

**Table 5.1.2a** Segregation ratios and T-DNA loci numbers

Number of Kan <sup>R</sup> plants	Number of Kan <sup>S</sup> plants	Number of unlinked T-DNA loci
3	1	1
15	1	2
63	1	3
255	1	4

Fifteen of the independent T2 lines that were isolated in section 5.1.1 were surface sterilised and germinated on ½ MS10 SS supplemented with 35 mg/L kanamycin sulphate. Approximately 7 DAG, the plates were scored for the ratio of Kan<sup>R</sup> seedlings to Kan<sup>S</sup> seedlings (Appendix 3, Table 1). This revealed that all of the plants were hemizygous and had a number of T-DNA loci ranging from 1 to 4 (Table 5.1.2b).

**Table 5.1.2b** Number of T-DNA loci in pKNAT6::GUS lines

Line	T-DNA loci	Line	T-DNA loci	Line	T-DNA loci
1	3-4	6	1	11	1
2	1	7	1	12	1
3	1	8	1	13	1
4	1	9	1	14	2
5	1	10	1-2	15	2

Four kanamycin-resistant plants (denoted x.1 to x.4) from each line were removed from the selective plates and transplanted to soil. T3 seed was collected as individuals from each plant.

In order to identify a transgenic line that had a typical root expression pattern, T2 seed from each line was surface sterilised and germinated on ½ MS10 SS medium. 9 days after germination (DAG), whole seedlings were stained histochemically for GUS activity (section 2.3.2). To determine the optimum staining time, seedlings from each line were stained for 3 hours, 6 hours and 16 hours. Microscopic examination of the seedlings indicated that a staining period of 16 hours was required for easy visualisation of GUS activity.

The staining patterns that were obtained are summarised in Table 5.1.2c

**Table 5.1.2c Summary of root expression patterns in 15 independent T2 pKNAT6::GUS transgenic lines**

Line	Root staining pattern	Line	Root staining pattern
1	No staining	9	No staining
2	No staining	10	Hypocotyl and root vasculature, fades towards root tip. Bright at bases of laterals. In petioles of cotyledons and true leaves
3	Hypocotyl and root vasculature, fades towards root tip. At bases of laterals. Hydathodes of cotyledons and true leaves	11	No staining
4	No staining	12	No staining
5	Hypocotyl and root vasculature. Fades towards root tip. Bright at bases of laterals. Cotyledons and true leaves and their petioles	13	Patchy staining in cotyledons.
6	In crown and at bases of laterals.	14	Lateral and main root tips, hypocotyl and shoot apex. In root vasculature, fades towards root tip. At bases of laterals. Cotyledon vasculature.
7	No staining	15	Hypocotyl and petiole vasculature. In root vasculature, fades towards root tip. At bases of laterals
8	No staining		

Based on this screen, three lines that showed a typical root expression pattern were selected for further analysis. These lines were 3, 10 and 15.

The T3 seed harvested from kanamycin-resistant individual plants above was subjected to kanamycin segregation analysis as above to identify lines that were homozygous for the T-DNA insertion. Lines 3.1, 10.1 and 15.1 were shown to be homozygous. The seed was bulked up and T4 seed was used for analysis in sections 5.1.3-5.1.6.

In addition, in order to investigate *KNAT6* promoter activity in other organs, each T2 GUS line was also grown in soil in a controlled environment room, and mature rosette leaves as well as inflorescences (consisting of stems, floral parts, cauline leaves and siliques) were stained. The staining period used was 16 hours. The expression patterns in other tissues are summarised in Table 5.1.2d

**Table 5.1.2d Summary of expression patterns in aerial parts of 15 independent T2 pKNAT6::GUS transgenic lines**

Line	Staining pattern	
	Mature rosette leaves	Inflorescence
1	Petiole vasculature	Anthers in buds, anthers in open flowers and at silique bases
2	No staining	Anthers of buds, stipules on cauline leaves
3	Hydathodes, petiole vasculature	Cauline hydathodes, anthers in buds and open flowers, base of buds, open flowers and siliques
4	No staining	Anthers in some buds
5	Petiole vasculature, faint in hydathodes	Bases of siliques and open flowers. Cauline leaf petioles and main stem. Anthers in buds and open flowers
6	Faint in hydathodes	At silique bases
7	No staining	Very faint in anthers in buds
8	No staining	Anthers in buds
9	No staining	Anthers in buds
10	No staining	At bases of buds, open flowers and siliques. In anthers in buds. Some in anthers and petals of open flowers. In main stem and some in cauline leaf vasculature.
11	No staining	Anthers in buds, some in main stem
12	No staining	No staining
13	No staining	Anthers in buds
14	No staining	In anthers and stigma in buds. At bases of buds, siliques and flowers. In anthers of open flowers.
15	In primary vascular strand	In main stem vasculature and at base of cauline petioles. At base of flowers and siliques. In anthers of open flowers

### 5.1.3 Developmental expression of GUS under the *KNAT6* promoter in seedling roots and hypocotyl

The T4 homozygous seed identified in section 5.1.2 for three p*KNAT6*::GUS lines (3.1, 10.1. and 15.1) showing representative root expression was used to examine the activity of the *KNAT6* promoter during development of *Arabidopsis* seedlings.

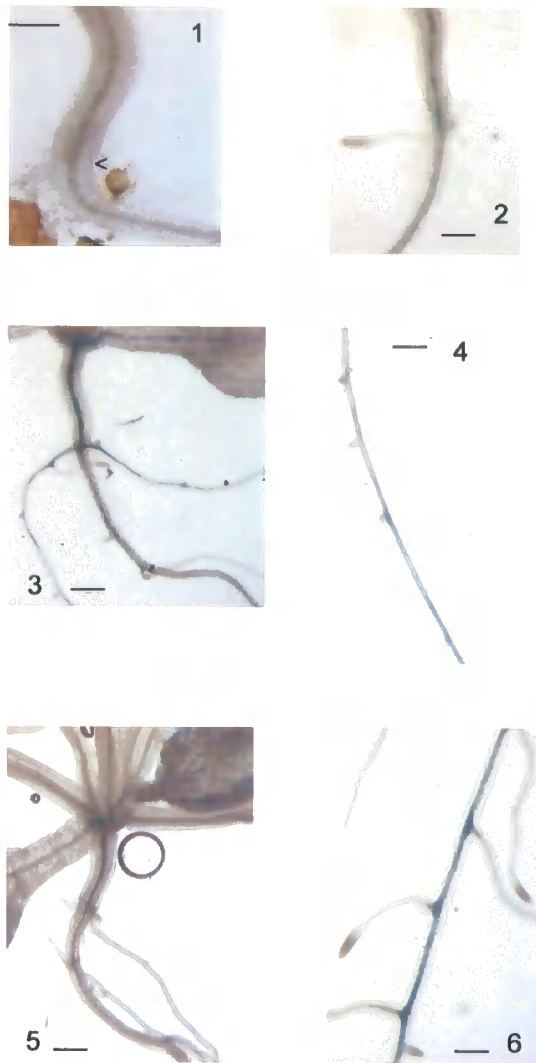
Seed from each of these lines was surface sterilised and germinated on ½ MS10 SS medium. At 3 days after germination (DAG), the seedlings were transferred to ½ MS10 vertical plates (section 2.2.1). Seedlings were removed at 3, 6, 9, 12 and 14 DAG and stained histochemically for GUS activity for 16 hours. The seedlings were then destained in 70% v/v ethanol until the tissue had cleared before being mounted in 50% v/v glycerol and examined by light microscopy (section 2.3.2).

Although the expression patterns observed in the seedlings were similar between the three lines examined, there was variability in the level of staining in seedlings from the same transgenic line at each time point, with a proportion of seedlings showing no staining. However, representative seedlings from each time point are shown in Figure 5.1.3a. In all cases where root expression is observed, the expression appears to be in the inner cell layers (stele).

At 3 DAG, GUS expression was seen around the crown (i.e. at the bottom of the hypocotyl and at the top of the main root). At 6 DAG, expression was seen in the hypocotyl, in the main root and at the bases of lateral roots. The GUS expression in the main root was strongest at the crown and faded towards the root tip. At 9 DAG, GUS expression could be seen in the hypocotyl, as well as in the main root and at the lateral root bases. The expression in the main root extended towards the root tip until just distal to the position of the last lateral roots to emerge (e.g. Figure 5.1.3a (4), (6)). Expression could also be seen in the stele of some older lateral roots and at the bases of secondary lateral roots (e.g. Figure 5.1.3a (3)). By 12 DAG, expression was downregulated in the hypocotyl, at the top of the main root and in older lateral root bases. Expression could still be seen in the bases of some secondary lateral roots, in the main root towards the tip and at the bases of younger primary lateral roots (e.g. Figure

**Figure 5.1.3a** GUS expression in pKNAT6::GUS Line 3.1

Bar approx. 3 mm



- (1) GUS expression in hypocotyl, 3 DAG
- (2) GUS expression in hypocotyl and main root, 6 DAG
- (3) GUS expression in hypocotyl, main root, lateral roots and at lateral root bases, 9 DAG
- (4) GUS expression in main root, 9 DAG
- (5) GUS expression is downregulated in hypocotyl, main root and older lateral roots, 12 DAG
- (6) GUS expression in main root and at young lateral root bases, 12 DAG

5.1.3a (6)). At 14 DAG, the expression pattern was similar to that seen at 12 DAG (data not shown).

In summary, GUS expression was localised in the main root in a broadly similar area to where primary lateral roots were emerging and elongating, but disappeared after the primary lateral roots had reached a certain length. GUS expression was occasionally seen in the stele of older primary lateral roots close to the main root and at the bases of secondary lateral roots. GUS expression is stronger at the lateral root bases than in the stele of the main root. Lateral root primordia and the root tips did not show GUS expression.

#### **5.1.4 Response of the *KNAT6* promoter to plant growth regulators**

As well as examining the expression of the GUS reporter gene over a developmental time course, the response of the promoter to various plant growth regulators was also examined to determine whether the gene might be hormonally regulated.

Seed from each T4 homozygote p*KNAT6*::GUS line identified in section 5.1.2 was surface sterilised and germinated in ½ MS10 SS medium. At 5 days after germination (DAG), seedlings were transferred to ½ MS10 medium supplemented with a different plant growth regulator (Table 5.1.4a). Control seedlings from each line were transferred to ½ MS10 without hormones. Seedlings were removed from this medium at 3, 6 and 9 days post transfer (PT) and stained histochemically for GUS expression for 16 hours. The seedlings were then cleared using 70% v/v ethanol before being mounted in 50% v/v glycerol and examined using a microscope (section 3.2.3).

**Table 5.1.4a Plant growth regulators used to examine promoter activity**

Plant growth regulator	Working concentration	Action
1-NAA	10 $\mu\text{M}$	auxin analogue which enters the cell by diffusion
BA	10 $\mu\text{M}$	cytokinin analogue
ACC	10 $\mu\text{M}$ and 100 $\mu\text{M}$	ethylene precursor
TIBA	25 $\mu\text{M}$	auxin transport inhibitor which inhibits the efflux carrier function
NPA	10 $\mu\text{M}$	auxin transport inhibitor which inhibits the efflux carrier function

Although the expression patterns observed in the seedlings was similar between the three lines examined, there was variability in the level of staining in seedlings from the same transgenic line at each time point. In all cases where root expression is discussed, the expression appears to be in the stele.

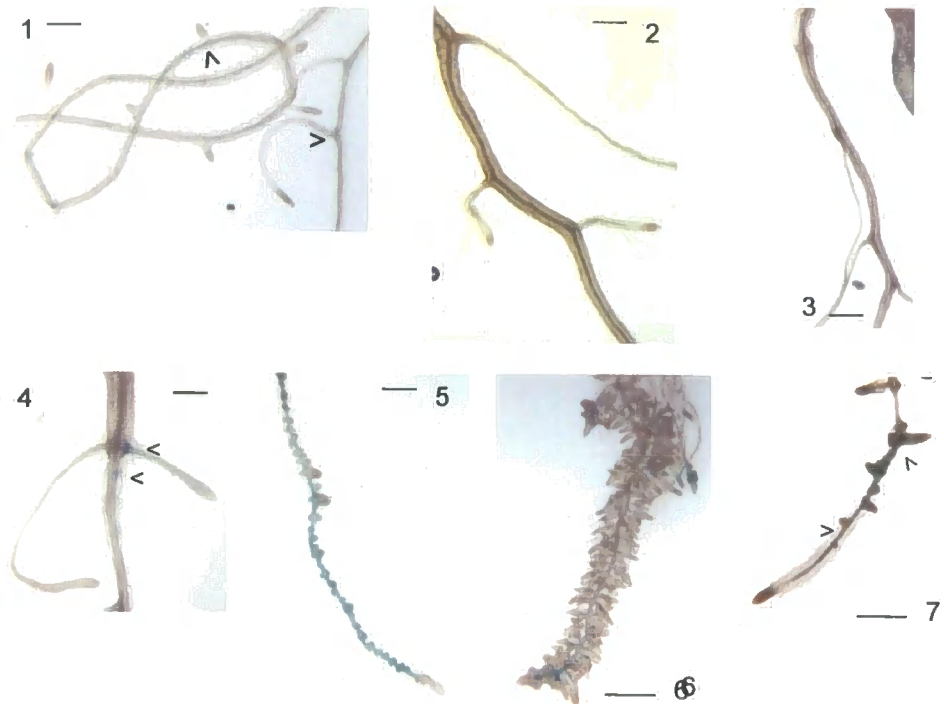
The control seedlings where no exogenous hormone treatment was used show a similar expression pattern to those examined in section 5.1.3 (Figure 5.1.4a (1)). At 3d PT GUS expression was seen in the hypocotyl, main root stele and at the bases of primary lateral roots. GUS expression was strongest at the top of the main root, and faded towards the root tip. GUS expression was downregulated by 6d PT in the hypocotyl, in the stele at the top of the main root and in the bases of older primary lateral roots, but could still be seen in the main root towards the root tip and at the bases of young lateral root. A similar pattern was seen in seedlings 9d PT. Note that there was no expression in the root tips.

Treatment with 10  $\mu\text{M}$  ACC and 100  $\mu\text{M}$  ACC did not lead to any significant alteration in GUS expression (data not shown).

On treatment with BA, some GUS expression could still be seen in the hypocotyl and at the lateral root bases at 3d PT and 6d PT, but this had disappeared by 9d PT (Figure 5.1.4a (2)).

**Figure 5.1.4a** Response of the *KNAT6* promoter to plant growth regulators

Bar approx 3 mm. Arrows indicate low level GUS expression



- (1) GUS expression in main root where young lateral roots developing, 9d PT no treatment
- (2) No GUS expression in main root or at lateral root bases, 9d PT 10  $\mu$ M BA
- (3) No GUS expression in the hypocotyl and main root or lateral root bases, 9d PT 10  $\mu$ M NPA
- (4) GUS expression is down regulated in the hypocotyl, but can be seen at the lateral root base, 9d PT 25  $\mu$ M TIBA
- (5) GUS expression in the main root, lateral roots and main root tip, 3d PT 10  $\mu$ M 1-NAA
- (6) GUS expression at the tip of the main root and in some lateral roots, 9d PT 10  $\mu$ M 1-NAA
- (7) GUS expression of pKNAT6::GUS Line 10.1 in *rty* background, 6 DAG

Treatment with the auxin efflux carrier inhibitor NPA (Figure 5.1.4a (3)) lead to a downregulation of GUS expression by 9d PT whereas treatment with the auxin influx carrier inhibitor TIBA (Figure 5.1.4a (4)) did not lead to a significant decrease compared with untreated seedlings.

Seedlings treated with the synthetic auxin analogue 1-NAA showed GUS expression in the hypocotyl and in the main root stele over the whole length of the root at 3d PT (Figure 5.1.4a (5)). A similar pattern was seen 6d PT. By 9d PT GUS expression had been downregulated in the hypocotyl and in the top of the main root, but was still expressed in the lower part of the main root including the root tip (Figure 5.1.4a (6)). At all time points, GUS expression was seen in some of the lateral root bases. There was no global increase in *KNAT6* promoter activity on treatment with 1-NAA, but the pattern of GUS expression was altered, with expression seen closer to the root tip than in untreated seedlings.

To support the results obtained on treatment of pKNAT6::GUS seedlings with 1-NAA, the pKNAT6::GUS construct was introduced into the *rtv* background by crossing (section 2.2.5). F2 seed obtained for crosses between pKNAT6::GUS lines 10.1 and 15.1 and the *rtv* mutant was surface sterilised and plated onto ½ MS10 SS medium (section 2.1.1). At 6 DAG, the plates were examined and plants exhibiting the *rtv* phenotype were removed and stained histochemically for GUS activity for 16 hours (section 2.3.2). The seedlings were then destained in 70% v/v ethanol before being mounted in 50% v/v glycerol and examined by light microscopy (section 2.3.2).

The GUS expression pattern in the crosses between the *rtv* mutant and the pKNAT6::GUS lines was similar to that seen on treatment with the auxin analogue 1-NAA. GUS expression was seen in the main root, at the bases of lateral roots and at the root tip (Line 10.1, Figure 5.1.4a (7)) or at the bases of lateral roots (Line 15.1, data not shown). In general, the level of GUS expression was lower in the *rtv* cross than on treatment with 1-NAA, especially with Line 15.1. These results will be discussed further in section 8.3.5.

## **5.2 The *KNAT6* promoter is expressed in the phloem poles of the *Arabidopsis* root**

The data presented in section 5.1 indicated that the *KNAT6* promoter was expressed in the seedling root during development, and that this expression appeared to be in the stele of the root. To localise this expression to a specific cell layer(s), plants expressing GFP under the control of the *KNAT6* promoter were examined using Laser Scanning Confocal Microscopy (LSCM). This data was then confirmed by sectioning the p*KNAT6*::GUS lines and by analysing the p*KNAT6*::GUS construct in a mutant background lacking the cell layer in which the *KNAT6* promoter was found to be active.

### **5.2.1 Construction of the promoter::GFP vector pEGFP<sub>er</sub>**

As a suitable vector to allow the production of promoter::GFP fusions was not available, the initial part of this work involved the construction of the promoter::GFP vector pEGFP<sub>er</sub>, which contained the pUC19 multiple cloning site followed by an GFP cassette and the 35S terminator. The GFP cassette consisted of the EGFP coding sequence (Enhanced GFP) (Cormack *et al.*, 1996) with a 5' translational enhancer from Tobacco Etch Potivirus (TEVL). The EGFP coding sequence included an N-terminal signal peptide from chitinase that allowed the GFP to enter the endoplasmic reticulum (ER) as well as a C-terminal KDEL ER retention signal. The targeting and retention of GFP to the ER has been shown to increase intensity of the GFP signal and also to prevent deleterious effects on cells expressing the GFP reporter gene (<http://www.plantsci.cam.ac.uk/Haseloff/GFP/mgfp4.html>). The promoter which was isolated in section 5.1.1 was used to produce a p*KNAT6*::GFP construct which was introduced into *Arabidopsis*. The cloning strategy is shown in Figure 5.2.1a. For the amplification of the CaMV 35S terminator, the primers were 35S T5' (*SacI*) and 35S T3' (*EcoRI*), and for the GFP cassette they were KDEL (*SacI*) and TEVL (*SmaI*).

The Expand™ High Fidelity PCR system (section 2.8.2) was used to amplify the fragments from the p*KAR6*-GFP vector. The reaction products were analysed by gel electrophoresis (section 2.5.1) and bands of the expected sizes (944 bp for the GFP cassette and 240 bp for the 35S terminator) were obtained (Figure 5.2.1b). The bands were cut out and purified using the QIAquick® Gel

**Figure 5.2.1a** Cloning strategy for the production of pEGFPer and pKNAT6::GFP

CaMV 35S terminator with SacI and EcoRI linkers and GFP cassette with SacI and SmaI linkers amplified from the pKAR6-GFP vector



CaMV terminator and GFP cassette cloned into the pCR®2.1-TOPO vector, sequenced and then excised with the appropriate restriction endonucleases



CaMV terminator ligated into pUC19 vector linearised with SacI and EcoRI. Recombinant plasmid isolated



GFP cassette ligated into pUC19::35S terminator linearised with SacI and SmaI. Recombinant plasmid isolated, named pEGFPer



*KNAT6* promoter fragment with HindIII and XbaI linkers ligated into the pEGFPer vector linearised with HindIII and XbaI. Recombinant plasmid isolated



pKNAT6::GFP cassette excised as a HindIII/EcoRI fragment and ligated into the pCIRCE binary vector linearised with HindIII and EcoRI



Recombinant plasmid isolated and sequenced to verify construct

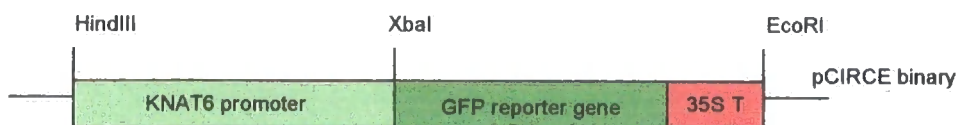
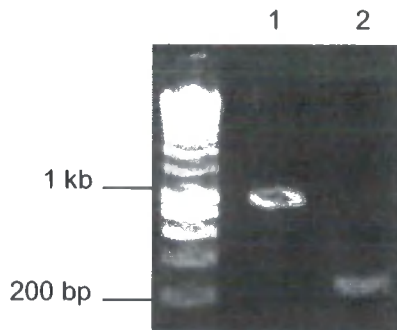


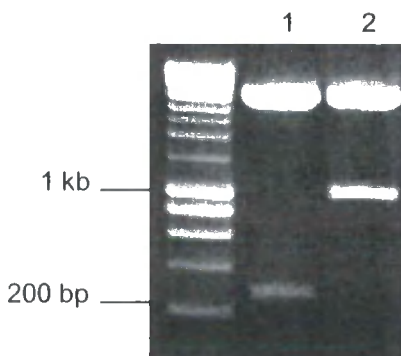
**Figure 5.2.1b** Amplification of 35S terminator and GFP cassette from the pKAR6-GFP vector



Lane 1 shows the 944 bp  
GFP cassette

Lane 2 shows the 240 bp  
35S terminator

**Figure 5.2.1c** Release of 35S terminator and GFP cassette from the pCR®2.1-TOPO vector



Lane 1 shows the 240 bp 35S  
terminator released after  
digestion with SacI/EcoRI

Lane 2 shows the 944 bp GFP  
cassette released after  
digestion with SacI/SmaI

Extraction kit (section 2.4.7) before being cloned into the pCR®2.1-TOPO vector (section 2.7.4) and introduced into chemically competent *E. coli*. Putative positive white colonies were checked by colony PCR (section 2.8.1) using the universal primers *M13F* and *M13R* and those with inserts of the correct size were used to prepare plasmid DNA (section 2.4.1). Sequencing with *M13F* and *M13R* confirmed that no errors had been introduced into the DNA sequence during PCR amplification.

The plasmids were then digested using the appropriate restriction endonucleases (section 2.7.1) to release the 35S terminator (*SacI* and *EcoRI*) and the GFP cassette (*SacI* and *SmaI*) from the pCR®2.1-TOPO vector backbone. At the same time, the pUC19 vector was digested with *SacI* and *EcoRI* and dephosphorylated (section 2.7.2) to prevent religation during the subsequent cloning steps. The digests were analysed by gel electrophoresis (Figures 5.2.1c and d) and the bands of interest cut out and purified as before.

The 35S terminator fragment was then ligated into the digested pUC19 vector (section 2.7.3) and introduced into chemically competent *E. coli*. Putative positive colonies were checked by colony PCR using the 35S T5' (*SacI*) and 35S T3' (*EcoRI*) primers and a colony with an insert of the correct size was used to prepare plasmid DNA.

The pUC19 vector containing the 35S terminator was digested with *SmaI* and *SacI*, dephosphorylated and analysed by gel electrophoresis (Figure 5.2.1e). The linearised vector was cut out and purified before being ligated to the GFP cassette and introduced into chemically competent *E. coli*. Putative positive colonies were checked by colony PCR using the *KDEL* (*SacI*) and *TEVL* (*SmaI*) primers. A colony containing an insert of the correct size was used to prepare plasmid DNA. The completed pEGFPer vector was then sequenced with *M13F* and *M13R* to confirm that it was correct.

### **5.2.2 Production and isolation of pKNAT6::GFP Arabidopsis**

The pEGFPer vector produced in section 5.2.1 was used to produce a pKNAT6::GFP construct which was introduced into *Arabidopsis*. As mentioned above, the promoter fragment that was isolated in section 5.1.1 and used to

**Figure 5.2.1d** 2.7 kb pUC19 linearised with SacI/EcoRI

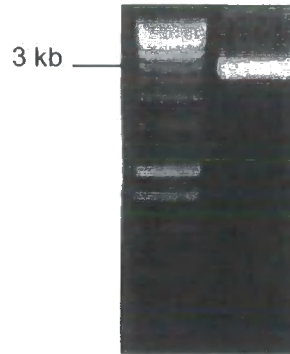
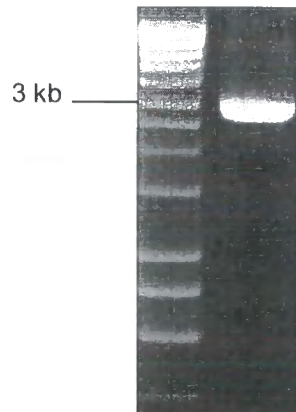


**Figure 5.2.1e** 2.95 kb pUC19::35S terminator linearised with SmaI/SacI



analyse promoter activity using the GUS reporter gene was also used to make the GFP reporter construct (Figure 5.2.1a).

The promoter fragment was released from the pCR®2.1-TOPO vector by digestion with HindIII and XbaI. The pEGFPer vector was also digested with these restriction endonucleases before being dephosphorylated. Both digests were analysed by gel electrophoresis (Figures 5.2.2a and b). The bands corresponding to the *KNAT6* promoter and the digested pEGFPer vector were cut out of the gel and purified using the QIAquick® Gel Extraction kit. The promoter fragment was then ligated into the pEGFPer vector and introduced into chemically competent *E. coli*. Putative positive colonies were checked by colony PCR using the *Promoter For* and *Promoter Rev* primers and a colony containing an insert of the correct size was used to prepare plasmid DNA.

The pKNAT6::GFP cassette was then released from the pEGFPer vector backbone by digestion with EcoRI and HindIII. The binary vector pCIRCE was also digested with these enzymes and then dephosphorylated. Both digests were analysed by gel electrophoresis (Figures 5.2.2c and d) before the bands of interest were cut out and purified as above. The promoter::GFP cassette was then ligated into the digested pCIRCE and introduced into chemically competent *E. coli*. White putative positive colonies were checked by colony PCR using the *Promoter For* and *Promoter Rev* primers. A colony containing an insert of the correct size was used to prepare plasmid DNA (section 2.4.2).

Sequencing with the *M13F*, *M13R* and *Cds For* primers verified that the completed construct was correct before the plasmid was introduced into electrocompetent *Agrobacterium tumefaciens* strain C58C3 by electroporation. Positive colonies were checked by colony PCR as above, and a positive colony was selected and used to introduce the construct into *Arabidopsis* var. Col-0 by the dipping method.

T1 seed from the dipped plants was collected and sown onto ½ MS10 SS medium supplemented with 35 mg/L kanamycin sulphate and 200 mg/L augmentin. Kanamycin-resistant seedlings were transferred to soil 7-10 days after germination (DAG) and T2 seed was harvested as individual lines.

**Figure 5.2.2a** Release of the 2.1 kb promoter fragment from pCR®2.1 -TOPO by digestion with HindIII/XbaI

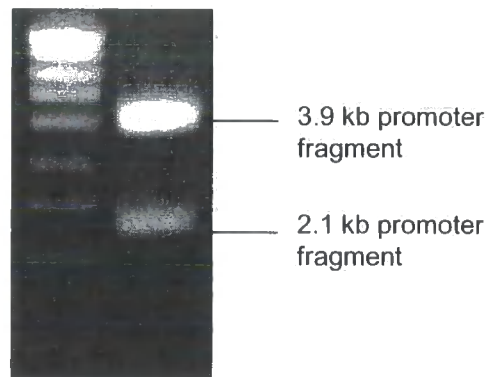


**Figure 5.2.2b** Linearisation of the 3.9 kb pEGFPper vector by digestion with HindIII/XbaI

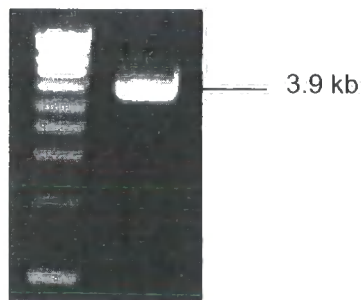


**Figure 5.2.2c** Release of the 3.5 kb pKNAT6::GFP cassette from pEGFPer by digestion with EcoRI/HindIII

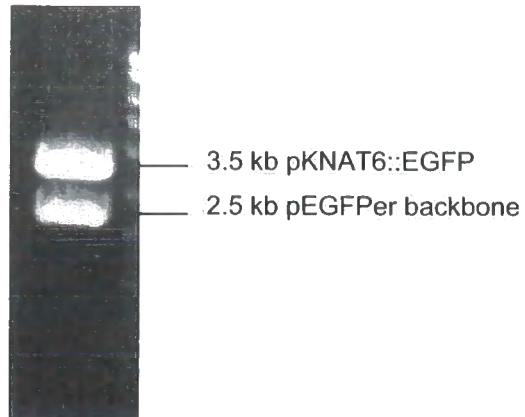
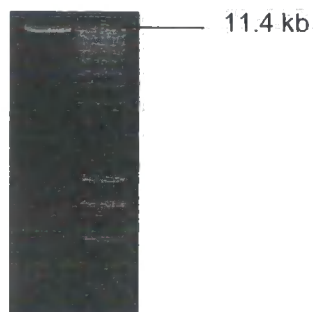


**Figure 5.2.2d** 11.4 kb pCIRCE linearised with EcoRI/HindIII



The T2 seed was sown onto ½ MS10 SS medium supplemented with 35 mg/L kanamycin sulphate to allow the number of segregating T-DNA loci in each line to be estimated (see section 5.1.2 and Table 5.1.2a). The numbers of kanamycin-resistant and kanamycin-sensitive seedlings were counted (Table 2, Appendix 3) and the number of T-DNA loci in each line is shown in Table 5.2.2a below. All of the plants were hemizygous and had a number of T-DNA loci ranging from 1 to 4.

**Table 5.2.2a** Number of T-DNA loci in pKNAT6::GFP lines

Line	Number of T-DNA loci	Line	Number of T-DNA loci
GFP1	2-3	GFP9	1
GFP2	1	GFP10	1
GFP3	1	GFP11	1
GFP4	1	GFP12	1
GFP5	2-3	GFP13	1
GFP6	1	GFP14	1
GFP7	1	GFP15	1
GFP8	1	GFP16	1

Four kanamycin-resistant plants (denoted *a-d*) were removed from each T2 segregation plate and grown on in soil. T3 seed was then collected from each of these individual plants. The T3 seed from plant *a* from each line was subjected to kanamycin selection as before. Resistant seedlings from each line were removed, mounted in 50% v/v glycerol then screened for GFP activity in the root using a fluorescence microscope. A summary of the range of GFP root expression patterns is shown in Table 5.2.2b.

**Table 5.2.2b** Root expression patterns in pKNAT6::GFP lines

Line	Het/Homozygote	Expression pattern
GFP1a	Heterozygote	Present at lateral bases, low in stele
GFP2a	Homozygote	Present at lateral bases, low in stele
GFP3a	Heterozygote	Bright at lateral bases, low in stele
GFP4a	Heterozygote	Very bright in lateral bases and in stele
GFP5a	Homozygote	Present at lateral bases, low in stele
GFP6a	Homozygote	Present at lateral bases, low in stele
GFP7a	Heterozygote	No expression
GFP8a	Heterozygote	No expression
GFP9a	Homozygote	Very bright in lateral bases and in stele
GFP10a	Homozygote	No expression
GFP11a	Homozygote	Present at some lateral bases, not in stele
GFP12a	Heterozygote	No expression
GFP13a	Homozygote	Very bright in lateral bases and in stele
GFP14a	Heterozygote	Present at some lateral bases, not in stele
GFP15a	Heterozygote	No expression
GFP16a	Heterozygote	Very bright in lateral bases and in stele

In all cases, the expression in the inner cell layers (stele) reduced towards the root tip in the same way as the GUS expression observed in section 5.1.2. Overall, the GFP expression seen in these lines was in good agreement with that observed for the pKNAT6::GUS lines isolated in section 5.1.2.

Five lines from the 16 analysed were selected for further analysis based on strong expression of the GFP reporter gene in the stele and at the bases of the lateral roots. These lines were GFP3, GFP4, GFP9, GFP13 and GFP16.

Homozygous lines were required for further analysis of GFP expression (section 5.2.3). Homozygous lines were identified above for GFP9 and GFP13 (GFP9a and GFP13a). For those which were hemizygous (GFP3, GFP4 and GFP16), T3 seed from plants *b*, *c* and *d* was sown on ½ MS10 SS medium supplemented with 35 mg/L kanamycin sulphate as before. Seed from GFP3d,

GFP4*c* and GFP16*d* was shown to be homozygous and was used for analysis in section 5.2.3.

### **5.2.3 Confocal imaging of pKNAT6::GFP *Arabidopsis***

The five homozygous lines that showed strong GFP expression identified in section 5.2.2 were further analysed by Laser Scanning Confocal Microscopy (LSCM).

T3 seed from lines GFP3*d*, GFP4*c*, GFP9*a*, GFP13*a* and GFP16*d* were sown on ½ MS10 SS medium. Six days after germination, seedlings were prepared and analysed by confocal microscopy as detailed in section 2.3.5. Samples were oriented so that the xylem pole was horizontal (Figure 5.2.3a).

The confocal imaging revealed that the GFP was not expressed in the same plane as the xylem poles, but was expressed in the cells immediately above and below the xylem pole (with respect to the sample orientation, refer to Figure 5.2.3a) although it was more difficult to visualise the GFP expression below the xylem pole due to the increase in the thickness of the tissue which had to be penetrated by the laser. In these samples, the cells that are directly above and below the xylem poles are the phloem poles. Seedlings from all five of the lines that were examined showed expression in the same cell layers. Figure 5.2.3b shows examples of GFP expression in the phloem poles of the main root as well as the expression adjacent to a lateral root primordium and an emerged lateral root.

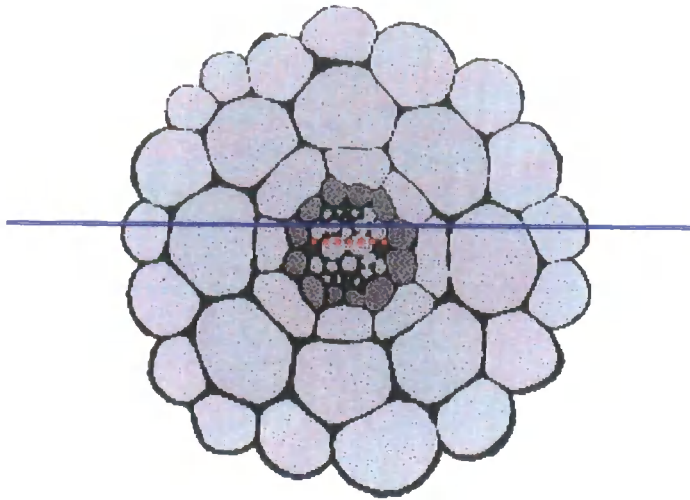
The confocal analysis indicates that the *KNAT6* promoter is active in the phloem poles of the *Arabidopsis* root.

### **5.2.4 Sectioning of pKNAT6::GUS *Arabidopsis* roots**

To support the finding that the *KNAT6* promoter is expressed in the phloem poles of the *Arabidopsis* seedling root, pKNAT6::GUS lines 3.1, 10.1 and 15.1 were used to prepare transverse root sections.

Seed was surface sterilised and sown onto ½ MS10 SS medium (section 2.2.1). Six days after germination (DAG), the seedlings were stained for GUS activity

**Figure 5.2.3a** Orientation of root samples for LSCM



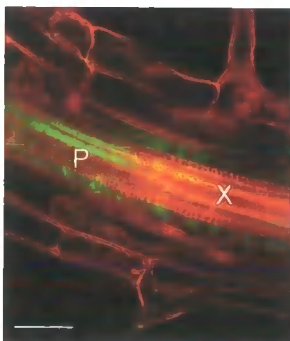
The blue line indicates the plane of optical sections taken during confocal analysis of pKNAT6::GFP transgenic lines

The xylem pole is indicated by the red dotted line

**Figure 5.2.3b** GFP expression in pKNAT6::GFP at 6 DAG

(i) pKNAT6::GFP line 3d

Bar approx. 50  $\mu\text{m}$



P denotes where the phloem pole, with GFP expression, is in the plane of focus.

X denotes where the xylem pole, with no GFP expression, is in the plane of focus

**Figure 5.2.3b cont.** GFP expression in pKNAT6::GFP at 6 DAG

Bar approx. 50  $\mu$ m

**(ii) pKNAT6::GFP line 4c**



1 and 3 indicate GFP expression in the phloem poles above and below the xylem pole

2 indicates the plane of the xylem pole, with no GFP expression



4 indicates GFP expression in the phloem pole above the xylem at the base of a lateral root

5 indicates the plane of the xylem pole at the base of a lateral root with no GFP expression

**(iii) pKNAT6::GFP line 16d**



1 indicates GFP expression in the phloem pole above the xylem pole next to a lateral root primordium

2 indicates the plane of the xylem pole next to a lateral root primordium with no GFP expression

and then embedded in either paraffin (section 2.3.3) or Historesin (2.3.4) before being sectioned. The sections were mounted on slides and examined as described in sections 2.3.3 and 2.3.4. Sections were taken from the main root just below the root/hypocotyl junction for all samples apart from line 3.1 embedded in Historesin, where samples were taken from further down the main root towards the root tip.

Of the samples embedded in paraffin, only those from Line 10.1 were good enough to allow the GUS expression to be localised to a specific cell layer. The GUS expression in these sections was seen in the phloem poles of the root vascular tissue (Figure 5.2.4a). Most interestingly, GUS expression was seen in the phloem poles adjacent to the point where a new lateral root was initiating (Figure 5.2.4a).

The sections from the Historesin embedded roots from lines 10.1 and 15.1 also show that the GUS staining is localised in the phloem poles of the root vascular tissue (Figure 5.2.4b). The sections from line 3.1 which were embedded in Historesin were taken from further down the main root and show more widespread staining in the vasculature (Figure 5.2.4b). The difference in area of the root that was sectioned may account for the variation in the cell type that shows GUS staining.

### **5.2.5 Analysis of pKNAT6::GUS in the *wol* mutant background**

As described in section 1.3.3, the *woodenleg* (*wol*) mutant in *Arabidopsis* is a radial pattern mutant that has fewer cells in the vascular system in comparison with the wild type. All of these cells differentiate to form xylem elements, leading to a lack of phloem cells in the mutant (Scheres *et al.*, 1995).

F2 seed was obtained for crosses (section 2.2.5) between pKNAT6::GUS lines 10.1 and 15.1 and *wol* mutants. F2 seed was surface sterilised and plated onto ½ MS10 SS medium (section 2.1.1). At 6 DAG, the plates were examined and plants exhibiting *wol* phenotype were removed and stained histochemically for GUS activity for 16 hours (section 2.3.2). The seedlings were then destained in 70% v/v ethanol before being mounted in 50% v/v glycerol and examined by light microscopy (section 2.3.2). Wild type seedlings from the *wol* cross were

**Figure 5.2.4a** Paraffin sections from pKNAT6::GUS line 10.1

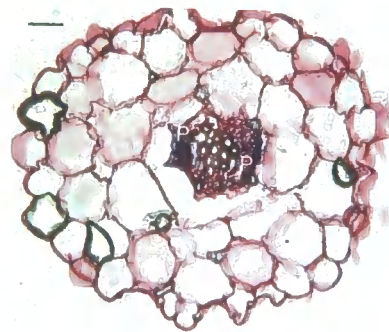
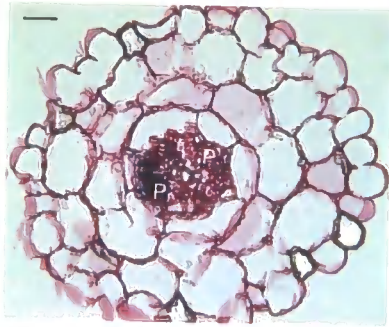
P denotes the phloem poles

X denotes the xylem pole

L denotes initiating lateral root

(i) GUS expression in the phloem poles of the vascular bundle in *Arabidopsis* seedling roots

Bar approx. 20  $\mu$ m



(ii) GUS expression in the phloem poles of the vascular bundle during lateral root initiation

Bar approx. 20  $\mu$ m

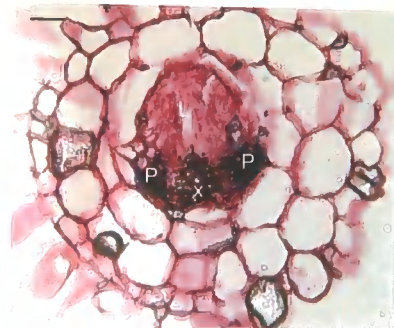


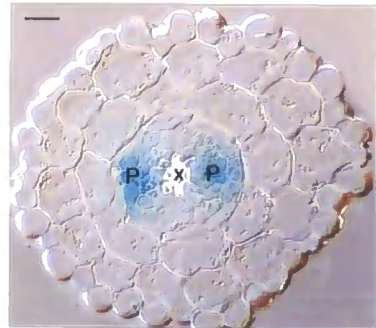
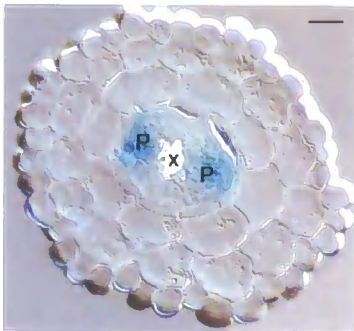
**Figure 5.2.4b** Histoiresin sections from pKNAT6::GUS lines

P denotes the phloem poles

X denotes the xylem pole

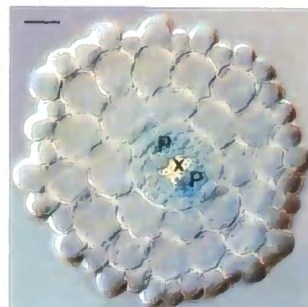
(i) pKNAT6::GUS 10.1

Bar approx. 10  $\mu$ m



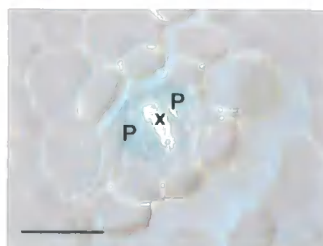
(ii) pKNAT6::GUS 15.1

Bar approx. 10  $\mu$ m



(iii) pKNAT6::GUS 3.1

Bar approx. 15  $\mu$ m



removed and stained in the same way to act as a control showing GUS expression in a wild type background. Representative seedlings from the crosses are shown in Figure 5.2.5a.

The expression patterns in the wild type plants were as described in section 5.1.3 i.e. expression was seen in the hypocotyl, main root phloem poles and at the bases of the lateral roots.

No GUS expression was seen in root or hypocotyl when pKNAT6::GUS was introduced into the *wo1* background. Occasionally, GUS expression was detected in the cotyledons of crosses using pKNAT6::GUS 10.1. The presence of the GUS gene in F2 progeny was confirmed by the presence GUS staining in seedlings with a wild type phenotype. The expression pattern of the *KNAT6* promoter in relation to possible gene function is discussed in Chapter 8.

### **5.3 Analysis of *KNAT6* transcript levels**

Analysis of the *KNAT6* transcript was carried out using two different methods: northern analysis and Reverse Transcriptase-mediated PCR (RT-PCR).

#### **5.3.1 Northern analysis of the *KNAT6* transcript in different tissues**

*Arabidopsis* var. C24 seeds were surface sterilised and grown on ½ MS10 SS medium (section 2.2.1). Whole seedlings were harvested at 3 days after germination (DAG), 5 DAG and 9 DAG and stored at -80°C until required for RNA extraction. In addition, at 14 DAG, roots and aerial parts from seedlings were harvested and stored as above.

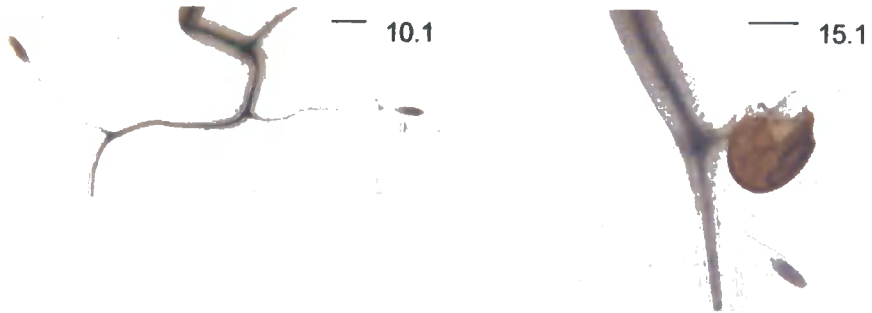
Wild type C24 seeds were also sown on soil and grown in a controlled-environment room (section 2.2.2). Mature rosette leaves, cauline leaves, stems, flowers and siliques were harvested from these plants and stored at -80°C until required for RNA extraction.

RNA was extracted from the tissues according to the Logeman RNA extraction method detailed in section 2.4.5. 20 µg of total RNA from each tissue was then subjected to formaldehyde gel electrophoresis (section 2.5.2) before being stained with ethidium bromide to allow visualisation of the RNA (section 2.5.3

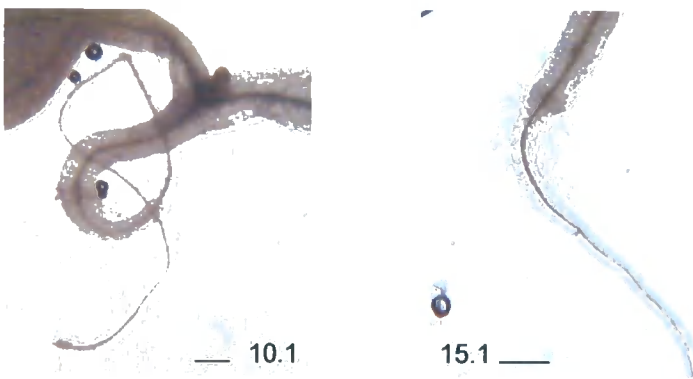
**Figure 5.2.5a** Expression of pKNAT6::GUS in the *wo/* background

Bar approx. 3 mm

(i) GUS expression in pKNAT6::GUS lines, 6 DAG



(ii) GUS expression in of pKNAT6::GUS in *wo/* background, 6 DAG



and Figure 5.3.1a). The RNA was then transferred to membrane by northern blotting (section 2.6.2).

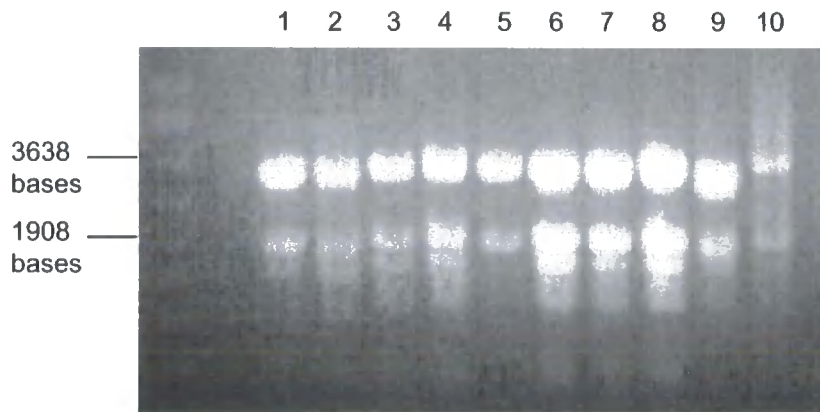
As a loading control, the membrane was first hybridised with a probe corresponding to the *ACTIN1* (*ACT1*) transcript. The probe was prepared by amplification from pCR<sup>®</sup>2.1::ACT using the *ACT For* and *ACT Rev* primers. The resulting band was purified from an agarose gel (section 2.4.7) before being labelled with [<sup>32</sup>P]α-dCTP (section 2.6.4). Prehybridisation and hybridisation was carried out according to the Denhardt's protocol (section 2.6.7). The blot was then washed to 90% stringency (section 2.6.9) and exposed to autoradiography film for 3 days. The autoradiograph is shown in Figure 5.3.1a.

After autoradiography, the blot was stripped as detailed in section 2.6.11. The blot was then rehybridised with a *KNAT6*-specific probe. The original probe sequence was the same as that used for genomic Southern analysis as described in section 4.7 (i.e. the 5' end of *KNAT6* consisting of the 5' UTR and exon 1 amplified by PCR from the cloned full length cDNA using the *Cds For* and *Probe R* primers under standard PCR conditions). This probe was chosen for its specificity to the *KNAT6* transcript. The PCR fragment was purified from an agarose gel and labelled with [<sup>32</sup>P]α-dCTP in the same way as for the *ACT1* probe. After prehybridisation and hybridisation as above, the blot was washed to 90% stringency and exposed to autoradiography film for 4 weeks.

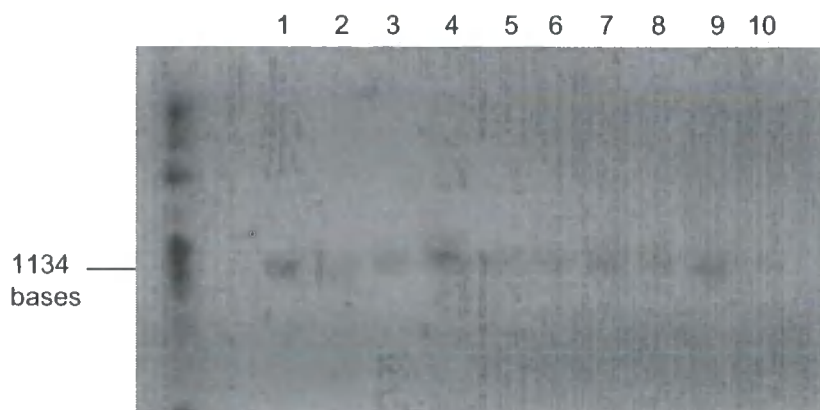
Upon development of the autoradiogram, no signal could be seen (data not shown). It was thought possible that the *KNAT6* transcript was present at low levels, and that use of a longer probe may allow its detection. Therefore, the full length original splice coding sequence from section 4.6 was used as a probe. The probe was prepared by amplification of the cloned fragment by PCR using the *Cds For* and *3' UTR-116* primers. The resulting PCR product was purified from an agarose gel and then labelled with [<sup>32</sup>P]α-dCTP in the same way as above. Prehybridisation and hybridisation was carried out using the Denhardt's system. In addition, the hybridisation protocol was modified to include 10% w/v polyethylene glycol (PEG) 8,000 MW as a volume excluder to increase the sensitivity of the hybridisation. The blot was then washed to 85% stringency exposed to autoradiography film for 4 weeks. On development of the

**Figure 5.3.1a** Northern analysis of transcripts in *Arabidopsis* tissues

(i) Gel electrophoresis of RNA samples used for northern analysis



(ii) Hybridisation of RNA samples from *Arabidopsis* tissues with the *ACT1* probe



autoradiogram, no bands could be detected (data not shown) and it was concluded that the *KNAT6* transcript was below the level of detection.

### 5.3.2 RT-PCR analysis of the *KNAT6* transcript in seedlings

As mentioned in section 5.3.1, the *KNAT6* transcript was not detected on a northern blot using 20 µg of total RNA from various tissues, including some samples from seedlings. Therefore, semi-quantitative RT-PCR was used to determine *KNAT6* transcript levels in seedlings over a developmental time course.

Root and aerial tissue was harvested from *Arabidopsis* Col-0 seedlings grown on ½ MS10 SS medium at 3 DAG, 6 DAG, 9 DAG, 12 DAG and 14 DAG. These time points were the same as those used for the GUS staining experiments detailed in section 5.1.3. RNA was extracted from the tissue samples using the RNeasy kit (section 2.4.6) before being quantified spectrophotometrically (section 2.4.10).

As mentioned in section 2.12, semi-quantitative RT-PCR relies on the selection of a standard transcript that acts as a “loading control” with which to compare the gene of interest. The loading control should be expressed at the same level in each of the tissues of interest. For this work, the *ACT1* transcript (*ACTIN1*) was selected. This gene is expressed at low but equal levels in root and aerial vegetative parts of *Arabidopsis* seedlings (An *et al.*, 1996).

Primers with similar annealing temperatures that give products of similar lengths are used to amplify the control gene and the gene of interest from a standard amount of RNA. The amplification of *ACT1* was carried out using *ACT For* and *ACT Rev* primers and the amplification of *KNAT6* used *HD Exon 1* and *HD Exon 4 Rev* primers. These primers were designed around introns to allow PCR products from contaminating genomic DNA to be distinguished from product from the *KNAT6* or *ACT1* transcripts (Table 5.3.2a).

**Table 5.3.2a** Sizes of PCR products from cDNA and genomic DNA templates

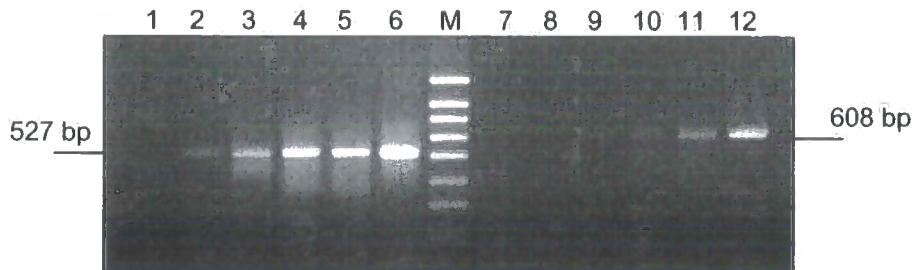
Gene	Primers	cDNA product size	Genomic product size
<i>ACT1</i>	<i>ACT For</i> and <i>ACT Rev</i>	527 bp	638 bp
<i>KNAT6</i>	<i>HD Exon 1</i> and <i>HD Exon 4 Rev</i>	608 bp	4518 bp

Before the relative amounts of the *ACT1* and *KNAT6* transcripts in the samples can be determined, the number of cycles where PCR amplification is in the exponential stage must be determined. The RNA sample obtained from *Arabidopsis* aerial parts harvested 6 DAG was used for cycle quantification.

Cycle quantification was carried out according to the method given in section 2.12. The RNA was first treated with DNase to remove any contaminating DNA. Although the primers amplify products of different sizes from DNA and RNA, amplification from DNA would compete with that from RNA and may alter the results. After DNase treatment, five identical reactions for each primer pair (*ACT For* + *ACT Rev* and *HD Exon 1* + *HD Exon 4 Rev*) were set up. Each reaction contained 1 µg of RNA. In addition, a negative control reaction for each primer pair where the AMV reverse transcriptase was omitted was also prepared. This negative control acted to show that none of the other components of the reaction mixture were contaminated with either of the transcripts of interest.

The reactions were then subjected to amplification as detailed in section 2.12. The PCR machine was programmed for 40 cycles of amplification as detailed in section 2.12. However, a single sample for each primer pair was removed after 20, 25, 30 and 35 cycles. The remaining samples as well as the negative controls were left until the run was complete, giving 40 cycles amplification in total. 10 µl of each PCR product was then analysed by gel electrophoresis (Figure 5.3.2a). The negative controls showed no product as expected and indicated that there was no contamination in the system. Amplification in the exponential phase was seen between 20 and 30 cycles for the *ACT1* transcript and between 30 and 40 cycles for *KNAT6*. Therefore, *ACT1* transcript quantification was carried out with 25 cycles amplification and *KNAT6* transcript quantification was carried out with 35 cycles amplification.

**Figure 5.3.2a** Cycle quantification from amplification of *ACT1* and *KNAT6* transcripts from Arabidopsis RNA



Lanes 1 and 7 show the -RT negative controls with 40 cycles amplification.

The other samples are as follows:

Lane	Sample
2	<i>ACT1</i> transcript, 20 cycles
3	<i>ACT1</i> transcript, 25 cycles
4	<i>ACT1</i> transcript, 30 cycles
5	<i>ACT1</i> transcript, 35 cycles
6	<i>ACT1</i> transcript, 40 cycles
8	<i>KNAT6</i> transcript, 20 cycles
9	<i>KNAT6</i> transcript, 25 cycles
10	<i>KNAT6</i> transcript, 30 cycles
11	<i>KNAT6</i> transcript, 35 cycles
12	<i>KNAT6</i> transcript, 40 cycles
M	size markers

2 µg of each of the 10 RNA samples prepared as detailed above were treated with DNase as before. 1 µg of RNA was used in a RT-PCR reaction using the *ACT1* primers with 25 cycles of amplification and 1 µg was used in a RT-PCR reaction using the *KNAT6* primers with 35 cycles of amplification. 10 µl of each PCR product was analysed by gel electrophoresis (Figure 5.3.2b). To verify that the correct transcript had been amplified from the RNA, the product obtained with the *ACT1* primers and the *KNAT6* primers using RNA from *Arabidopsis* aerial parts harvested 3 DAG was sequenced with the appropriate forward primer.

The *ACT1* transcript that was amplified was constant in the samples, indicating that the same amount of RNA was used in each sample. The amount of *KNAT6* transcript that was amplified was also constant in each sample. This indicated that *KNAT6* is expressed at similar levels in root and aerial tissues in seedlings between 3 and 14 days after germination (DAG).

The agreement between the analysis of the *KNAT6* transcript levels with the GUS histochemical analysis carried out in section 5.1.3 will be discussed more in section 8.3.4.

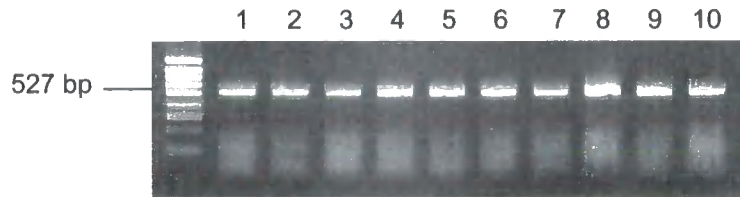
#### **5.4 Localisation of *KNAT6* protein using GFP::*KNAT6* protein fusions**

The cell type in which the *KNAT6* promoter was active was investigated using the GUS and GFP reporter genes (sections 5.1.5 and 5.2.3). However, there is evidence that both the transcript and protein of the class 1 *KNOX* gene *KN1* are trafficked (section 1.4.2.4). To investigate the localisation of the *KNAT6* protein in a particular cell type, as well as its subcellular localisation, constructs for the expression of C and N terminal *KNAT6*::GFP protein fusions were made and introduced into *Arabidopsis*.

The C terminal and N terminal protein fusions of the GFP reporter gene to *KNAT6* were made using different systems as detailed below.

**Figure 5.3.2b** Analysis of transcript levels in *Arabidopsis* seedlings

(i) *ACT1* transcript after 25 cycles amplification in *Arabidopsis* seedling tissues



(ii) *KNAT6* transcript after 35 cycles amplification in *Arabidopsis* seedling tissues



Lanes for (i) and (ii) are as follows

Lane	Sample
1	3 DAG seedling aerial parts
2	3 DAG seedling roots
3	6 DAG seedling aerial parts
4	6 DAG seedling roots
5	9 DAG seedling aerial parts
6	9 DAG seedling roots
7	12 DAG seedling aerial parts
8	12 DAG seedling roots
9	14 DAG seedling aerial parts
10	14 DAG seedling roots

#### 5.4.1 Production of plants expressing a C terminal *KNAT6*::GFP protein fusion

The C terminal fusion was made using the p35S::*fusion-GFP* vector. This vector contained the CaMV 35S promoter to drive expression of the fusion protein followed by a small multiple cloning site upstream of the coding sequence for smGFP (Davis and Vierstra, 1998) and the CaMV 35S terminator. The smGFP does not contain an ATG, so allowing translation of a single protein consisting of the *KNAT6* and GFP coding sequences. An overview of the strategy is shown in Figure 5.4.1a.

Primers (*GFP-RE2-F* and *GFP-RE2-R*) were designed to allow the amplification of the *KNAT6* coding region. These primers included *Sma*I sites to allow cloning into the p35S::*fusion-GFP* vector. A small part of the *KNAT6* 5' UTR (downstream of any ORFs which start with an ATG) was included in the construct. The reverse primer did not include the *KNAT6* stop codon and was designed to ensure that the *KNAT6* coding sequence was in frame with the GFP coding sequence. The positions of the primers in the *KNAT6* transcript are shown in Figure 5.4.1b.

The primers were used to amplify the *KNAT6* coding region from the original splice fragment that was cloned in section 4.6 using the Expand™ High Fidelity PCR system (section 2.8.2). The PCR products were analysed by gel electrophoresis (section 2.5.1) and a band of 945 bp was obtained as expected (Figure 5.4.1c). The band was cut out and purified using the QIAquick® Gel Extraction kit (section 2.4.7) before being cloned into the pCR®2.1-TOPO (section 2.7.4). The ligation mix was introduced into chemically competent *E. coli* and white putative positive colonies were checked by colony PCR (section 2.8.1) using the universal primers *M13F* and *M13R*. A colony containing an insert of the correct size was selected and used to prepare plasmid DNA (section 2.4.1).

The plasmid containing the *KNAT6* coding sequence was sequenced using the *M13F* and *M13R* primers to confirm that no errors had been introduced during the PCR amplification. This plasmid was then digested with *Sma*I (section 2.7.1) to release the insert. At the same time, the p35S::*fusion-GFP* vector was

**Figure 5.4.1a** C terminal KNAT6::GFP protein fusion construct cloning strategy

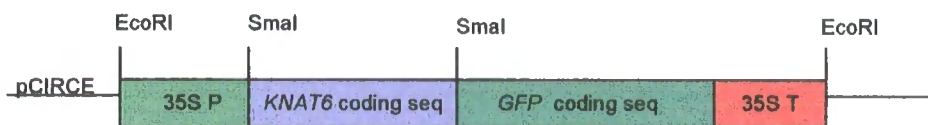
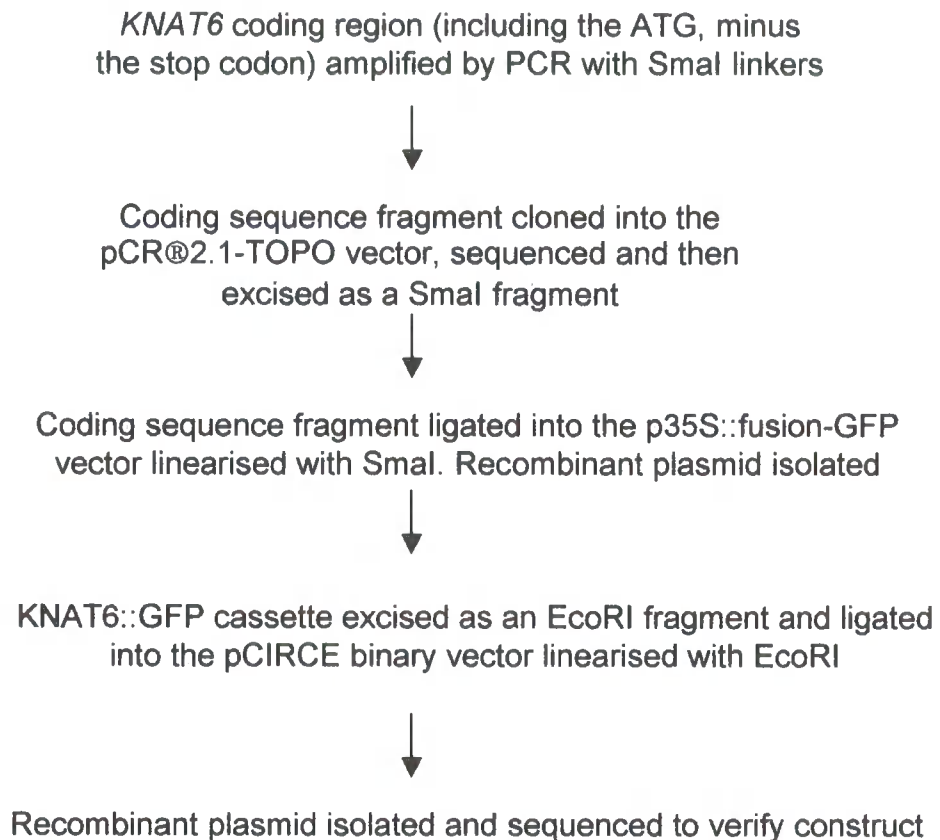


**Figure 5.4.1b** KNAT6 coding region used for C terminal  
KNAT6::GFP protein fusions

The upstream ORF is shown underlined

The *KNAT6* ATG is shown in **red**

The GFP-RE2-F and GFP-RE2-R primer are  
shown in **green**

The *KNAT6* stop (TGA) is shown in **orange**

GAGCCTTTTAGCATATGTCCTTTTTCGTAATTATCATTTTATTTTC  
TTCTCCGTTAACTTTTCATATCTTTTTCTTCCAAAAGAAAATAAATT  
AAGATCCCTCGAGCCTCTCTCTCTCTACACACTCCCATAGAAA  
TAAATATTTTCAAGAACC AAAAGTTTGTTATAAGCGGTTTCATAT  
TATTCCTTCATCGATTCTTGATTTTGCAAGAAGACAATTCAAGA  
AAGCGATTTAGAAGACGGAGGAGTTCTTACCGGAGATCTTATAC  
TT**ATG**GATGGAATGTACAATTTCCATTCCGGCCGGTGATTATTCAG  
ATAAGTCGGTTCTGATGATGTCACCGGAGAGTCTCATGTTTCCTT  
CCGATTACCAAGCTTTGCTATGTTCCCTCCGCCGGTGAAAATCGT  
GTCTCTGATGTTTTCGGATCCGACGAGCTACTCTCAGTAGCCGT  
CTCCGCTTTGTGCTCGGAGGCGGCTTCGATCGCTCCGGAGATC  
CGAAGAAATGATGATAACGTTTCTCTAACTGTCATCAAAGCTAAA  
ATCGCTTGTATCCTTCGTATCCTCGCTTACTTCAAGCTTACATC  
GATTGCCAAAAGGTCGGAGCACCACCGGAGATAGCGTGTTTACT  
AGAGGAGATTCAACGGGAGAGTGATGTTTATAAGCAAGAGGTTG  
TTCCTTCTTCTTGCTTTGGAGCTGATCCTGAGCTTGATGAATTTA  
TGGAACGTA CTGCGATATATTAGTGAAATACAAATCGGATCTAG  
CAAGACCGTTTGACGAGGCAACGTGTTTCTTGAACAAGATTGAG  
ATGCAGCTACGGAACCTATGTA CTGGTGTGCGAGTCTGCCAGGG  
GAGTTTCTGAGGATGGTGTAAATATCATCTGACGAGGAACTGAGT  
GGAGGTGATCATGAGGTAGCAGAGGATGGGAGACAAAGATGTG  
AAGACCGGGACCTCAAAGATAGGTTGCTACGCAAATTTGGAAGC  
CGTATTAGTACTTTAAAGCTTGAGTTCTCAAAGAAGAAGAAGAAA  
GGAAAGTTACCAAGAGAAGCAAGACAAGCTCTTCTTGATTGGTG  
GAATCTCCATTATAAGTGGCCTTACCCTACTGAAGGAGATAAGAT  
AGCATTAGCTGATGCAACGGGGTTAGACCAAAAACAAATCAACA  
ATTGGTTTATAAACCAAAGGAAACGTCATTGGAAGCCATCAGAGA  
ATATGCCTTTCGCTATGATGGATGATTCTAGT**GGATCATTCTTTA**  
**CCGAGGAATGA**

**Figure 5.4.1c** Amplification of the 945 bp *KNAT6* coding sequence by PCR

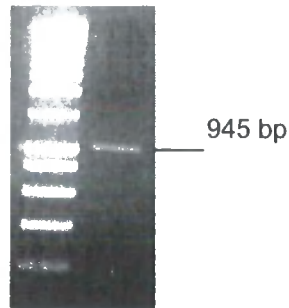


**Figure 5.4.1d** Release of 945 bp *KNAT6* coding region from the pCR®2.1-TOPO vector by digestion with *Sma*I

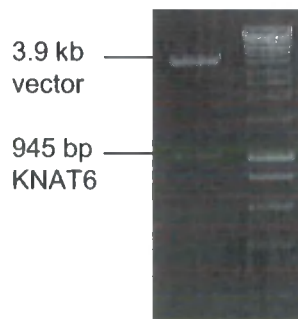
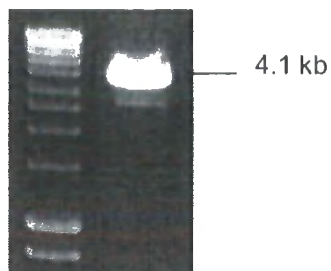


**Figure 5.4.1e** Linearisation of the 4.1 kb p35S::fusion-GFP vector by digestion with *Sma*I



digested with *Sma*I before being dephosphorylated (section 2.7.1) to prevent religation during the subsequent cloning steps. Both digests were analysed by gel electrophoresis (Figures 5.4.1d and e).

The *KNAT6* fragment was then ligated into the linearised p35S::fusion-GFP vector (section 2.7.3) and introduced into chemically competent *E. coli*. Putative positive colonies were checked by colony PCR using the *Probe F* and *5' RACE 1* primers. Plasmid was prepared from 5 positive colonies (section 2.4.1). As the *KNAT6* fragment could have ligated into the p35S::fusion-GFP vector in either orientation, further PCR was carried out on these plasmids to determine the orientation of the *KNAT6* fragment. A forward primer to the 35S promoter, *35S P1*, was used in conjunction with either the *Probe F* primer or the *5' RACE 1* primer. Standard PCR was carried out on the plasmids with these primer pairs and the products analysed by gel electrophoresis (Figure 5.4.1f). The results are summarised in Table 5.4.1a.

**Table 5.4.1a** PCR reactions to determine *KNAT6* orientation in the p35S::fusion-GFP vector

Reaction	Plasmid	Reverse primer	Product size, bp	Present?
1	1	<i>5' RACE 1</i>	600	No
2	1	<i>Probe F</i>	1,124	Yes
3	2	<i>5' RACE 1</i>	600	No
4	2	<i>Probe F</i>	1,124	Yes
5	3	<i>5' RACE 1</i>	600	No
6	3	<i>Probe F</i>	1,124	Yes
7	4	<i>5' RACE 1</i>	600	No
8	4	<i>Probe F</i>	1,124	Yes
9	5	<i>5' RACE 1</i>	600	Yes
10	5	<i>Probe F</i>	1,124	No

Plasmid 5 contains an insert in the correct orientation as indicated by the presence of a 600 bp product with the *35S P1* primer and the *Probe F* primer. This plasmid was digested with *Eco*RI to release the *KNAT6*::GFP cassette. The pCIRCE binary vector was also digested with *Eco*RI before being

**Figure 5.4.1f** Determination of insert orientation in recombinant p35S::KNAT6::GFP plasmids



Primer 2 was the 35S P1 primer in all reactions. Lanes are as follows:

Lane	Primer 1	Plasmid
1	5' RACE1	1
2	Probe F	1
3	5' RACE1	2
4	Probe F	2
5	5' RACE1	3
6	Probe F	3
7	5' RACE1	4
8	Probe F	4
9	5' RACE1	5
10	Probe F	5

dephosphorylated as before. Both digests were analysed by gel electrophoresis (Figure 5.4.1g and h) before the appropriate bands were cut out and purified. The expression cassette was then ligated into the digested pCIRCE and introduced into chemically competent *E. coli*. White putative positive colonies were checked by colony PCR using the *GFP-RE2-F* and *GFP-RE2-R* primers. A positive colony was selected and plasmid was prepared (section 2.4.2) and then sequenced using the 35S *P1* primer and a reverse primer to the 35S terminator, 35S *T1*, to verify that the construct was correct.

The plasmid was then introduced into electrocompetent *Agrobacterium tumefaciens* strain C58C3 (section 2.2.3). Putative positive colonies were checked by colony PCR using the *GFP-RE2-F* and *GFP-RE2-R* primers. A positive colony was then used to introduce the construct to *Arabidopsis* var. Col-0 using the dipping method (section 2.2.4).

T1 seed from the dipped plants was collected and sown on ½ MS10 SS medium supplemented with 35 mg/L kanamycin sulphate and 200 mg/L augmentin. Kanamycin-resistant seedlings were transferred to soil 7-10 DAG and T2 seed was harvested as individual lines.

#### **5.4.2 Production of plants expressing an N-terminal alcohol-inducible GFP::*KNAT6* fusion protein**

The N terminal fusion was made using the GATEWAY™ cloning system. The *KNAT6* coding region was introduced into the GATEWAY™ compatible entry vector pENTR3c by restriction endonuclease digestion and ligation. The *KNAT6* coding region was then mobilised into the binary vector pBinAGRFAN via a series of LR and BP reactions (see section 2.7.5 and Figure 5.4.2a). pBinAGRFAN utilises the alcohol-inducible *AlcA/AlcR* system to drive expression of the fusion protein via the CaMV 35S promoter (Figure 5.4.2b). The GFP variant in this vector is also smGFP (Davis and Vierstra, 1998). In this case, the smGFP coding sequence does not include a stop codon to allow translation of a single protein from the GFP and *KNAT6* coding sequences.

Primers (*GFP-GW2-F* and *GFP-GW2-R*) were designed to allow the amplification of the *KNAT6* coding sequence. These primers included EcoRI

**Figure 5.4.1g** Release of the 2.4kb KNAT6::GFP fusion cassette from the p35S::fusion-GFP vector by digestion with EcoRI

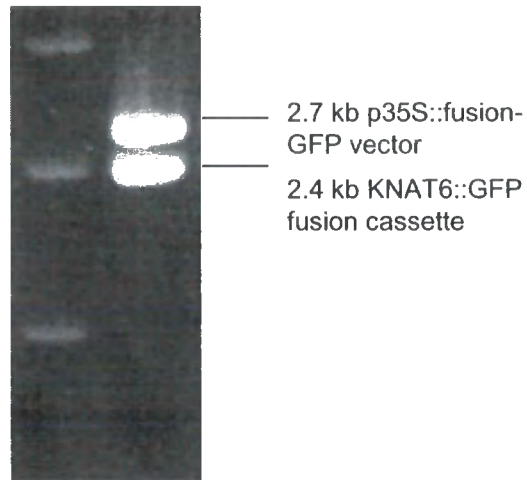


**Figure 5.4.1h** Linearisation of the 11.4 kb pCIRCE vector by digestion with EcoRI

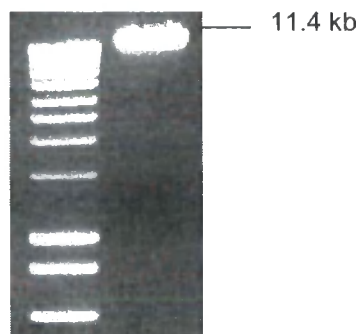


**Figure 5.4.2a** GATEWAY™ cloning strategy for the production of N terminal GFP::KNAT6 fusions

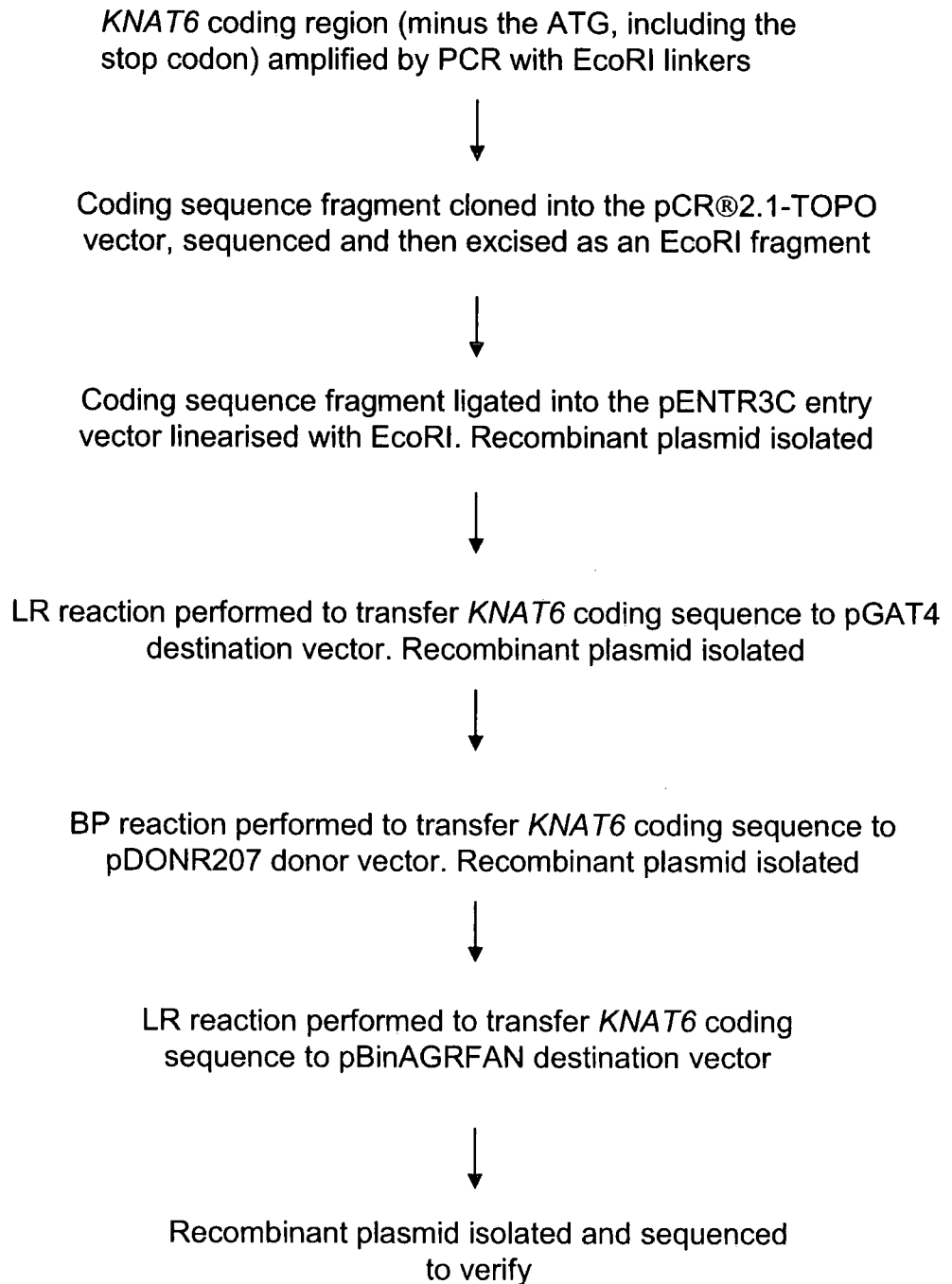


**Figure 5.4.2b** The alcohol-inducible system and N-terminal GFP::KNAT6 fusion protein construct

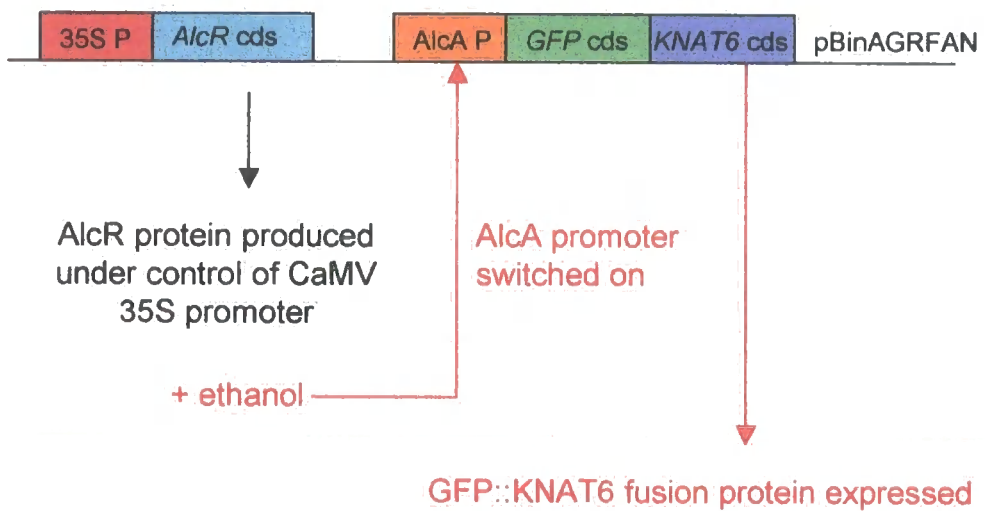
The CaMV 35S promoter is shown in red

The AlcR coding sequence is shown pale blue

AlcA promoter is shown in orange

The GFP coding sequence is shown in green

The KNAT6 coding sequence is shown in dark blue



sites to allow cloning into the pENTR3C entry vector. The forward primer did not include the *KNAT6* ATG and was designed to ensure that the *KNAT6* coding sequence was in frame with the GFP coding sequence. The positions of the primers in the *KNAT6* transcript are shown in Figure 5.4.2c.

The primers were used to amplify the *KNAT6* coding region from the original splice fragment that was cloned in section 4.6 using the Expand™ High Fidelity PCR system (section 2.8.2). The PCR products were analysed by gel electrophoresis (section 2.5.1) and a band of 900 bp was obtained as expected (Figure 5.4.2d). The band was cut out and purified using the QIAquick® Gel Extraction kit (section 2.4.7) before being cloned into the pCR®2.1-TOPO (section 2.7.4). The ligation mix was introduced into chemically competent *E. coli* and putative positive colonies were checked by colony PCR (section 2.8.1) using the universal primers *M13F* and *M13R*. A colony containing an insert of the correct size was selected and used to prepare plasmid DNA (section 2.4.1). The plasmid was then sequenced using *M13F* and *M13R* to verify that no errors had been introduced during the PCR amplification.

The plasmid was then digested with EcoRI (section 2.7.1) to release the *KNAT6* coding sequence fragment. The pENTR3C entry vector was also digested with EcoRI to release the cytotoxic *ccdB* gene from the vector backbone before being dephosphorylated (section 2.7.2). Both digests were analysed by gel electrophoresis (Figure 5.4.2e) and the appropriate bands were cut out and purified as above. The *KNAT6* fragment was ligated into the linearised pENTR3C vector and then introduced into chemically competent *E. coli*. Putative positive colonies were checked by colony PCR using primers designed around the pENTR3C multiple cloning site (*pENTR3CF* and *pENTR3CR*) and six colonies containing the *KNAT6* insert were identified.

As the *KNAT6* fragment could have ligated into pENTR3C in either orientation, further PCR was carried out on the colonies to determine the orientation of the inserts. The *GFP-GW2-R* primer was used in conjunction with either the *pENTR3CF* primer or the *pENTR3CR* primer. A band of approximately 1,200 bp was seen in the reaction with either the *GFP-GW2-R* primer + *pENTR3CF* or the *GFP-GW2-R* primer + *pENTR3CR*. Colony PCR was carried out and the

**Figure 5.4.2c** *KNAT6* coding region used for N terminal GFP::*KNAT6* protein fusions

The *KNAT6* ATG is shown in **red**

The *GFP-GW2-F* and *GFP-GW2-R* primers are underlined

The *KNAT6* stop codon (TGA) is shown in **orange**

**ATG**GATGGAATGTACAATTTCCATTCCGGCCGGTGATTATTCAGAT  
AAGTCGGTTCTGATGATGTCACCGGAGAGTCTCATGTTTCCTTC  
CGATTACCAAGCTTTGCTATGTTCTCCGCCGGTGAAAATCGTG  
TCTCTGATGTTTTCGGATCCGACGAGCTACTCTCAGTAGCCGTC  
TCCGCTTTGTCGTCGGAGGCCGGCTTCGATCGCTCCGGAGATCC  
GAAGAAATGATGATAACGTTTCTCTAACTGTCATCAAAGCTAAAA  
TCGCTTGTCATCCTTCGTATCCTCGCTTACTTCAAGCTTACATCG  
ATTGCCAAAAGGTCGGAGCACCACCGGAGATAGCGTGTTTACTA  
GAGGAGATTCAACGGGAGAGTGATGTTTATAAGCAAGAGGTTGT  
TCCTTCTTCTTGCTTTGGAGCTGATCCTGAGCTTGATGAATTTAT  
GGAAACGTA CTGCGATATATTAGTGAAATACAAATCGGATCTAGC  
AAGACCGTTTGACGAGGCAACGTGTTTCTTGAACAAGATTGAGA  
TGCAGCTACGGAACCTATGTA CTGGTGTGCGAGTCTGCCAGGGG  
AGTTTCTGAGGATGGTGTAAATATCATCTGACGAGGAACTGAGTG  
GAGGTGATCATGAGGTAGCAGAGGATGGGAGACAAAGATGTGA  
AGACCGGGACCTCAAAGATAGGTTGCTACGCAAATTTGGAAGCC  
GTATTAGTACTTTAAAGCTTGAGTTCTCAAAGAAGAAGAAGAAAG  
GAAAGTTACCAAGAGAAGCAAGACAAGCTCTTCTTGATTGGTGG  
AATCTCATTATAAGTGGCCTTACCCTACTGAAGGAGATAAGATA  
GCATTAGCTGATGCAACGGGGTTAGACCAA AAAACAATCAACAA  
TTGGTTTATAAACCAAAGGAAACGTCATTGGAAGCCATCAGAGAA  
TATGCCTTTTCGCTATGATGGATGATTCTAGTGGATCATTCTTTAC  
CGAGGAATGA

**Figure 5.4.2d** Amplification of the 900 bp *KNAT6* coding sequence with *EcoRI* linkers by PCR

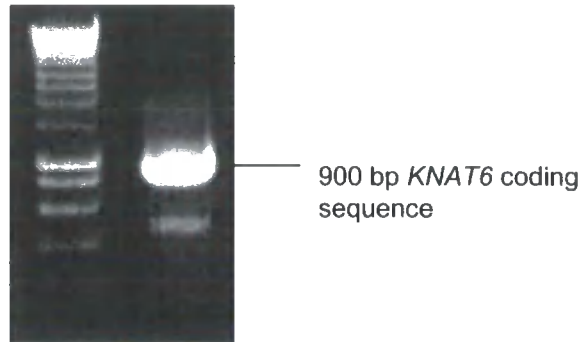
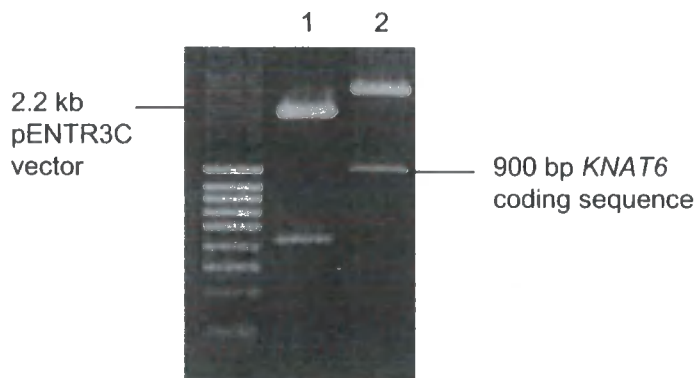


**Figure 5.4.2e** Preparation of fragment for cloning the *KNAT6* coding sequence into the pENTR3C entry vector



Lane 1 shows the linearisation of the 2.2 kb pENTR3C entry vector and the release of the 500 bp cytotoxic *ccdB* gene by digestion with *EcoRI*.

Lane 2 shows the release of the 900 bp *KNAT6* coding sequence from the 3.9 kb pCR@2.1-TOPO vector by digestion with *EcoRI*

products analysed by gel electrophoresis (Figure 5.4.2f). A summary of the PCR results is shown in Table 5.4.2a.

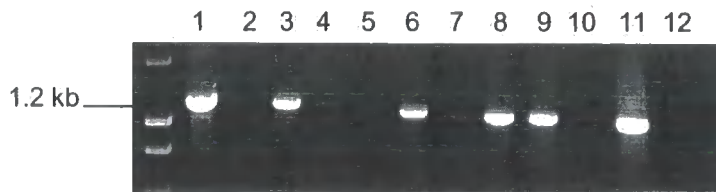
**Table 5.4.2a** Determination of *KNAT6* coding sequence orientation in pENTR3C by PCR

Reaction	Colony	Reverse primer	1,200 bp product?
1	1	<i>pENTR3CF</i>	Yes
2	1	<i>pENTR3CR</i>	No
3	2	<i>pENTR3CF</i>	Yes
4	2	<i>pENTR3CR</i>	No
5	3	<i>pENTR3CF</i>	No
6	3	<i>pENTR3CR</i>	Yes
7	4	<i>pENTR3CF</i>	No
8	4	<i>pENTR3CR</i>	Yes
9	5	<i>pENTR3CF</i>	Yes
10	5	<i>pENTR3CR</i>	No
11	6	<i>pENTR3CF</i>	Yes
12	6	<i>pENTR3CR</i>	No

Colonies that showed a band in the reaction with *pENTR3CF* were selected as having the *KNAT6* fragment in the correct orientation. Colony 1 was selected and used to prepare plasmid DNA (section 2.4.1). The *KNAT6* fragment was then mobilised to the pGAT4 destination vector via the LR reaction (section 2.7.5). The clonase reaction was introduced into chemically competent *E. coli* and plasmid was prepared from four putative positive colonies. Plasmid was digested with either EcoRI or XbaI and analysed by gel electrophoresis (Figure 5.4.2g). All of the plasmids had an insert of the correct size.

Colony 1 was selected and used in the BP reaction with the donor vector pDONR207 (section 2.7.5). The clonase reaction was introduced into *E. coli* as before and plasmid was prepared from five colonies and analysed by digestion with EcoRI (Figure 5.4.2.h). All plasmids contained an insert and plasmid 3 was selected for the final LR reaction between pDONR207 containing the *KNAT6* coding sequence and pBinAGRFAN. The reaction was introduced into *E. coli*

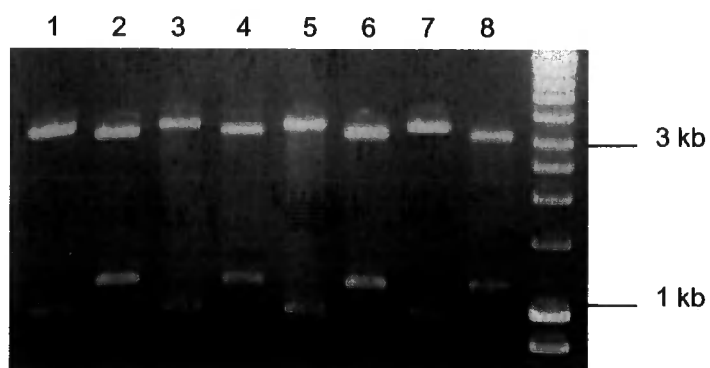
**Figure 5.4.2f** Determination of orientation of KNAT6 coding sequence fragments into pENTR3C



PCR was carried out using the GFP-GW2-R primer with either the pENTR3CF or the pENTR3CR primer

Lane	Primer	Colony
1	<i>pENTR3CF</i>	1
2	<i>pENTR3CR</i>	1
3	<i>pENTR3CF</i>	2
4	<i>pENTR3CR</i>	2
5	<i>pENTR3CF</i>	3
6	<i>pENTR3CR</i>	3
7	<i>pENTR3CF</i>	4
8	<i>pENTR3CR</i>	4
9	<i>pENTR3CF</i>	5
10	<i>pENTR3CR</i>	5
11	<i>pENTR3CF</i>	6
12	<i>pENTR3CR</i>	6

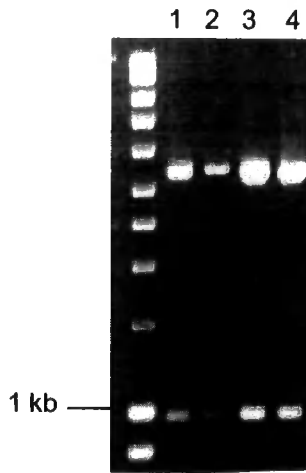
**Figure 5.4.2g** Diagnostic digests of the *KNAT6* coding sequence in the pGAT4 vector



A 0.9 kb fragment is released from the pGAT4 vector on digestion with *EcoRI*, and a 1.2 kb fragment is released on digestion with *XbaI*.

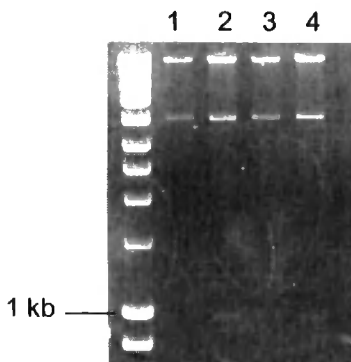
Lane	Plasmid	Digest
1	1	<i>EcoRI</i>
2	1	<i>XbaI</i>
3	2	<i>EcoRI</i>
4	2	<i>XbaI</i>
5	3	<i>EcoRI</i>
6	3	<i>XbaI</i>
7	4	<i>EcoRI</i>
8	4	<i>XbaI</i>

**Figure 5.4.2h** Diagnostic digests of the *KNAT6* coding sequence in the pDONR207 vector



Lanes 1-4 show the release of the 900 bp *KNAT6* coding sequence from the pDONR207 donor vector by digestion with EcoRI.

**Figure 5.4.2i** Diagnostic digests of the *KNAT6* coding sequence in the pBinAGRFAN vector



Lanes 1-4 show the release of the 900 bp *KNAT6* coding sequence from the pBinAGRFAN destination vector by digestion with EcoRI.

and plasmid was prepared from four colonies and analysed as above (Figure 5.4.2i). All four plasmids contained the correct insert.

Plasmid 1 was sequenced with the *Probe F* and *HD Exon 5* primers to ensure that the construct was correct. The pBinAGRFAN vector containing the *KNAT6* coding sequence was then introduced into electrocompetent *Agrobacterium tumefaciens* strain C58C3 (section 2.2.3). Putative positive colonies were checked using the *GFP-GW2-F* and *GFP-GW2-R* primers and a colony containing the plasmid was used to introduce the construct into *Arabidopsis* var. Col-0 by the dipping method (section 2.2.4).

T1 seed from the dipped plants was collected and sown onto ½ MS10 SS medium supplemented with 35 mg/L kanamycin sulphate and 200 mg/L augmentin. Kanamycin-resistant seedlings were transferred to soil 7-10 days after germination (DAG) and T2 seed was harvested as individual lines. Time constraints meant that this T2 seed was not analysed further.

## 5.5 Summary

The results presented in this chapter detailed the production and analysis of pKNAT6::GUS expressing plants. This showed that the *KNAT6* promoter was active in the hypocotyl and the phloem poles of the main root, especially at the bases of emerged lateral roots. The GUS expression was strongest at the crown and faded towards the root tip. In addition, GUS appeared to be expressed predominantly in areas of the main root where lateral roots were emerging. The activity of the *KNAT6* promoter in the phloem poles of roots was confirmed by the analysis of plants expressing pKNAT6::GFP. Analysis of crosses where the pKNAT6::GUS Lines 10.1 and 15.1 were introduced the *wol* background revealed that the *KNAT6* promoter was not active in the roots of plants where the phloem poles were absent.

Treatment of pKNAT6::GUS lines with plant hormones was also carried out. The synthetic auxin analogue 1-NAA appeared to alter the *KNAT6* promoter activity and lead to expression of GUS at the root tip while the cytokinin analogue BA caused downregulation. The auxin efflux carrier inhibitor NPA also reduced *KNAT6* promoter activity while the auxin efflux carrier inhibitor TIBA

and the ethylene precursor ACC did not appear to significantly affect promoter activity. In addition, introduction of GUS lines 10.1 and 15.1 into a *ry* background showed a similar expression pattern as on treatment with 1-NAA, especially in Line 10.1.

The *KNAT6* transcript was not detectable by northern analysis, but semi-quantitative RT-PCR indicated that the *KNAT6* transcript was present in the roots and aerial parts of *Arabidopsis* seedlings over a developmental time course.

Finally, plants carrying a C terminal KNAT6::GFP fusion protein under control of the CaMV 35S promoter and an N terminal alcohol-inducible GFP::KNAT6 fusion protein were generated and are awaiting analysis.

## Chapter 6 Functional Analysis of *KNAT6* using transgenics

Functional analysis of the *KNAT6* gene was attempted by investigating the effects of misexpression (sense overexpressing constructs) and downregulation (antisense and RNAi) of *KNAT6*. The Cauliflower Mosaic Virus 35S (CaMV 35S) RNA gene promoter was used to drive sense and antisense gene expression in transgenic plants. RNAi constructs were made using two different regions of the *KNAT6* coding region, with each region being introduced into plants under control of both the CaMV 35S promoter and the *KNAT6* promoter.

### 6.1 Overexpression and antisense of *KNAT6*

Sense and antisense expression constructs were made using the pDH51 vector, which contains the CaMV 35S promoter and terminator separated by a multiple cloning site. Overexpression of the *KNAT6* transcript was used to examine the effect of misexpression of this gene *in vivo*. Downregulation of *KNAT6* using an antisense approach was also attempted. The cloning strategy is shown in Figure 6.1a.

#### 6.1.1 Production of *KNAT6* overexpression and antisense plants

When designing the constructs, as much 5' UTR as possible was included in case it was required for efficient expression of *KNAT6*. As mentioned in section 4.1, several ORFs were identified in the 5' UTR of the *KNAT6* cDNA. Inclusion of these in the overexpressing constructs was avoided as they may have provided an alternative translation start that could have reduced the amount of *KNAT6* protein that was produced. The *Cds For* primer was designed just downstream of the ORF closest to the *KNAT6* ATG, and included an Xba1 site for the cloning steps (Figure 6.1.1a). The 3' UTR of *KNAT6* was also included in the construct. The 3' UTR-116 primer was resynthesised with an Xba1 site for use in this work.

Poly(A)<sup>+</sup> from NAA-treated *Arabidopsis* roots was used for reverse transcription with the Oligo d(T)<sub>15</sub> adaptor primer (section 2.9.1). The resulting cDNA was purified as detailed in section 2.9.2 before being used as a PCR template with the Expand™ High Fidelity PCR system (section 2.8.2) using the *Cds For* and 3' UTR-116 Xba1 primers. The resulting 1.3 kb PCR product (Figure 6.1.1b) was

**Figure 6.1a** Sense and antisense construct cloning strategy

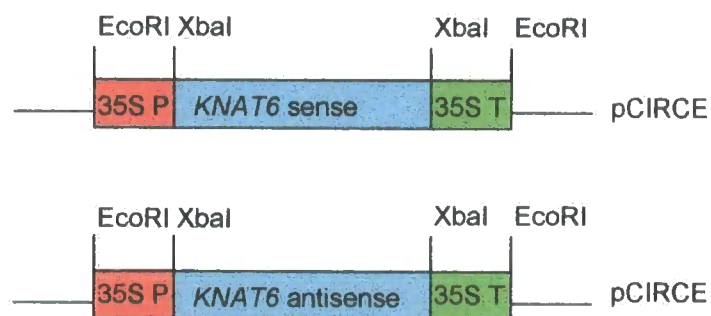
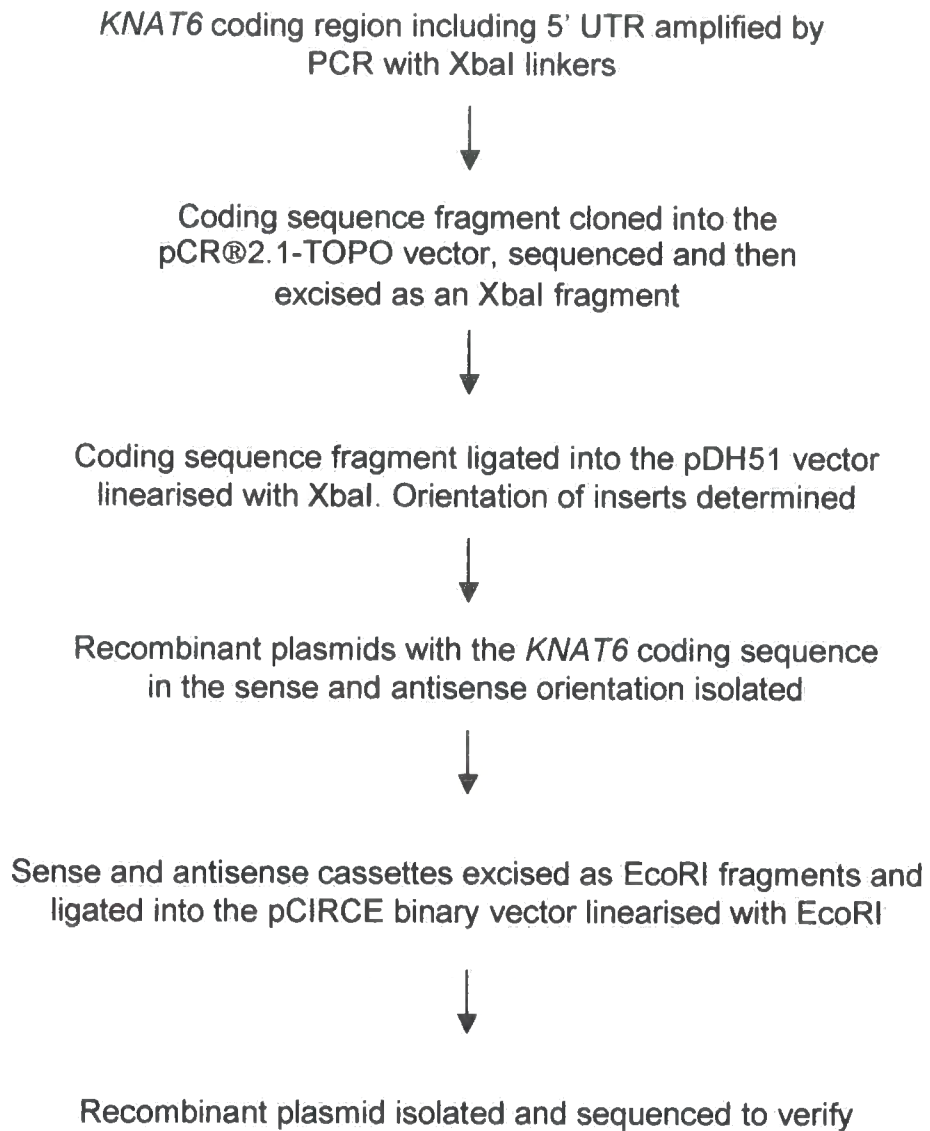


**Figure 6.1.1a** *KNAT6* fragment used for production of sense and antisense constructs

- 5' UTR
- ATG of closest upstream ORF in 5' UTR
- Coding sequence
- 3' UTR
- Extra bases in alternate splice isoform

The *Cds For* and *3' UTR-116* primers are underlined

ATAACACAGCCTTGGACCTTTCTTAGATATATATGTTAGGAAGGCCTTATC  
 TCGACCTATGAAGCCTGAAGCTCCATTGAGCCTTTTAGCATATGTCCTTTT  
 TCGTAATTATCATTTTATTTTTCTTCTCCGTTAACTTTTCATATCTTTTTCTTC  
 CAAAAGAAAATAAATTAAGATCCCTCGAGCCTCTCTCTCTCTCTACACACT  
 CCCATAGAAATAAATATTTTCAAGAACCAAAAAGTTTGTTATAAGCGGTTTC  
 ATATTATTCTTCTTCATCGATTCTTGATTTTGAAGAAGACAATTCAAGAAA  
 GCGATTTAGAAGACGGAGGAGTTCTTACCGGAGATCTTATACTTATGGAT  
 GGAATGTACAATTTCCATTCGGCCGGTGATTATTCAGATAAGTCGGTTCTG  
 ATGATGTCACCGGAGAGTCTCATGTTTCTTCCGATTACCAAGCTTTGCTA  
 TGTTCTCCGCCGGTGAAAATCGTGTCTCTGATGTTTTCCGATCCGACGA  
 GCTACTCTCAGTAGCCGTCTCCGCTTTGTCTCGTCGGAGGCCGCTTCGATCG  
 CTCCGGAGATCCGAAGAAATGATGATAACGTTTCTCTAACTGTCATCAAAG  
 CTAAAATCGCTTGTCATCCTTCGTATCCTCGCTTACTTCAAGCTTACATCG  
 ATTGCCAAAAGAAACAGGTCGGAGCACCACCGGAGATAGCGTGTTTACTA  
 GAGGAGATTCAACGGGAGAGTGATGTTTATAAGCAAGAGGTTGTTCTTC  
 TTCTTGCTTTGGAGCTGATCCTGAGCTTGATGAATTTATGGAAACGACTG  
 CGATATATTAGTGAAATACAAATCGGATCTAGCAAGACCGTTTGACGAGGC  
 AACGTGTTTCTTGAACAAGATTGAGATGCAGCTACGGAACCTATGTAAGG  
 TGTCGAGTCTGCCAGGGAGTTTCTGAGGATGGTGTAAATATCATCTGACG  
 AGGAACTGAGTGGAGGTGATCATGAGGTAGCAGAGGATGGGAGACAAAG  
 ATGTGAAGACCGGGACCTCAAAGATAGGTTGCTACGCAAATTTGGAAGCC  
 GTATTAGTACTTTAAAGCTTGAGTTCTCAAAGAAGAAGAAGAAAGGAAAGT  
 TACCAAGAGAAGCAAGACAAGCTTCTTCTGATTGGTGGAACTCCATTATA  
 AGTGGCCTTACCCTACTGAAGGAGATAAGATAGCATTAGCTGATGCAACG  
 GGGTTAGACCAAAAACAAATCAACAATTGGTTTATAAACCAAAGGAAACGT  
 CATTGGAAGCCATCAGAGAATATGCCTTTTCGCTATGATGGATGATTCTAGT  
 GGATCATTCTTACCAGGAATGAATTTATTTATGGTACTTATTTAACGTTG  
 ATTTAAAGATGGATGTATAATTCTGCCTTGCTTTGCCGACAAAGGAAAAA  
 AGAAAGAAAGAGTGAAGCATGGACGACACATGAAATGGATCTTACACTCA  
 CTCACATG

**Figure 6.1.1b** Amplification of the 1.3 kb *KNAT6* fragment with XbaI linkers by PCR

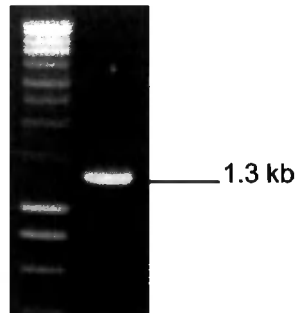
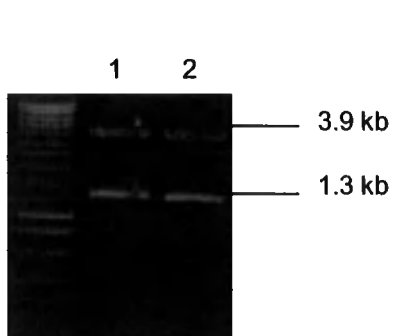


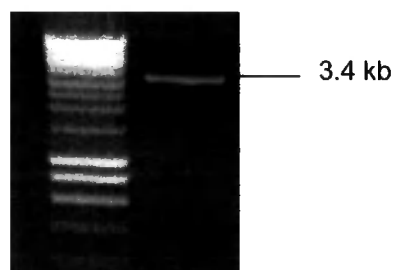
**Figure 6.1.1c** Release of the 1.3 kb *KNAT6* fragment from the pCR@2.1-TOPO



Lane 1 shows the release of the 1.3 kb alternative splice *KNAT6* coding sequence from the 3.9 kb pCR@2.1-TOPO vector by digestion with EcoRI

Lane 2 shows the release of the 3.9 kb original splice *KNAT6* coding sequence from the 3.9 kb pCR@2.1-TOPO vector by digestion with EcoRI

**Figure 6.1.1d** Linearisation of the 3.4 kb pDH51 vector by digestion with EcoRI



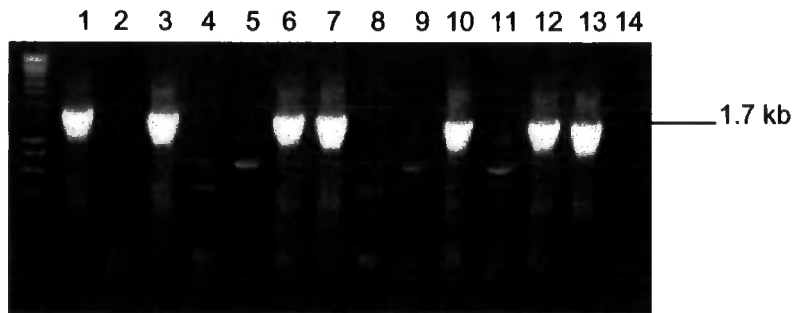
cut out and purified (section 2.4.7), cloned into the pCR®2.1-TOPO vector (section 2.7.4) and the resulting colonies checked by colony PCR (section 2.8.1) using the universal primers *M13F* and *M13R*. Plasmid DNA was prepared from colonies with an insert of the correct size. Sequencing with *M13F* and *M13R* primers was then used to determine which isoform had been cloned and to ensure that no errors had been introduced to the sequence during PCR amplification.

After identification of both the original and alternate splice *KNAT6* cloned cDNAs, the plasmids were digested with *Xba*1 (section 2.7.1) to release the *KNAT6* fragment. The pDH51 vector was also digested with *Xba*1 before being dephosphorylated to prevent religation (section 2.7.2). The digests were analysed by gel electrophoresis (Figure 6.1.1c and d) and the appropriate bands were cut out and purified using the QIAquick® Gel Extraction kit (section 2.4.7).

Each of the *KNAT6* fragments were then ligated into the linearised pDH51 vector as described in section 2.7.3 and introduced into chemically competent *E. coli* (section 2.7.6). As the same restriction site was used on both ends of the *KNAT6* fragments, inserts could ligate into pDH51 in either orientation. This allowed the overexpressing (sense) and the antisense cassettes to be generated with a single ligation step for each *KNAT6* cDNA. To determine the orientation of the inserts, colony PCR was carried out on putative positive colonies using the CaMV 35S promoter primer *35s ENH For* and either the *Cds For* primer or the *3' UTR -116 Xba1* primer. A product of 1721 bp was expected in either the reaction with the *3' UTR -116 Xba1* primer or with the *Cds For* primer, depending on the insert orientation. The colony PCR results are shown in Figures 6.1.1e and 6.1.1f.

For each *KNAT6* cDNA, single colonies containing either a sense or an antisense cassette were selected and are shown in Table 6.1.1a

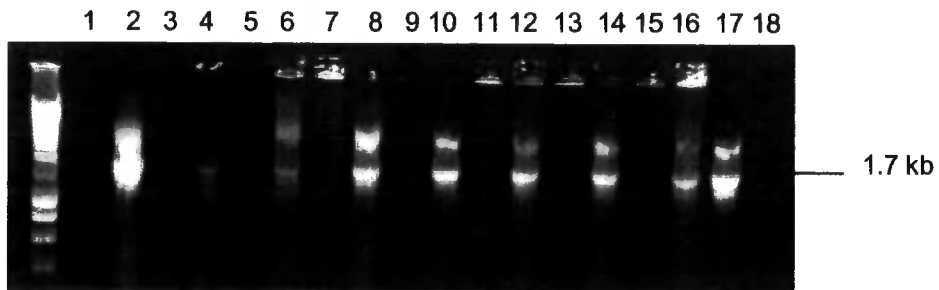
**Figure 6.1.1e** Colony PCR to determine the insert orientation of original splice *KNAT6* fragments into the pDH51 vector



PCR was carried out using the *35S ENH For* primer and one other primer as follows:

Lane	Colony	Primer 2
1	1	<i>Cds For</i>
2	1	<i>3' UTR-116 Xbal</i>
3	2	<i>Cds For</i>
4	2	<i>3' UTR-116 Xbal</i>
5	3	<i>Cds For</i>
6	3	<i>3' UTR-116 Xbal</i>
7	4	<i>Cds For</i>
8	4	<i>3' UTR-116 Xbal</i>
9	5	<i>Cds For</i>
10	5	<i>3' UTR-116 Xbal</i>
11	6	<i>Cds For</i>
12	6	<i>3' UTR-116 Xbal</i>
13	7	<i>Cds For</i>
14	7	<i>3' UTR-116 Xbal</i>

**Figure 6.1.1f** Colony PCR to determine the insert orientation of alternate splice *KNAT6* fragments into the pDH51 vector



PCR was carried out using the *35S ENH For* primer and one other primer as follows:

Lane	Colony	Primer 2
1	1	<i>Cds For</i>
2	1	<i>3' UTR-116 Xbal</i>
3	2	<i>Cds For</i>
4	2	<i>3' UTR-116 Xbal</i>
5	3	<i>Cds For</i>
6	3	<i>3' UTR-116 Xbal</i>
7	4	<i>Cds For</i>
8	4	<i>3' UTR-116 Xbal</i>
9	5	<i>Cds For</i>
10	5	<i>3' UTR-116 Xbal</i>
11	6	<i>Cds For</i>
12	6	<i>3' UTR-116 Xbal</i>
13	7	<i>Cds For</i>
14	7	<i>3' UTR-116 Xbal</i>
15	8	<i>Cds For</i>
16	8	<i>3' UTR-116 Xbal</i>
17	9	<i>Cds For</i>
18	9	<i>3' UTR-116 Xbal</i>

**Table 6.1.1a** Colonies containing *KNAT6* sense and antisense cassettes

<i>KNAT6</i> cDNA	Orientation	Colony number
Original splice	Sense	3
Original splice	Antisense	1
Alternate splice	Sense	6
Alternate splice	Antisense	13

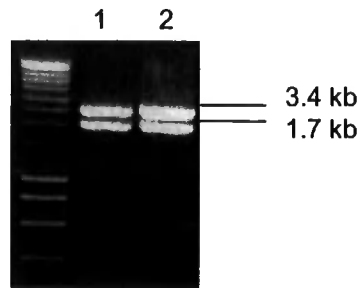
These four colonies were used to prepare plasmid DNA. The 1700 bp cassettes were then released from the pDH51 vector by restriction endonuclease digestion with EcoR1. The pCIRCE binary vector was also digested with EcoR1 before being dephosphorylated as before. The digests were analysed by gel electrophoresis (Figure 6.1.1g, h and i) before the appropriate bands were purified from the gel.

Each cassette was then ligated into the linearised pCIRCE and the products introduced into chemically competent *E. coli*. White recombinant colonies were checked by colony PCR using the *35S ENH For* primer and either the *3' UTR-116 XbaI* primer (for sense constructs) or the *Cds For* primer (for antisense constructs). Plasmid DNA was prepared from colonies containing the recombinant pCIRCE plasmid using the Qiagen Midi Prep kit (section 2.4.2). The plasmids were sequenced with *M13F* and *M13R* primers to confirm the construct was correct.

The plasmids were then introduced into electrocompetent *Agrobacterium tumefaciens* strain C58C3 as described in section 2.2.3. Colonies were checked by colony PCR using the *35S ENH For* primer and either the *3' UTR-116 XbaI* primer (for sense constructs) or the *Cds For* primer (for antisense constructs).

Positive colonies were selected and used for introduction of the constructs to *Arabidopsis* var. Columbia by the dipping method (section 2.2.4). T1 seed from the dipped plants was sown on ½ MS10 SS medium supplemented with 35 mg/L kanamycin sulphate and 200 mg/L augmentin. Kanamycin-resistant transformed seedlings remained green while sensitive seedlings became bleached 7-10 days after germination (DAG) on the selective medium.

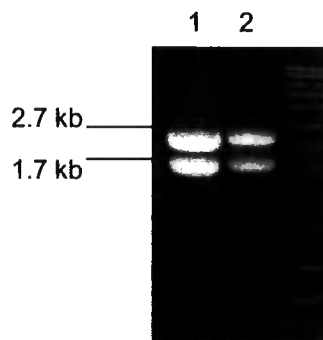
**Figure 6.1.1g** Release of 1.7 kb original splice 35S::KNAT6 cassettes from the 3.4 kb pDH51 vector by digestion with EcoRI



Lane 1 shows the sense cassette

Lane 2 shows the antisense cassette

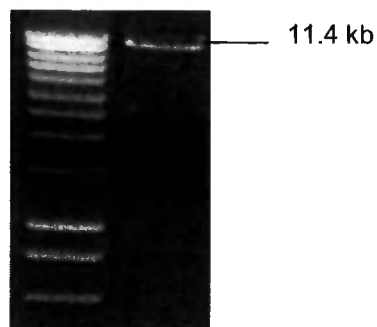
**Figure 6.1.1h** Release of 1.7 kb alternate splice 35S::KNAT6 cassettes from the 2.7 kb pDH51 vector by digestion with EcoRI



Lane 1 shows the sense cassette

Lane 2 shows the antisense cassette

**Figure 6.1.1i** Linearisation of the 11.4 kb pCIRCE vector by digestion with EcoRI



Transformed plants were transferred to soil and T2 seed collected as individual lines.

### 6.1.2 Isolation of *KNAT6* overexpressing lines

The number of unlinked T-DNA loci in a hemizygous line can be estimated by the ratio of kanamycin-resistant ( $\text{Kan}^{\text{R}}$ ) seedlings to kanamycin-sensitive ( $\text{Kan}^{\text{S}}$ ) seedlings (Table 6.1.2a).

**Table 6.1.2a** Segregation ratios and T-DNA loci numbers

Number of $\text{Kan}^{\text{R}}$ plants	Number of $\text{Kan}^{\text{S}}$ plants	Number of unlinked T-DNA loci
3	1	1
15	1	2
63	1	3
255	1	4

T2 seed (section 6.1.1) from 30 individual p35S::*KNAT6* original splice lines (S1-S30) and 30 individual p35S::*KNAT6* alternative splice lines (asS6-asS36) were surface sterilised and germinated on ½ MS10 SS supplemented with 35 mg/L kanamycin sulphate. Approximately 7 DAG, the plates were scored for the ratio of  $\text{Kan}^{\text{R}}$  seedlings to  $\text{Kan}^{\text{S}}$  seedlings (Appendix 3, Tables 3 and 4). This revealed that all of the plants were hemizygous and had a number of T-DNA loci ranging from 0 to 4 (Table 6.1.2b and c).

**Table 6.1.2b** Number of T-DNA loci present in p35S::KNAT6 original splice (S) lines

Line	T-DNA loci	Line	T-DNA loci	Line	T-DNA loci
S1	1-2	S11	2	S21	1
S2	1	S12	1	S22	4
S3	2-3	S13	1	S23	2
S4	1	S14	2-3	S24	1
S5	2	S15	4	S25	2
S6	1	S16	3-4	S26	3-4
S7	1	S17	2-3	S27	3
S8	2	S18	1	S28	1
S9	1	S19	1	S29	3
S10	1	S20	1	S30	1

**Table 6.1.2c** Number of T-DNA loci present in p35S::KNAT6 alternative splice (asS) lines

Line	T-DNA loci	Line	T-DNA loci	Line	T-DNA loci
asS6	1	asS17	3	asS27	1
asS7	1	asS18	0	asS28	2-3
asS8	1-2	asS19	3	asS29	1
asS9	1	asS20	1-2	asS30	1
asS11	1	asS21	1	asS31	1
asS12	1	asS22	2-3	asS32	2-3
asS13	3	asS23	1	asS33	1
asS14	2	asS24	1	asS34	1
asS15	1	asS25	3-4	asS35	1
asS16	3	asS26	2-3	asS36	1

Four kanamycin-resistant T2 plants (denoted *a-d*) from each segregation plate were transferred to soil and the T3 seed was collected from individual plants. No aerial phenotype was observed in these T2 plants.

### 6.1.3 Screening of T2 *KNAT6* overexpressing lines for a root phenotype

As the activity of the *KNAT6* promoter had been localised to the stele of the root and the lateral root bases, it was hypothesised that *KNAT6* may play a role in some aspect of lateral root development. Although the transformed T2 plants identified in section 6.1.2 were hemizygous for the T-DNA insertion (meaning that some of the plants examined were untransformed), it was expected that any dominant overexpression would have been visible. Therefore, the T2 plants were screened in an attempt to identify a root phenotype caused by the overexpression of *KNAT6*. Six T2 plants from each of the S lines analysed in Table 6.1.2b and six or eight T2 plants from each of the asS lines analysed in Table 6.1.2c (except for asS18 which does not contain a T-DNA) were grown on vertical plates (section 2.2.1) to allow the roots to be examined.

Seeds were surface sterilised and germinated on  $\frac{1}{2}$  MS10 SS medium and then transferred at 3 DAG to  $\frac{1}{2}$  MS10 medium on vertical plates. Wild type Columbia (Col-0) plants were grown in the same way to act as a control. As the T-DNA carrying the *KNAT6* overexpressing construct was segregating in the seedling population that was examined, no measurements (such as root length) were recorded. The roots of these plants were examined at 10 DAG, and any plants that showed a difference in root growth (i.e. root length, lateral root number or lateral root positioning) or aerial growth compared with the Col-0 control were transplanted to soil and grown on (Tables 6.1.3a and b). Only one of these plants (S29.1) showed an aerial T2 phenotype. This plant had lobed leaves.

T3 seed from each plant was collected and then subjected to kanamycin segregation analysis to determine if the T2 plant was hemizygous, homozygous or untransformed (Tables 6.1.3a and b). It should be noted that most of the plants for which no seed was collected died due to technical problems with the greenhouse rather than because of a possible phenotype.

**Table 6.1.3a** Genotype of T2 S seedlings showing a putative phenotype on vertical plates

Line.plant	Putative phenotype	Genotype
S2.2	Short main root, few laterals	Heterozygote
S3.2	Very short main root	Heterozygote
S7.6	Short root, few laterals	Heterozygote
S8.3	Short root, two laterals at same position	Heterozygote
S8.4	Main root split by lateral	Heterozygote
S9.1	Main root split by lateral	Wild type
S9.3	Main root split by lateral	Heterozygote
S9.6	Laterals initiate close to root tip	Heterozygote
S10.4	Main root split by lateral	Homozygote
S11.1	Two laterals at same position, stunted aerials	Homozygote
S11.4	Two laterals at same position, stunted aerials	No seed
S11.6	Two laterals at same position, stunted aerials	No seed
S14.5	Two lateral at same position	Wild type
S15.1	Very short main root	Homozygote
S15.6	Laterals initiate close to root tip	Homozygote
S16.1	Main root split by lateral	Homozygote
S17.4	Two laterals at same position	Heterozygote
S18.1	Two laterals at same position	Heterozygote
S18.2	Main root split by lateral	Heterozygote
S19.5	Increased laterals	Wild type
S19.6	Increased laterals	Wild type
S20.1	Callusing at shoot apex	No seed
S20.4	Short lateral roots	Heterozygote
S26.1	Anthocyanin accumulation, stunted, green roots	No seed
S26.5	Anthocyanin accumulation, stunted, green roots	No seed
S26.6	Two laterals at same position	Homozygote
S28.5	Hypocotyl split by lateral	Wild type
S29.1	Radially swollen hypocotyl	Heterozygote

**Table 6.1.3b** Genotype of T2 asS seedlings showing a putative phenotype on vertical plates

Line.plant	Putative phenotype	Genotype
asS6.1	Short main root	No seed
asS6.3	Short main root	No seed
asS9.3	Short main root	Homozygote
asS11.4	Short main root, some curly laterals	Heterozygote
asS11.6	Short main root, some curly laterals	Homozygote
asS12.1	Short main root, some curly laterals	No seed
asS12.2	Short main root, some curly laterals	Heterozygote
asS12.3	Short main root, some curly laterals	No seed
asS14.3	Main root split by lateral	Heterozygote
asS15.6	Main root split by lateral	No seed
asS15.7	Very short main root	Heterozygote
asS16.3	Main root/hypocotyl split by anchor root	Homozygote
asS17.3	Main root split by lateral	Heterozygote
asS19.4	Main root split by lateral	No seed
asS19.7	Main root split by lateral	No seed
asS19.8	Main root split by lateral	Homozygote
asS20.1	Short main root	Heterozygote
asS21.6	Two laterals at same position	Homozygote
asS22.2	Main root split by lateral	No seed
asS22.3	Short root, single lateral	No seed
asS22.4	Main root split by lateral	No seed
asS23.2	Main root split by lateral	Wild type
asS24.6	Main root split by lateral	Wild type
asS24.8	Main root split by lateral	No seed
asS25.4	Leaf-like outgrowth on leaf	Heterozygote
asS26.6	Main root split by lateral	Wild type
asS27.8	Short main root	Heterozygote
asS28.3	Main root split by lateral	Heterozygote
asS28.4	Very short main root	Homozygote
asS28.5	Main root split by lateral	Heterozygote
asS29.1	Main root split by lateral	Wild type
asS29.7	Main root split by lateral	Wild type
asS29.8	Short main root	No seed
asS33.5	Swollen lateral root	Wild type
asS33.6	Short main root	No seed
asS34.2	Short main root	Heterozygote

**Figure 6.1.3a** shows an example of a lateral root splitting a main root in plant S18.2

As can be seen from the tables above, some seedlings that were selected as having a putative phenotype were in fact untransformed. In addition, some of the Col-0 wild type plants which were included as controls occasionally showed some of the putative phenotypes such as a lateral root splitting the main root, the positioning of two lateral roots close together (lateral roots should not normally be initiated at the same position) and a short main root (data not shown). As these phenomena were observed in the wild type plants, it appeared that this was normal variation in the population of *Arabidopsis* seedlings.

However, there still remains the possibility that these phenomena may occur at higher incidence in the plants that overexpressed either of the *KNAT6* isoforms.

#### **6.1.4 Analysis of aerial parts in T3 *KNAT6* overexpressing lines**

Despite the lack of an obvious root phenotype in the T2 seedlings transformed with *KNAT6* overexpressing constructs, two plants showed a putative aerial phenotype that was reminiscent of the effects of overexpressing other *KN1* Class I genes (section 1.4.2). These two plants were S29.1 (lobed leaves in soil grown plants) and asS25.4 (leaf-like outgrowth on leaf on vertical plates). To investigate this further, T3 plants from S and asS lines that had a putative phenotype as described in Tables 6.1.3a and b, and which were kanamycin-resistant (indicating the presence of a T-DNA) were analysed.

In addition, for the same lines as above, T3 seed from the T2 plants *a-d* which were removed from kanamycin selection plates (section 6.1.2) were subjected to kanamycin segregation analysis to determine if they were hemizygous or homozygous. In most cases, a homozygous plant was selected and used for further analysis. Where no homozygote was identified, a heterozygote was used instead. The genotypes of these plants are shown in Table 6.1.4a

**Figure 6.1.3a** Splitting of the main root by initiating lateral roots



Col-0

(i) Normal lateral root growth



S18.2 (see Table 6.1.3a)

(ii) Lateral roots occasionally split the main root

**Table 6.1.4a** Genotypes of Kan<sup>R</sup> S and asS plants used for aerial analysis

Line	Genotype	Line	Genotype
S2 <i>d</i>	Homozygote	asS11 <i>b</i>	Heterozygote
S3 <i>d</i>	Homozygote	asS12 <i>b</i>	Homozygote
S7 <i>a</i>	Homozygote	asS14 <i>b</i>	Homozygote
S8 <i>d</i>	Homozygote	asS15 <i>d</i>	Homozygote
S9 <i>c</i>	Homozygote	asS16 <i>b</i>	Homozygote
S10 <i>b</i>	Homozygote	asS17 <i>b</i>	Heterozygote
S11 <i>c</i>	Homozygote	asS19 <i>a</i>	Homozygote
S14 <i>b</i>	Homozygote	asS20 <i>b</i>	Homozygote
S15 <i>b</i>	Homozygote	asS21 <i>b</i>	Heterozygote
S16 <i>a</i>	Homozygote	asS23 <i>b</i>	Heterozygote
S17 <i>a</i>	Heterozygote	asS24 <i>b</i>	Heterozygote
S18 <i>d</i>	Heterozygote	asS25 <i>b</i>	Homozygote
S19 <i>b</i>	Heterozygote	asS26 <i>b</i>	Homozygote
S20 <i>d</i>	Homozygote	asS27 <i>b</i>	Homozygote
S26 <i>c</i>	Homozygote	asS28 <i>b</i>	Homozygote
S28 <i>d</i>	Homozygote	asS29 <i>b</i>	Homozygote
S29 <i>a</i>	Homozygote	asS33 <i>c</i>	Homozygote
asS9 <i>b</i>	Homozygote	asS34 <i>b</i>	Heterozygote

Seed from these lines was sown in soil and grown in a controlled environment room. The original splice S plants showed an aerial phenotype at approximately 28 DAG, whereas the alternate splice asS plants remained wild type in appearance. A summary of the range of phenotypes observed in the S plants is shown in Table 6.1.4b.

**Table 6.1.4b** Summary of phenotypes in plants expressing original splice (S) *KNAT6*

Lines	Phenotype
S8 <i>d</i>	Wild type
S2.2, S3.2, S3 <i>d</i> , S11.1, S11 <i>c</i> , S15 <i>b</i> , S18 <i>d</i> , S28 <i>d</i> , S29.1	Slightly curled leaves
S7.6, S8.4, S9.6, S9.3, S20.4, S26.6,	Curled leaves
S7 <i>a</i> , S8.3,	Small curled leaves
S2 <i>d</i> , S9 <i>c</i> , S10 <i>b</i> , S18.1, S14 <i>b</i>	Curled and lobed leaves
S15.1, S19 <i>b</i> , S29 <i>a</i>	Curled, thickened and widened leaves
S10.4, S18.2, S20 <i>d</i> , S26 <i>c</i>	Curled, lobed and widened leaves
S15.6	Small, curled, thickened and lobed leaves
S16 <i>a</i> , S17.4, S17 <i>a</i>	Small, curled, thickened and widened leaves
S16.1	Curled, lobed, thickened and widened leaves

The following lines were selected to do a development series as they showed a range of phenotypes: S2*d*, S7*a*, S9*c*, S10.4, S14*b* and S15.6. Seed from these lines as well as from all of the asS lines were sown in soil and grown in a controlled environment room. The plants were photographed at 14, 21, 28 and 35 DAG. The plants all showed a wild type phenotype until 21 DAG, when the sense phenotype becomes visible. The asS lines remained wild type in appearance throughout the time course. The six sense lines listed above, the Col-0 control and a representative from the asS lines (asS16.3) are shown at 21, 28 and 35 DAG in Figures 6.1.4a-i.

As the results in Table 6.1.4b show, seedlings which were selected from the vertical plates used in the root growth screen (section 6.1.3) as well as kanamycin-resistant seedlings removed from segregation analysis plates (section 6.1.2) showed the *KNAT6* original splice (S) overexpressing phenotype. In many cases there is wide variability between plants from the same transgenic line e.g. compare the phenotypes of S8*d* and S8.3. Also note that the T3 S29.1 plants analysed in this generation did not have a strong phenotype despite the T2 S29.1 plant having a lobed leaf phenotype. Silencing

**Figure 6.1.4a** Col-0 developmental series

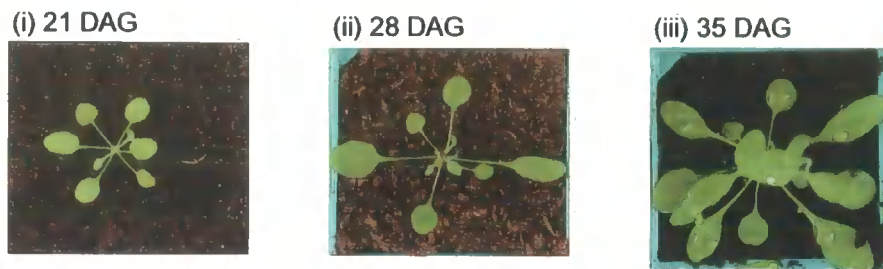


**Figure 6.1.4b** asS16.3 developmental series

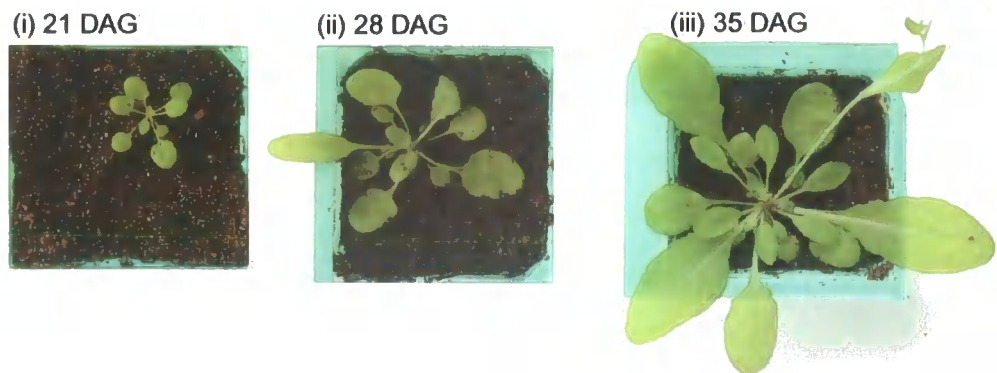


**Figure 6.1.4c** S2*d* developmental series

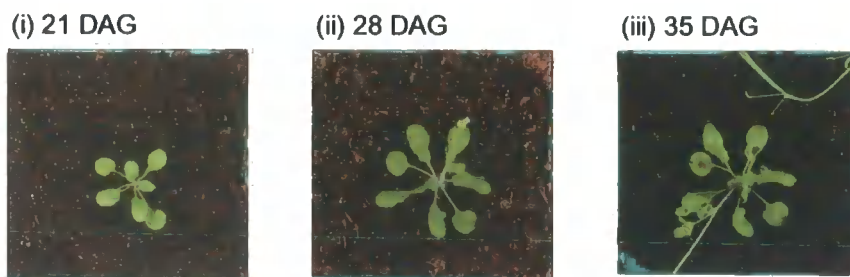
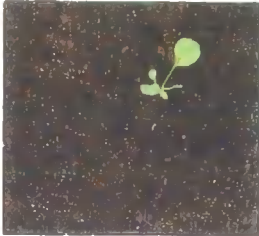


**Figure 6.1.4d S7a developmental series**

(i) 21 DAG



(ii) 28 DAG



(iii) 35 DAG



**Figure 6.1.4e S9c developmental series**

(i) 21 DAG



(ii) 28 DAG



(iii) 35 DAG

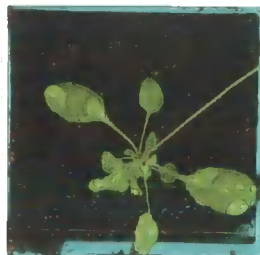
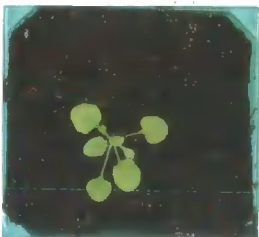


**Figure 6.1.4f S10.4 developmental series**

(i) 21 DAG



(ii) 28 DAG



(iii) 35 DAG



**Figure 6.1.4g** S14*b* developmental series

(i) 21 DAG



(ii) 28 DAG



(iii) 28 DAG

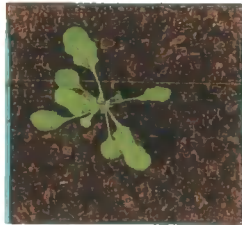


**Figure 6.1.4h** S15.6 developmental series

(i) 21 DAG



(ii) 28 DAG



(iii) 28 DAG



**Figure 6.1.4i** Leaf phenotype of 35S::*KNAT6* plants, 46 DAG

Bar approx. 0.5 cm



of the expression of the transgene could have caused this. In addition, no phenotype was seen with any of the asS plants, despite the outgrowth on the leaf seen on plant asS25.4. It was concluded that this was an example of natural variation rather than a true phenotype.

### **6.1.5 Analysis of roots in T3 *KNAT6* overexpressing lines**

As an aerial phenotype was identified in the T3 seedlings carrying the *KNAT6* S (original splice) constructs which was not seen in the T2 seedlings, the roots of T3 homozygous seedlings were examined.

The six homozygous transgenic lines that showed a range of aerial phenotypes and were examined above (S15.6, S10.4, S2*d*, S9*c*, S7*a* and S14*b*) were used for root growth assays, along with a Col-0 control. Seeds were surface sterilised and germinated on ½ MS10 SS medium. At 3 DAG, ten seedlings per line were transferred to ½ MS10 onto vertical plates. The length of the main root as well as the number of laterals and the distance between the root tip and the youngest lateral root were recorded at 3, 6, 9 and 12 DAG.

The average length of the main root at each time point was calculated for each S line (Figure 6.1.5a). These results indicated that there was no difference between transgenic lines and the Col-0 control apart from in line S7*a* where root growth was retarded. The average distance from the root tip to the last lateral root to emerge was also calculated for each time point (Figure 6.1.5b). This also indicated that there was no difference between the transgenic lines and the Col-0 control, apart from in line S7*a*, where lateral roots initiated closer to the primary root tip than in wild type.

The average number of lateral roots and anchor roots which each S line produced at each time point was calculated (Figures 6.1.5c and d), and these also showed no difference with the Col-0 control, apart from in the case of line S7*a* where fewer lateral and anchor roots were produced. The values that were used to plot these graphs are shown in Appendix 4. These results are discussed in section 8.4.1.

**Figure 6.1.5a** Length of the primary root in T3 S lines

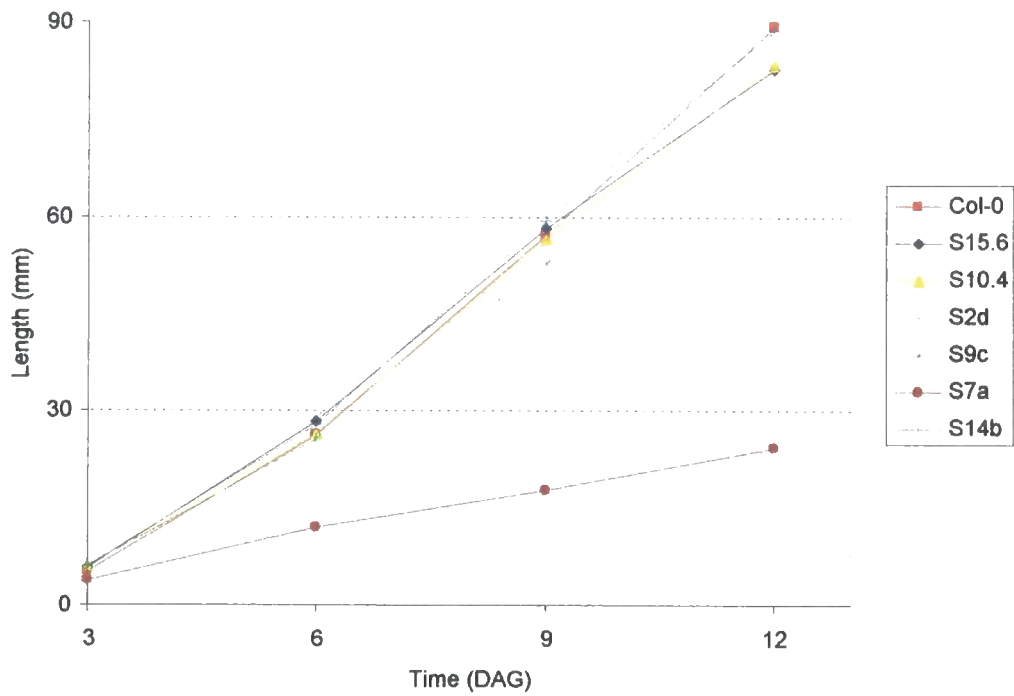


**Figure 6.1.5b** Distance from the primary root tip to the last lateral root to emerge in T3 S lines

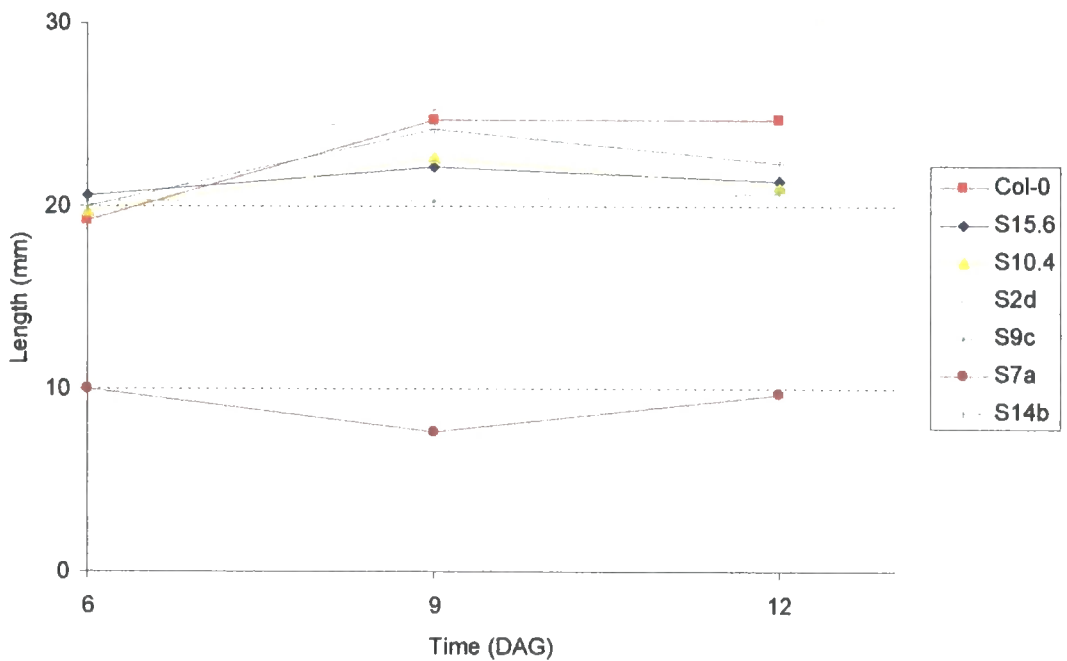


**Figure 6.1.5c** Number of lateral roots produced by T3 S lines

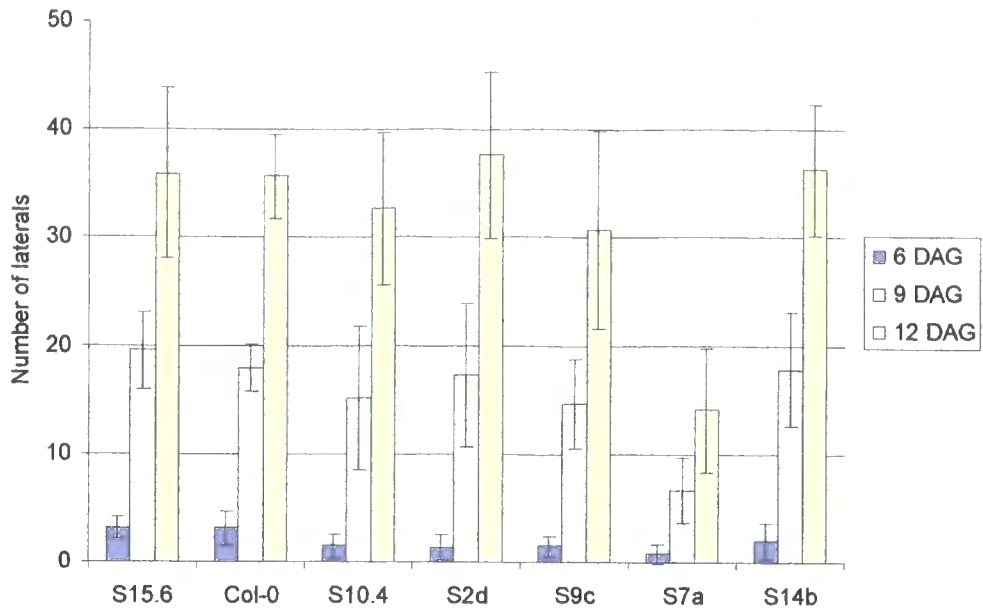
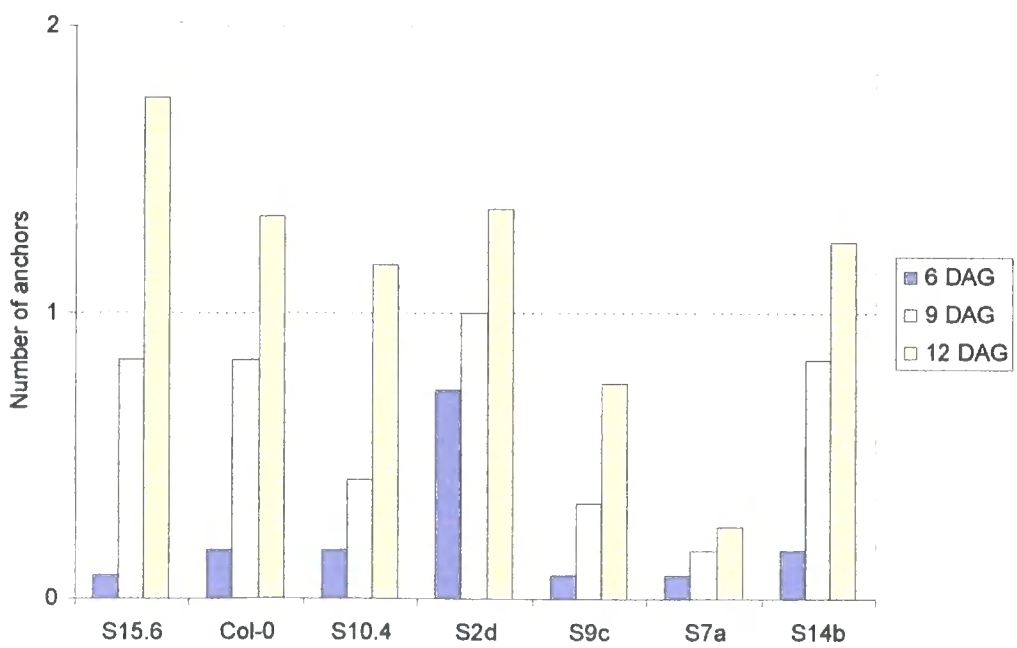


**Figure 6.1.5d** Number of anchor roots produced by T3 S lines



Note that roots of these homozygous lines did not show an increase in the frequency of characteristics that were originally used to select transformants in section 6.1.2 such as a lateral root splitting the main root.

The roots of the asS lines were not examined again as they had no aerial phenotype. The differences in phenotype seen between S and asS lines are discussed in section 8.4.1.

### **6.1.6 Isolation of *KNAT6* antisense lines**

As mentioned in section 6.1.2, the number of unlinked T-DNA loci in a hemizygous line can be estimated by the ratio of kanamycin-resistant ( $\text{Kan}^{\text{R}}$ ) seedlings to kanamycin-sensitive ( $\text{Kan}^{\text{S}}$ ) seedlings (Table 6.1.2a).

T2 seed was collected from 30 individual lines of the antisense p35S::*KNAT6* original splice (AS1-AS30) and from individual lines of the antisense p35S::*KNAT6* alternative splice (asAS) identified in section 6.1.

Seed from the original splice antisense lines AS1-AS30 was analysed. T2 seed were surface sterilised and germinated on  $\frac{1}{2}$  MS10 SS supplemented with 35 mg/L kanamycin sulphate. Approximately 7 DAG, the plates were scored for the ratio of  $\text{Kan}^{\text{R}}$  seedlings to  $\text{Kan}^{\text{S}}$  seedlings (Appendix 3). This revealed that all of the plants were hemizygous and had a number of T-DNA loci ranging from 1 to 4 (Table 6.1.6a).

**Table 6.1.6a** Number of T-DNA loci present in antisense p35S::KNAT6 original splice (AS) lines

Line	T-DNA loci	Line	T-DNA loci	Line	T-DNA loci
AS1	2	AS11	2-3	AS21	2-3
AS2	1-2	AS12	1	AS22	1
AS3	1	AS13	1	AS23	3-4
AS4	1	AS14	1-2	AS24	1
AS5	1	AS15	4	AS25	2-3
AS6	1	AS16	1-2	AS26	1
AS7	2	AS17	1	AS27	1-2
AS8	1	AS18	1	AS28	1-2
AS9	2	AS19	1	AS29	1
AS10	2	AS20	1	AS30	1

Four kanamycin-resistant T2 plants (denoted *a-d*) from each segregation plate were transferred to soil and the T3 seed collected as individuals.

### 6.1.7 Screening of T2 *KNAT6* antisense lines for a root phenotype

A root growth screen was performed on the T2 plants in the same way as for the T2 sense lines (section 6.1.3) even though these plants were hemizygous. Seeds were surface sterilised and germinated on ½ MS10 SS medium and then transferred at 3 DAG to ½ MS10 on vertical plates. Wild type Col-0 plants were grown in the same way to act as a control. At 10 DAG, the roots were examined and any plants that showed a difference in root growth (i.e. root length, lateral root number or lateral root positioning) or aerial growth compared with the Col-0 control were transplanted to soil and grown on (Table 6.1.7a). As in section 6.1.3, no actual measurements were recorded as two discrete populations (i.e. wild type and transgenic) were not being examined. None of these T2 plants showed an aerial phenotype. T3 seed was harvested from these plants.

**Table 6.1.7a** T2 AS seedlings showing a putative phenotype on vertical plates

Line.plant	Putative phenotype
AS2.5, AS13.5	Few laterals
AS3.2, AS6.5, AS10.3, AS10.6, AS18.4, AS20.2	Short root, laterals close tip
AS7.5, AS7.6, AS14.4, AS16.1, AS19.5	Short root
AS9.5, AS13.1, AS13.3, AS16.1, AS16.4, AS18.3, AS18.6, AS19.4, AS22.3, AS26.1,	Two laterals at same position
AS14.5	Cotyledons callusing, two laterals at same position
AS26.6, AS28.6, AS29.6, AS30.1	Main root split by lateral

The phenotypes identified in these plants are similar to those seen in the sense plants in section 6.1.3. As before, these phenotypes were occasionally seen in the wild type Col-0 control (data not shown). There still remained the possibility that the frequency of these characteristics differed between the wild type and antisense plants.

No further analysis was carried out on these plants and it was hoped that the isolation of a T-DNA knockout or the production of RNAi downregulated plants might help with the identification of a *KNAT6* deficient phenotype.

## 6.2 RNAi *KNAT6* lines

The pRNAi vector was used in the production of RNAi lines. This vector contains the CaMV 35S promoter and terminator as well as an ampicillin-based hinge region. RNAi plants were used to examine the effects of downregulating *KNAT6* expression *in vivo* as this technique can give more efficient and reliable downregulation of the target gene than antisense.

Two regions of the *KNAT6* coding region were used to make RNAi constructs. Both of these regions were at the 5' end of the coding sequence away from the highly conserved homeodomain and ELK domains to avoid non-specific downregulation of any other *KN1* Class 1 homeobox genes. The pRNAi vector

contained two small multiple cloning sites (MCSs) on either side of the ampicillin-based hinge region. To allow the formation of the hairpin loop required for downregulation, each coding sequence fragment was cloned into the 5' multiple cloning site in the antisense orientation and into the 3' multiple cloning site in the sense orientation (section 1.1.4). After both *KNAT6* coding regions had been cloned into the vector to give cassettes where expression was mediated by the CaMV 35S promoter, this promoter was replaced by the *KNAT6* native promoter. The native promoter sequence used was the same as that used for both the promoter::*GUS* and promoter::*GFP* constructs detailed in sections 5.1 and 5.2. A schematic of the cloning strategy is shown in Figure 6.2a.

### 6.2.1 Production of 35S::*KNAT6* RNAi plants

Primers were designed to two regions of the *KNAT6* coding region. Each region required the design of two primers to allow its amplification, and these primers were synthesised with different restriction sites to allow the directional cloning of the fragments into the different MCSs of the pRNAi vector. The primer pairs are detailed in Table 6.2.1a. The positions of these primers in the *KNAT6* coding region is shown in Figure 6.2.1a.

**Table 6.2.1a** Primer pairs for amplification of *KNAT6* coding sequence fragments for use in RNAi constructs

Coding sequence fragment	Forward primer	Reverse primer	Orientation in pRNAi
1	<i>RNAiF1(BglII)</i>	<i>RNAiR1(SphI)</i>	sense
1	<i>RNAiF1(SpeI)</i>	<i>RNAiR1(XbaI)</i>	antisense
2	<i>RNAiF2(BglII)</i>	<i>RNAiR2(SphI)</i>	sense
2	<i>RNAiF2(SpeI)</i>	<i>RNAiR2(XbaI)</i>	antisense

PCR using each of the above primer pairs was carried out using the Expand™ High Fidelity PCR system (section 2.8.2). The template for this PCR was the cloned original splice cDNA amplified up from NAA-treated root RNA in section 6.1.1. Analysis of the PCR products revealed that bands of 319 bp using the F1 and R1 primer pairs and of 270 bp using the F2 and R2 primer pairs were

**Figure 6.2a** RNAi construct cloning strategy

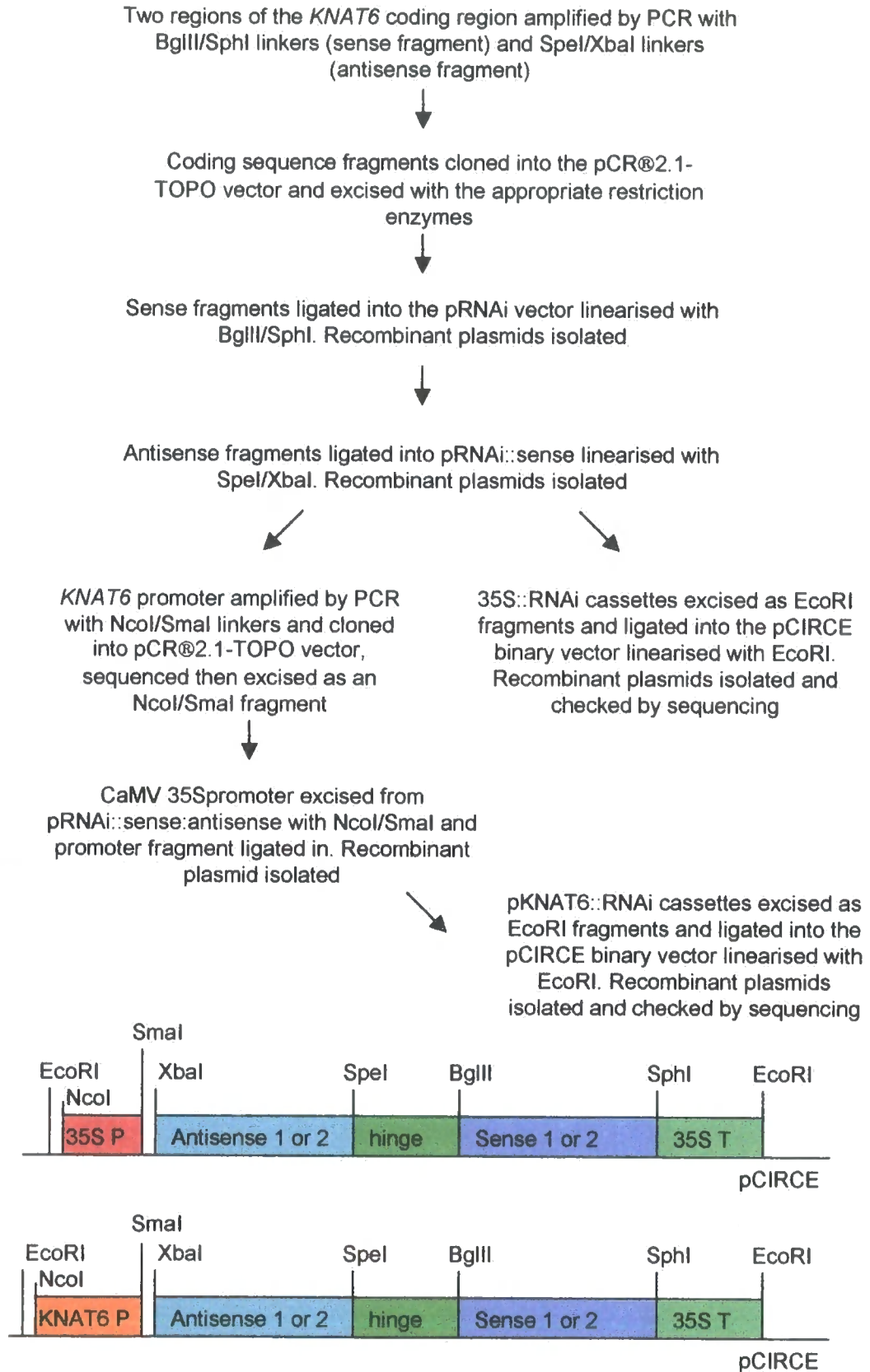


**Figure 6.2.1a** *KNAT6* coding sequence fragments used for production of RNAi constructs

The RNAi 1 fragment is shown in blue

The RNAi 2 fragment is shown in green

The ELK and homeobox regions are underlined

ATGGATGGAATGTACAATTTCCATTCCGGCCGGTGATTATTCAGATAAGTC  
GGTTCTGATGATGTCACCGGAGAGTCTCATGTTTCCTCCGATTACCAAG  
CTTTGCTATGTTCCCTCCGCCGGTAAAATCGTGTCTCTGATGTTTTCGGA  
TCCGACGAGCTACTCTCAGTAGCCGTCTCCGCTTTGTCGTCGGAGGCCG  
CTTCGATCGCTCCGGAGATCCGAAGAAATGATGATAACGTTTCTCTAACT  
GTCATCAAAGCTAAAATCGCTTGTATCCTTCGTATCCTCGCTTACTTCAA  
GCTTACATCGATTGCCAAAAGGTCGGAGCACCACCGGAGATAGCGTGTT  
TACTAGAGGAGATTCAACGGGAGAGTGATGTTTATAAGCAAGAGGTTGTT  
CCTTCTTCTTGCTTTGGAGCTGATCCTGAGCTTGATGAATTTATGAAAC  
GTA CTGCGATATATTAGTGAAATACAAATCGGATCTAGCAAGACCGTTTG  
ACGAGGCAACGTGTTTCTTGAACAAGATTGAGATGCAGCTACGGAACCT  
ATGTA CTGGTGTGCGAGTCTGCCAGGGGAGTTTCTGAGGATGGTGTAAATA  
TCATCTGACGAGGAACTGAGTGGAGGTGATCATGAGGTAGCAGAGGATG  
GGAGACAAAGATGTGAAGACCGGGACCTCAAAGATAGGTTGCTACGCAA  
ATTTGGAAGCCGTATTAGTACTTTAAAGCTTGAGTTCTCAAAGAAGAAGA  
AGAAAGGAAAGTTACCAAGAGAAGCAAGACAAGCTCTTCTTGATTGGTG  
GAATCTCCATTATAAGTGGCCTTACCCTACTGAAGGAGATAAGATAGCAT  
TAGCTGATGCAACGGGGTTAGACCAAAAACAAATCAACAATTGGTTTATA  
AACCAAAGGAAACGTCATTGGAAGCCATCAGAGAATATGCCTTTCGCTAT  
GATGGATGATTCTAGTGGATCATTCTTTACCGAGGAATGA

obtained (Figure 6.2.1b). These PCR products were cloned directly into the pCR®2.1-TOPO vector (section 2.7.4). Colony PCR was performed on white, putative positive colonies (section 2.8.1) using the universal primers *M13F* and *M13R* and a plasmid containing the correct insert was prepared for each of the four *KNAT6* coding sequence fragments.

Each plasmid was then digested using the appropriate restriction endonucleases (section 2.7.1) i.e. *Bgl*III and *Sph*I for the sense fragments and *Spe*I and *Xba*I for the antisense fragments, to release the insert from the pCR®2.1-TOPO vector (Figure 6.2.1c). The bands corresponding to the *KNAT6* fragments were then cut out and purified using the QIAquick® Gel Extraction kit (section 2.4.7). The pRNAi vector was also digested with *Bgl*III and *Sph*I (Figure 6.2.1c), before being dephosphorylated (section 2.7.2) and then purified from a gel as above.

Each of these two sense fragments was then ligated into the digested pRNAi and introduced into chemically competent *E. coli* (sections 2.7.3 and 2.7.6). The resulting colonies were checked by colony PCR using the primers originally used to amplify the inserted sense fragments (see Table 6.2.1a). A colony containing the insert of the correct size was then used to prepare plasmid DNA. These two plasmids (pRNAi::sense1 and pRNAi::sense2) were then digested with *Spe*I and *Xba*I (Figure 6.2.1d), analysed by gel electrophoresis and purified as before. Ligation of the appropriate purified antisense fragment with the cut plasmids (i.e. pRNAi + sense fragment 1 with antisense fragment 1 and pRNAi + sense fragment 2 with antisense fragment 2) was carried out and the ligations were introduced into *E. coli* as before.

As the vector already contained a *KNAT6* fragment, colony PCR was carried out using a primer to the 35S promoter, *35S P1*, and the forward primer which was used for amplification of the fragment originally (i.e. *RNAiF1(SpeI)* or *RNAiF2(SpeI)*). This allowed the identification of colonies that contained the antisense insert, and therefore the complete RNAi cassette. Plasmids, denoted pRNAi1 and pRNAi2, were prepared from single positive colonies before the RNAi cassettes were released by digestion with *Eco*RI. The digests were analysed by gel electrophoresis (Figure 6.2.1e) and the cassettes purified from

**Figure 6.2.1b** Amplification of *KNAT6* coding sequence fragments for RNAi constructs by PCR

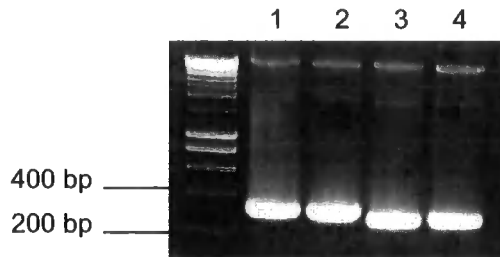


**Figure 6.2.1c** Preparation of *KNAT6* coding sequence fragments and pRNAi vector for ligations

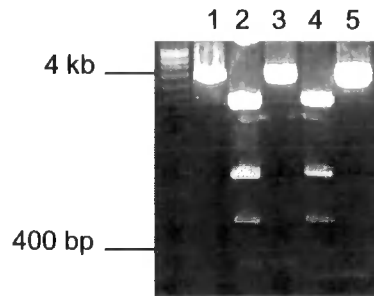
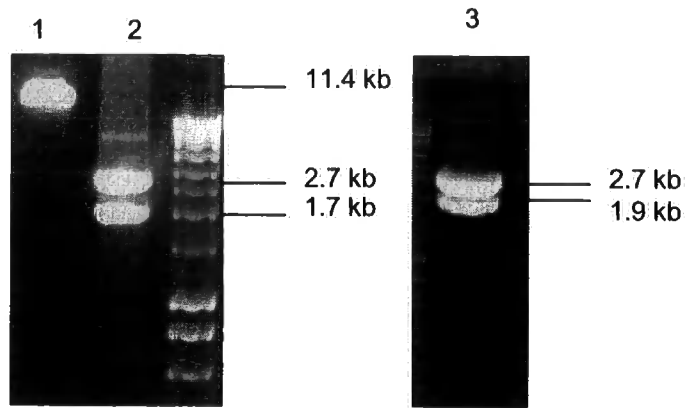


**Figure 6.2.1d** Linearisation of pRNAi::sense1 and pRNAi::sense2 by digestion with *SpeI*/*XbaI*



**Figure 6.2.1e** Preparation of pCIRCE and RNAi cassettes for ligations



Lane 1: 11.4kb pCIRCE linearised by digestion with EcoRI

Lane 2: 1.7 kb RNAi2 cassette released from 2.7 kb pRNAi by digestion with EcoRI

Lane 3: 1.8 kb RNAi1 cassette released from 2.7 kb pRNAi by digestion with EcoRI

the gel. In addition, the pCIRCE binary vector was digested with EcoRI, dephosphorylated and then purified from a gel in the same way as pRNAi (Figure 6.2.1e).

Finally, the two cassettes, RNAi1 and RNAi2, containing the *KNAT6* fragments were ligated into pCIRCE. The ligations were introduced into *E. coli* as before and putative positive white colonies were checked by colony PCR using the RNAiF and RNAiR primers which were originally used to amplify up the *KNAT6* coding region fragments (Table 6.2.1a). Positive colonies were used to prepare plasmids (as detailed in section 2.4.2) that were checked by sequencing with the universal primers *M13F* and *M13R*. This confirmed that the constructs were correct and so the plasmids were introduced into electrocompetent *Agrobacterium tumefaciens* strain C58C3 (section 2.2.3). *Agrobacterium* colonies were checked by colony PCR using the RNAiF and RNAiR primers as above.

Positive colonies were selected and used for introduction of the constructs to *Arabidopsis* var. Columbia by the dipping method (section 2.2.4). Seed from the dipped plants was sown on ½ MS10 SS medium supplemented with 35 mg/L kanamycin sulphate and 200 mg/L augmentin. Transformed plants, denoted RNAi1 and RNAi2, were identified and seed collected as individual lines.

### 6.2.2 Production of pKNAT6::*KNAT6* RNAi plants

The *Promoter For* and *Promoter Rev* primers that were used in section 5.1.1 to clone the *KNAT6* promoter region were resynthesised with new restriction sites to allow the replacement of the CaMV 35S promoter with the *KNAT6* native promoter. *RNAipromF* contains an NcoI and *RNAipromR* contains a SmaI site. These two primers were then used to reamplify the cloned promoter obtained in section 5.1.1 using the Expand™ High Fidelity PCR system (section 2.8.2). The PCR products were analysed by gel electrophoresis and a band of 2074 bp was obtained as expected (Figure 6.2.2a). This band was cut out, purified and then cloned into the pCR®2.1-TOPO (section 2.7.4). Putative positive white colonies were checked by colony PCR using the universal primers *M13F* and *M13R* and a positive colony was identified and used to prepare plasmid DNA (sections 2.8.1 and 2.4.1). The plasmid was then sequenced with *M13F*, *M13R*, *Prom*

**Figure 6.2.2a** Amplification of the 2.1 kb *KNAT6* promoter fragment with *Nco*I/*Sma*I linkers by PCR

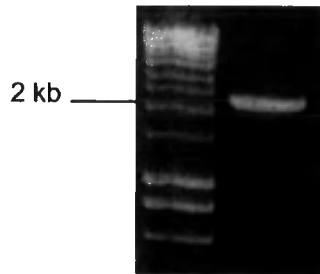


**Figure 6.2.2b** Release of the 2.1 kb *KNAT6* promoter fragment from pCR®2.1-TOPO by digestion with *Nco*I/*Sma*I

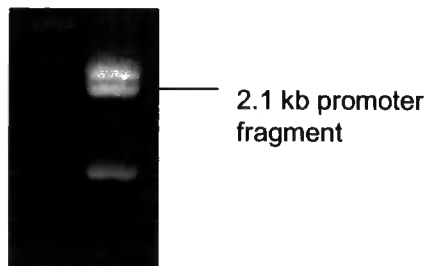
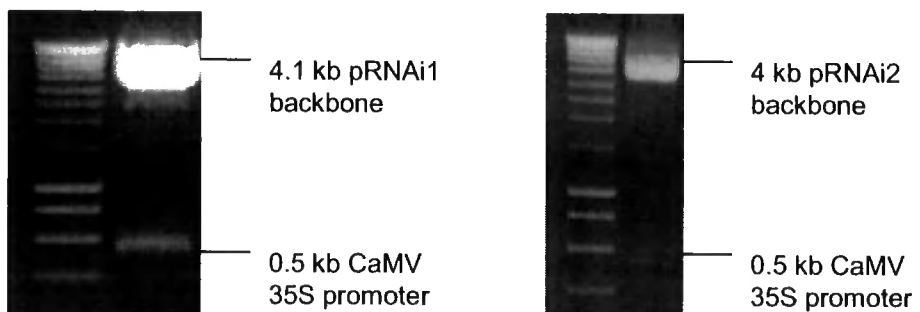


**Figure 6.2.2c** Release of the 0.5 kb CaMV 35S promoter fragment from pRNAi1 and pRNAi2 by digestion with *Nco*I/*Sma*I

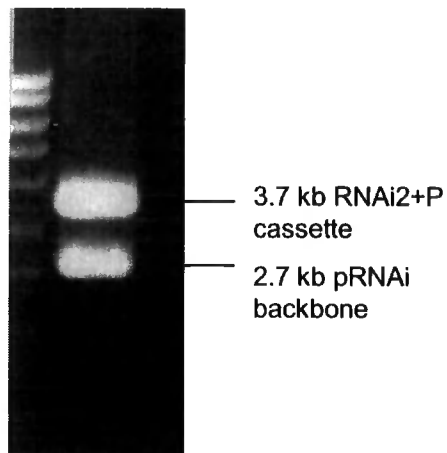
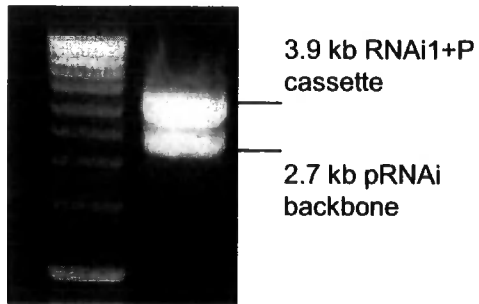


*Seq For* and *Prom Seq Rev*. This revealed that one of the two apparent errors identified in the promoter in section 5.1.1 had reverted to the correct base (indicating that this was probably a sequencing error rather than a PCR error), and that one further error had been introduced. However, as this new error was more than 1 kb upstream of the ATG, it was not thought that this would influence promoter activity greatly.

The plasmid DNA was then digested using *NcoI* and *SmaI* to release the promoter fragment (Figure 6.2.2.b). In addition, the pRNAi1 and pRNAi2 plasmids produced in section 6.2.1 were digested with *NcoI* and *SmaI* to release the CaMV 35S promoter (Figure 6.2.2c). The *KNAT6* promoter fragment and the pRNAi1 and 2 vectors without the 35S promoter were purified from the gel before the promoter fragment was ligated into each pRNAi vector. The ligations were introduced into *E. coli* and putative positive colonies were analysed by colony PCR using the *RNAipromF* and *RNAipromR* primers. Those colonies containing an insert of the correct size were used to prepare plasmid DNA. These plasmids, denoted pRNAi1+P and pRNAi2+P were then digested with *EcoRI* to release the RNAi1+P and RNAi2+P cassettes (Figure 6.2.2d). These cassettes were then ligated into the pCIRCE linearised with *EcoRI* that was prepared in section 6.2.1. Colony PCR was carried out on white putative positive colonies using the *RNAipromF* and *RNAipromR* primers and a single positive colony from each ligation was used to prepare plasmid DNA (section 2.4.2). Sequencing with *M13F*, *M13R* and the *Cds For* primers confirmed that the constructs were correct.

The RNAi1+P and RNAi2+P cassettes in pCIRCE were introduced into *Agrobacterium tumefaciens* strain C58C3 by electroporation (section 2.2.3), positive colonies were identified by colony PCR as above and used for introduction of the constructs into *Arabidopsis* var. Columbia by the dipping method (section 2.2.4). Seed from the dipped plants was sown on ½ MS10 SS medium supplemented with 35 mg/L kanamycin sulphate and 200 mg/L augmentin. Transformed plants, denoted RNAi1+P and RNAi2+P, were identified and seed collected as individual lines.

**Figure 6.2.2d** Release of RNAi1+P and RNAi2+P cassettes from pRNAi1+P and pRNAi2+P plasmids by digestion with EcoRI



### 6.2.3 Isolation of homozygous *KNAT6* RNAi lines

T2 seed from 10 individual lines from each transformation with an RNAi construct i.e. RNAi1, RNAi2, RNAi1+P and RNAi2+P that was collected in sections 6.2.1 and 6.2.2 was surface sterilised and germinated on ½ MS10 SS supplemented with 35 mg/L kanamycin sulphate. Approximately 7 DAG, the plates were scored for the ratio of Kan<sup>R</sup> seedlings to Kan<sup>S</sup> seedlings (Appendix 3, Table 7). This revealed that all of the plants were hemizygous and had a number of T-DNA loci ranging from 0 to 4 (Table 6.2.3.a).

Four kanamycin-resistant seedlings (denoted *a-d*) from each transformed line were transferred to soil from the selective plates and the T3 seed was harvested as individual lines.

As no clear phenotype was observed in the root growth assays using hemizygous sense and antisense lines, homozygous T3 seeds were identified by kanamycin segregation analysis and used for the RNAi root growth assays.

**Table 6.2.3a** Number of T-DNA loci present in RNAi lines

Line	T-DNA loci	Line	T-DNA loci
RNAi1 1	1-2	RNAi1+P 1	1
RNAi1 2	2-3	RNAi1+P 2	1
RNAi1 3	1	RNAi1+P 3	1-2
RNAi1 4	1-2	RNAi1+P 4	1
RNAi1 5	2-3	RNAi1+P 5	1
RNAi1 6	1	RNAi1+P 6	1
RNAi1 7	2-3	RNAi1+P 7	1
RNAi1 8	1	RNAi1+P 8	1
RNAi1 9	1	RNAi1+P 9	1
RNAi1 10	3	RNAi1+P 10	1-2
RNAi1 11	1-2	RNAi1+P 11	1
RNAi1 12	1	RNAi1+P 12	2
RNAi1 13	1-2	RNAi1+P 13	1
RNAi1 14	1	RNAi1+P 14	2
RNAi1 15	1	RNAi1+P 15	2
RNAi2 1	1	RNAi2+P 1	1
RNAi2 2	1	RNAi2+P 2	1
RNAi2 3	1-2	RNAi2+P 3	1
RNAi2 4	1	RNAi2+P 4	1
RNAi2 5	1	RNAi2+P 5	1
RNAi2 6	2	RNAi2+P 6	1
RNAi2 7	1	RNAi2+P 7	1-2
RNAi2 8	2-3	RNAi2+P 8	1
RNAi2 9	1	RNAi2+P 9	2
RNAi2 10	0	RNAi2+P 10	4
RNAi2 11	1	RNAi2+P 11	1
RNAi2 12	1	RNAi2+P 12	1
RNAi2 13	1	RNAi2+P 13	1
RNAi2 14	1	RNAi2+P 14	1-2
RNA12 15	1	RNAi2+P 15	1

For each RNAi construct, ten homozygote lines were identified (Table 6.2.3b) and used in section 6.2.4 below.

**Table 6.2.3b** T3 homozygous RNAi lines

Line	Homozygotes
RNAi1	1d, 2b, 3d, 4c, 5b, 6d, 7d, 9b, 11c, 12b
RNAi2	1a, 2a, 4c, 5a, 6c, 7a, 8b, 9a, 11d, 13d
RNAi1+P	1c, 2b, 3d, 5a, 7c, 9b, 10a, 12c, 14b, 15d
RNAi2+P	1a, 3a, 4c, 9b, 10a, 11a, 12a, 13a, 14b, 15a

#### 6.2.4 Analysis of homozygous *KNAT6* RNAi lines

Ten plants from each homozygous RNAi line were grown on vertical plates to allow root growth measurements to be taken. Seeds were surface sterilised and germinated on ½ MS10 SS medium and then transferred at 3 DAG to ½ MS10 medium on vertical plates. The length of the roots was measured at 3 DAG, 6 DAG, 9 DAG and 12 DAG. In addition, at each time point the number of lateral roots and anchor roots was recorded as well as the distance from the root tip to the last lateral root to emerge. Wild type Col-0 plants were grown in the same way to act as a control.

The average root length for each line was calculated at each time point (Figures 6.2.4a-d). There was no difference between the root length of any of the RNAi lines and the Col-0 control.

The average distance from the root tip to the last lateral root to emerge was also calculated for each line at each time point (Figures 6.2.4e-h). For the Col-0 control, this distance increased so that there was a greater distance from the root tip to the last lateral root to emerge as time progressed. However, in the RNAi1, RNAi2 and RNAi1+P (Figures 6.2.4e-g), this distance decreases i.e. the plants initiate lateral roots closer to the root tip with time. For the RNAi2+P plants, this is more variable, with some of the plants showing a similar trend to the Col-0 plants, and some showing a decrease in this distance. This result is discussed in section 8.4.2.



**Figure 6.2.4c** Length of primary root in homozygous RNAi1+P plants

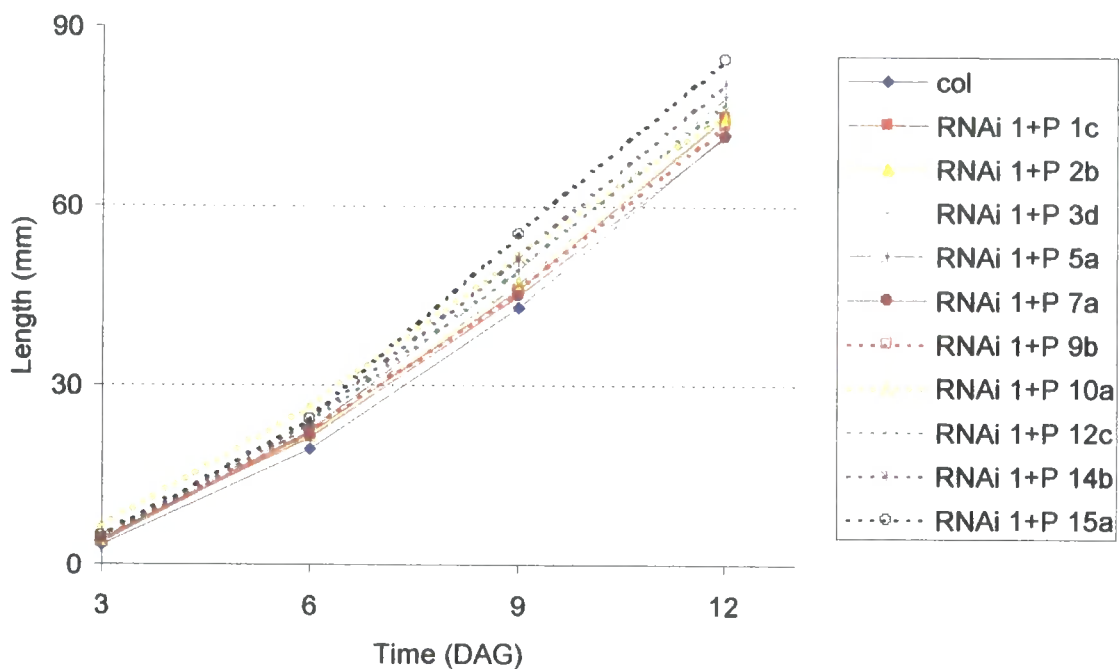


**Figure 6.2.4d** Length of primary root in homozygous RNAi2+P plants

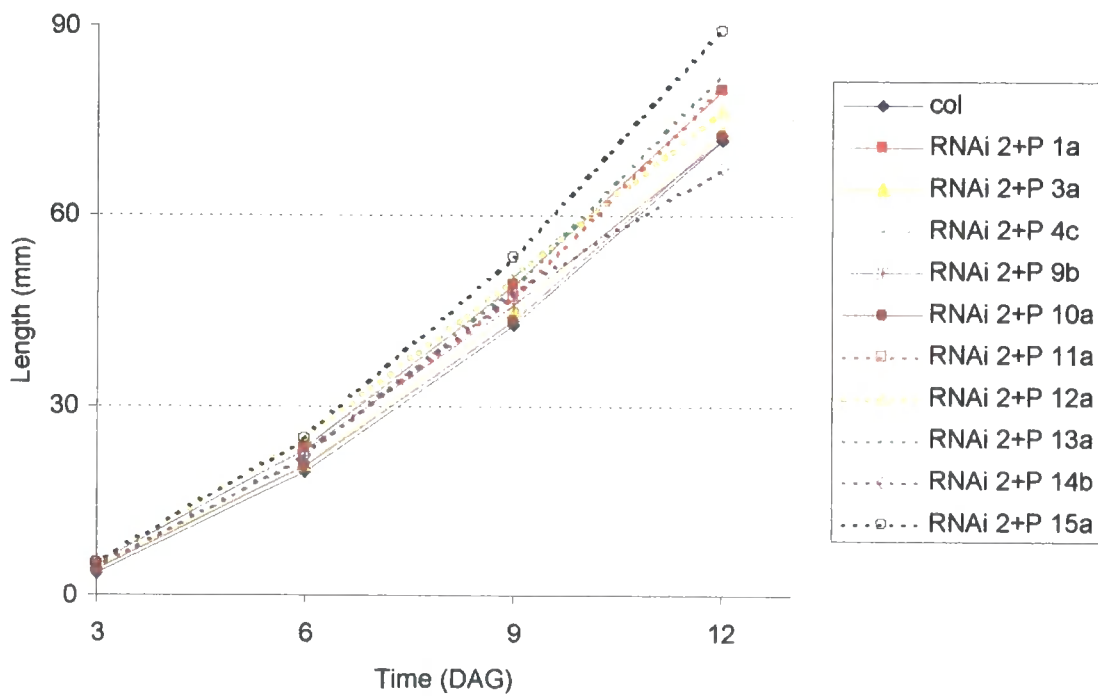


**Figure 6.2.4e** Distance from the primary root tip to the last lateral root primordium to emerge in homozygous RNAi1 plants

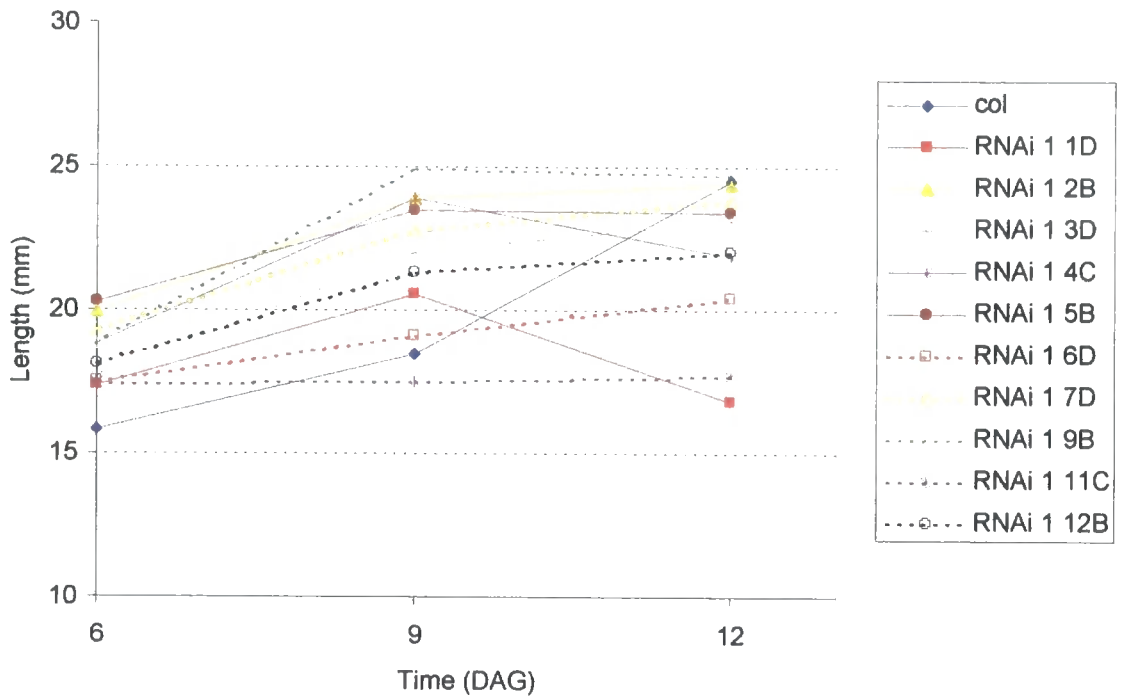


**Figure 6.2.4f** Distance from the primary root tip to the last lateral root primordium to emerge in homozygous RNAi2 plants

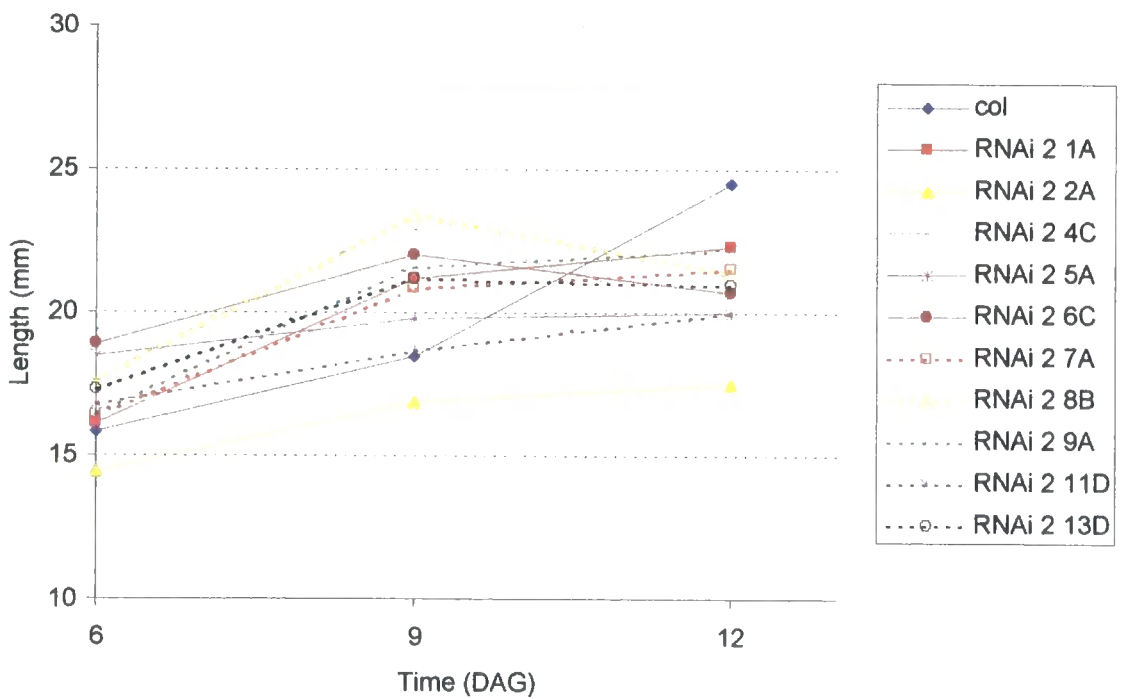


**Figure 6.2.4g** Distance from the primary root tip to the last lateral root primordium to emerge in homozygous RNAi1+P plants

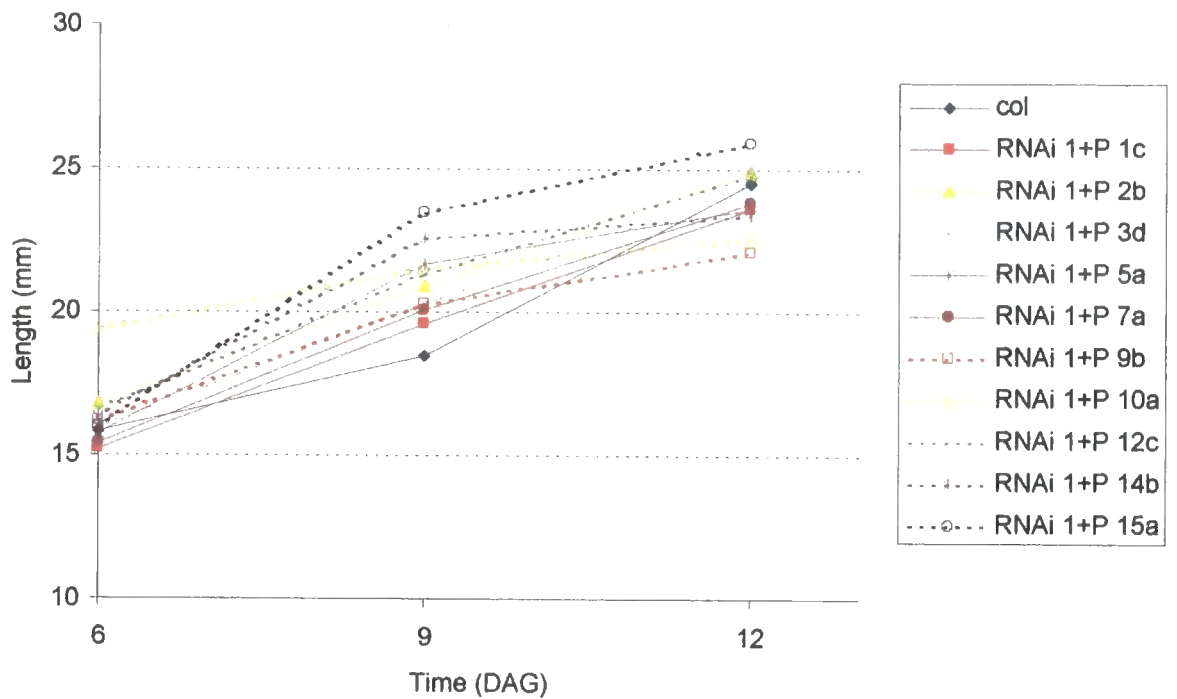


**Figure 6.2.4h** Distance from the primary root tip to the last lateral root primordium to emerge in homozygous RNAi2+P plants

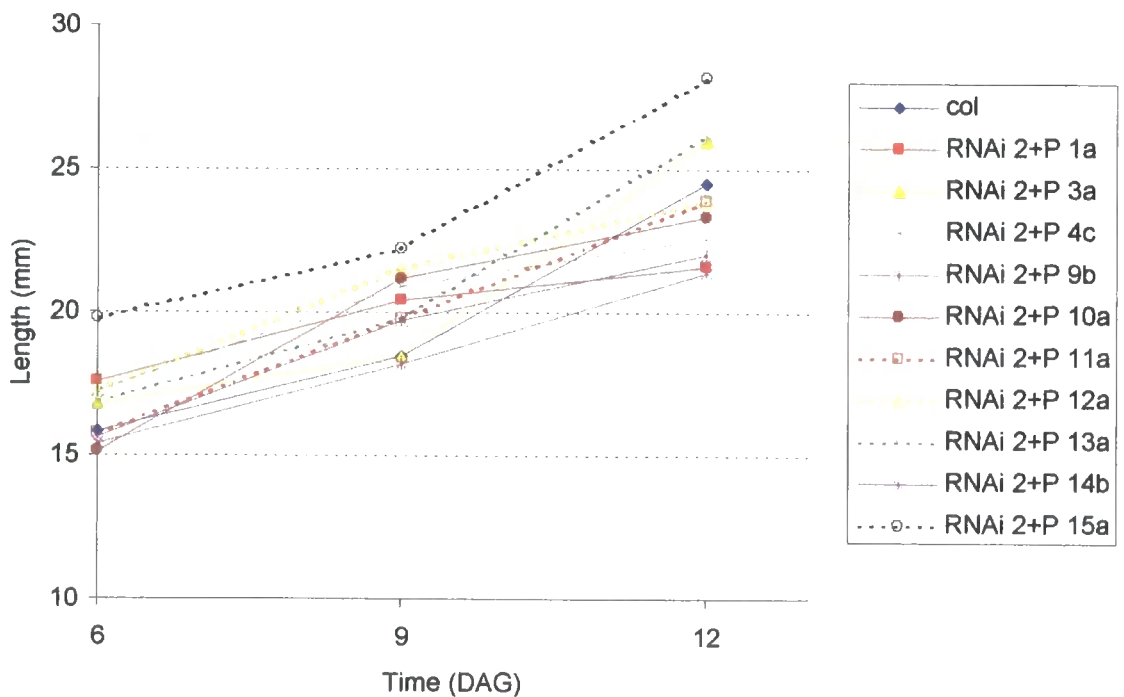


**Figure 6.2.4i** Number of lateral roots produced by homozygous RNAi1 plants

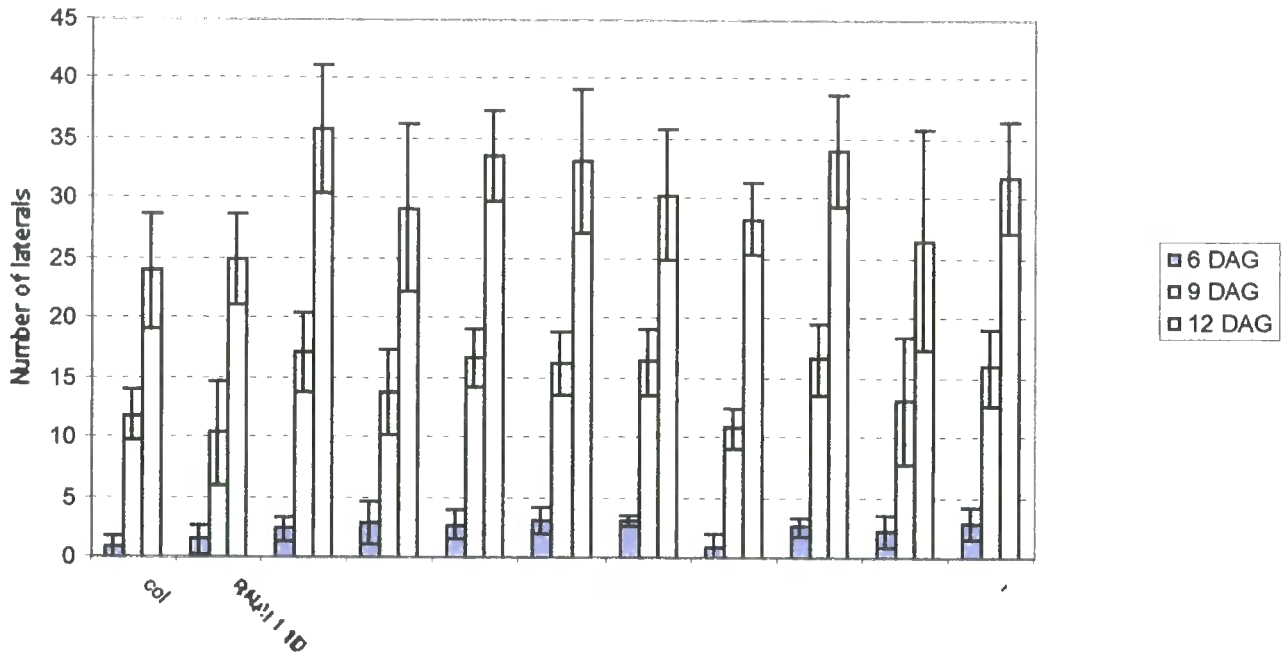


**Figure 6.2.4j** Number of lateral roots produced by homozygous RNAi2 plants

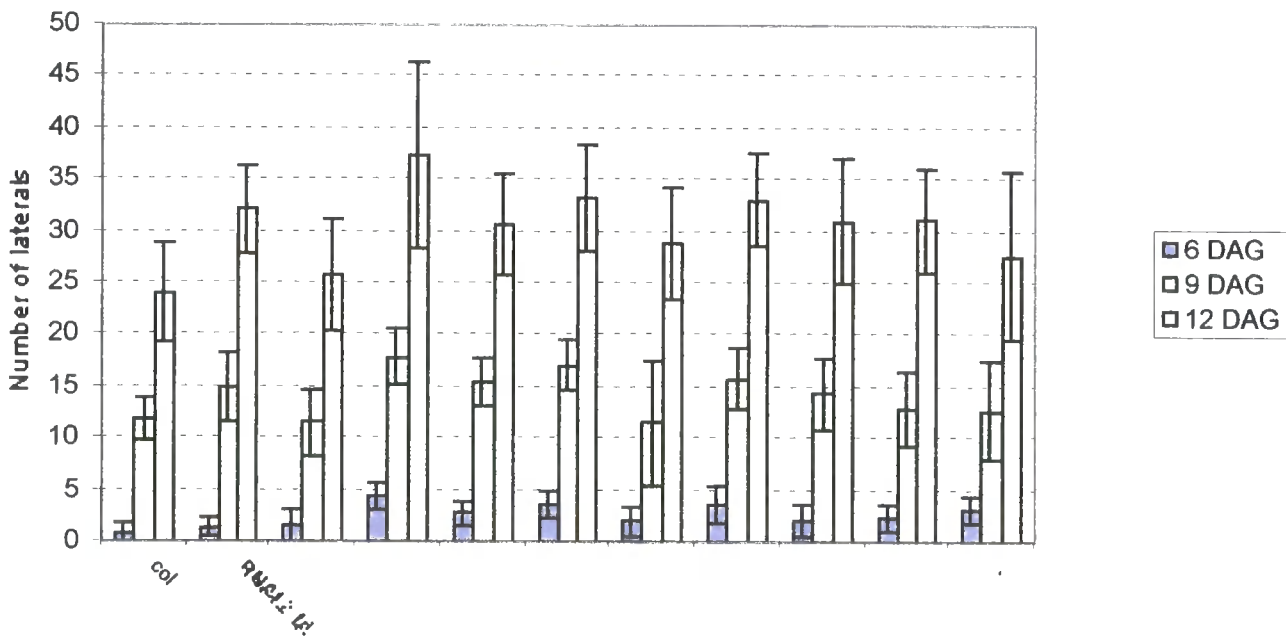


**Figure 6.2.4k** Number of lateral roots produced by homozygous RNAi1+P plants

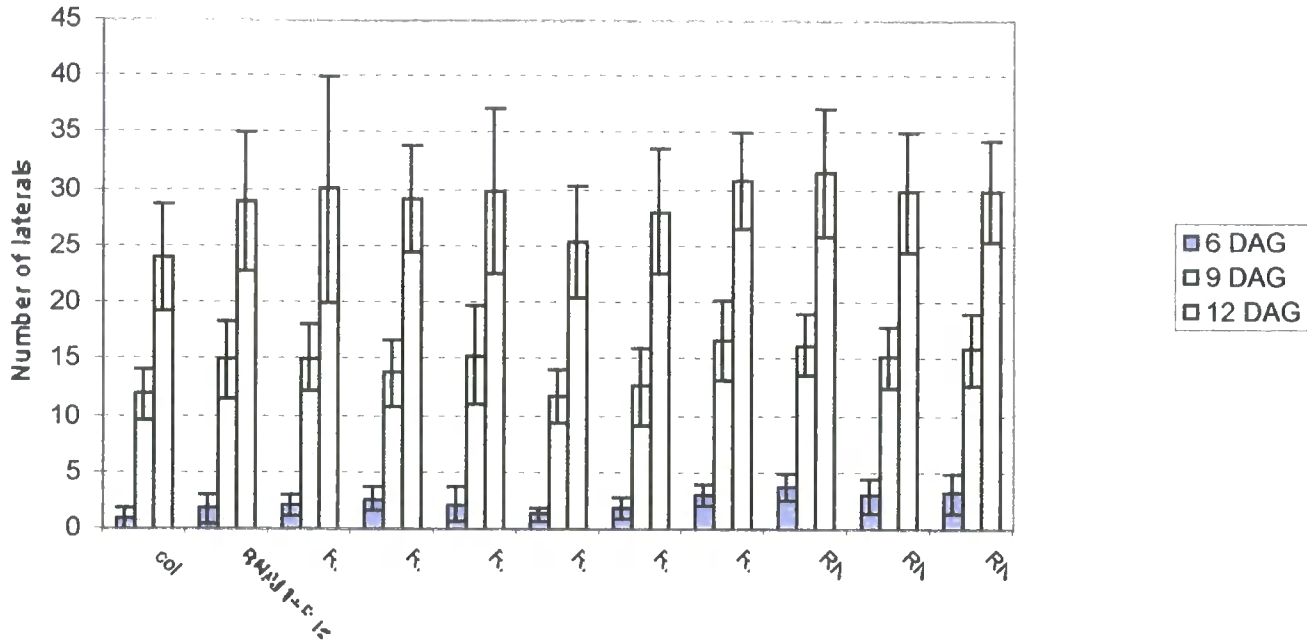


**Figure 6.2.4l** Number of lateral roots produced by homozygous RNAi2+P plants

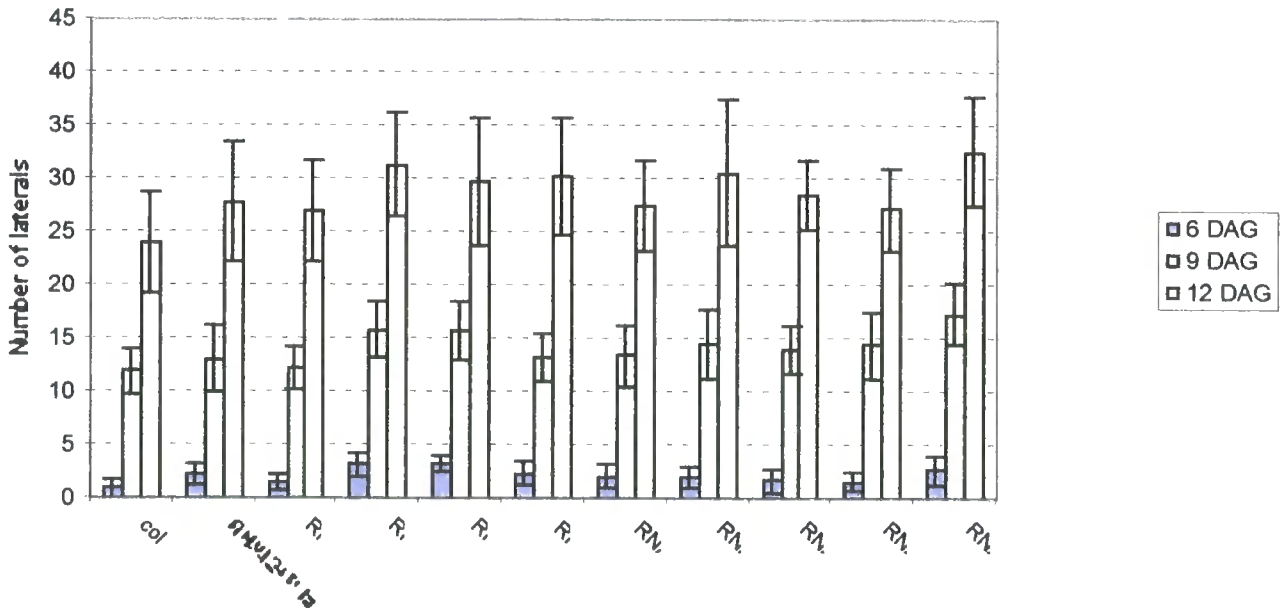


**Figure 6.2.4m** Number of anchor roots produced by homozygous RNAi1 plants

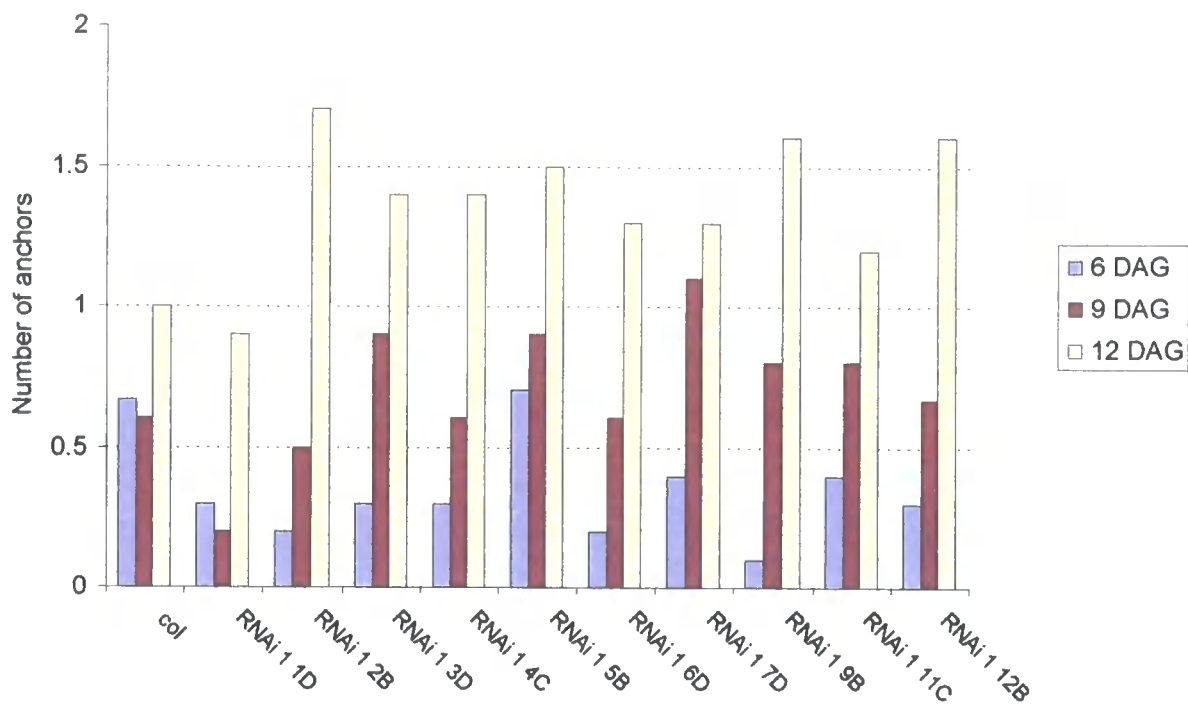


**Figure 6.2.4n** Number of anchor roots produced by homozygous RNAi2 plants

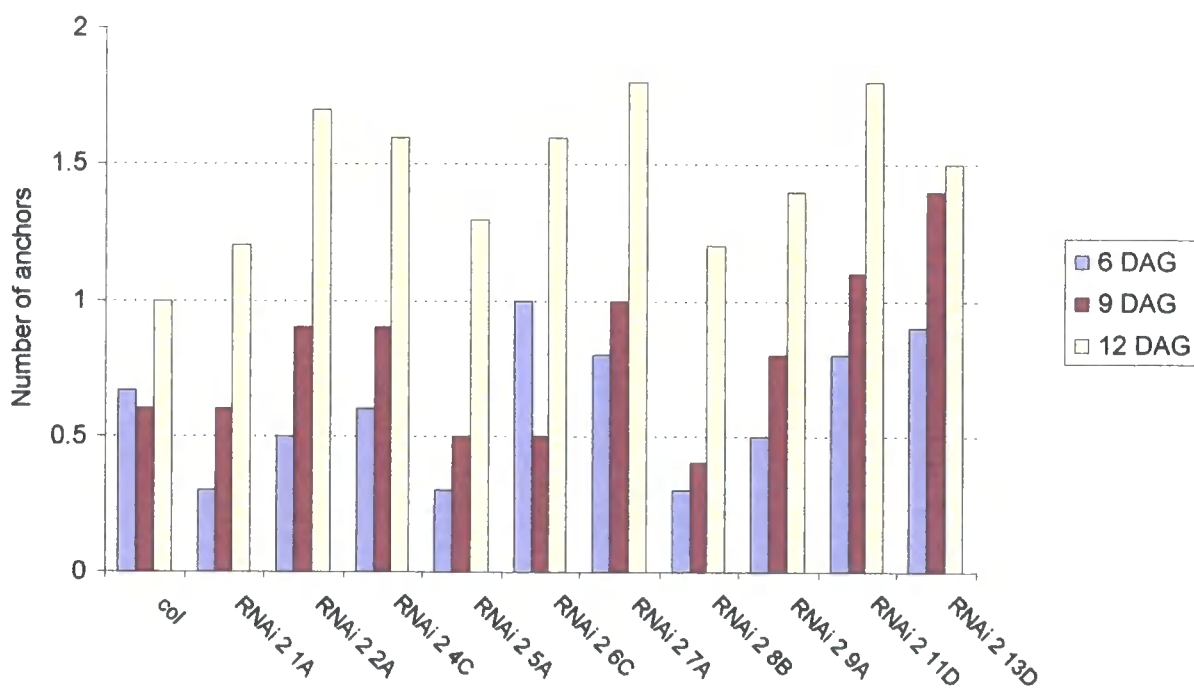


**Figure 6.2.4o** Number of anchor roots produced by homozygous RNAi1+P plants

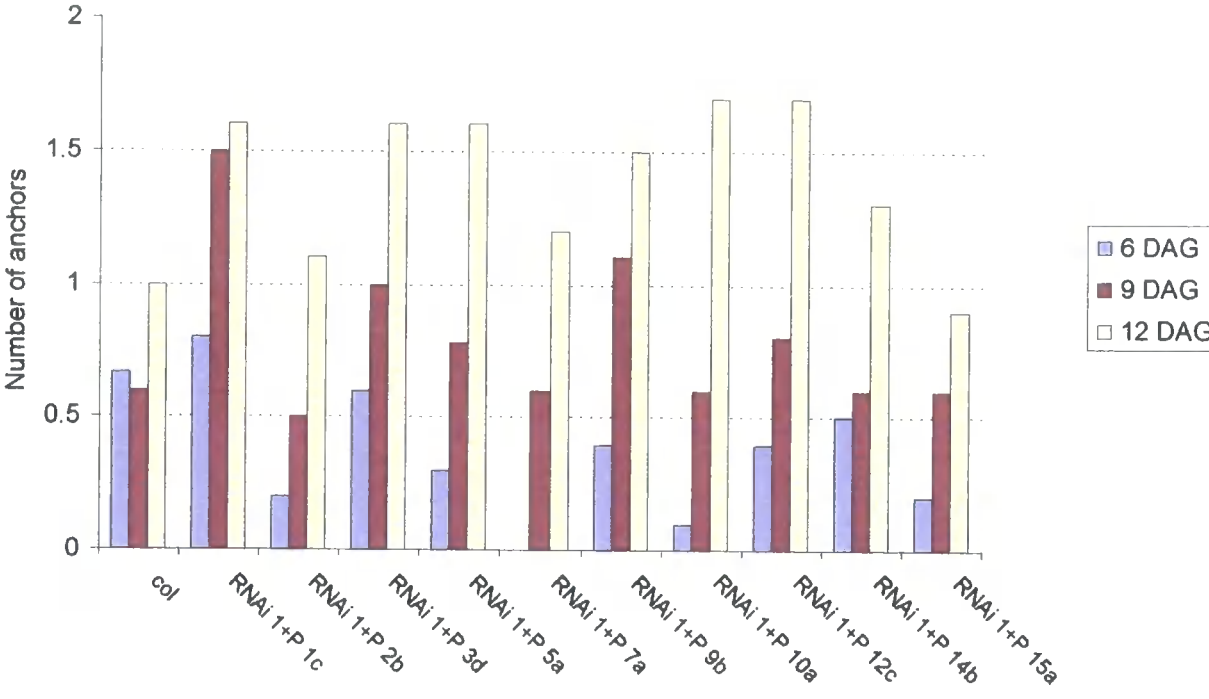
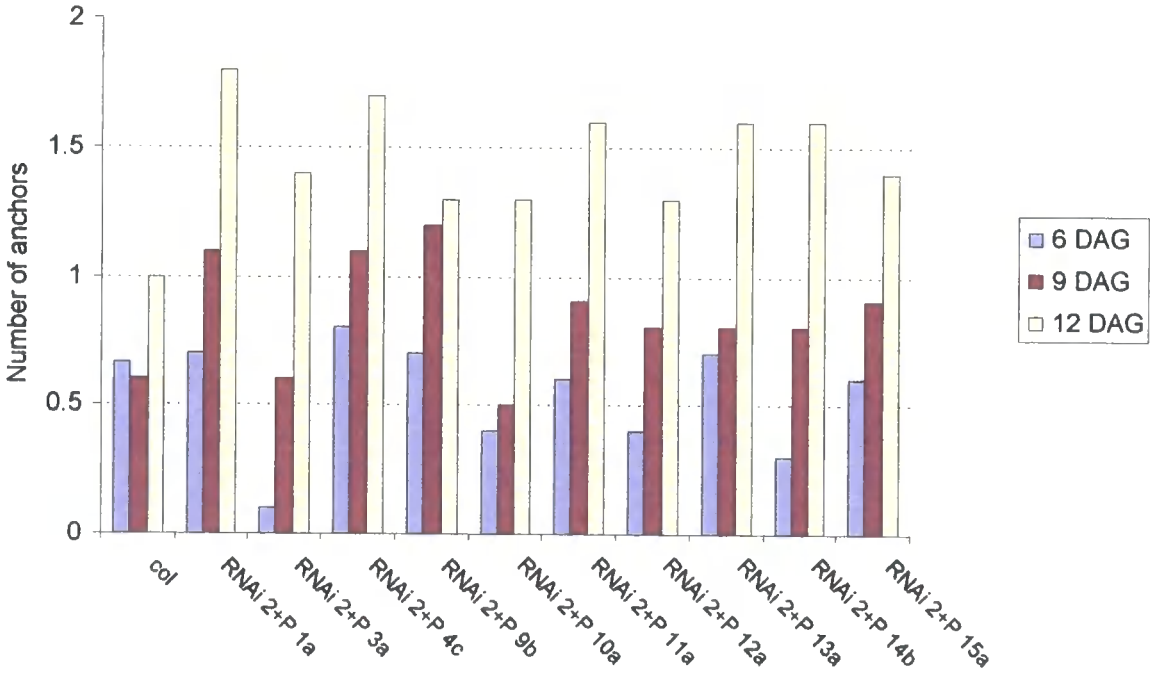


**Figure 6.2.4p** Number of anchor roots produced by homozygous RNAi2+P plants



The average number of lateral roots and anchor roots produced by each transgenic line at each time point was also calculated (Figures 6.2.4i-p) but these did not appear different from the Col-0 control.

The data used to plot these graphs is shown in Appendix 4.

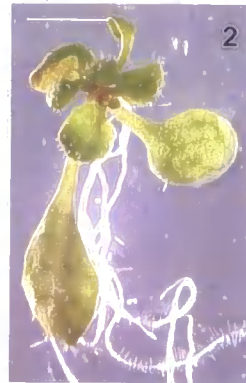
As in the case of the sense and antisense plants analysed in sections 6.1.3 and 6.1.6, occasional plants with short roots or with laterals initiating close together were observed but these were at low frequency within each homozygous line. It also appeared that plants with short roots were always those that were growing into the medium rather than on its surface. Some of the plants, including Col-0 controls, had an unusual aerial phenotype where apical dominance appeared to have broken, leading to the initiation of leaves from the axillary buds. In addition, some of the RNAi plants showed evidence of callus formation on the cotyledons, and a very small number of plants showed a much more severe aerial phenotype where the SAM appeared to initiate many leaf-like structures. These phenotypes were never seen in the Col-0 controls. Figure 6.2.4q shows examples of the range of phenotypes seen in RNAi plants and Col-0 controls.

A summary of the range of putative phenotypes seen in the T3 homozygous RNAi lines is given in Table 6.2.4a. The number in brackets is the number of plants in a given line showing the phenotype. These results are discussed in section 8.4.2.

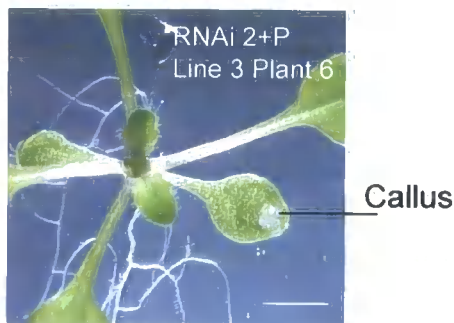
**Figure 6.2.4q** Range of putative phenotypes in RNAi plants

Bar approx. 5 mm

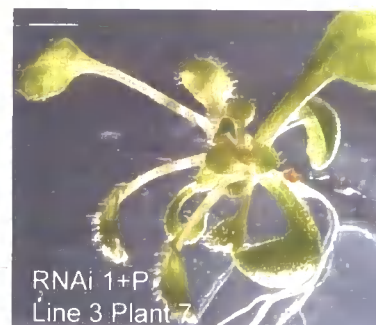
(i) Col-0 plants showing normal development (1) and a break in apical dominance (2)



(ii) RNAi plant showing callusing on cotyledons



(iii) RNAi plant showing a break in apical dominance



(iv) RNAi plants showing callusing at the shoot apex



(v) RNAi plants with severe apical phenotype



**Table 6.2.4a Range of putative phenotypes seen in T3 homozygous RNAi lines**

Phenotype	Line				
	Col-0	RNAi1	RNAi2	RNAi1+P	RNAi2+P
Cotyledons callusing	-	1d(3) 2b(1) 6d(4) 11c(1)	4c(3) 5a(1) 8b(1) 9a(2) 13d(1)	9b(1) 10a(1) 14b(1)	4c(1) 10a(1) 12a(1) 13a(1) 15a(1)
Apical dominance broken	(1)	1d(1) 11c(1)	1a(1) 9a(1) 13d(1)	3d(1) 9b(1) 14b(1) 15d(2)	1a(2) 11a(1)
Cotyledons callusing and apical dominance broken	-	3d(1)	-	5a(3)	-
Severe apical phenotype	-	1d(1) 11c(2)	-	-	-

Seed from these T3 homozygous RNAi lines was also sown in soil and grown in the environment room. No aerial phenotype was observed for these plants after 6 weeks of growth.

### 6.3 Summary

The results indicated in this chapter indicate that only the original splice (S) isoform of *KNAT6* is capable of producing the characteristic leaf phenotype seen when other KNOX class 1 genes are overexpressed. There was no clear root phenotype in plants which displayed the aerial phenotype, although one line did show a reduction in root length, the number of lateral and anchor roots which were produced as well as an alteration in lateral root distribution. This result is discussed further in section 8.4.1.

Antisense suppression of *KNAT6* did not produce a clearly visible phenotype in any of the parameters examined under the experimental conditions used here.

It may be that *KNAT6* is redundant, or it may be that the antisense suppression has not worked efficiently.

Analysis of RNAi lines gave no strong root phenotype being visible. However, some plants showed an aerial phenotype that was characterised by callus formation on the cotyledons as well as more severe apical defects.

## Chapter 7 Identification of *KNAT6* insertion mutants

In addition to the transgenic approaches described in Chapter 6, a number of different *Arabidopsis* insertion mutant libraries were screened to identify a *KNAT6* knockout.

The *Arabidopsis* Knockout Facility collection was screened by PCR for a T-DNA knockout of the *KNAT6* gene. In addition, collections generated at the Salk Institute, the Torrey Mesa Research Institute (TMRI), the Cold Spring Harbor Laboratory (CSHL) and the John Innes Research Centre and Sainsbury Laboratory that had sequence data available, were searched.

### 7.1 Screening the *Arabidopsis* Knockout Facility Alpha collection

The Alpha collection of T-DNA insertion lines at the *Arabidopsis* Knockout Facility (KO facility) at the University of Wisconsin Biotechnology Centre (<http://www.biotech.wisc.edu/Arabidopsis>) consisted of 60,480 lines that were organised into pools to allow efficient screening by PCR (Krysan *et al.*, 1999). The T-DNA insertions were produced using the pD991 vector that is a derivative of pCGN1547 (McBride and Summerfelt, 1990). The PCR reactions were carried out at the Centre with the primers specific for *KNAT6* and the products returned for analysis. The pooling strategy and the insertion screening strategy is shown in Figure 7.1a. The *Arabidopsis* ecotype that was used to produce the Alpha collection was *Ws*.

PCR primers, designated *ATKO For1* and *ATKO Rev1*, were designed to amplify the complete *KNAT6* genomic region according to the parameters detailed by the KO facility. The primers designed were 29 bp in length and had a GC content of 34 – 50% overall. The GC content of the 3' end of the primer was less than 50% and the last two bases at the 3' end of the primer contained a maximum of a single C or G.

The *KNAT6* primers, which amplify a 5.4 kb fragment, were tested along with control primers (*Con-1A* and *Con-1B*) and the T-DNA left border primer *JL-202* designed by the KO facility. Test PCR reactions with various primer

**Figure 7.1a** Pooling and screening strategy for KO facility

Alpha collection

(i) Pooling strategy

Vacuum infiltration of  
15,000 plants and  
isolation of 60,480 Kan<sup>R</sup>  
plants



6,720 J pools generated  
by combining seed from  
9 Kan<sup>R</sup> plants



270 H pools of 225 lines  
generated by combining  
seed from 25 pools of 9.  
DNA extracted



30 X pools of 2025 lines  
generated by combining  
DNA from 9 pools of 225.

(ii) Insertion screening strategy

Primary PCR screen using DNA  
from 30 X pools using 5' gene  
primer and T-DNA left border  
primer



Confirm positives by  
southern blot and  
sequencing



Secondary PCR screen  
using DNA from H pools  
corresponding to X pool  
which contained hit



Tertiary PCR on DNA from J  
pools corresponding to H pool  
which contained hit



Identify individual plant by  
extracting DNA from single  
plants in the J pool which  
contained hit

combinations as detailed in Table 7.1a were performed as described by the KO facility (section 2.8.3).

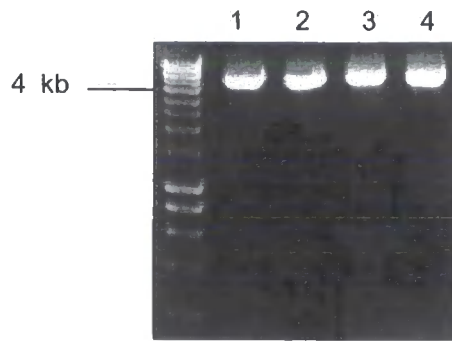
**Table 7.1a** Reactions performed to test primers for KO facility screening

Reaction	Primer 1	Primer 2	Primer 3
1	<i>Con-1A</i>	<i>Con-1B</i>	-
2	<i>Con-1A</i>	<i>Con-1B</i>	<i>JL-202</i>
3	<i>ATKO For1</i>	<i>ATKO Rev1</i>	-
4	<i>ATKO For1</i>	<i>ATKO Rev1</i>	<i>JL-202</i>

The *Con-1A* and *Con-1B* primers amplified a 5 kb fragment of the *Arabidopsis* genome and were used to test PCR conditions in this lab and provide a standard with which to judge the gene specific primers. Reaction 2 tested the compatibility of *Con-1A* and *Con-1B* with the border primer *JL-202*. Reaction 3 tested the gene specific primers and reaction 4 tested the compatibility of the gene specific primers with the border primer *JL-202*.

5 µl of each PCR product was analysed by gel electrophoresis (Figure 7.1b). The amount of PCR product in reactions 1 and 3 was similar, indicating that the gene specific primers worked well (by comparison with the control primers) under the PCR conditions used. The amount of PCR products in lanes 3 and 4 was also similar, indicating that the gene specific primers were compatible with the left border primer *JL-202*. Having demonstrated that the ATKO primers designed to *KNAT6* were suitable for use in the PCR screen, primers were desiccated and sent to the KO facility. As shown in Figure 7.1a, the DNA from the T-DNA tagged lines was organised into 30 pools. To allow the detection of an insertion in either orientation, two PCR reactions were carried out on each pool, one using the *ATKO For1* primer with *JL-202* and one using the *ATKO Rev1* with *JL-202*. In addition, a control reaction was performed using the *ATKO For1* and *Rev1* primers with wild type *Ws* DNA as a template. The PCR reactions were returned and analysed by running 5 µl of each PCR product out on a gel (Figure 7.1c) before transferring the DNA to membrane by Southern blotting as described in section 2.6.1.

**Figure 7.1b** Compatibility of *ATKO For1* and *ATKO Rev1* primers used to screen to *Arabidopsis* KO facility collection



Lane 1: *Con-1A* and *Con-1B* primers give a 5 kb band

Lane 2: *Con-1A*, *Con-1B* and *JL-202* primers give a 5 kb band

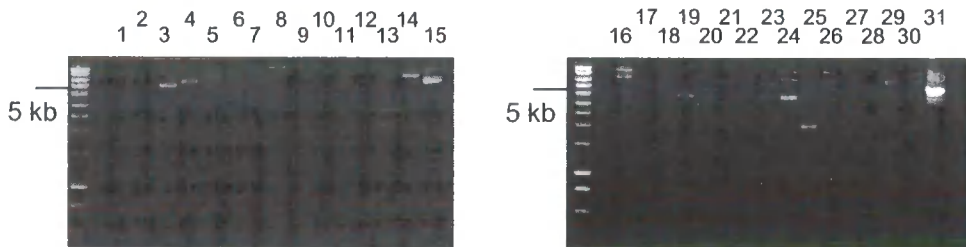
Lane 3: *ATKO For1* and *ATKO Rev1* primers give a 5.4 kb band

Lane 4: *ATKO For1*, *ATKO Rev1* and *JL-202* primers give a 5.4 kb band

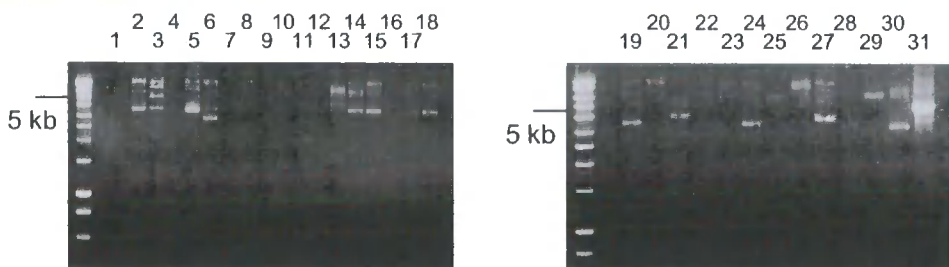
**Figure 7.1c** Analysis of primary PCR products using *ATKO For1* and *ATKO Rev1* primers by gel electrophoresis

In parts (i) and (ii), lanes 1-30 denote PCR reactions using DNA from X pools 1-30 as a template. Lane 31 in each case is the positive control using the *ATKO For1* and *ATKO Rev1* primers with wild type Ws DNA as a template.

(i) *ATKO For1* and *JL-202*



(ii) *ATKO Rev1* and *JL-202*



The blots were probed with the complete *KNAT6* genomic sequence. The probe template was prepared by standard PCR (section 2.8.1) using the cloned genomic *KNAT6* sequence from section 3.10 amplified with the 5' *UTR*+51 and 3' *UTR*-116 primers. This probe template was then used to prepare a [<sup>32</sup>P]α-dCTP radiolabelled probe (section 2.6.4) that was hybridised to the membrane using the Church system (section 2.6.5). The membrane was washed to 100% stringency (section 2.6.8) before being exposed to autoradiography film overnight (section 2.6.10). The autoradiographs are shown in Figure 7.1d. The positive control had worked as expected and indicated that the PCR had been successful. There were various putative positives in the PCR reactions carried out using the pooled DNA, and these are listed in Table 7.1b.

**Table 7.1b** Putative positives in DNA pools

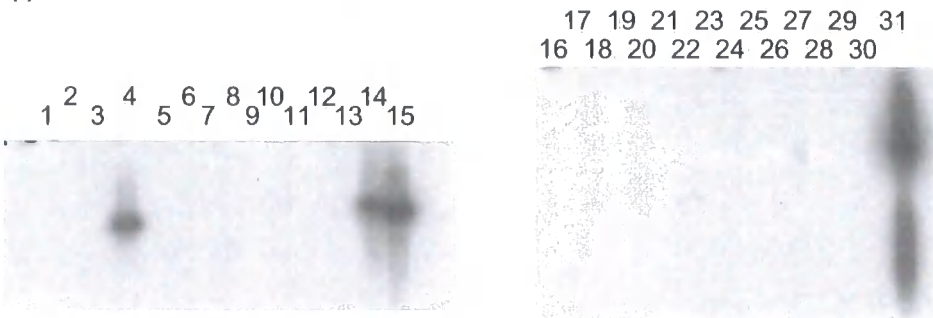
<i>KNAT6</i> primer	DNA Pool	Approx. size of putative positive, kb
<i>ATKO For1</i>	4	6.0
<i>ATKO For1</i>	14	9.0
<i>ATKO For1</i>	15	6.0
<i>ATKO For1 and Rev1</i>	31	Positive control, 5.4 kb
<i>ATKO Rev1</i>	2	3.2
<i>ATKO Rev1</i>	3	3.2
<i>ATKO Rev1</i>	5	3.2
<i>ATKO Rev1</i>	14	3.2
<i>ATKO Rev1</i>	15	3.2
<i>ATKO Rev1</i>	17	3.2
<i>ATKO Rev1</i>	18	3.2
<i>ATKO Rev1</i>	19	3.0
<i>ATKO Rev1</i>	30	4.0
<i>ATKO For1 and Rev1</i>	31	Positive control, 5.4 kb

To confirm that the putative positives identified by Southern blotting were true insertions in the *KNAT6* gene, the fragments corresponding to the hybridising bands were isolated and sequenced. 10 µl from each PCR reaction that contained a putative positive as listed in Table 7.1b was purified using the High

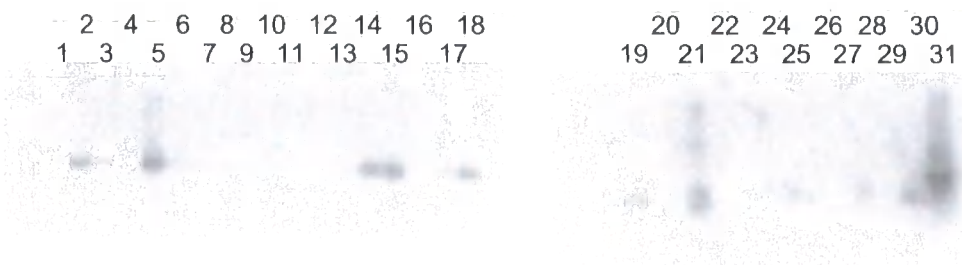
**Figure 7.1d** Hybridisation of primary PCR products obtained using the *ATKO For1* and *ATKO Rev1* primers to the complete *KNAT6* genomic sequence

In parts (i) and (ii), lanes 1-30 denote PCR products using DNA from X pools 1-30 as a template. Lane 31 in each case is the positive control using the *ATKO For1* and *ATKO Rev1* primers with wild type Ws DNA as a template.

(i) *ATKO For1* and *JL-202*



(ii) *ATKO Rev1* and *JL-202*



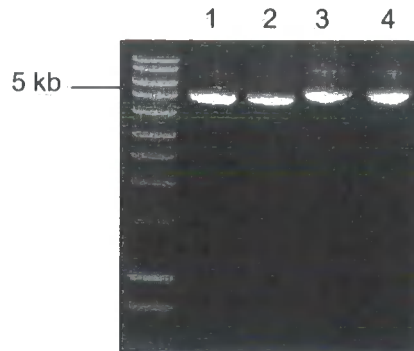
Pure PCR Product Purification kit (section 2.4.8) and eluted in 50 µl of the elution buffer provided. The purified PCR products were then reamplified using the same conditions as for the original screening (section 2.8.3), except that the number of cycles was decreased from 36 to 25. The reamplified fragments were separated by gel electrophoresis before the bands of interest (corresponding to the putative positives identified above) were cut out and purified using the QIAquick® Gel Extraction kit (section 2.4.7). These purified bands were then cloned into the pCR®2.1-TOPO vector (section 2.7.4). White putative positive colonies were checked by colony PCR (section 2.8.1) using the universal primers *M13F* and *M13R*. Positive colonies were used to prepare plasmid DNA (section 2.4.1) and the plasmids were sequenced with *M13F* and *M13R*.

Sequencing of the putative positives obtained using the *ATKO For1* primer revealed that they were true insertions as they consisted of a junction between plant genomic DNA and the T-DNA left border, but that they were downstream of the experimentally determined 3' UTR. As these positives were downstream of *KNAT6*, it seemed unlikely that these insertions would result in a downregulation of gene expression and so they were not pursued further.

Sequencing of the putative positives obtained using the *ATKO Rev1* primer revealed that these products were in fact double primed by this primer. This was due to the fact that a region in exon 3 acted as a primer binding site for the *ATKO Rev1* primer.

Although a true positive may still have been identified despite the double priming by the *ATKO Rev1* primer, this could have led to a positive being missed if amplification of the double primed product outcompeted that of a product primed by the *ATKO Rev1* primer and the *JL-202* primer. Therefore, a new reverse primer, *ATKO Rev4*, was designed and tested as before. The four test PCR reactions were carried out as described in Table 7.1a but with *ATKO Rev1* being replaced with *ATKO Rev4*. The test PCRs showed that the *ATKO Rev4* primer was compatible with both *ATKO For1* and *JL-202* (Figure 7.1e). This primer was then sent to the KO facility as before and the PCR reactions were returned for analysis. Again, 5 µl of each PCR product was analysed by gel electrophoresis (Figure 7.1f) before being transferred to membrane by

**Figure 7.1e** Compatability of *ATKO For1* and *ATKO Rev4* primers used to screen to *Arabidopsis* KO facility collection



Lane 1: *Con-1A* and *Con-1B* primers give a 5 kb band

Lane 2: *Con-1A*, *Con-1B* and *JL-202* primers give a 5 kb band

Lane 3: *ATKO For1* and *ATKO Rev4* primers give a 5.4 kb band

Lane 4: *ATKO For1*, *ATKO Rev4* and *JL-202* primers give a 5.4 kb band



Southern blotting and then hybridised to the complete *KNAT6* genomic sequence. The autoradiograms were exposed for 3 days before being developed. The positive control had worked as expected, and there was a putative positive in the PCR products obtained from DNA pool 1 (Figure 7.1g). However, the band corresponding to the positive in this pool was visible in all other pools on the gels (see Figure 7.1f), and it was not possible to reamplify this product in the same way as for the other putative positives analysed above. It was therefore concluded that this was also an artefact and was not pursued further.

## 7.2 Isolation of SALK lines containing an insertion in *KNAT6*

The Salk Institute (La Jolla, California, USA) holds a collection of 150,000 T-DNA tagged insertion mutants (the Salk Institute Genomic Analysis Library, SIGnAL). The insertion mutants were produced in a Col-0 background using the binary vector pROK2 (Baulcombe *et al.*, 1986) that confers kanamycin resistance to transformed plants.

The T-DNA/plant junctions from single transformed lines were being sequenced at the time of this work, and the database of insertions was available at <http://signal.salk.edu/cgi-bin/tdnaexpress>. The database was searched using the *Arabidopsis* Genome Initiative (AGI) identifier for *KNAT6*, AT1G23380 (available at the *Arabidopsis* Information Resource (TAIR), <http://arabidopsis.org>).

Two positives, SALK\_047931 and SALK\_054482, were identified in the collection and T3 seed was obtained from the Nottingham *Arabidopsis* Stock Centre (NASC, <http://nasc.nott.ac.uk/home.html>). The position of the inserts is shown in Figure 7.2a.

As these lines are segregating T3 seeds, and only a few seeds were provided, the presence of the T-DNA insertion in individual plants was initially confirmed by PCR. Primers to the *KNAT6* genomic region surrounding the T-DNA insertion were used in conjunction with the pROK2 left border primer *LBb1* which was used to sequence the plant/T-DNA junctions at the Salk Institute. DNA was extracted from leaf tissue from single soil grown T3 plants using the

**Figure 7.1g** Hybridisation of primary PCR products obtained using the *ATKO For1* and *ATKO Rev4* primers to the complete *KNAT6* genomic sequence

Lanes 1-30 denote PCR products using DNA from X pools 1-30 as a template. Lane 31 is the positive control using the *ATKO For1* and *ATKO Rev4* primers with wild type Ws DNA as a template.

Arrowhead indicates putative positive in DNA pool 1

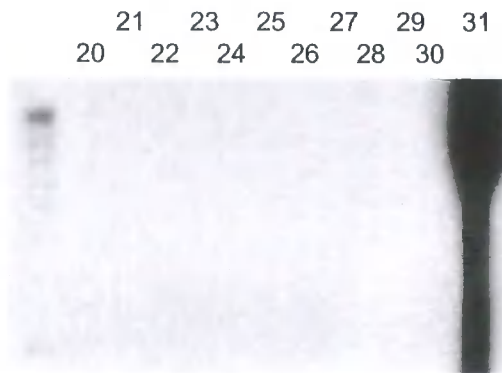
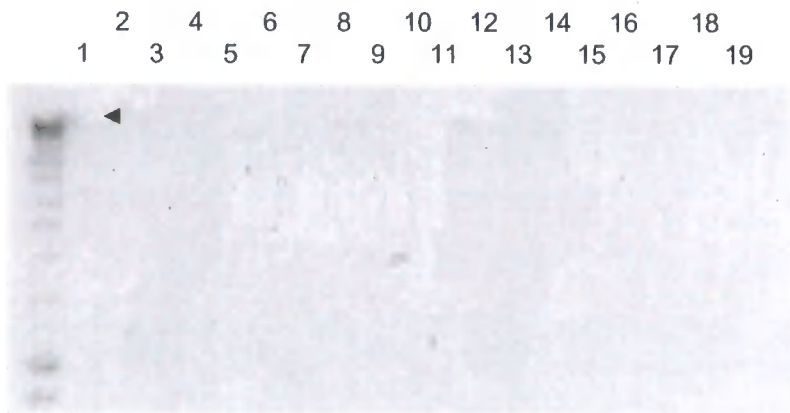
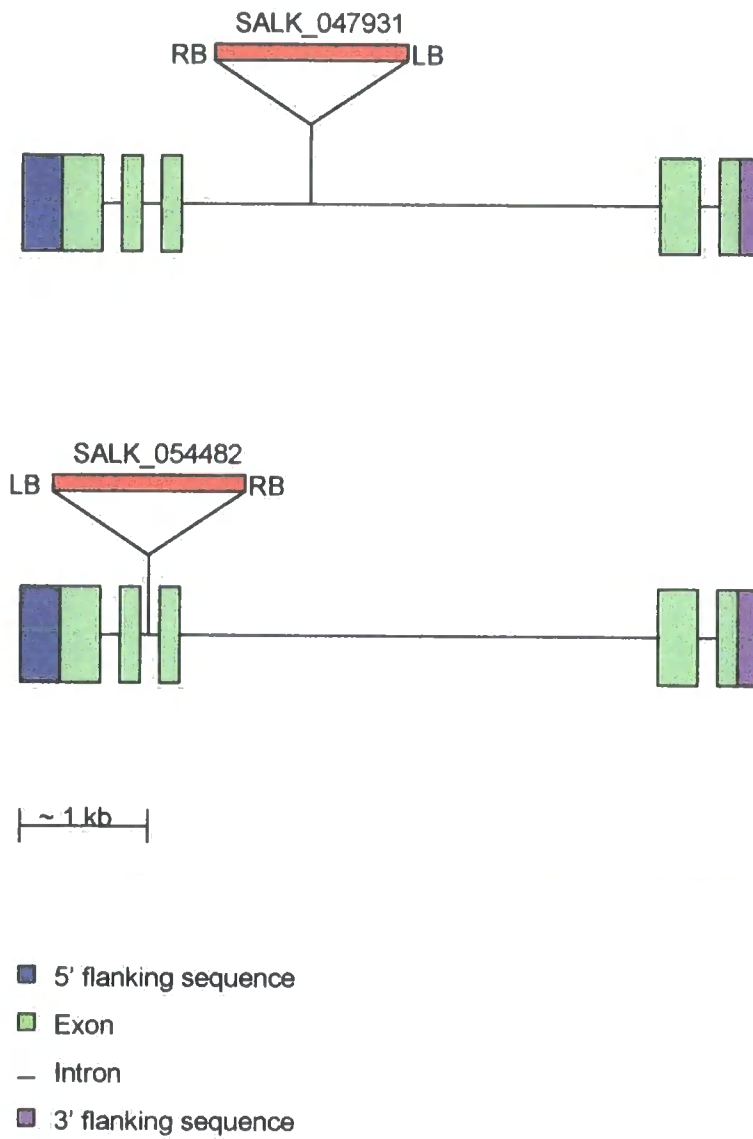


**Figure 7.2a** Positions of insertion in SALK\_047931 and SALK\_054482



quick extraction method detailed in section 2.4.4. Standard PCR with an anneal temperature of 60°C and 35 cycles was then carried out (section 2.8.1) on the DNA from each plant to confirm the presence of an insert.

[A] SALK\_047931 was analysed using the following *KNAT6* primers in conjunction with *LBb1*: *SALK\_047931 Rev1*, *SALK\_047931 Rev2* and *SALK\_047931 For*. The positions of these primers in relation to the T-DNA insert are shown in Figure 7.2b.

The following PCR reactions (Table 7.2a) were performed on DNA from eleven T3 plants to confirm the presence of an insert in *KNAT6*. The *LBb1* primer was used in all reactions. PCR products were analysed by gel electrophoresis (Figure 7.2c). A band of 478 bp was expected using the *SALK\_047931 Rev1* primer in conjunction with *LBb1* and of 766 bp when using the *SALK\_047931 Rev2* primer in conjunction with *LBb1* in plants where an insert was present.

The PCR reactions indicated that there were T-DNA insertions in plants 2, 4, 6, 8 and 11, and that there is a possible insert in plant 10 (the plant/T-DNA junction was amplified with the *SALK\_047931 Rev2* primer but not the *SALK\_047931 Rev1* primer). The products obtained were of the expected sizes.

**Figure 7.2b** Primer positions around the SALK\_47931 insertion

Exon 3 is shown in red

SALK\_47931For is shown in green

SALK\_47931 Rev1 is shown in blue

SALK\_47931 Rev2 is shown in purple

The T-DNA insertion site and orientation is shown in orange

GAAACGTA CTACTGCGATATATTAGTGAAATACAAATCGGATCTAGCAAGACCGTT  
TGACGAGGCAACGTGTTTCTTGAACAAGATTGAGATGCAGCTACGGAACCTA  
TGTACTGGTGTGCGAGTCTGCCAGGGGAGTTTCTGGTATGTCTTAAATTATCC  
CTCTCTGGTTCGGTCTTTTAGTGGTTCATTTTGTGGTTAGTTCTGAATGATT  
CTTTGATCTTTCCGTGGTTTTTCATTAATAATATCCTTTCCTCGATATTTCCA  
TAGGGTTTTGATTCATATGACCAGTTTCTGAAAAATGATTGGTAGCTTGTTGA  
TAGAATAACCCTAGGCTTTTGAAGTGATCAGAAAGCAAATAGATAAAAAATG  
AAAAAAAAGAAGATAAACCCCTAGCTACAAGTTTCATTTCCATAGCTATTTTTCC  
CTTGATGGGTTTTGTTTTGTGTGTGCTTTTCTTTGGGCACGTTGAAACTCTG  
GAGACAAAGATCTGTTAAGGTGTTGTGCAATTATTTACTCGTTCATTTAATG  
TTTTAGCCATGGGATTAGGGTGTGGAGTGTGGTGGGATTTCCTCTTCTTC  
TTGTTGTTGATCTTTGTGCTAATCATACAAATTTACTTTATATCTTTTTCTCT  
CTTTCTCTGTCAGAAAGAAAATGGTGTAGAAAGCAATAAACTTTTGTGGTAGA  
GATTCTGATTTTGACGTTTCAGAGGCTTGTGCGTACTGAATGTTTTTTCAAC  
TTGTTGCTTTTTCTAGTGAAAAACCAATTGACAGAAAAACCTAGTCATAACT  
TTAACAATATGTGTAGTTGATTTTTCATGAGCTTCTTTTGCTTCACTTCTCGT  
TTAACAATAAGTAAGTATAAGTACTAGTCATAACTCATAAGTCGTTCACTCTT  
GTTTATGGGTAACAACCTTATTAGGTTACCAGTTTTTCTAAGACTTCAACTTCT  
TTTGGT CAGATGATTATTAATAACCAATAAGCCATAAGAGTTATTAGCTGTAAT  
TCCTCTTTAAGCTCATTACAGATTCTCTGGATCGGAATTA RB LB  
TAAGCGTGTTAGATAATTTTACGATTAATTTCTGTTATATCTTAATAACACA  
CCATATAATTTTTCTATCTAATTAATAGGTTAAAACAATAAAGTTAAAATTGTA  
TTTTAAATTTAATATAGAAGTCTACAAAACGACATTCTTTGTGAAATAAAAAATTT  
AATCCTGAATTCGACATTTATTATGAAGAACGTAACCTTTGGTCTATTTCAAGTT  
TCAATGATCTGAGAACAAGAGTAGGGAGATTTTTGTTGATCATCGGAAATAGT  
ATCATTGCCAAGTGGCCACTCTTATCTGCATGTTCTTGTGGAGTCTTGTTGG  
ACTTATATGTAAGTAATAAACCAAAACTGACTCAATTTTGAAGCGATTTAAAAG  
TCTAGGTTTTATGCTTATACATGAATGAAATGCTTCAAATAAGTACTTTCTTT  
GTGGTTTACTGATATTATCTCTTTAGACCACATATTGTA CTACTACA ACTAGCAAAA  
ACATTGTGGCCATAACAAATCAACCGATCAGGTTAGCTAGAAATACTGATCCT  
TAGGAGTTTTTTTTTAATACAATAAAATAGAAGAAAAACTCCAGCTGAAAGAG  
TTAGCTGTAAAGAAATGAAACTCCATAGATTGGTAGACTTTTTTTTCAGCTTTG  
CAGGAGTTTTCCATTATC

**Figure 7.2c** Identification of plants carrying an insertion in *KNAT6* corresponding to SALK\_47931



The lane numbers indicate the number of the plant whose DNA was used as a PCR template

The forward primer in all reactions was *LBb1*

The reverse primer was *SALK\_047931 Rev1* in lanes 1-11 and *SALK\_047931 Rev2* in lanes 12-22

A band of 478 bp was expected in plants containing an insert where the *SALK\_047931 Rev1* primer was used

A band of 766 bp was expected in plants containing an insert where the *SALK\_047931 Rev2* primer was used.

**Table 7.2a** PCR to confirm presence of T-DNA inserts in T3 SALK\_047931 individuals

Plant	Reverse primer	Insert?
1	<i>SALK_047931 Rev1</i>	No
2	<i>SALK_047931 Rev1</i>	Yes
3	<i>SALK_047931 Rev1</i>	No
4	<i>SALK_047931 Rev1</i>	Yes
5	<i>SALK_047931 Rev1</i>	No
6	<i>SALK_047931 Rev1</i>	Yes
7	<i>SALK_047931 Rev1</i>	No
8	<i>SALK_047931 Rev1</i>	Yes
9	<i>SALK_047931 Rev1</i>	No
10	<i>SALK_047931 Rev1</i>	No
11	<i>SALK_047931 Rev1</i>	Yes
1	<i>SALK_047931 Rev2</i>	No
2	<i>SALK_047931 Rev2</i>	Yes
3	<i>SALK_047931 Rev2</i>	No
4	<i>SALK_047931 Rev2</i>	Yes
5	<i>SALK_047931 Rev2</i>	No
6	<i>SALK_047931 Rev2</i>	Yes
7	<i>SALK_047931 Rev2</i>	No
8	<i>SALK_047931 Rev2</i>	Yes
9	<i>SALK_047931 Rev2</i>	No
10	<i>SALK_047931 Rev2</i>	Yes
11	<i>SALK_047931 Rev2</i>	Yes

The PCR products obtained from plants 2, 4, 6, 8 and 11 using the *SALK\_047931 Rev1* primer and the product obtained from plant 10 using the *SALK\_047931 Rev2* primer were cloned directly into the pCR®2.1-TOPO vector (section 2.7.4). White putative positive colonies were checked by colony PCR (section 2.8.1) using the universal primers *M13F* and *M13R*, and colonies containing an insert of the correct size were used to prepare plasmid DNA

(section 2.4.1). Sequencing using *M13F* and *M13R* primers confirmed that the PCR products were in fact the amplified T-DNA/plant DNA junction.

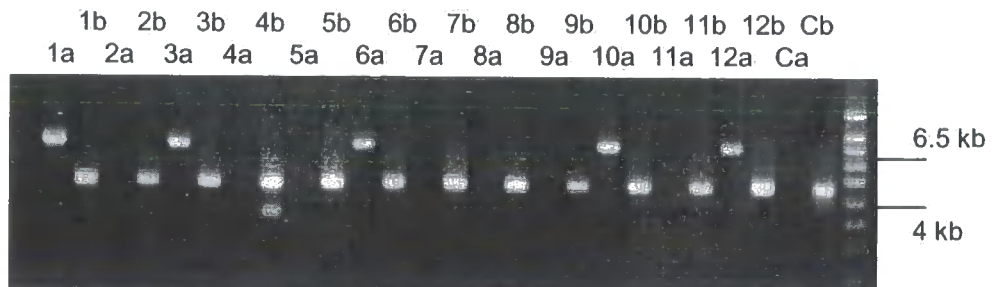
To determine if these individuals were homozygous or hemizygous for the T-DNA insertion, T4 seed from the individual plants was sown on ½ MS10 SS medium supplemented with 35 mg/l kanamycin sulphate and scored for kanamycin resistance 7 days after germination (DAG). However, despite the successful amplification of the plant/T-DNA junction, all of the plants were kanamycin sensitive. It has been reported that many of the T-DNA insertion lines in the SALK collection exhibit silencing of the introduced kanamycin resistance gene, leading to a lack of kanamycin resistance even where the T-DNA was present (<http://signal.salk.edu/cgi-bin/tdnaexpress>).

Several attempts were made to determine whether the T3 individuals were hemizygous or homozygous using PCR, but the results obtained were extremely unreliable and it was not always possible to repeat the original PCR amplification detailed in Table 7.2a successfully. This could be due to poor quality of DNA preps or possibly due to the primers not being especially good pairs. The experiment was not pursued further due to time constraints, but clean DNA preparations and a redesign of the primers may help to solve the problems and allow genotyping of the T3 individuals and T4 progeny by PCR.

[B] SALK\_054482 was analysed using the *Probe F* and 5' *RACE1* primers in conjunction with *LBb1*. These primer positions in relation to the T-DNA insert (according to the SALK database) are shown in Figure 7.2d. Use of the *Probe F* primer in conjunction with 5' *RACE1* amplified the wild type gene (481 bp) and use of *Probe F* in conjunction with *LBb1* (548 bp) amplified the plant/T-DNA junction. Therefore, plants that were wild type, hemizygous or homozygous could be identified by PCR (Table 7.2b). The reactions were performed on DNA from twelve T3 plants and analysed by gel electrophoresis (Figure 7.2e). The reverse primer used in each reaction was *Probe F*.



**Figure 7.2e** Identification of plants carrying an insertion in *KNAT6* corresponding to SALK\_54482



The lane numbers indicate the number of the plant whose DNA was used as the PCR template

The forward primer in all reactions was *ProbeF*

The reverse primer was *LBb1* in lanes marked a and *5'RACE1* in lanes marked b

A band of 548 bp was expected in plants containing an insert in *KNAT6* where the *ProbeF* and *LBb1* primers were used

A band of 481 bp was expected in plants containing a wild type copy of *KNAT6* where the *5'RACE1* and *LBb1* primer were used

**Table 7.2b** PCR to confirm presence of T-DNA inserts in T3 SALK\_054482 individuals

Plant	Forward primer	Genotype
1	<i>LBb1</i>	Heterozygote
1	<i>5' RACE1</i>	
2	<i>LBb1</i>	Wild type
2	<i>5' RACE1</i>	
3	<i>LBb1</i>	Heterozygote
3	<i>5' RACE1</i>	
4	<i>LBb1</i>	Wild type
4	<i>5' RACE1</i>	
5	<i>LBb1</i>	Wild type
5	<i>5' RACE1</i>	
6	<i>LBb1</i>	Heterozygote
6	<i>5' RACE1</i>	
7	<i>LBb1</i>	Wild type
7	<i>5' RACE1</i>	
8	<i>LBb1</i>	Wild type
8	<i>5' RACE1</i>	
9	<i>LBb1</i>	Wild type
9	<i>5' RACE1</i>	
10	<i>LBb1</i>	Heterozygote
10	<i>5' RACE1</i>	
11	<i>LBb1</i>	Wild type
11	<i>5' RACE1</i>	
12	<i>LBb1</i>	Heterozygote
12	<i>5' RACE1</i>	
Col-0	<i>LBb1</i>	Wild type
Col-0	<i>5' RACE1</i>	

As can be seen from the gel in Figure 7.2e, a 700 bp band was obtained after PCR using the *LBb1* and *Probe F* primers. This is larger than the 548 bp band which was expected upon amplification of the plant/T-DNA junction. To verify

the sequence of these bands, the 700 bp PCR products from these reactions were cloned directly into the pCR®2.1-TOPO vector (section 2.7.4). White putative positive colonies were checked by colony PCR using *M13F* and *M13R* primers (section 2.8.1) and those containing an insert of the correct size were used to prepare plasmid DNA (section 2.4.1). Sequencing with *M13F* and *M13R* revealed that the T-DNA insert was in fact downstream of the insertion site indicated by the SALK database. The experimentally determined insertion site is shown in Figure 7.2f.

Therefore, as the T-DNA insertion is downstream of the site indicated by the SALK line sequenced fragment, the primers that were used for genotyping were both upstream of the insertion site (see Figure 7.2f). Therefore, a new reverse primer will have to be selected and used to genotype the plants.

Although the T3 plants have not been genotyped successfully, T4 seed from individual plants 1,3,6,10 and 12 was sown onto ½ MS10 SS medium supplemented with 35 mg/l kanamycin sulphate and scored for kanamycin resistance 7 days after germination (DAG). All plants showed 100% green, kanamycin resistant seedlings, apart from plant 12 which had a few sensitive seedlings in a predominantly resistant background. The high proportion of kanamycin resistant plants indicated that there might be more than one T-DNA insertion in this line. If these multiple T-DNAs are segregating independently it should be possible to screen individual T5 plants that only contain the T-DNA insertion in *KNAT6*.

No further work was carried out on these lines due to time constraints, but in the future, T5 seed could be grown and genotyped by PCR as above and then checked by kanamycin segregation for the number of T-DNAs. Southern analysis could then be used to confirm the number of T-DNA insertions in these individuals. For lines that contain only a single T-DNA in *KNAT6*, homozygous lines could be identified by PCR or by kanamycin segregation analysis in subsequent generations.

**Figure 7.2f** Primer positions around the revised SALK\_54482 insertion

Exons 1, 2 and 3 are shown in red

*ProbeF* is shown in blue

5'RACE1 is shown in green

The revised T-DNA insertion site and orientation is shown in orange

```
ATGGATGGAATGTACAATTTCCATTCGGCCGGTGATTATTCAGATAAGTC
GGTTCTGATGATGTACCGGAGAGTCTCATGTTTCCTTCCGATTACCAAG
CTTTGCTATGTTCTCCGCCGGTGAAAATCGTGTCTCTGATGTTTTCGGA
TCCGACGAGCTACTCTCAGTAGCCGTCTCCGCTTTGTCGTCCGAGGCGGC
TTCGATCGCTCCGGAGATCCGAAGAAATGATGATAACGTTTCTCTAACT
GTCATCAAAGCTAAAATCGCTTGTCATCCTTCGTATCCTCGCTTACTTCA
AGCTTACATCGATTGCCAAAAGGTGATCGTTAACTCTTCTTTTTTATC
ACTTAGATAAAAATCTAGGTTTTACTTTTTAAAGATAAAGATAAGATTGA
GAAGCITTTGATATTTGATTGTTTTTTTTATAATTTATGGTTTAAACAATTT
CATAATTTAGAAAACAGGTCGGAGCACCAACCGGAGATAGCGTGTTTACTA
GAGGAGATTC AACGGGAGAGTGATGTTTATAAGCAAGAGGTTGTTCTT
CTTCTTGCTTTGGA GCTGATCCTGAGCTTGATGAATTTATGGTCTCTCTCT
TTTTTCCCTCGATTTTTTTTTTCGGATTTTTATTTTGTTAAAATATTTTTTT
TT LB _____ RB
GGAAATTTTTGTA CTTAAGAAGATAATTTATTATCAGGAAACGTA CTGC
GATATATTAAGTGAAATACAAATCGGATCTAGCAAGACCGTTTGACGAGG
CAACGTGTTTCTTGAACAAGATTGAGATGCAGCTACGGAACCTATGTAC
TGGTGTCGAGTCTGCCAGGGGAGTTTCTG
```

### 7.3 Other sequenced *Arabidopsis* insertion mutant libraries

In addition to the Salk Institute collection discussed in section 7.2, several other insertion mutant libraries for which sequence data was available were searched as described below.

#### [A] Syngenta *Arabidopsis* Insertion Library (SAIL)

Formerly known as the GARLIC collection, the SAIL collection was produced at the Torrey Mesa Research Institute (TMRI, San Diego, California, USA). 100,000 T-DNA insertion mutant lines were produced in a Col-0 background using two different vectors, pCSA110 and pDAP101 (McElver *et al.*, 2001), with the transformants produced with the pCSA110 vector also carrying the *qrt* mutation. The database was searched by emailing the sequence of interest to TMRI (<http://www.tmri.org>). The search results were then returned by email as BLAST results. The submission of the complete *KNAT6* genomic region, including 2 kb of putative promoter, did not reveal a positive.

#### [B] Cold Spring Harbor *Arabidopsis* Genetrap (GT) lines

This collection was produced at the Cold Spring Harbor Laboratory (CSHL, Long Island, New York, USA) and consists of 14,547 insertion mutant lines in a Col-0 background. At the time of this work, 13,587 inserts had been sequenced. These lines were generated by introducing a transposon into the *Arabidopsis* genome using the pWS32 vector (Sundaresan *et al.*, 1995). The lines are gene trap (GT) lines where integration of the transposon led to the production of a GUS fusion protein in many cases. GUS staining patterns are also available for many of the lines. The database was available at (<http://genetrap.cshl.org>) and was searched using the GenBank accession number for *KNAT6* (AB072361, see section 4.6).

Although a positive was identified in this database (GT8310), CSHL were interested in working on this line, and were in the process of characterising the insertion locus. Seed was only available to carry out a specific experiment to be done in collaboration, and this was not pursued further during the course of this work.

[C] The *Arabidopsis thaliana* Insertion Database (AtIDB)

The AtIDB combines sequence data from insertion mutation libraries at the John Innes Centre (Norwich, UK) and the Sainsbury Laboratory (Norwich, UK) as well as the CSHL GT lines detailed above.

The transgenic lines generated at the John Innes Centre and the Sainsbury Laboratory consists of 48,000 transposon insertions (Tissier *et al.*, 1999). The T-DNA/plant junctions from these lines are currently being sequenced.

The AtIDB was available at <http://atidb.cshl.org> and was searched with the *KNAT6* genomic sequence using the BLAST programme against the sequenced inserts in the database. No positives were revealed.

#### **7.4 Summary**

The work carried out in this chapter showed that the *Arabidopsis* Knockout Facility Alpha collection did not contain an insert in the *KNAT6* gene. However, two insertions in *KNAT6* were identified in the Salk Institute collection. The insertion in SALK\_047931 is located in intron 3 and the insertion in SALK\_054482 is located in intron 2. Further analysis of these lines will be required to isolate plants containing homozygous insertions in the *KNAT6* gene. In addition, one other insertion in *KNAT6* was identified in the CSHL GeneTrap lines but this was not available for release.

## Chapter 8 Discussion

Plant homeobox genes can be classified into seven families based on their sequence. One of these families, the *KNOX* family, is characterised by the presence of an atypical homeodomain as well as various other conserved domains. The *KNOX* family can be further divided into two subfamilies, class 1 and class 2, based on both sequence and function. Class 1 genes are involved in maintenance of meristematic tissues whereas the function of class 2 genes is less well understood. In *Arabidopsis*, *KNOX* class 1 genes include *STM*, *KNAT1* and *KNAT2*. This work describes the isolation and characterisation of a fourth member, *KNAT6*.

The aim of this chapter is to discuss the results presented in the previous five chapters in the context of what is currently known about the function of class 1 *KNOX* genes in plant development. Future work that is required for further clarification of the role of *KNAT6* is also included.

### **8.1 Isolation of a novel homeobox gene from *Arabidopsis* root using 3' RACE**

Chapter 3 detailed the experiments that allowed a fragment of the *KNAT6* coding sequence to be isolated from *Arabidopsis* root tissue using a 3' RACE-based approach. Although this approach was successful in that it allowed the isolation of *KNAT6*, it is possible that other homeobox genes that are expressed in root were not isolated for a number of reasons.

The use of the *STM* coding sequence as a probe for the identification of homeobox sequences that were amplified during 3' RACE may have prevented the detection of sequences from families that have diverged from the Class 1 *KNOX* genes. Therefore, it is possible that the detection of a Class 1 homeobox gene was biased by the use of this probe.

In addition, the treatment of root tissue with the synthetic auxin analogue NAA may have led to downregulation of transcription of genes which are normally negatively regulated by this plant hormone.

It is interesting to note that no homeobox sequences that are known to be expressed in root were identified in this screen. These include the class 2 *KNOX* genes *KNAT3*, *KNAT4* and *KNAT5* (Serikawa *et al.*, 1996) as well as the HD-*GL2* gene *GLABRA2* which is involved in controlling the development of root hairs (Cristina *et al.*, 1996, Masucci *et al.*, 1996). It may be that these genes were not identified due to the factors mentioned above.

## **8.2 Sequence analysis**

As described in Chapter 3, the complete *KNAT6* transcript was isolated using a combination of PCR-based approaches including 3' and 5' RACE. Analysis of this transcript was carried out as described in Chapter 4.

### **8.2.1 Prediction of the *KNAT6* ATG**

As described in section 4.1.1, examination of the sequence adjacent to the *KNAT6* ATG that was predicted in the GenBank database revealed a second in-frame ATG 9 bases upstream. To determine which of these two ATGs was more likely to be the true ATG used for translation of the *KNAT6* protein, the Kozak Scanning Hypothesis (Kozak, 1981) was used to predict which ATG more likely to be used for translation initiation.

In prokaryotes, the ATG is selected by the Shine Dalgarno sequence. This purine rich sequence is found within the 10 bases upstream of the ATG initiation codon (Lewin, 1995). Examination of eukaryotic sequences indicated that there is greater heterogeneity within the region of a message preceding the initiation codon. Therefore, the original scanning hypothesis proposed that there was no particular sequence required for eukaryotic translation initiation, and that it was the first ATG that was used. (Kozak, 1980). However, as more sequences were analysed, it was revealed that the nucleotides flanking the initiator codon are not random. In particular, the bases at the -3 and the +4 positions are important, and purine bases (A or G) are conserved at these positions (Kozak, 1981). Therefore it appears that the context of the ATG that is important, rather than the presence of a "leader" sequence as found in prokaryotes.

More recently, the consensus sequence for translation initiation has been determined for dicotyledonous plants (Joshi *et al.*, 1997). This consensus

sequence was used in section 4.1.1 to predict which ATG was more likely to be used for translation of the *KNAT6* protein.

Although neither sequence fits the consensus exactly, the upstream ATG shares the highly conserved G (67% of examined sequences) at the +4 position, whereas the downstream ATG has a T (12% of examined sequences) at this position. At the -3 position, the upstream sequence contains a C (8% of examined sequences) whereas the downstream sequence contains a G (22% of sequences). Therefore, it is likely that the upstream ATG is the ATG used for translation initiation of the *KNAT6* protein.

### **8.2.2 Analysis of the *KNAT6* transcript**

To confirm that the complete coding sequence had been isolated using 5' RACE, the sequence upstream of the predicted ATG was analysed.

Five small ORFs upstream of the ATG were identified (section 4.1.2). However, analysis using the splice site prediction software at the NetPlantGene server, as well as their location upstream of the predicted *KNAT6* ATG, indicated that they were not part of the *KNAT6* coding sequence.

These upstream ORFs may be required for translational regulation. Early work on the role of 5' UTR ORFs in translational regulation was carried out using the *GCN4* gene of *Saccharomyces cerevisiae* (For review see Geballe and Morris, 1994). *GCN4* encodes a transcription factor that positively regulates amino acids biosynthetic genes under conditions of amino acid starvation (Hinnebusch, 1997). The *GCN4* 5' UTR contains 4 ORFs which control transcriptional regulation of the *GCN4* protein. These ORFs are designated upstream ORF1-4 (uORF), with uORF1 being closest to the 5' end of the UTR. In the absence of amino acid starvation, translation begins at uORF1 and the reinitiates at uORF4 after termination of the uORF1 peptide. However, under conditions of amino acid starvation, reinitiation bypasses uORF5 and begins at the start of the *GCN4* protein. This has been shown to be due to differences in the phosphorylation status of a subunit of initiation factor-2 (eIF-2 $\alpha$ ) (Hinnebusch, 1996; Gaba *et al.*, 2001).

Translational control of plant proteins has also been shown to involve uORFs. For example, the mRNA of the maize *Opaque2* gene is inhibited by the presence of several small ORFs that are located in the 5' UTR (Lohmer *et al.*, 1993).

Although some of the 5' UTR was included in overexpressing constructs (section 6.1.1), inclusion of the ORFs that are present in the 5' UTR of the *KNAT6* cDNA was avoided as they may have provided an alternative translation start that could have reduced the amount of *KNAT6* protein that was produced.

It is possible that the 5' UTR sequence that was isolated experimentally in section 3.9 was not full length. This was indicated by the identification of likely TATA boxes more than 35 bp upstream of the experimentally determined 5' UTR (section 4.5). The full extent of the 5' UTR could be determined accurately using techniques such as RNase protection assays (Casson *et al.*, 2002).

### **8.2.3 *KNAT6* is a Class 1 *KNOX* gene**

As described in section 3.8, a PCR product that was generated by 3' RACE with the *HD-KN1* primers also hybridised to the *STM* probe. This fragment was cloned and sequenced before being compared with the sequences in the GenBank database. This analysis revealed that the fragment was part of the last exon and 3' UTR of a novel homeobox gene that was assigned to a predicted GeneScan gene on chromosome 1 (GenBank Accession numbers AC007945 and AC005292, available at <http://www.ncbi.nlm.nih.gov>). These two chromosomal sequences were aligned and shown to be overlapping, indicating that there is a single copy of this region rather than a duplicated gene in different parts of the *Arabidopsis* genome. The predicted gene was annotated as a homologue of the homeobox gene *ATK1* (Dockx *et al.*, 1995). *ATK1* has also been isolated as *KNAT2* (Lincoln *et al.*, 1994)) and is a class 1 *KNOX* gene (section 1.4.2). The isolation of the complete coding sequence of *KNAT6* revealed that its sequence was different to, but most similar to, that of *KNAT2*.

Several other pieces of evidence also indicated that *KNAT6* is a class 1 *KNOX* gene.

The positions of the *KNAT6* introns are conserved with those in other *KNOX* genes. There is an intron in a conserved position near the N-terminal end of the second helix in the homeobox region which is conserved between all other *KNOX* genes and which has also been identified in *KNAT6* (section 4.2). In addition, *KNAT6* does not contain another small intron upstream of the homeobox in the ELK domain that is conserved only in Class 2 *KNOX* genes.

Isolation of the complete *KNAT6* coding sequence (section 3.7-3.9) allowed the *KNAT6* protein sequence to be predicted and analysed (section 4.3). This indicated that the predicted protein sequence contained all of the protein domains previously identified in Class 1 *KNOX* genes (section 4.3). These domains include the homeodomain itself as well as the ELK and MEINOX domains and the GSE box. The roles of these domains were discussed in section 1.4.2.2. The three additional amino acids in the *KNAT6* homeodomain that are characteristic of all the TALE superfamily genes were also identified in the *KNAT6* predicted protein sequence.

Less analysis has been carried out on the HD-*KN1* Class 2 sequences, but these genes also contain the homeodomain, the ELK domain and the MEINOX domains. The presence of a GSE box in the Class 2 protein sequences was not readily identifiable by alignment with the Class 1 genes.

Finally, phylogenetic analysis using the PHYLIP package of programmes (Felsenstein, 1989) was performed to confirm that *KNAT6* was a member of the *KNOX* class 1 subfamily (section 4.4).

### **8.3 Expression analysis**

Determination of the expression pattern of *KNAT6* was carried out using several methods. The promoter sequence was analysed for conserved motifs, and the promoter activity during development of seedling roots and in response to exogenously applied plant hormones was investigated using promoter::*GUS* and promoter::*GFP* fusions. p*KNAT6*::*GUS* plants were histologically stained and sectioned to determine the specific cell type in which the *KNAT6* promoter was active, and this was confirmed using the *GFP* reporter gene. In addition,

the levels of the *KNAT6* transcript were measured by Northern blotting and semi-quantitative RT-PCR.

### 8.3.1 Identification of conserved motifs in the *KNAT6* promoter

Sequence analysis of 2 kb of the 5' flanking region upstream of the *KNAT6* ATG was carried out using the PLACE database ([www.dna.affrc.go.jp/htdocs/PLACE](http://www.dna.affrc.go.jp/htdocs/PLACE), (Higo *et al.*, 1999)). This revealed that there are motifs for several promoter activities in this region (section 4.5).

There are eleven copies of a motif (ATATT) which is associated with root expression within the 2 kb region. This root motif was originally identified in the *rolD* promoter of *Agrobacterium rhizogenes* and has been shown to direct expression of the GUS reporter gene in tobacco roots (Elmayan and Tepfer, 1995).

Two auxin response elements (CATATG) at positions -309 and -1736 (Xu *et al.*, 1997) were identified as well as an ethylene response element (ERE, ATTTCAAA) at position 294 (Montgomery *et al.*, 1993). However, these two motifs were not isolated from *Arabidopsis* (the auxin response element is a soybean sequence and the ERE is a tomato sequence) and it is not known how efficiently they function in this species. In addition, one of the auxin response elements as well as the ERE are positioned approximately 1700 bp upstream of the *KNAT6* coding region so they may not have formed part of the *KNAT6* promoter (normally most cis-acting promoter elements are found within 1 kb of the ATG).

The 2 kb upstream sequence was also searched for the AuxRE motif TGTCTC. This sequence was isolated from the soybean GH3 promoter and was used to make the DR5 synthetic promoter that directs high auxin inducibility in several species including *Arabidopsis* (Ulmasov *et al.*, 1995, Ulmasov *et al.*, 1997). This motif was not identified in the *KNAT6* promoter.

Although several motifs were identified in the *KNAT6* promoter, this does not in itself prove that *KNAT6* gene expression is influenced by these sequences. In addition, some of these motifs are located more than 1 kb upstream of the

*KNAT6* ATG and may not form part of the *KNAT6* promoter. For example, the use of the GUS reporter gene to analyse the same 2 kb of *KNAT6* promoter does not indicate that ethylene influences *KNAT6* promoter activity (section 5.1.4). However, treatment with the auxin analogue NAA shifts the expression of GUS towards the root tip, although there is no global increase of GUS expression in the root (section 5.1.4). In addition, the identification of eleven root motifs in the promoter region is supported by the experimentally determined expression of *KNAT6* in the root.

### **8.3.2 GUS expression level is variable in pKNAT6::GUS lines**

Three independent transgenic lines that express the GUS reporter gene under control of the *KNAT6* promoter were examined over a developmental time course (section 5.1.3), and the response of these lines to exogenously applied plant hormones was investigated (section 5.1.4)

GUS expression was absent in approximately 30% of seedlings during these analyses. Although the number of unlinked T-DNA loci was determined by kanamycin segregation analysis (section 5.1.2), it is still possible that there were a number of T-DNAs at each insertion locus. It has been documented that an increase in the copy number of a transgene can lead to a decrease in the transgene expression level (Matzke *et al.*, 1989, Van Blokland *et al.*, 1994), and this cosuppression may account for the GUS-negative transformants.

It is also possible that expression of the *KNAT6* gene is transient in the plant. Therefore, as staining of pKNAT6::GUS plants at a particular time in development represents only a snapshot of promoter activity, this may at least partially explain why not all of the seedlings show GUS activity at a given time point.

### **8.3.3 *KNAT6* promoter activity is localised to the phloem poles of the mature root**

The data presented in section 5.2 demonstrate that the *KNAT6* promoter is active in the phloem poles of the root.

The roots of seedlings which expressed the pKNAT6::GUS construct were also sectioned to allow the GUS expression to be localised to specific cell layers (section 5.2.4). Sections were taken from the main root adjacent to the hypocotyl in all cases apart from Line 3.1, where sections were taken from further down the root towards the root tip for technical reasons.

The examination of pKNAT6::GUS Lines 10.1 and 15.1 by sectioning indicates that the *KNAT6* promoter is active in the phloem poles of the mature root in *Arabidopsis*. This is supported by the analysis of pKNAT6::GFP lines, where GFP expression was also seen in the phloem poles (section 5.2.3).

The *woodenleg* (*wol*) mutation was first identified as a radial pattern mutant that has fewer cells in the vascular bundle in comparison with the wild type, and where all of these cells differentiate to form xylem elements (Scheres *et al.*, 1995). Therefore, in this mutant there are no phloem poles, which have been identified as a site of pKNAT6::GUS activity. As expected, no GUS expression was seen in root or hypocotyl when pKNAT6::GUS lines were introduced into the *wol* background (section 5.2.5). This is consistent with the findings presented above where pKNAT6::GUS activity is restricted to the phloem poles.

Sectioning of pKNAT6::GUS Line 3.1 indicated that the *KNAT6* promoter may be more widely expressed in the vascular tissue closer to the root apex. This difference in the staining pattern may reflect the part of the root that was sectioned and examined. *KNAT6* may be required in different parts of the root during different phases of development, and its expression pattern may alter during development. Alternatively, it may be that there are slight differences in the expression patterns between these two lines and that the *KNAT6* promoter is expressed in a wider range of vascular cells throughout the whole root in Line 3.1. Future examination of sections taken towards the root apex from Lines 10.1 and 15.1 may help to resolve this.

It has been demonstrated that the *Kn1* protein and transcript can move between different cell types (Kim *et al.*, 2002, Lucas *et al.*, 1995). It is possible that the *KNAT6* transcript and/or protein are also trafficked in this way. It would be useful to examine the localisation of the *KNAT6* transcript by in situ

hybridisation and the *KNAT6* protein using an antibody. This would allow the cellular localisation of the transcript and the protein to be localised directly rather than inferring *KNAT6* localisation by *pKNAT6::GUS* expression. This will help identify the cells in which *KNAT6* functions.

#### **8.3.4 Analysis of *KNAT6* transcript levels**

As described in section 5.3, the *KNAT6* transcript was not detected by Northern analysis, but semi-quantitative RT PCR indicated that the *KNAT6* transcript was expressed at approximately equal levels in roots and aerial parts of developing seedlings between 3 and 14 DAG.

Although the *KNAT6* promoter was active throughout a similar domain of the root during seedling development (i.e. in the primary root in the region where lateral roots were emerging), the percentage of the root that this region constitutes decreases as the root system elaborates. Therefore, it might have been expected that *KNAT6* transcript levels would decrease over time. There are several reasons why the activity of the promoter as determined by the GUS reporter gene may not correlate exactly with levels of the *KNAT6* transcript itself.

It may be that GUS may be expressed over the complete length of the root, but that the expression level is too low for detection using the GUS assay. Increasing the staining time during the GUS histochemical assay is a simple way to investigate this possibility.

It is also important to remember that there may not be a direct correlation between the amount of GUS protein that is present and the amount of *KNAT6* transcript. It has been shown that the GUS transcript and the GUS protein levels do not correlate well in all tissues (Topping *et al.*, 1991), so it is possible that there is also poor correlation between *KNAT6* transcript and GUS protein levels and care should be taken in making a direct inference between the two.

The presence of the *KNAT6* transcript does not necessarily indicate that *KNAT6* protein is present and functional. *KNAT6* may be regulated at the level of protein turnover as well as at the transcript level. In support of this, two regions

of the *KNAT6* protein, the ELK domain and the extreme C-terminal, have been identified as putative PEST sequences that are thought to act as a signal for rapid intracellular degradation of proteins (section 1.4.2.2). However, there is also some evidence for transcriptional regulation of *KNAT6* as levels of *KNAT6* transcript have been shown to be increased in the leaves of *as1* mutants (Semiarti *et al.*, 2001). The normal function of *AS1* is to repress transcription of class 1 *KNOX* genes in the leaves to allow cell differentiation via expression of GA biosynthesis genes.

It is also possible that the complete *KNAT6* promoter was not used to make the p*KNAT6*::GUS fusion. Although 2 kb of sequence upstream of the *KNAT6* ATG was isolated and used to drive GUS expression, it has been reported that sequences which control gene expression may also be present within the transcribed region of the gene. For example, *cis*-acting elements in the intragenic sequence of the *AGAMOUS* (*AG*) gene of *Arabidopsis* are required for repression of *AG* in vegetative tissues as well as correct spatial and temporal regulation of *AG* in early flower development (Sieburth and Meyerowitz, 1997). In support of this, *KNAT6* has a large intron that may contain further regulatory elements.

There is very little information on the expression pattern of *KNAT6* in the literature. It has been shown by RT-PCR that *KNAT6* is expressed at low levels in leaf tissue and at a higher level in the shoot apex (Semiarti *et al.*, 2001). There are no data for expression of *KNAT6* in root with which to compare the results obtained here.

### **8.3.5 Regulation of the *KNAT6* promoter by plant hormones**

In untreated seedlings, the GUS expression pattern indicated that the *KNAT6* promoter is active in the main root in a broadly similar area to where lateral roots are emerging and elongating. GUS is not expressed in lateral root primordia, and disappears after the primary lateral roots have emerged. GUS expression was occasionally seen in the stele of older primary lateral roots close to the main root and at the bases of secondary lateral roots. GUS expression is stronger at the lateral root bases than in the stele of the main root. The primary and lateral root tips did not show GUS expression.

The responses of the *KNAT6* promoter to exogenous plant hormones can be summarised as follows. The synthetic auxin analogue NAA altered the *KNAT6* promoter activity and led to expression of GUS at the root tip, while the cytokinin analogue BA caused downregulation. The auxin efflux carrier inhibitor NPA also reduced *KNAT6* promoter activity while the auxin efflux carrier inhibitor TIBA and the ethylene precursor ACC did not appear to significantly affect promoter activity.

In addition to treatment with exogenous NAA, the response of the *KNAT6* promoter to auxin was also investigated by examination of p*KNAT6*::GUS in the *rtv* mutant background. The *rtv* mutant has increased levels of auxin and shows a massive increase in the number of lateral and adventitious roots that are produced (section 1.2.1.1). In this respect, the *rtv* phenotype resembles the effect of treating wild type seedlings with the auxin analogue NAA.

In general, the level of GUS expression was lower in the *rtv* background than on treatment with NAA, especially in Line 15.1, but the expression patterns were similar with GUS expression in the main root, at the bases of lateral roots and at the root tip (Line 10.1) or at the bases of lateral roots (Line 15.1).

The difference in response of the *KNAT6* promoter to the auxin efflux carrier inhibitors TIBA and NPA could indicate that different concentrations of these inhibitors are required for complete inhibition of auxin transport. It has been reported that 5-10  $\mu\text{M}$  NPA is sufficient to give complete inhibition of lateral root initiation in *Arabidopsis*, presumably due to complete inhibition of auxin transport (Casimiro *et al.*, 2001). As 10  $\mu\text{M}$  NPA was used in this study, complete inhibition should have occurred. It is possible that the concentration of TIBA that was used (25  $\mu\text{M}$ ) did not give complete inhibition and that this explains the difference in response of the promoter. In support of this, it has been shown that growth on 20  $\mu\text{M}$  TIBA leads to a less drastic inhibition of root growth and lateral root formation than growth on 20  $\mu\text{M}$  NPA (Mattsson *et al.*, 1999).

The effects of TIBA and NPA on the vascular system in the *Arabidopsis* root have also been reported (Mattsson *et al.*, 1999). Treatment of plants with NPA and TIBA causes an increase in the size of the vascular bundle. The number of xylem strands is increased, and these are randomly distributed. They do not elongate or align properly, leading to xylem vessels that are interrupted. Therefore, alterations in the vascular tissue may also account for the decrease in pKNAT6::GUS expression, as cells of the stele which normally express pKNAT6::GUS may be lost.

Although TIBA and NPA have been widely used to examine the developmental effects of disrupting polar auxin transport, it has recently been noted that these inhibitors do not specifically block the efflux carrier, but in fact inhibit the trafficking of the efflux carrier in the cell (Geldner *et al.*, 2001, Geldner *et al.*, 2003). Therefore, it may be difficult to draw conclusions about the effects of blocking auxin transport when the inhibitor used may have wider effects on cellular functions.

It would be preferable to examine the effects of reduced auxin transport by analysis of the expression of pKNAT6::GUS in the *aux1-100* background where the proposed auxin influx carrier *AUX1* is non-functional. F2 seed for this cross has been obtained and is awaiting analysis.

Overexpression of a fusion protein between KNAT2 and the glucocorticoid (GR) receptor in *Arabidopsis* has allowed the effects of various hormones on KNAT2 function to be investigated (Hamant *et al.*, 2002). Activation of the KNAT2-GR fusion led to delayed leaf senescence and a higher rate of shoot initiation. These two processes are also induced by cytokinin and repressed by ethylene. In addition, induction caused the production of lobed leaves characteristic of the overexpression of class 1 *KNOX* genes. This phenotype was partially repressed by the addition of the ethylene precursor ACC, and by the *ctr1* mutation that causes a constitutive ethylene response (section 1.2.3).

*KNAT2* is expressed in the L3 layer and in the rib zone of the SAM (Hamant *et al.*, 2002). Treatment with ACC restricts this expression pattern and reduces the size of the L3 layer. This can be reversed by the activation of the KNAT2::GR

protein fusion. Conversely, the *KNAT2* expression domain is enlarged in the *etr1* mutant background where ethylene responses are reduced, and also on treatment with cytokinin.

Therefore, it appears that ethylene acts to repress *KNAT2* function whereas cytokinin enhances it, and that these two hormones act antagonistically in the SAM via *KNAT2* to regulate meristem activity.

*KNAT2* expression in the root has been determined by analysis of p*KNAT2*::GUS fusions (O. Hamant, pers. com.). Expression is weak in the primary root but is upregulated where lateral roots emerge. No expression is detected in the root meristem or in the elongation zone of the primary root. In this respect, expression of *KNAT2* is similar to that of *KNAT6* in the *Arabidopsis* primary root.

However, it appears that regulation of *KNAT2* and *KNAT6* by plant hormones in the root differs. p*KNAT2*::GUS expression in the root is increased on cytokinin treatment, and ectopic expression is seen in the elongation zone of lateral roots. A decrease in p*KNAT2*::GUS expression is seen on treatment with ACC. This is not in agreement with the observed response of p*KNAT6*::GUS to these two plant hormones, where cytokinin causes downregulation of expression and ACC does not cause any alteration of expression.

There is no detailed information on which cells in the root express p*KNAT2*::GUS, but it appears to be in the inner cell layers (O. Hamant, pers. com.) and it is possible that *KNAT2* and *KNAT6* are expressed in the same cells. Therefore, it appears possible that *KNAT2* and *KNAT6* may act antagonistically in the root.

The use of plant hormones is a simple method for the initial investigation of the response of promoter::reporter fusions. However, there are problems associated with this approach in that the chemicals used may not actually be specific for purpose for which they are used (such as in the case of TIBA and NPA mentioned above). The use of genetic methods such as the analysis of

crosses may give more reliable results in the investigation of *KNAT6* promoter activity.

## **8.4 Functional analysis**

Functional analysis of the *KNAT6* gene was performed by (a) overexpressing the *KNAT6* coding sequence under control of the 35S promoter, and (b) the generation of antisense and RNAi lines, the aim of which was to downregulate *KNAT6* expression.

### **8.4.1 Overexpression of *KNAT6***

As described in Chapter 4, two isoforms of *KNAT6* mRNA have been isolated from NAA-treated *Arabidopsis* roots, and these two transcripts have been shown to arise from a single genomic locus (section 4.7). The “alternative splice” isoform differs from the “original splice” isoform by the insertion of two amino acids in the conserved MEINOX domain (section 4.6).

This alternative splicing may be the result of a splicing error, or it may be a functional isoform that plays a different role in the plant. Both of these scenarios are a possibility, as discussed in section 1.3.3.

As discussed in section 4.6, an independent group has isolated both of these isoforms and submitted the sequences to GenBank. Therefore it is highly unlikely that these two isoforms are an artefact of the isolation procedure used here. However, to confirm the presence of these two isoforms in multiple samples, PCR using primers specific to each isoform could be designed. The technique could be used semi-quantitatively to determine the relative abundances of each isoform in different tissues or after different treatments. This could be used to confirm the hypothesis that the original, shorter isoform is more abundant in NAA-treated root tissue (section 4.6), and to determine if NAA treatment alters the relative amount of these transcripts.

Overexpression of the original splice isoform under control of the 35S promoter leads to the generation of the characteristic lobed leaf phenotype observed on overexpression of other class 1 *KNOX* genes (section 6.1.4). It would be useful to determine if *KNAT6* is indeed expressed at higher levels in these plants using

RT-PCR. The roots of transgenic lines that show this phenotype were also examined for alterations in root length, the number of anchor roots produced as well as the number and position of lateral roots. Six homozygous transgenic lines were examined, but only one of these showed a root phenotype (section 6.1.5a). It therefore appears likely that this phenotype is not the result of overexpression of *KNAT6* but may be an insertional mutation caused by the integration of the T-DNA. Therefore, it appears that overexpression of the original isoform of *KNAT6* does not cause a root phenotype.

Overexpression of the alternative splice isoform does not lead to the generation of the lobed leaf phenotype observed in original splice 35S::*KNAT6* plants (section 6.1.4), although to confirm this, increased expression of the alternative *KNAT6* isoform should be determined using RT-PCR.

The addition of two amino acids to the MEINOX domain could either abolish or modify the function of this domain. It appears that the alternative splice isoform does not function in the leaf to generate the typical class 1 *KNOX* gene overexpression phenotype, but it is still possible that this isoform could function in the root. The roots of alternative splice 35S::*KNAT6* homozygous plants could be examined to determine if this is the case.

Alternative splicing of homeobox genes is known to play a role in their function. The rice *OSH45* homeobox gene has been shown to have two different transcription initiation sites. This allows the production of several different mRNA species from a single genomic locus (Tamaoki *et al.*, 1995). One cDNA, *OSH45*, consists of exon 1 and 3-7 while the second cDNA *OSH42* consists of exons 2-7. In addition to this, the C-terminal of both of these cDNAs are alternatively spliced by the use of three different splice acceptor sites in intron 6, giving a total of six different transcripts. *OSH45* is expressed constitutively while *OSH42* is expressed in vegetative aerial tissues but not in flowers or roots. The alternative splicing in intron 6 is not tissue specific. The proteins that are encoded by these cDNAs also appear to have different transactivational activities, with exon 1 (that is present in *OSH45* but not in *OSH42*) acting to suppress transactivational activity. It has been suggested that the *OSH45*

protein may function as a competitive inhibitor of OSH42 by occupying the same DNA binding sites without activating transcription.

It is possible then that the two isoforms of *KNAT6* may function in a similar way with the alternative splice isoform (that does not induce a lobed leaf phenotype) functioning to repress the activity of the original splice isoform that can induce the lobed leaf phenotype.

#### **8.4.2 Downregulation of *KNAT6***

No clear phenotype was observed in *KNAT6* antisense plants that were generated, as described in section 6.1.7. It has been reported that antisense suppression does not always cause efficient downregulation of the target gene (Chuang and Meyerowitz, 2000). No further analysis was carried out on these plants.

Four different RNAi constructs were made using two parts of the *KNAT6* coding sequence under the control of either the *KNAT6* promoter or the 35S promoter. Analysis of 10 homozygous lines for each of these constructs was then performed (section 6.2). There did not appear to be any difference between the length of the primary root or the number of lateral roots or anchor roots that were produced by RNAi lines.

However, it did appear that RNAi1, RNAi2 and RNAi1+P plants initiate lateral roots closer to the root tip. For the RNAi2+P plants, this is more variable, with some of the plants showing a similar trend to the Col-0 plants, and some showing a decrease in this distance. It is difficult to say if this is significant, as some variability was also seen in 35S::*KNAT6* original splice sense lines when this parameter was measured (compare Figure 6.1.5b with Figures 6.2.4e-h). Initially, RT-PCR should be used to confirm that these RNAi plants do have reduced levels of the *KNAT6* transcript. To confirm the putative root phenotype, measurements from the root tip to the last lateral root to emerge should be repeated.

In addition to this possible root phenotype, it was also noted that some plants showed an aerial phenotype. The range of phenotypes that were seen are summarised in Table 6.2.4a.

A small proportion of seedlings exhibited a break in apical dominance, including Col-0 controls. Although the controls can occasionally show this phenotype, it may be that it occurs at higher frequency in the RNAi lines. Analysis of a greater number of both wild type and transgenic plants may help to resolve this.

In addition, some seedlings carrying each of the four RNAi constructs showed callus formation on the cotyledons. This was never observed on Col-0 control plants. In RNAi1 and RNAi1+P lines, cotyledon callusing and a break in apical dominance was combined. In some seedlings transformed with RNAi1, seedlings showed a more severe apical phenotype where the SAM appeared to initiate many small leaf-like structures (see Figure 6.2.4q (v)).

All four RNAi constructs cause callusing of cotyledons but a combination of a break in apical dominance and cotyledon callusing was only observed in plants carrying RNAi1 or RNAi1+P constructs. Furthermore, the most severe apical phenotype was only observed in plants carrying the RNAi1 construct. This may reflect a higher efficiency of the 5' end of the *KNAT6* transcript at inducing RNAi downregulation of the endogenous transcript. Increased cytokinin levels can cause the release of lateral buds from dormancy (Klee and Lanahan, 1995), and callus formation may also reflect alterations in the level of hormones such as cytokinin and/or auxin.

The putative phenotypes discussed below are not an artefact of the RNAi vector as suppression of other genes using this vector gives different phenotypes to those described here (S. Casson, pers. com.). Therefore, the results presented here indicate that a decrease in *KNAT6* levels in RNAi plants may perturb hormone levels in the plant.

#### **8.4.3 *KNAT6* may be partially redundant**

Several pieces of information indicate that *KNAT6* may be partially redundant. The phylogenetic analysis presented in section 4.4 indicates that *KNAT6* is very

closely related to the Class 1 homeobox gene *KNAT2*. Therefore, it is likely that these two genes share some functional redundancy. It appears that *KNAT2* gene knockouts have no phenotype (O. Hamant, pers. com.) and it may be that *KNAT2* and *KNAT6* share some functional redundancy.

As described in section 6.1.4, overexpression of the shorter original isoform of *KNAT6* leads to a lobed leaf phenotype which is similar to that seen when *KNAT1* and *KNAT2* are overexpressed in *Arabidopsis*. This indicates that *KNAT6* may be involved in the same pathways or may have some overlapping functions with these other *KNOX* genes.

Mutations in the MYB transcription factor *AS1* result in plants that have abnormal leaves, with marginal outgrowths or lobes (section 1.4.2.5). *AS1* related to *ROUGH SHEATH2 (RS2)* in maize and *PHANTASTICA (PHAN)* in *Antirrhinum* (Byrne et al., 2000). All three genes are expressed in lateral organ primordia and act as negative regulators of *KNOX* genes (Byrne et al., 2000; Ori et al., 2000; Semiarti et al., 2001; Timmermans et al., 1999; Tsiantis et al., 1999; Waites et al., 1998; Byrne et al., 2002).

*as1* suppresses the *stm* mutant phenotype, so that double mutants have an *as1* vegetative shoot. Therefore, this genetic interaction indicates that *STM* normally prevents *AS1* expression in the SAM to maintain its undifferentiated state (Byrne et al., 2000). Triple *as1/stm/bp* mutants, have a phenotype that is comparable to *stm* single mutants, indicating that *BP/KNAT1* is required for meristem maintenance in the absence of *STM* (Byrne et al., 2002).

*stm/knat2* double mutants have a *stm* phenotype and *KNAT2* expression is also absent in *stm* mutants. This is consistent with a genetic hierarchy whereby *STM* negatively regulates *AS1*, which in turn negatively regulates *KNAT2*. However, although it has been shown that *KNAT2* is regulated by *AS1*, *knat2* knockout plants have no phenotype either alone or in combination with *as1* or *as2*. This indicates either that misexpression of *KNAT2* is not required for these phenotypes, or that *KNAT2* is redundant with another homeobox gene, most likely *KNAT6*.

No clear phenotype was identified in *KNAT6* antisense lines (although transcript levels in these lines were not examined), and there is a subtle effect on root development when *KNAT6* transcript levels presumably are reduced in RNAi lines. In these RNAi lines, no clear aerial phenotype was observed, despite the expression of *KNAT6* in aerial parts of the plant (sections 5.1.2 and 5.3.2). There are several explanations for these observations. It may be that a low level of transcript is present in *KNAT6* RNAi lines and that this is responsible for the subtle phenotype, or it may be that the role of *KNAT6* in root development is partially redundant with another gene. As mentioned above, the most likely candidate for redundancy with *KNAT6* is the closely related *KNAT2* gene, and it has been reported that *KNAT2* is expressed in the root (section 8.3.5).

To distinguish between these two possibilities, isolation and characterisation of null *knat6* mutants as well as generation of *knat2/knat6* double mutants will clarify the role of *KNAT6* in plant development and reveal any partial redundancy between *KNAT2* and *KNAT6*. The putative insertion mutants isolated in section 7.2 will be characterised to determine if they are indeed null alleles.

## **8.5 Roles of *KNAT6* in plant development**

The previous sections in this discussion deal with particular data on the expression and function of *KNAT6* that was collected in the results chapters. The aim of the final section in this chapter is to provide a number of alternative models for possible roles of *KNAT6* in the plant during development.

### **8.5.1 *KNAT6* may play a similar role to other class 1 *KNOX* genes in the shoot**

The similarity in phenotype between 35S::*KNAT6*, 35S::*KNAT1* and 35S::*KNAT2* plants implies that *KNAT6* may play a similar role to these genes in *Arabidopsis*.

As discussed in section 1.4.2.5, the plant hormone cytokinin appears to function in some of the same pathways as class 1 *KNOX* genes. Some authors have noted that tobacco plants which overexpress *Kn1* or *KNAT1* share some similarities, such as a reduction in apical dominance and the formation of

epiphylllic shoots, with plants which overproduce cytokinin (Rupp *et al.*, 1999). However, overexpression of *KNOX* genes does not lead to reduced root growth that is characteristic of cytokinin treatment, which indicates that other pathways are also involved.

The position of cytokinin in relation to *KNOX* genes in these pathways is not clear, with some workers proposing that cytokinin is upstream, and some proposing it is downstream, from *KNOX* genes (section 1.4.2.5). The observation that overexpression of the cytokinin biosynthesis *ipt* gene leads to accumulation of *STM* and *KNAT1* transcripts (Rupp *et al.*, 1999), and that overexpression of *Kn1* and *KNAT1* leads to elevated cytokinin levels (Ori *et al.*, 1999, Frugis *et al.*, 2001) could be explained by the existence of a feedback mechanism, although this remains undefined at the molecular level.

Alternatively, it is possible that misexpression of *KNOX* genes in tissues where they are not normally expressed (as is the case with 35S::KN1 and 35S::KNAT1) confers a novel function to these genes. As discussed in section 1.4.2.3, homeobox genes may be able to function as activators or repressors of transcription. Therefore, *KNOX* genes may carry out different functions at different stages of development or in different tissues depending on what other coregulatory proteins are present. This model could in theory be extended to explain alteration in the function of these genes when they are ectopically expressed. This may help to explain why cytokinin appears to act both upstream and downstream of *KNOX* genes in the plant.

The overexpression phenotype of *KNAT6* in the shoot is similar to that seen on overexpression of other class 1 *KNOX* genes and, as it has been demonstrated that this can lead to cytokinin accumulation, this result indicates that *KNAT6* functions to upregulate cytokinin biosynthesis. However, some RNAi plants also showed a phenotype that is similar to plants that have higher levels of cytokinin. Therefore it appears from these results that *KNAT6* would normally function to repress cytokinin synthesis in the plant. It has also been noted as part of this work that exogenous application of cytokinin represses *KNAT6* promoter activity.

It is not possible to draw further conclusions on the relative positions of *KNAT6* and cytokinin in developmental pathways from the results presented here although it does appear that hormone levels may be altered in plants with altered *KNAT6* expression.

### **8.5.2 *KNAT6* may be involved in vascular development**

The *KNAT6* promoter is active in the phloem poles of the root vascular tissue. It has been reported that other class 1 *KNOX* genes are expressed in vascular tissues. For example, the maize homeobox genes *Kn1* and *RS1* are expressed in the developing stem of maize seedlings (Jackson *et al.*, 1996). In the developing stem, *Kn1* is expressed in the ground tissue, with the exception of some provascular strands that are associated with the developing lateral veins. *RS1* is also expressed in the provascular strands of the stem, including cells that are not labelled by *Kn1*. *Kn1* is expressed in some of the developing vascular strands of the inflorescence stem. *RS1* is also expressed in the ground tissue of the inflorescence stem but not in the same provascular cells which express *Kn1*. In addition, *RS1* and *KNOX4* are expressed weakly in roots although no information is available for the cell type in which these genes are expressed (Kerstetter *et al.*, 1994).

In *Arabidopsis*, the class 1 *KNOX* genes *KNAT1*, *KNAT2* and *STM* are also expressed in the stem of the plant. Expression of *STM* in the stem is absent from cells around the vascular strands (Long *et al.*, 1996). *KNAT1* is expressed in cells that are adjacent to the developing vasculature in the stem (Lincoln *et al.*, 1994). *KNAT2* is also expressed in vascular strands near the shoot apex and in inflorescence stems (Laufs *et al.*, 1998, Dockx *et al.*, 1995).

Therefore, as class 1 *KNOX* genes are expressed in the developing vascular tissue of maize and *Arabidopsis*, it is reasonable that they may be involved in vascular tissue development. This is supported by the phenotype of the *Kn1* mutant, where vascular development is affected and knots associated with the vascular tissue develop (Vollbrecht *et al.*, 1991).

Mutations in *AS1* and *AS2*, which are both negative regulators of class 1 *KNOX* genes, also lead to defects in vascular development. Normally, the primary vein

of *Arabidopsis* leaves grows acropetally in the centre of the leaf. Towards the leaf apex, the primary vein splits and forms secondary veins that grow basipetally towards the primary vein. Additional secondary veins differentiate as the lamina expands and they are connected almost symmetrically to the primary vein (Semiarti *et al.*, 2001).

*as2* leaves show a thinner primary vein as well as asymmetric development and less efficient connections of secondary veins (Semiarti *et al.*, 2001). The pattern of venation is also less complex than in *AS2* plants, although differentiation of vascular elements such as xylem and phloem still occurs. In addition, *as2* mutants may have an increased number of vascular bundles in the petiole of leaves. *as1* plants have a similar phenotype (Semiarti *et al.*, 2001).

Consistent with the observation that *as1* and *as2* have a similar morphology to 35S::*KNAT1* plants, there is an accumulation of *KNAT1*, *KNAT2* and *KNAT6* transcripts in the leaves of these mutants (Semiarti *et al.*, 2001). Other groups have also reported that *KNAT1* and *KNAT2* accumulate in the leaves of *as1* (Byrne *et al.*, 2000) and *as2* (Ori *et al.*, 2000). In addition, 35S::*KNAT1* plants show an enlargement in secondary veins (Chuck *et al.*, 1996).

Therefore, there is a possible correlation between *KNOX* gene repression in the leaf and correct vein formation. It is possible that *KNAT6* is required for development of phloem. It may act as a signal that specifies phloem identity or it may prevent all of the vascular tissues from becoming xylem elements. The development of xylem and phloem is mediated by plant hormones such as auxin (Davies, 1995).

To determine if *KNAT6* plays a role in the development of vascular tissue, 35S::*KNAT6* lines can in the future be examined to determine if these plants show a similar phenotype to 35S::*KNAT1* plants. It will also be interesting to examine the vascular tissue of *Arabidopsis* plants where *KNAT6* function is impaired, either in RNAi or insertion mutant lines.

The expression of p*KNAT6*::GUS in several mutants which show defects in vascular patterning can be investigated. These include *gollum* (*glm*), which is

characterised by defective radial patterning, and disorganised vascular tissues with an incomplete pericycle layer, and the components of the auxin perception pathway *bodenlos (bdl)* and *monopteros (mp)* that are defective in formation of continuous vascular strands. *fass* seedlings have an enlarged vascular cylinder which may contain more than two protoxylem poles. More than one vascular strand has also been observed in *hydra* mutants (Souter *et al.*, 2002). This increase in vascular strands has been correlated with an increase in the number of cotyledons which are formed (Torres-Ruiz and Jürgens, 1994). T2 seed from all of these crosses has been generated and is awaiting analysis, and it will be interesting to examine the activity of the *KNAT6* promoter in these backgrounds, as well as in the *as1* and *as2* mutants.

### **8.5.3 *KNAT6* may be a regulator of lateral root initiation**

Lateral root primordia are initiated by divisions in pericycle cells that are in contact with the underlying protoxylem cells of the xylem pole (Dubrovsky *et al.*, 2001). Those pericycle cells that are adjacent to the phloem poles do not divide. Initiation of lateral roots occurs behind the root tip in the zone of differentiation, where the pericycle cells are not actively dividing (Malamy and Benfey, 1997).

As discussed in section 1.3.3.1, it is thought that the cell cycle status of pericycle cells in files adjacent to xylem poles or phloem poles is different, with those that are adjacent to phloem poles remaining in the G1 phase and those that are adjacent to the xylem poles progressing to the G2 phase. It may be that xylem pole pericycle cells are more susceptible to lateral root initiation as they have already completed DNA synthesis (S phase) and are arrested immediately prior to the mitotic phase (M), whereas phloem pole pericycle cells are arrested prior to the S phase.

It has been hypothesised that a negative regulator of lateral root development may be present in phloem pole pericycle cells. This negative signal could be encoded by cell cycle regulatory genes which inhibit cell cycle progression when overexpressed in *Arabidopsis* such as *SUC1/CKS1At*, which inhibits G1 to S and G2 to M transitions (De Veylder *et al.*, 2001b), or could be one of a number of cyclin-dependent kinase inhibitors (CKIs) (De Veylder *et al.*, 2001a).

Cell cycle regulation in the xylem pericycle is known to be mediated by auxin, as inhibition of polar auxin transport using NPA blocks lateral root initiation (section 1.3.3.2). Auxin has recently been shown to promote lateral root initiation by stimulating the G1 to S transition in xylem pole pericycle cells (Himanen *et al.*, 2002). In young roots where lateral roots are being initiated, the CKI gene *KRP2* is expressed in the phloem pole pericycle. In older tissues, where no laterals are normally formed, expression was seen in the xylem pole pericycle cells, or around the whole pericycle. *KRP2* expression was also observed opposite a developing lateral root in the xylem pole pericycle. Therefore, it appears that this gene is required for inhibition of cell division in cells that do not form lateral roots. This is supported by the observation that overexpression of *KRP2* prevents pericycle activation and reduces the number of lateral roots which are formed.

The expression pattern of *KNAT6* in the phloem poles of the root as determined by p*KNAT6*::GUS activity allows one to speculate that this gene may also play a role in regulation of lateral root development. As *KNAT6* is expressed in the phloem pole, rather than in the phloem pole pericycle cells, this would require trafficking of the *KNAT6* transcript or protein, or the production of a transportable signal by *KNAT6*. The ability of the *KNAT6* protein to be trafficked between different cells can be investigated in the future by the analysis of *KNAT6*::GFP protein fusions which were generated as part of this work. In addition, localisation of the *KNAT6* transcript could be investigated using in situ hybridisation, and protein localisation could be investigated by immunolocalisation if a *KNAT6* antibody were raised. Differences in these two expression patterns may reveal differences in the localisation of the *KNAT6* transcript and protein.

Based on GUS expression in the stele of the primary root in p*KNAT6*::GUS lines, it does not appear that *KNAT6* is expressed in the zone of lateral root initiation close to the root tip. Therefore, *KNAT6* may not be involved in control of initiation of lateral roots at this position in *Arabidopsis*. A separate negative regulator of lateral root initiation may be required in the zone of differentiation to prevent phloem pole pericycle cells from initiating lateral roots at this position. However, the putative phenotype in RNAi plants, where lateral roots are

initiated closer to the root tip, may indicate a role for *KNAT6* in lateral root initiation at this position.

*KNAT6* appears to be expressed in the zone of lateral root emergence. Auxin is also implicated in the emergence steps during lateral root initiation as discussed in section 1.3.3. Analysis of the levels of auxin in the *Arabidopsis* root reveals that a gradient is present, with a high concentration at the crown that decreases towards the root tip (Marchant *et al.*, 2002). Then, at the root tip itself, auxin accumulates to give a higher concentration. The expression data inferred from p*KNAT6*::GUS lines indicate that *KNAT6* appears to be expressed in a zone of intermediate auxin concentration which correlates roughly with the zone of lateral root emergence. Therefore, there is a possible link between the auxin gradient required for lateral root emergence and *KNAT6*.

It may be that the concentration of auxin in the zone of lateral root emergence could induce formation of lateral roots from phloem pole pericycle cells at this position, and that *KNAT6* acts as an inhibitor here. p*KNAT6*::GUS is not expressed in the older primary root, and it may be that *KNAT6* is no longer required at this position, for example if the pericycle cells are no longer responsive to auxin and therefore cannot form lateral roots.

Although auxin is required for lateral root development, it is likely that the ratio of auxin to cytokinin is also important (Davies, 1995). The downregulation of p*KNAT6*::GUS by exogenous addition of BA could be explained if this causes a change in the auxin to cytokinin ratio which prevents lateral root initiation, such that the inhibitory effects of *KNAT6* are not required. Indeed, lateral roots were not initiated on treatment with BA in this work.

During the course of this work, p*KNAT6*::GUS seedlings were examined after 3, 6 and 9 days treatment on NAA. After 3 days' treatment, when lateral roots have been initiated along the whole length of the root apart from at the tip, p*KNAT6*::GUS expression has shifted to the root tip. The expression of p*KNAT6*::GUS at this position may be significant as this is the only part of the root where lateral roots are still emerging. Therefore, this may support the hypothesis above that *KNAT6* is required specifically at the position of lateral

root emergence. The investigation of pKNAT6::GUS expression after shorter treatments with NAA will indicate if *KNAT6* is upregulated along the root during the period when lateral roots emerge simultaneously over the whole root, and will help to clarify this point. GUS histochemical staining of plants which carry pKNAT6::GUS in the *rtv* background over a developmental time course can also be carried out to this end.

The *alf3-1* mutant is characterised by lateral roots that emerge and then arrest (Celenza *et al.*, 1995). As the *alf3-1* mutant can be rescued by growth on the IAA precursor indole, it is thought that the role of the *ALF3-1* gene product is maintain auxin levels in the primordium at a level which is required to keep the cells viable. This could either be by *de novo* synthesis of auxin in the primordium, or by auxin transport to the primordium. Investigation of the activity of the *KNAT6* promoter in this mutant background may help to dissect the role of *KNAT6* in relation to the emergence steps of lateral roots in *Arabidopsis*.

In addition, the expression of pKNAT6::GUS in *lax3* and *aux1-100* backgrounds can be investigated. These mutants show reduced numbers of lateral roots (section 1.2.1.2), and this may correlate with a reduced expression domain of *KNAT6* if *KNAT6* is indeed required at positions of lateral root emergence.

Expression of *KNAT1* in the SAM is seen as two stripes in the peripheral zone that appears to mark the boundary between the cells of the meristem, and the cells which will form the next leaves (Hake and Ori, 2002). This is similar to the expression of the maize class 1 *KNOX* gene *RS1*, which is expressed in a ring around the lateral organ primordia adjacent to the meristem (Jackson *et al.*, 1996). It has been proposed that the misexpression of class 1 *KNOX* genes creates ectopic boundaries (Ori *et al.*, 2000). In 35S::*KNAT1* plants, the sinuses between the lobes on the leaves consist of cells which have meristem-like properties whereas the lobes consist of cells with leaf-like properties. This juxtaposition is similar to the situation seen in the SAM where leaves are initiated. Consistent with this model is the expression of *KNAT1* and *KNAT2* in the sinuses. It seems possible that *KNAT6* may play a similar role in the development of the root, where it may be involved specifying which cells will form lateral roots, and cells which will not.

#### 8.5.4 *KNAT6* may play a role in control of root architecture

As well as expression in the stele of the main root, p*KNAT6*::GUS is strongly expressed at the bases of the lateral roots.

Analysis of the *bp* mutant (a null allele of *KNAT1*) has indicated that this gene plays a role in the development of the *Arabidopsis* inflorescence stem (Douglas *et al.*, 2002). In wild type plants, the inflorescence stem consists of an outer layer of epidermis surrounding 4-5 layers of ground tissue (chlorenchyma). The inner part of the stem consists of alternating vascular bundles and interfascicular fibres that surround central pith. The pattern is altered at positions where nodes join the main stem. Here, a discrete vascular bundle in the stem adjacent to the region of attachment of the lateral organ is absent. This is a result of branching of the vascular bundle into the lateral organ to connect it into the vascular system of the rest of the plant. In the node itself, vascular bundles that are on the adaxial side are smaller than those on the abaxial side. In addition, the chlorenchyma is interrupted adjacent to the lateral organs at the nodes, so that a collar of achlorophyllous tissue is produced distal to the node. This indicates that a downregulation of chlorenchyma development occurs adjacent to the lateral organs.

In the *bp* mutant, this achlorophyllous tissue is expanded to include a larger portion of the stem circumference, and also extends basipetally into the internodes which underlie cauline leaves and floral nodes to form a stripe of achlorophyllous tissue. These stripes are always positioned over the vascular bundle which is associated with the lateral organ from which the stripe originated.

This suggests that a repressor of chlorenchyma development normally functions in the plant to produce achlorophyllous tissues at the nodes (Douglas *et al.*, 2002). The enlargement of this domain in *bp* mutants suggests that *BP* normally restricts the domain of action of this repressor. As there is a link between the *bp* stripe and the vascular bundle, this suggests that there is a link between the repressor and the vasculature. For example, the flux of the repressor through the vascular tissue may alter differentiation in the overlying tissues. Therefore,

BP may function to repress the action of this “asymmetrising” molecule, and may provide the switch between the symmetrical internodes and the asymmetrical nodes in the inflorescence stem.

Supporting evidence for this link between the *bp* stripe and the vasculature comes from the observation that overexpression of class 1 *KNOX* genes such as in the *knotted1* mutant in maize and 35S::KNAT1 plants leads to ectopic meristem formation near leaf veins.

The localisation of pKNAT6::GUS expression in the phloem poles of root vascular tissue may imply that *KNAT6* performs a similar function in the root, where it is required for the regulation of lateral root spacing in the same way as *BP* is required in the stem.

This is supported by the putative root phenotype observed in RNAi lines where lateral roots appear to be produced closer to the root tip. This indicates that *KNAT6* may normally function to repress the initiation of lateral roots in the *Arabidopsis* root.

The genes which are downstream of *KNAT6*, and which may play a role in control of lateral root spacing are currently unknown. *LAX3* is one candidate downstream gene. *LAX3* has similarity to *AUX1* and is expressed in the mature vasculature of the root where it is thought to deliver auxin to the lateral root primordia (M. Bennett, pers. com.). *lax3* plants show reduced numbers of lateral roots compared to wild type plants. The investigation of the expression of *LAX3* in plants where *KNAT6* is downregulated (either RNAi lines or insertion mutants) will indicate if *KNAT6* normally regulates *LAX3* to control lateral root spacing.

## 8.6 Conclusions

This work describes the isolation and preliminary characterisation of the *Arabidopsis* class 1 *KNOX* gene *KNAT6*.

The expression and functional analysis presented here indicates that *KNAT6* may play similar roles to other class1 *KNOX* genes in the maintenance of cell identity or function. In addition, *KNAT6* may also be involved in aspects of

lateral root and vascular tissue development as well as in the control of root architecture. Further work that has been proposed throughout this chapter should clarify the role of *KNAT6* in plant development.

## References

- Alberts, B., Bray, D., Lewis, J., Raff, M., Roberts, K., and Watson, J.D. (1994) *Molecular Biology of the Cell* Garland Publishing.
- Alonso, J.M., Hirayama, T., Roman, G., Nourizadeh, S., and Ecker, J.R. (1999) *EIN2*, a bifunctional transducer of ethylene and stress responses in *Arabidopsis*. *Science*, 284, 2148-2152.
- An, Y.-Q., Huang, S., McDowell, J.M., McKinney, E.C., and Meagher, R.B. (1996) Conserved expression of the *Arabidopsis ACT1* and *ACT3* actin subclass in organ primordia and mature pollen. *The Plant Cell*, 8, 15-30.
- Ashikari, M., Wu, J., Yano, M., Sasaki, T., and Yoshimura, A. (1999) Rice gibberellin-insensitive dwarf mutant gene *Dwarf1* encodes the  $\alpha$ -subunit of GTP-binding protein. *Proceedings of the National Academy of Sciences*, 96, 10284-10289.
- Ausubel, F.M., Brent, R., Kingston, R.E., Moore, D.D., Seidman, J.G., Smith, J.A., and Struhl, K. (1994) *Current Protocols in Molecular Biology* John Wiley and Sons.
- Barton, K. and Poethig, S. (1993) Formation of the shoot apical meristem in *Arabidopsis thaliana*: an analysis of development in the wild type and in the *shootmeristemless* mutant. *Development*, 119, 823-831.
- Baulcombe, D.C., Saunders, G.R., Bevan, M.W., Mayo, M.A., and Harrison, B.D. (1986) Expression of biologically active viral satellite RNA from the nuclear genome of transformed plants. *Nature*, 321, 446-449.
- Beeckman, T., Burssens, S., and Inzé, D. (2001) The peri-cell-cycle in *Arabidopsis*. *Journal of Experimental Botany*, 52, 403-411.
- Bellaoui, M., Pidkowich, M., Samach, A., Kushalappa, K., Kohalmi, S., Modrusan, Z., Crosby, W., and Haughn, G. (2001) The *Arabidopsis* BELL1 and KNOX TALE homoeodomain proteins interact through a domain conserved between plants and animals. *The Plant Cell*, 13, 2455-2470.
- Bennett, M.J., Marchant, A., Green, H.G., May, S.T., Ward, S.P., Millner, P.A., Walker, A.R., Schulz, B., and Feldmann, K.A. (1996) *Arabidopsis AUX1* gene: a permease-like regulator of Root Gravitropism. *Science*, 273, 948-950.
- Berleth, T. and Jürgens, G. (1993) The role of the *monopteros* gene in organising the basal body region of the *Arabidopsis* embryo. *Development*, 118, 575-587.
- Berleth, T. and Mattsson, J. (2000) Vascular development: tracing signals along veins. *Current Opinion in Plant Biology*, 3, 406-411.

Bernard, P., Kezdy, K.E., van Melder, L., Steyaert, J., Wyns, L., Pato, M.M., Higgins, P.N., and Couturier, M. (1993) The F-plasmid CCDB protein induces efficient ATP-dependent DNA cleavage by gyrase. *Journal of Molecular Biology*, 234, 534-541.

Bertolino, E., Reimund, B., Wildt-Perinic, D., and Clere, R.G. (1995) A novel homeobox protein which recognises a TGT core and functionally interferes with a retinoid-responsive motif. *Journal of Biological Chemistry*, 270, 31178-31188.

Bevan, M. (1984) Binary *Agrobacterium* papers for plant transformation. *Nucleic acids research*, 12, 8711-8721.

Bhalerao, R., Eklöf, J., Ljung, K., Marchant, A., Bennett, M., and Sandberg, G. (2002) Shoot-derived auxin is essential for lateral root emergence in *Arabidopsis* seedlings. *The Plant Journal*, 29, 325-332.

Bharathan, G., Janssen, B.-J., Kellogg, E.A., and Sinha, N. (1999) Phylogenetic relationships and evolution of the *KNOTTED* class of plant homeodomain proteins. *Mol. Biol. Evol.*, 16, 553-563.

Bleeker, A.B., Estelle, M.A., Somerville, C., and Kende, H. (1988) Insensitivity to ethylene conferred by a dominant mutation in *Arabidopsis thaliana*. *Science*, 241, 1086-1089.

Boerjan, W., Cervera, M.-T., Delarue, M., Beeckman, T., Dewitte, W., Bellini, C., Caboche, M., Van Onckelen, H., Van Montague, M., and Inzé, D. (1995) *superroot*, a recessive mutation in *Arabidopsis*, confers auxin overproduction. *Plant Cell*, 7, 1405-1419.

Bowman, J. and Eshed, Y. (2000) Formation and maintenance of the shoot apical meristem. *Trends in Plant Science*, 5, 110-115.

Bürglin, T. (1997) Analysis of TALE superclass homeobox genes (MEIS, PBC, KNOX, Iroquois, TGIF) reveals a novel domain conserved between plants and animals. *Nucleic acids research*, 25, 4173-4180.

Bürglin, T. (1998) The PBC domain contains a MEINOX domain - Coevolution of Hox and TALE homeobox genes? *Development, Genes and Evolution*, 208, 113-116.

Byrne, M.E., Barley, R., Curtis, M., Arroyo, J., Dunham, M., Hudson, A., and Martienssen, R. (2000) *Asymmetric leaves1* mediates leaf patterning and stem cell function in *Arabidopsis*. *Nature*, 408, 967-971.

Byrne, M.E., Simorowski, J., and Martienssen, R. (2002) *ASYMMETRIC LEAVES1* reveals knox gene redundancy in *Arabidopsis*. *Development*, 129, 1957-1965.

- Camilleri, C., Azimzadeh, J., Pastuglia, M., Bellini, C., and Grandjean, O. (2002) The *Arabidopsis* TONNEAU2 gene encodes a putative novel protein phosphatase 2A regulatory subunit essential for control of the cortical cytoskeleton. *The Plant Cell*, 14, 833-845.
- Carthew, R. (2001) Gene silencing by double-stranded RNA. *Current Opinion in Cell Biology*, 13, 244-248.
- Casimiro, I., Marchant, A., Bhalerao, R., Beeckman, T., Dhooge, S., Swarup, R., Graham, N., Inzé, D., Sandberg, G., Casero, P., and Bennett, M. (2001) Auxin transport promotes *Arabidopsis* lateral root initiation. *The Plant Cell*, 13, 843-852.
- Casson, S.A., Chilley, P.M., Topping, J.F., Evans, I.M., Souter, M.A., and Lindsey, K. (2002) The POLARIS gene of *Arabidopsis* encodes a predicted peptide required for correct root growth and leaf vascular patterning. *Plant Cell* 14, 1705-1721.
- Celenza, J., Gristafi, P., and Fink, G. (1995) A pathway for lateral root formation in *Arabidopsis thaliana*. *Genes and Development*, 9, 2131-2142.
- Chalfie, M., Tu, Y., Euskirchen, G., Ward, W., and Prasher, D. (1994) Green fluorescent protein as a marker for gene expression. *Science*, 263, 802-805.
- Chang, C. and Stadler, R. (2001) Ethylene hormone receptor action in *Arabidopsis*. *BioEssays*, 23, 619-627.
- Chang, C.-F., Kwok, S.F., Bleeker, A.B., and Meyerowitz, E.M. (1993) *Arabidopsis* ethylene-response gene *ETR1*: similarity of product to two-component regulators. *Science*, 262, 539-544.
- Cheng, J.-C., Seeley, K., and Sung, Z. (1995) *RML1* and *RML2*, *Arabidopsis* genes required for cell proliferation at the root tip. *Plant Physiology*, 107, 365-376.
- Chien, J.C. and Sussex, I.M. (1996) Differential regulation of trichome formation on the adaxial and abaxial leaf surfaces by gibberellins and photoperiod in *Arabidopsis thaliana* (L.) Heynh. *Plant Physiology*, 111, 1321-1328.
- Christensen, S.K., Dagenais, N., Chory, D., and Weigel, D. (2000) Regulation of auxin response by the protein kinase PINOID. *Cell*, 100, 469-478.
- Chuang, C.-F. and Meyerowitz, E.M. (2000) Specific and heritable genetic interference by double stranded RNA in *Arabidopsis thaliana*. *Proceedings of the National Academy of Sciences*, 97, 4985-4990.
- Chuck, G., Lincoln, C., and Hake, S. (1996) *KNAT1* induces lobed leaves with ectopic meristems when overexpressed in *Arabidopsis*. *Plant Cell*, 8, 1277-1289.

- Church, G. and Gilbert, W. (1984) Genomic sequencing. Proceedings of the National Academy of Sciences, 81, 1991-1995.
- Clark, K.L., Larsen, P.B., Wang, X., and Chang, C. (1998) Association of the *Arabidopsis* *CTR1* Raf-like kinase with the *ETR1* and *ERS* ethylene receptors. Proceedings of the National Academy of Sciences, 95, 5401-5406.
- Clarke, J.H., Tack, D., Findlay, K., van Montague, M., and van Lijsebettens, M. (1999) The *SERRATE* locus controls the formation of the early juvvenile leaves and phase length in *Arabidopsis*. Plant Journal, 20, 493-501.
- Clough, S. and Bent, A. (1998) Floral dip: a simplified method for *Agrobacterium*-mediated transformation of *Arabidopsis thaliana*. The Plant Journal, 16, 735-743.
- Cormack, B., Valdivia, R., and Falkow, S. (1996) FACS-optimised mutants of the green fluorescent protein (GFP). Gene, 173, 33-38.
- Craig, K.L. and Tyers, M. (1999) The F-box: a new motif for ubiquitin dependent proteolysis in cell cycle regulation and signal transduction. Biophys Mol Biol, 72, 299-328.
- Cristina, M.D., Sessa, G., Dolan, L., Linstead, P., Baima, S., Ruberti, I., and Morelli, G. (1996) The *Arabidopsis* *Athb-10* (*GLABRA2*) is an HD-Zip protein required for regulation of root hair development. The Plant Journal, 10, 393-402.
- Croy, R.R.D., ed. (1993) Plant Molecular Biology Labfax. Biosis Scientific Publishers  
Blackwell Scientific Publications, Oxford.
- D'Agostino, I.B. and Keiber, J.J. (1999) Molecular mechanisms of cytokinin action. Current Opinion in Plant Biology, 2, 359-364.
- Dale, P.J., Marks, M.S., Brown, M.M., Woolston, C.J., Gunn, H.V., Mullineaux, P.M., Lewis, D.M., Kemp, J.M., Chen, D.F., Gilmore, D.M., and Flavell, R.B. (1989) Agroinfection of wheat: inoculation of *in vitro* grown seedlings and embryos. Plant Science, 63, 237-245.
- Davies, P.J. (1995) Plant hormones: physiology, biochemistry and molecular biology, 2 edn. Kluwer Academic Publishers, Dordrecht.
- Davis, S. and Vierstra, R. (1998) Soluble, highly fluorescent variants of green fluorescent protein (GFP) for use in higher plants. Plant Molecular Biology, 36, 521-528.
- De Veylder, L., Beeckman, T., Beemster, G.T.S., Krols, L., Terras, F., Landrieu, I., Van Der Schueren, E., Maes, S., Naudts, M., and Inze, D.

(2001a) Functional analysis of cyclin-dependent kinase inhibitors of *Arabidopsis*. *The Plant Cell*, 13, 1653-1667.

De Veylder, L., Beeckman, G.T.S., Beeckman, T., and Inze, D. (2001b) *CKS1At* overexpression in *Arabidopsis thaliana* inhibits growth by reducing meristem size and inhibiting cell-cycle progression. *The Plant Journal*, 25, 617-626.

del Pozo, J.C. and Estelle, M. (1999) The *Arabidopsis* cullin AtCUL1 is modified by the ubiquitin related protein RUB1. *Proceedings of the National Academy of Sciences*, 96, 15342-15347.

del Pozo, J.C., Timpte, C., Tan, S., Callis, J., and Estelle, M. (1998) The ubiquitin-related protein RUB1 and auxin response in *Arabidopsis*. *Science*, 280, 1760-1763.

Dewitte, W., Chiappetta, A., Azmi, A., Witters, E., Strnad, M., Rembur, J., Noin, M., Chriqui, D., and van Onckelen, H. (1999) Dynamics of cytokinins in apical shoot meristemes of a day neutral tobacco during floral transition and flower formation. *Plant Physiology*, 119, 111-121.

Dill, A., Jung, H.-S., and Sun, T.-p. (2001) The DELLA motif is essential for gibberellin-induced degradation of RGA. *Proceedings of the National Academy of Sciences*, 98, 14162-14167.

Dill, A. and Sun, T.-p. (2001) Synergistic de-repression of gibberellin signaling by removing *RGA* and *GAI* function in *Arabidopsis thaliana*. *Genetics*, 159, 777-785.

Dockx, J., Quaedvlieg, N., Keultjes, G., Kock, P., Weisbeek, P., and Smeekens, S. (1995) The homeobox gene *ATK1* of *Arabidopsis thaliana* is expressed in the shoot apex of the seedling and in flowers and inflorescence stems of mature plants. *Plant Molecular Biology*, 28, 723-737.

Dolan, L., Janmaat, K., Willemsen, V., Linstead, P., Poethig, S., Roberts, K., and Scheres, B. (1993) Cellular organisation of the *Arabidopsis thaliana* root.

Douglas, S.J., Chuck, G., Dengler, R.E., Pelecanda, L., and Riggs, C.D. (2002) *KNAT1* and *ERECTA* regulate inflorescence architecture in *Arabidopsis*. *The Plant Cell*, 14, 547-558.

Dubrovsy, J.G., Rost, T.L., Colon-Cardoma, A., and Doerner, P. (2001) Early primordium morphogenesis during lateral root initiation in *Arabidopsis thaliana*. *Planta*, 214, 30-36.

Edwards, K., Johnstone, A., and Thompson, C. (1991) A simple and rapid method for the preapration of plant genomic DNA for PCR analysis. *Nucleic acids research*, 19, 1349.

- Elliott, R.C., Smith, J.L., Lester, D.R., and Reid, J.B. (2001) Feedforward regulation of gibberellin deactivation in pea. *Journal of Plant Growth Regulation*, 20, 87-94.
- Elmayan, T. and Tepfer, M. (1995) Evaluation in tobacco of the organ specificity and strength of the rolD promoter, domain A of the 35S promoter and the 35S2 promoter. *Transgenic Research*, 4, 388-396.
- Eshed, Y., Baum, S., and Bowman, J. (1999) Distinct mechanisms promote polarity establishment in carpels of *Arabidopsis*. *Cell*, 99, 199-209.
- Felsenstein, J. (1989) PHYLIP: Phylogeny Inference Package (version 3.2). *Cladistics*, 5, 164-166.
- Frank, M., Rupp, H.-M., Prinsen, E., Motyka, V., Van Onckelen, H., and Schumling, T. (2000) Hormone autotrophic growth and differentiation identifies mutant lines of *Arabidopsis* with altered cytokinin and auxin content or signalling. *Plant Physiology*, 122, 721-729.
- Friml, J. (2003) Auxin transport - shaping the plant. *Current Opinion in Plant Biology*, 6, 7-12.
- Friml, J. and Palme, K. (2002) Polar auxin transport - old questions and new concepts. *Plant Molecular Biology*, 49, 273-284.
- Frugis, G., Giannino, D., Mele, G., Nicolodi, C., Chiappetta, A., Bitonti, M., Innocenti, A., Dewitte, W., Onckelen, H., and Mariotti, D. (2001) Overexpression of *KNAT1* in lettuce shifts leaf determinate growth to a shoot-like intermediate growth associated with an accumulation of isopentyl-type cytokinins. *Plant Physiology*, 126, 1370-1380.
- Fujisawa, Y., Kato, T., Ohki, S., Ishikawa, A., Kitano, H., Sasaki, T., Asahi, T., and Iwasaki, Y. (1999) Suppression of the heterotrimeric G protein causes abnormal morphology, including dwarfism, in rice. *Proceedings of the National Academy of Sciences*, 96, 7575-7580.
- Gaba, W., Wang, Z., Krishnamoorthy, T., Hinnebusch, A.G., and Sachs, M.S. (2001) Physical evidence for distinct mechanisms of translational control by upstream open reading frames. *EMBO J.*, 20, 6453-6463.
- Galweiler, L., Guan, C., Muller, A., Wisman, E., Mendgen, K., Yephremov, A., and Palme, K. (1998) Regulation of polar auxin transport by AtPIN1 in *Arabidopsis* vascular tissue. *Science*, 282, 2226-2230.
- Geballe, A.P. and Morris, D.R. (1994) Initiation codon within 5'-leaders of mRNAs as regulators of translation. *Trends in Biochemical Sciences*, 19, 159-164.
- Geldner, N., Anders, N., Wolters, H., Keicher, J., Kornberger, W., Muller, A., Delbarre, A., Ueda, T., Nakano, A., and Jürgens, G. (2003) The *Arabidopsis*

GNOM ARF-GEF mediates endosomal recycling, auxin transport and auxin dependent plant growth.

Geldner, N., Friml, J., Stierhof, Y.-D., Jürgens, G., and Palme, K. (2001) Auxin transport inhibitors block *PIN1* cycling and vesicle trafficking. *Nature*, 413, 425-428.

Gilroy, S. and Jones, R.L. (1994) Perception of gibberellin and abscisic acid at the external face of the plasma membrane of barley (*Hordeum vulgare* L.) aleurone protoplasts. *Plant Physiology*, 104, 1185-1192.

Gocal, G.F.W., Sheldon, C.C., Gubler, F., Moritz, T., Bagnall, D.B., MacMillan, C.P., Li, S.F., Parish, R.W., Dennis, E.S., Weigel, D., and King, R.W. (2001) *GAMYB*-like genes, flowering and gibberellin signaling in *Arabidopsis*. *Plant Physiology*, 127, 1682-1693.

Granger, C.L., Callos, J.D., and Medford, J.I. (1996) Isolation of an *Arabidopsis* homologue of the maize homeobox *Knotted-1* gene. *Plant Molecular Biology*, 31, 373-378.

Grant, S.G.N., Jessee, J., Bloom, F.R., and Hanahan, D. (1990) Differentiation plasmid rescue from transgenic mouse DNAs into *Escherichia coli* methylation-restriction mutants. *Proceedings of the National Academy of Sciences*, 87, 4645-4649.

Gray, W.M., del Pozo, J.C., Walker, L., Hobbie, L., Risseuw, E., Banks, T., Crosby, W., Yang, M., Ma, H., and Estelle, M. (1999) Identification of an SCF ubiquitin ligase complex required for auxin response in *Arabidopsis thaliana*. *Genes and Development*, 13, 1678-1691.

Gray, W.M. and Estelle, M. (2000) Function of the ubiquitin-proteasome pathway in auxin response. *Trends in Biochemical Sciences*, 25, 133-138.

Grebe, M., Friml, J., Swarup, R., Ljung, K., Sandberg, G., Terlou, M., Palme, K., Bennett, M., and Scheres, B. (2002) Cell polarity signalling in *Arabidopsis* involves a BFA-sensitive auxin influx pathway. *Current Biology*, 12, 329-334.

Guzman, P. and Ecker, J.R. (1990) Exploiting the triple response of *Arabidopsis* to identify ethylene-related mutants. *The Plant Cell*, 2, 513-523.

Hake, S. and Ori, N. (2002) Plant morphogenesis and KNOX genes. *Nature Genetics*, 31, 121-122.

Hamann, T., Benkova, E., Bäurle, I., Kientz, M., and Jürgens, G. (2003) The *Arabidopsis* *BODENLOS* gene encodes an auxin response protein inhibiting *MONOPTEROS*-mediated embryo patterning. *Genes and Development*, 16, 1610-1615.

Hamann, T., Mayer, U., and Jürgens, G. (1999) The auxin-insensitive *bodenlos* mutation affects primary root formation and apical-basal patterning in the *Arabidopsis* embryo. *Development*, 126, 1387-1395.

Hamant, O., Nogue, F., Belles-Boix, E., Jublot, D., Grandjean, O., Traas, J., and Pautot, V. (2002) The *KNAT2* homeodomain protein interacts with ethylene and cytokinin signalling. *Plant Physiology*, 130, 657-665.

Harberer, G. and Keiber, J.J. (2002) Cytokinins. New insights into a classic phytohormone. *Plant Physiology*, 128, 354-362.

Hardtke, C.S. and Berleth, T. (1998) The *Arabidopsis* gene *MONOPTEROS* encodes a transcription factor mediating embryo axis formation and vascular development. *The EMBO Journal*, 17, 1405-1411.

Haseloff, J., Siemering, K.R., Prasher, D.C., and Hodge, S. (1997) Removal of a cryptic intron and subcellular localisation of green fluorescent protein are required to mark transgenic *Arabidopsis* plants brightly. *Proceedings of the National Academy of Sciences*, 94, 2122-2127.

Hass, J., Park, E.C., and Seed, B. (1996) Codon usage limitation in the HIV-1 envelope glycoprotein. *Current Biology*, 6, 315-324.

Hay, A., Kaur, H., Phillips, A., Hedden, P., Hake, S., and Tsiantis, M. (2002) The gibberellin pathway medates *KNOTTED1*-type homeobox function in plants with different body plans. *Current Biology*, 12, 1557-1565.

Hebsgaard, S., Korning, P., Tolstrup, N., Engelbrecht, J., Rouze, P., and Brunak, S. (1996) Splice site prediction in *Arabidopsis thaliana* pre-mRNA by combining local and global sequence information. *Nucleic acids research*, 24, 3439-3452.

Hedden, P. and Phillips, A.L. (2000) Gibberellin metabolism: New insights revealed by the genes. *Trends in Plant Science*, 5, 523-530.

Higo, K., Ugawa, Y., Iwamoto, M., and Korenaga, T. (1999) Plant cis-acting regulatory DNA elements (PLACE) database. *Nucleic acids research*, 27, 297-300.

Hilhorst, H.W.M. and Karssen, C.M. (1988) Dual effect of light on the gibberellin- and nitrate-stimulated seed germination of *Sisymbrium officinale* and *Arabidopsis thaliana*. *Plant Physiology*, 86, 591-597.

Himanen, K., Boucheron, E., Vanneste, S., de Almeida Engler, J., Inze, D., and Beeckman, T. (2002) Auxin-mediated cell cycle activation during early lateral root initiation. *The Plant Cell*, 14, 2339-2351.

Hinnebusch, A.G. (1996). Translational control of *GCN4*: gene specific regulation by phosphorylation of eIF2. In *Translational control* (eds J.W.B.

Hershey, M.B. Mathews and N. Sonenberg), pp. 199-244. Cold Spring Harbour Laboratory, New York.

Hinnebusch, A.G. (1997) Translational control of yeast *GCN4*: a window on factors which control initiator-tRNA binding to the ribosome. *Journal of Biological Chemistry*, 272, 21661-21664.

Hooley, R., Beale, M.H., and Smith, S.J. (1991) Gibberellin perception at the plasma membrane of *Avena fatua* aleurone protoplasts. *Planta*, 183, 274-280.

Hua, J. and Meyerowitz, E.M. (1998) Ethylene responses are negatively regulated by a receptor gene family in *Arabidopsis thaliana*. *Cell*, 94, 261-271.

Imamura, A., Hanaki, N., Nakamura, A., Suzuki, T., Taniguchi, M., Kiba, T., Ueguchi, C., Sugiyama, T., and Mizuno, T. (1999) Complication and characterisation of *Arabidopsis thaliana* response regulators implicated in His-Asp phosphorelay signal transduction. *Plant and Cell Physiology*, 40, 733-742.

Inoue, T., Higuchi, M., Hashimoto, Y., Seki, M., Kobayashi, M., Kato, T., Tabata, S., Shinozaki, K., and Kakimoto, T. (2001) Identification of *CRE1* as a cytokinin receptor for *Arabidopsis*. *Nature*, 409, 1060-1063.

Itoh, H., Ueguchi-Tanaka, M., Sato, Y., Ashikari, M., and Matsuoka, M. (2002) The gibberellin signaling pathway is regulated by the appearance and disappearance of *SLENDER RICE1* in nuclei. *The Plant Cell*, 14, 57-70.

Iwakawa, H., Ueno, Y., Semiarti, E., Onouchi, H., Kojima, S., Tsukaya, H., Hasebe, M., Soma, T., Ikezaki, M., Machida, C., and Machida, Y. (2002) The *ASYMMETRIC LEAVES2* gene of *Arabidopsis thaliana*, required for formation of a symmetric flat leaf lamina, encodes a member of a novel family of proteins characterised by cysteine repeats and a leucine zipper. *Plant and Cell Physiology*, 43, 467-478.

Jackson, D., Veit, B., and Hake, S. (1996) Expression of Maize *KNOTTED1* related homeobox genes in the shoot apical meristem predicts patterns of morphogenesis in the vegetative shoot. *Development*, 120, 405-413.

Jacobsen, S.E., Binkowski, K.A., and Olszewski, N.E. (1996) *SPINDLY*, a tetratricopeptide repeat protein involved in gibberellin signal transduction in *Arabidopsis*. *Proceedings of the National Academy of Sciences*, 93, 9292-9296.

Jacobsen, S.E. and Olszewski, N.E. (1993) Mutations at the *SPINDLY* locus of *Arabidopsis* alter gibberellin signal transduction. *The Plant Cell*, 5, 887-896.

Jefferson, R.A. (1989) The GUS reporter gene system. *Nature*, 342, 837-838.

Jefferson, R.A., Kavanagh, T.A., and Bevan, M.W. (1987) GUS fusions: b-glucuronidase as a sensitive and versatile gene fusion marker in higher plants. *EMBO J.*, 6, 3901-3907.

Jerpseth, b. (1992) *Strategies*, 5, 2-3.

Joshi, C.P., Zhou, H., Huang, X., and Chiang, V.L. (1997) Context sequences of translation initiation codon in plants. *Plant Molecular Biology*, 35, 993-1001.

Jürgens, G., Mayer, U., Torres-Ruiz, R.A., Berleth, T., and Misera, S. (1991) Genetic analysis of pattern formation in the *Arabidopsis* embryo. *Development*, Supplement 1, 27-38.

Kakimoto, T. (1996) *CKI1*, a histidine kinase homologue implicated in cytokinin signal transduction. *Science*, 274, 982-985.

Kamiya, Y. and García-Martínez, J. (1999) Regulation of gibberellin biosynthesis by light. *Current Opinion in Plant Biology*, 2, 398-403.

Kerstetter, R., Vollbrecht, E., Lowe, B., Veit, B., Yamaguchi, J., and Hake, S. (1994) Sequence analysis and expression patterns divide the maize *knotted1*-like homeobox genes into two classes. *The Plant Cell*, 6, 1877-1887.

Kerstetter, R.A., Laudencia-Chingcuano, D., Smith, L., and Hake, S. (1997) Loss-of-function mutations in the maize homeobox gene, *knotted1*, are defective in shoot meristem maintenance. *Development*, 124, 3045-3054.

Kieber, J.J., Rothenberg, M., Roman, G., Feldmann, K.A., and Ecker, J.R. (1993) CTR1, a negative regulator of the ethylene response pathway in *Arabidopsis*, encodes a member of the Raf family of protein kinases. *Cell*, 72, 427-441.

Kim, J.Y., Yuan, Z., Cilia, M., Khalfan-Jagani, Z., and Jackson, D. (2002) Intercellular trafficking of a *KNOTTED1* green fluorescent protein in the leaf and shoot meristem of *Arabidopsis*. *Proceedings of the National Academy of Sciences*, 99, 4103-4108.

King, J.J., Stimart, D.P., Fisher, R.H., and Bleeker, A.B. (1995) A mutation altering auxin homeostasis and plant morphology in *Arabidopsis*. *The Plant Cell*, 7.

King, K., Moritz, T., and Harberd, N. (2001) Gibberellins are not required for normal stem growth in *Arabidopsis thaliana* in the absence of *GAI* and *RGA*. *Genetics*, 159, 767-776.

Klee, H.J. and Lanahan, M.B. (1995). Transgenic plants in hormone biology. In *Plant hormones: physiology, biochemistry and molecular biology* (ed P.J. Davies). Kluwer Academic Publishers, Dordrecht.

- Koncz, C., Chua, N., and Schell, J., eds. (1992) *Methods in Arabidopsis research*. World Scientific Publishing Co. Pte. Ltd.
- Kowalczyk, M. and Sandberg, G. (2001) Quantitative analysis of indole-3-acetic acid metabolites in *Arabidopsis*. *Plant Physiology*, 127, 1845-1853.
- Kozak, M. (1980) Evaluation of the "scanning model" for initiation of protein synthesis in eucaryotes. *Cell*, 22, 7-8.
- Kozak, M. (1981) Possible role of flanking nucleotides in recognition of the AUG initiator codon by eukaryotic ribosomes. *Nucleic acids research*, 9, 5233-62.
- Krysan, P.J., Young, J.C., and Sussman, M.R. (1999) T-DNA as an insertional mutagen in *Arabidopsis*. *The Plant Cell*, 11, 2283-2290.
- Kubo, N., Harada, K., Hirai, A., and Kadowaki, K.-I. (1999) A single nuclear transcript encoding mitochondrial RPS14 and SDHB of rice is processed by alternative splicing: Common use of the same mitochondrial targeting signal for different proteins. *Proceedings of the National Academy of Sciences*, 96, 9207-9211.
- Laskowski, M., Williams, M., Nusbaum, H., and Sussex, I. (1995) The development of lateral root meristems is a two-stage process. *Development*, 121, 3303-3310.
- Laufs, P., Dockx, J., Kronenberger, J., and Traas, J. (1998) *MGOUN1* and *MGOUN2*: two genes required for primordium initiation at the shoot apical and floral meristems in *Arabidopsis thaliana*. *Development*, 125, 1253-1260.
- Lewin, B. (1995) *Genes V* Oxford University Press.
- Leyser, O. (2001) Auxin signalling: the beginning, the middle and the end. *Current Opinion in Plant Biology*, 4, 382-386.
- Liang, X., Oono, Y., Shen, N.F., Kohler, C., Li, K., Scolnik, P.A., and Theologis, A. (1995) Characterisation of two members (*ACS1* and *ACS3*) of the 1-aminocyclopropane-1-carboxylate synthase gene family of *Arabidopsis thaliana*. *Gene*, 167, 17-24.
- Lincoln, C., Long, J., Yamaguchi, J., Serikawa, K., and Hake, S. (1994) A *knotted1*-like homeobox gene in *Arabidopsis* is expressed in the vegetative meristem and dramatically alters leaf morphology when overexpressed in transgenic plants. *The Plant Cell*, 6, 1859-1876.
- Lindsey, K. and Topping, J. (1998) On the relationship between the plant cell and the plant. *Seminars in Cell and Developmental Biology*, 9, 171-177.

Lindsey, K., Topping, J.F., da Rocha, P.S.C.F., Horne, K.L., Muskett, P.R., May, V.J., and Wei, W. (1996) Insertional mutagenesis to dissect embryonic development in *Arabidopsis* Bios Scientific Publishers.

Liu, C.-M., Xu, Z.-H., and Chua, N.-H. (1993) Auxin polar transport is essential for the establishment of bilateral symmetry during early plant embryogenesis. *The Plant Cell*, 5, 621-630.

Ljung, K., Bhalerao, R., and Sandberg, G. (2001) Sites and homeostatic control of auxin biosynthesis in *Arabidopsis* during vegetative growth. *The Plant Journal*, 28, 465-474.

Logeman, J., Schell, J., and Willmitzer, L. (1987) Improved method for the isolation of RNA from plant tissues. *Analytical Biochemistry*, 163, 16020.

Lohmer, S., Maddaloni, M., Motto, M., Salamini, F., and Thompson, R. (1993) Translation of the maize transcriptional activator *Opaque2* is initiated by upstream open reading frames present in the leader sequence. *The Plant Cell*, 5, 65-73.

Lohrmann, J. and Harter, K. (2002) Plant two-component signalling systems and the role of response regulators. *Plant Physiology*, 128, 363-369.

Lomax, T.L., Muday, G.K., and Rubery, P.H. (1995). Auxin transport. In *Plant hormones: physiology, biochemistry and molecular biology* (ed P.J. Davies). Kluwer Academic Press, Dordrecht.

Long, J.A., Moan, E.I., Medford, J.I., and Barton, M.K. (1996) A member of the *KNOTTED* class of homeodomain proteins encoded by the *STM* gene of *Arabidopsis*. *Nature*, 379, 66-69.

Lorkovic, Z.J., Wieczorek-Kirk, D.A., Lambermon, M.H.L., and Filipowicz, W. (2000) Pre-mRNA splicing in higher plants. *Trends in Plant Science*, 5, 160-167.

Lucas, W.J., Bouche-Pillon, S., Jackson, P.J., Nguyen, L., Baker, L., Ding, B., and Hake, S. (1995) Selective trafficking of *KNOTTED1* homeodomain protein and its mRNA through plasmodesmata. *Science*, 270, 1980-1983.

MacKnight, R., Bancroft, I., Page, T., Lister, C., Schmidt, R., Love, K., Westphal, L., Murphy, G., Sherson, S., Cobbett, C., and Dean, C. (1997) *FCA*, a gene controlling flowering time in *Arabidopsis*, encodes a protein containing RNA-binding domains. *Cell*, 89, 737-745.

Mähönen, A.P., Bonke, M., Kauppinen, L., Riikonen, M., Benfey, P.N., and Helariutta, Y. (2000) A novel two component hybrid molecule regulates vascular morphogenesis of the *Arabidopsis* root. *Genes and Development*, 14, 2938-2943.

- Malamy, J.E. and Benfey, P.N. (1997) Organisation and cell differentiation in lateral roots of *Arabidopsis thaliana*. *Development*, 124, 33-44.
- Mano, S., Hayashi, M., and Nishimura, M. (1999) Light regulates alternative splicing of hydroxypyruvate reductase in pumpkin. *The Plant Journal*, 17, 309-320.
- Marchant, A., Bhalerao, R., Casimiro, I., Eklöf, J., Casero, P., Bennett, M., and Sandberg, G. (2002) *AUX1* promoter lateral root formation by facilitating indole-3-acetic acid distribution between sink and source tissues in the *Arabidopsis* seedling. *The Plant Cell*, 14, 589-597.
- Marchant, A., Kargul, J., May, S.T., Muller, P., Delbarre, A., Perrot-Rechenmann, C., and Bennett, M. (1999) *AUX1* regulates root gravitropism in *Arabidopsis* by facilitating auxin uptake within root apical tissues. *EMBO J.*, 18, 2066-2073.
- Masucci, J.D., Rerie, W.G., Foreman, D.R., Zhang, M., Galway, M.E., Marks, M.D., and Schiefelbein, J. (1996) The homeobox gene *GLABRA2* is required for position-dependent cell differentiation in the root epidermis of *Arabidopsis thaliana*. *Development*, 122, 1253-1260.
- Mattsson, J., Sung, Z.R., and Berleth, T. (1999) Responses of plant vascular systems to auxin transport inhibition. *Development*, 126, 2979-2991.
- Matzke, M.A., Matzke, A.J.M., Pruss, G.J., and Vance, V.B. (2001) RNA-based silencing strategies in plants. *Current Opinion in Genetics and Development*, 11, 221-227.
- Matzke, M.A., Primig, M., Trnovsky, J., and Matzke, A.J.M. (1989) Reversible methylation and inactivation in of marker genes in sequentially transformed tobacco. *EMBO J.*, 8, 643-649.
- Mayer, U., Buttner, G., and Jürgens, G. (1993) Apical-basal pattern formation in the *Arabidopsis* embryo: studies on the role of the *gnom* gene. *Development*, 117, 149-162.
- McBride, K.E. and Summerfelt, K.R. (1990) Improved binary vectors for *Agrobacterium*-mediated plant transformation. *Plant Molecular Biology*, 14, 269-276.
- McElver, j., Tzafrir, I., Aux, G., Rogers, R., Ashby, C., Smith, K., Thomas, C., Schetter, A., Zhou, Q., Cushian, M.A., Tossberg, J., Nickle, T., Levin, J.Z., Law, M., Meinke, D., and Patton, D. (2001) Insertional mutagenesis of genes required for seed development in *Arabidopsis thaliana*. *Genetics*, 159, 1751-1763.
- McGaw, B.A. and Burch, L.R. (1995). Cytokinin biosynthesis and metabolism. In *Plant Hormones: physiology biochemistry and molecular biology* (ed P.J. Davies). Kluwer Academic Publishers, Dordrecht.

McKeon, T.A., Fernandez-Maculet, J.C., and Yang, S.-F. (1995). Biosynthesis and metabolism of ethylene. In *Plant hormones: Physiology, biochemistry and molecular biology* (ed P.J. Davies). Kluwer Academic Publishers, Dordrecht.

Meisel, L. and Lam, E. (1996) The conserved ELK-homeodomain of *KNOTTED-1* contains two regions that signal nuclear localisation. *Plant Molecular Biology*, 30, 1-14.

Meyerowitz, E.M. (1987) *Arabidopsis thaliana*. *Annual review of genetics*, 93-111.

Montgomery, J., Goldman, S., Deikman, J., Margossian, L., and Fischer, R.L. (1993) Identification of an ethylene-responsive region in the promoter of a fruit ripening gene. *Proceedings of the National Academy of Sciences*, 90, 5939-5943.

Mushegian, A.R. and Koonin, E.V. (1996) Sequence analysis of eukaryotic developmental proteins: ancient and novel domains. *Genetics*, 144, 817-828.

Nagasaki, H., Sakamoto, T., Sato, Y., and Matsuoka, M. (2001) Functional analysis of the conserved domains of a rice KNOX homeodomain protein, OSH15. *The Plant Cell*, 13, 2085-2098.

Napier, R.M., David, K.M., and Perrot-Rechenmann, C. (2002) A short history of auxin-binding proteins. *Plant Molecular Biology*, 49, 339-348.

Nelson, T. (1998) Polarity, vascularisation and auxin. *Trends in Plant Science*, 3, 245-246.

Normanly, J. and Bartel, B. (1999) Redundancy as a way of life - IAA metabolism. *Current Opinion in Plant Biology*, 2, 207-213.

Ogas, J., Cheng, J.-C., Sung, Z.R., and Somerville, C. (1997) Cellular differentiation regulated by gibberellin in the *Arabidopsis thaliana* *pickle* mutant. *Science*, 277, 91-94.

Ogas, J., Kaufmann, S., Henderson, J., and Somerville, C. (1999) *PICKLE* is a CHD3 chromatin-remodeling factor that regulates the transition from embryonic to vegetative development in *Arabidopsis*. *Proceedings of the National Academy of Sciences*, 96, 13839-13844.

Okada, K., Ueda, J., Komaki, M.K., Bell, C.J., and Shimura, Y. (1991) Requirement of the auxin polar transport system in early stages of *Arabidopsis* floral bud formation. *The Plant Cell*, 3, 677-684.

Olszewski, N., Sun, T.-P., and Gubler, F. (2003) Gibberellin Signaling: Biosynthesis, Catabolism, and Response Pathways. *The Plant Cell*, Supplement, S61-80.

Ori, N., Eshed, Y., Chuck, G., Bowman, J., and Hake, S. (2000) Mechanisms that control *knox* gene expression in the *Arabidopsis* shoot. *Development*, 127, 5523-5532.

Ori, N., Juarez, M.T., Jackson, D., Yamaguchi, J., Banowetz, G.M., and Hake, S. (1999) Leaf senescence is delayed in tobacco plants expressing the maize homeobox gene *KNOTTED1* under the control of a senescence-activated promoter. *The Plant Cell*, 11, 1073-1080.

Ouellet, F., Overvoorde, P.J., and Theologis, A. (2001) IAA17/AXR3: Biochemical insight into an auxin mutant phenotype. *The Plant Cell*, 13, 829-841.

Parry, P.G., Delbarre, A., Marchant, A., Swarup, R., Napier, R., Perrot-Rechenmann, C., and Bennett, M. (2001a) Novel auxin transport inhibitors phenocopy the auxin influx carrier mutation *aux1*. *The Plant Journal*, 25, 399-406.

Parry, P.G., Marchant, A., May, S.T., Swarup, R., Swarup, K., James, N., Graham, N., Allen, T., Martucci, T., Yemm, A., Napier, R., Manning, K., King, G., and Bennett, M.J. (2001b) Quick on the uptake: characterisation of a family of plant auxin influx carriers. *Journal of Plant Growth Regulation*, 20, 217-225.

Pautot, V., Dockx, J., Hamant, O., Kronenberger, J., Grandjean, O., Jublot, D., and Traas, J. (2001) *KNAT2*: evidence for a link between Knotted-like genes and carpel development. *The Plant Cell*, 13, 1719-1734.

Peng, J., Carol, P., Richards, D.E., King, K.E., Cowling, R.J., Murphy, G.P., and Harberd, N.P. (1997) The *Arabidopsis* *GAI* gene defines a signalling pathway that negatively regulates gibberellin responses. *Genes and Development*, 11, 3194-3205.

Perazza, D., Vachon, G., and Herzog, M. (1998) Gibberellins promote trichome formation by up-regulating *GLABROUS1* in *Arabidopsis*. *Plant Physiology*, 117, 375-383.

Pickett, F.B., Wilson, A.K., and Estelle, M. (1990) The *aux1* mutation of *Arabidopsis* confers both auxin and ethylene resistance. *Plant Physiology*, 94, 1462-1466.

Pietrzak, M., Suillito, R.D., Hohn, T., and Potrykus, I. (1986) Expression in plants of two bacterial antibiotic resistance genes after protoplast transformation with a new transformation vector. *Nucleic acids research*, 14, 5857-5868.

Prigge, M.J. and Wagner, D.R. (2001) The *Arabidopsis* *SERRATE* gene encodes a zinc-finger protein required for normal shoot development. *The Plant Cell*, 13, 1263-1279.

Rashotte, A.M., Brady, S.R., Reed, R.C., Ante, S.J., and Muday, G.K. (2000) Basipetal auxin transport is required for gravitropism in the roots of *Arabidopsis*. *Plant Physiology*, 122, 481-490.

Reed, J.W. (2001) Roles and activities of Aux/IAA proteins in *Arabidopsis*. *Trends in Plant Science*, 6, 420-425.

Reed, R.C., Brady, S.R., and Muday, G.K. (1998) Inhibition of auxin movement from the shoot into the root inhibits lateral root development in *Arabidopsis*. *Plant Physiology*, 118, 1369-1378.

Reid, J.B. and Howell, S.H. (1995). Hormone mutants and plant development. In *Plant Hormones: Physiology, Biochemistry and Molecular Biology* (ed P.J. Davies). Kluwer Academic Publishers, Dordrecht.

Reid, M.S. (1995). Ethylene in plant growth, development and senescence. In *Plant hormones: Physiology, biochemistry and molecular biology* (ed P.J. Davies). Kluwer Academic Publishers, Dordrecht.

Rogers, S., Wells, R., and Rechsteiner, M. (1986) Amino acid sequences common to rapidly degraded proteins: the PEST hypothesis. *Science*, 234, 364-368.

Ross, J.J. (1998) Effects of auxin transport inhibitors on gibberellins in pea. *Journal of Plant Growth Regulation*, 17, 141-146.

Ross, J.J., O'Neill, D.P., Smith, J.J., Kerckhoffs, L.H.J., and Elliott, R.C. (2000) Evidence that auxin promotes gibberellin A1 biosynthesis in pea. *Plant Journal*, 21, 547-552.

Ruegger, M., Dewey, E., Hobbie, L., Brown, D., Bernasconi, P., Turner, J., Muday, G.K., and Estelle, M. (1997) Reduced naphthylphthalamic acid binding in the *tir3* mutant of *Arabidopsis* is associated with a reduction in polar auxin transport and diverse morphological defects. *The Plant Cell*, 9, 745-757.

Rupp, H.-M., Frank, M., Werner, T., Strnad, M., and Schmulling, T. (1999) Increased steady state mRNA levels of the *STM* and *KNAT1* homeobox genes in cytokinin overproducing *Arabidopsis thaliana* indicate a role for cytokinins in the shoot apical meristem. *The Plant Journal*, 18, 557-563.

Sakamoto, T., Kamiya, N., Ueguchi-Tanaka, M., Iwahori, S., and Matsuoka, M. (2001) KNOX homeodomain protein directly suppresses the expression of a gibberellin biosynthetic gene in the tobacco shoot apical meristem. *Genes and Development*, 15, 581-590.

Sakamoto, T., Nishimura, M., Tamaoki, M., Kuba, M., Tanaka, H., Iwahori, S., and Matsuoka, M. (1999) The conserved KNOX domain mediates specificity of tobacco *KNOTTED1*-type homeodomain proteins. *The Plant Cell*, 11, 1419-1431.

- Saleh, M., Rambaldi, I., Yang, X.-J., and Featherstone, M.S. (2000) Cell signalling switches HOX-PBX complexes from repressors to activators of transcription mediated by histone deacetylases and histone acetyltransferases. *Molecular and Cellular Biology*, 20, 8623-8633.
- Sambrook, J., Fritsch, E.F., and Maniatis, T. (1989) *Molecular Cloning: A Laboratory Manual*, 2 edn. Coldspring Harbour Laboratory Press.
- Schaller, G.E. and Bleeker, A.B. (1995) Ethylene-binding sites generated in yeast expressing the *Arabidopsis ETR1* gene. *Science*, 270, 1809-1811.
- Scheres, B., Di Laurenzio, L., Willemsen, V., Hauser, M.-T., Janmaat, K., Weisbeek, P., and Benfey, P.N. (1995) Mutations affecting the radial organisation of the *Arabidopsis* root display specific defects throughout the embryonic axis. *Development*, 121, 53-62.
- Scheres, B., Wolkenfelt, H., Willemsen, W., Terlouw, M., Lawson, E., Dean, C., and Weisbeek, P. (1994) Embryonic origin of the *Arabidopsis* primary root and root meristem initials. *Development*, 120, 2457-2487.
- Schmulling, T. (2001) CREAM of cytokinin signalling: receptor identified. *Trends in Plant Science*, 6, 281-284.
- Semiarti, E., Ueno, Y., Tsukaya, H., Iwakawa, H., Machida, C., and Machida, Y. (2001) The *ASYMMETRIC LEAVES2* gene of *Arabidopsis thaliana* regulates formation of a symmetric lamina, establishment of venation and repression of meristem-related homeobox genes in leaves. *Development*, 128, 1771-1783.
- Serikawa, K., Martinez-Laborda, A., and Zambryski, P. (1996) Three *knotted1*-like homeobox genes in *Arabidopsis*. *Plant Molecular Biology*, 32, 673-683.
- Serikawa, K.A., Martinez-Laborda, A., Kim, H.-S., and Zambryski, P.C. (1997) Localisation of the expression of *KNAT3*, a class 2 *knotted1*-like gene. *The Plant Journal*, 11, 853-861.
- Serikawa, K.A. and Zambryski, P.C. (1997) Domain exchanges between *KNAT3* and *KNAT1* suggest specificity of the kn1-like homeodomain requires sequences outside of the third helix and the N-terminal arm of the homeodomain. *The Plant Journal*, 11, 836-869.
- Sieberer, T., Seifert, G.J., Hauser, M.T., Grisafi, P., Fink, G., and Luschnig, C. (2000) Post-transcriptional control of the *Arabidopsis* auxin efflux carrier *EIR1* requires *AXR1*. *Current Biology*, 10, 1595-1598.
- Sieburth, L.E. and Meyerowitz, E.M. (1997) Molecular dissection of the *AGMOUS* control region shows that *cis* elements for spatial regulation are located intragenically. *The Plant Cell*, 9, 355-365.

Silverstone, A.L., Ciampaglio, C.N., and Sun, T.-p. (1998) The *Arabidopsis* RGA gene encodes a transcriptional regulator repressing the gibberellin signal transduction pathway. *The Plant Cell*, 10, 155-169.

Silverstone, A.L., Jung, H.-S., Dill, A., Kawaide, H., Kamiya, Y., and Sun, T.-p. (2001) Repressing a repressor: Gibberellin induced rapid reduction of the RGA protein in *Arabidopsis*. *The Plant Cell*, 13, 1555-1566.

Silverstone, A.L., Mak, P.Y.A., Casamitjana Martínez, E., and Sun, T.-p. (1997) The new RGA locus encodes a negative regulator of gibberellin response in *Arabidopsis thaliana*. *Genetics*, 146, 1087-1099.

Smith, L.G., Hake, S., and Sylvester, A.W. (1996) The *tangled-1* mutation alters cell division orientations throughout maize leaf development without altering leaf shape. *Development*, 122, 481-489.

Solano, R., Stepanova, A., Chao, Q., and Ecker, J.R. (1998) Nuclear events in ethylene signalling: a transcriptional cascade mediated by ETHYLENE-INSENSITIVE 3 and ETHYLENE-RESPONSE FACTOR1. *Genes and Development*, 12, 3703-3714.

Souter, M., Topping, J.F., Pullen, M., Friml, J., Palme, K., Hackett, R., Grierson, D., and Lindsey, K. (2002) *hydra* mutants of *Arabidopsis* are defective in sterol profiles and auxin and ethylene signalling. *The Plant Cell*, 14, 1017-1031.

Sponsel, V.M. (1995). The Biosynthesis and Metabolism of Gibberellins in Higher Plants. In *Plant Hormones: Physiology, Biochemistry and Molecular Biology* (ed P.J. Davies). Kluwer Academic Press, Dordrecht.

Steinmann, T., Geldner, N., Grebe, M., Mangold, S., Jackson, C.L., Paris, S., Gälweiler, L., Palme, K., and Jürgens, G. (1999) Coordinated polar localisation of auxin efflux carrier *PIN1* by *GNOM* ARF GEF. *Science*, 286, 316-318.

Stepanova, A. and Ecker, J.R. (2000) Ethylene signalling: from mutants to molecules. *Current Opinion in Plant Biology*, 3, 353-360.

Stomp, A.-M. (1990). Use of X-Gluc for histochemical localisation of glucuronidase. In *Editorial Comments*, Vol. 16, pp. 5. United State Biochemical, Cleveland.

Sundaresan, V., Springer, P., Volpe, T., Haward, S., Jones, J.D., Dean, C., Ma, H., and Martienssen, R. (1995) Patterns of gene action in plant development revealed by enhancer trap and gene trap transposable elements. *Genes and Development*, 9, 1797-1810.

Suzuki, S., Miwa, K., Ishikawa, K., Yamada, H., Aiba, H., and Mizuno, T. (2001a) The *Arabidopsis* sensor His-kinase, AHK4, can respond to cytokinins. *Plant and Cell Physiology*, 42, 107-113.

Suzuki, T., Imamura, A., Ueguchi, C., and Mizuno, T. (1998) Histidine-containing phosphotransfer (HPT) signal transducers implicated in His-to-Asp phosphorelay in *Arabidopsis*. *Plant and Cell Physiology*, 39, 1258-1268.

Suzuki, T., Ishikawa, K., Yamashino, T., and Mizuno, T. (2002) An *Arabidopsis* Histidine-containing phosphotransfer (HPT) factor implicated in phosphorelay signal transduction: overexpression of *AHP2* in plants results in hypersensitiveness to cytokinin. *Plant and Cell Physiology*, 43, 123-129.

Suzuki, T., Sakurai, K., Ueguchi, C., and Mizuno, T. (2001b) Two types of putative nuclear factors that physically interact with histidine-containing phosphotransfer (Hpt) domains, signaling mediators in His-to-Asp phosphorelay in *Arabidopsis thaliana*. *Plant and Cell Physiology*, 42, 37-45.

Swain, S.M., Tseng, T.S., and Olszewski, N.E. (2001) Altered expression of *SPINDLY* affects gibberellin response and plant development. *Plant Physiology*, 126, 1174-1185.

Swarup, R., Friml, J., Marchant, A., Ljung, K., Sandberg, G., Palme, K., and Bennett, M. (2001) Localisation of the auxin permease AUX1 suggests two functionally distinct hormone transport pathways operate in the *Arabidopsis* root. *Genes and Development*, 15, 2648-2653.

Taiz, L. and Zeiger, E. (1991) *Plant Physiology* Benjamin-Cummings Publishing, New York.

Tamaoki, M., Tsugawa, H., Minami, E., Kayano, T., Yamamoto, N., Kano-Murakami, Y., and Matsuoka, M. (1995) Alternative RNA products from a rice homeobox gene. *The Plant Journal*, 7, 927-938.

Tanaka-Ueguchi, M., Itoh, H., Oyama, N., Koshioka, M., and Matsuoka, M. (1998) Over-expression of a tobacco homeobox gene, NTH15, decreases the expression of a gibberellin biosynthetic gene encoding GA 20-oxidase. *The Plant Journal*, 15, 391-400.

Telfer, A., Bollman, K.M., and Poethig, R.S. (1997) Phase change and the regulation of trichome distribution in *Arabidopsis thaliana*. *Development*, 124, 645-654.

The *Arabidopsis* Genome Initiative (2000) Analysis of the genome sequence of the flowering plant *Arabidopsis thaliana*. *Nature*, 408, 796-815.

Thomas, S.G., Phillips, A.L., and Hedden, P. (1999) Molecular cloning and functional expression of gibberellin 2-oxidases, multifunctional enzymes involved in gibberellin deactivation. *Proceedings of the National Academy of Sciences*, 96, 4698-4703.

Thornton, T.M., Swain, S.M., and Olszewski, N.E. (1999) Gibberellin signal transduction presents . . . the SPY who O-GlcNAc'd me. *Trends Plant Sci.* 4, 424-428. *Trends in Plant Science*, 4, 424-428.

Timmermans, M.C., Hudson, A., Becraft, P.W., and Nelson, T. (1999) *ROUGH SHEATH2*: a Myb protein that represses knox homeobox genes in maize lateral organ primordia. *Science*, 284, 151-153.

Tissier, A.F., Marillionnet, S., Klimyuk, V., Patel, K., Torres, M.A., Murphy, G., and Jones, J.D. (1999) Multiple independent defective *Suppressor-mutator* transposon insertions in *Arabidopsis*: a tool for functional genomics. *The Plant Cell*, 11, 1841-1852.

Tiwari, S.B., Wang, X.-J., Hagen, G., and Guilfoyle, T. (2001) AUX/IAA proteins are active repressors, and their stability and activity are modulated by auxin. *The Plant Cell*, 13.

Topping, J.F. and Lindsey, K. (1995) Insertional mutagenesis and promoter trapping in plants for the isolation of genes and the study of development. *Transgenic Research*, 4, 291-305.

Topping, J.F. and Lindsey, K. (1997) Promoter trap markers differentiate structural and positional components of polar development in *Arabidopsis*. *The Plant Cell*, 9, 1713-1725.

Topping, J.F., May, V.J., Muskett, P.R., and Lindsey, K. (1997) Mutations in the *HYDRA1* gene of *Arabidopsis* perturb cell shape and disrupt embryonic and seedling morphogenesis. *Development*, 124, 4415-4424.

Topping, J.F., Wei, W., and Lindsey, K. (1991) Functional tagging of regulatory elements in the plant genome. *Development*, 112, 1009-1019.

Torres-Ruiz, R.A. and Jürgens, G. (1994) Mutations in the *FASS* gene uncouple pattern formation and morphogenesis in *Arabidopsis* development. *Development*, 120, 2967-2978.

Tsiantis, M., Brown, M.I., Skibinski, G., and Langdale, J.A. (1999) Disruption of auxin transport is associated with aberrant leaf development in maize. *Plant Physiology*, 121, 1163-8.

Ueguchi-Tanaka, M., Fujisawa, Y., Kobayashi, M., Ashikari, M., Iwasaki, Y., Kitano, H., and Matsuoka, M. (2000) Rice dwarf mutant *d1*, which is defective in the  $\alpha$ -subunit of the heterotrimeric G protein, affects gibberellin signal transduction. *Proceedings of the National Academy of Sciences*, 97, 11638-11643.

Ullah, H., Chen, J.G., Young, J.C., Im, K.H., Sussman, M.R., and Jones, A.M. (2001) Modulation of cell proliferation by heterotrimeric G protein in *Arabidopsis*. *Science*, 292, 2066-2069.

- Ulmasov, T. (1999a) Activation and repression of transcription by auxin response factors. *Proceedings of the National Academy of Sciences*, 96, 5844-5849.
- Ulmasov, T. (1999b) Dimerisation and DNA binding of auxin response factors. *The Plant Journal*, 19, 309-319.
- Ulmasov, T., Lui, Z.B., Hagen, G., and Guilfoyle, T.J. (1995) Composite structure of auxin response elements. *The Plant Cell*, 7, 1611-1623.
- Ulmasov, T., Murfett, J., Hagen, G., and Guilfoyle, T.J. (1997) Aux/IAA proteins repress expression of reporter genes containing natural and highly active synthetic auxin response elements. *The Plant Cell*, 9, 1963-1971.
- Van Blokland, R., Van der Geest, N., Mol, N.J.M., and Kooter, J.M. (1994) Transgene-mediated suppression of chalcone synthase expression in *Petunia hybrida* results from an increase in RNA turnover. *Plant Journal*, 6, 861-877.
- van den Berg, C., Willemsen, V., Hage, W., Weisbeek, P., and Scheres, B. (1995) Cell fate in the *Arabidopsis* root meristem determined by directional signalling. *Nature*, 378, 62-65.
- van den Berg, C., Willemsen, V., Hendriks, G., Weisbeek, P., and Scheres, B. (1997) Short-range control of cell division in the *Arabidopsis* root meristem. *Nature*, 390, 287-289.
- Venglat, S.P., Dumonceaux, T., Rozwadowski, K., Parnell, L., Babic, V., Keller, W., Martienssen, R., Selvaraj, G., and Datla, R. (2002) The homeobox gene *BREVIPEDICELLUS* is a key regulator of inflorescence architecture in *Arabidopsis*. *Proceedings of the National Academy of Sciences*, 99, 4730-4735.
- Vollbrecht, E., Veit, B., Sinha, N., and Hake, S. (1991) The developmental gene *KNOTTED1* is a member of the maize homeobox gene family. *Nature*, 350, 241-243.
- Wang, X.Q., Ullah, H., Jones, A.M., and Assmann, S.M. (2001) G protein regulation of ion channels and abscisic acid signaling in *Arabidopsis* guard cells. *Science*, 292, 2070-2072.
- Waterhouse, P.M., Graham, M.W., and Wang, M.-B. (1998) Virus resistance and gene silencing in plants can be induced by simultaneous expression of sense and antisense RNA. *Proceedings of the National Academy of Sciences*, 95, 13959-13964.
- White, J.G. and Amos, W.B. (1987) Confocal microscopy comes of age. *Nature*, 328, 183-184.

- White, J.G., Amos, W.B., and Fordham, M. (1987) An evaluation of confocal versus conventional imaging of biological structures by fluorescence light microscopy. *Journal of Cell Biology*, 105, 41-48.
- Whitty, C.D. and Hall, R.H. (1974) A cytokinin oxidase in *Zea mays*. *Can. J. Biochem*, 52, 781-799.
- Williams, R.W. (1998) Plant homeobox genes: many functions stem from a common motif. *BioEssays*, 20, 280-282.
- Wolbang, C.M. and Ross, J.J. (2001) Auxin promotes gibberellin biosynthesis in decapitated tobacco plants. *Planta*, 214, 153-157.
- Worley, C.K., Zenser, N., Ramos, J., Rouse, D., Leyser, O., Theologis, A., and Callis, J. (2000) Degradation of Aux/IAA proteins is essential for normal auxin signalling. *The Plant Journal*, 21, 553-562.
- Xu, N., Hagen, G., and Guilfoyle, T. (1997) Multiple auxin response modules in the *SAUR 15A* promoter. *Plant Science*, 126, 193-201.
- Yamada, H., Suzuki, T., Terada, K., Takei, K., Ishikawa, K., Miwa, K., Yamashino, T., and Y, M. (2001) The *Arabidopsis* AHK4 histidine kinase is a cytokinin-binding receptor that transduces cytokinin signals across the membrane. *Plant and Cell Physiology*, 42, 1017-1023.
- Yamaguchi, S. and Kamiya, Y. (2000) Gibberellin biosynthesis: Its regulation by endogenous and environmental signals. *Plant Cell Physiology*, 41, 251-257.
- Yamaguchi, S., Kamiya, Y., and Sun, T.-p. (2001) Distinct cell specific expression patterns of early and late gibberellin biosynthetic genes during *Arabidopsis* seed germination. *Plant Journal*, 443-453.
- Yanish-Perron, C., Vieira, J., and Messing, J. (1985) Improved M13 phage cloning vectors and host strains: nucleotide sequences of M13mp18 and pUC19 vectors. *Gene*, 33, 103-119.
- Zupan, J.R. and Zambryski, P. (1995) Transfer of T-DNA from *Agrobacterium* to the plant cell. *Plant Physiology*, 107, 1041-1047.

## Appendix 1 Primer sequences

### Primers

<b>35s ENH For:</b>	AACATGGTGGAGCACGACAC
<b>35s P1:</b>	GGCCATCGTTGAAGATGCCT
<b>35S T1:</b>	CCTAATTCCCTTATCTGGGA
<b>35S T3' (EcoRI):</b>	GAATTCCTTGCATGCCTGCAGGTC
<b>35S T5' (Sacl):</b>	GAGCTCGTCCGCAAAAATCACCAGT
<b>3' UTR – 51:</b>	CCTTTGTGGCAAGCAAGGCAG
<b>3' UTR – 116:</b>	CATGTGAGTGAGTGTAAGATCC
<b>3' UTR-116 XbaI:</b>	TCTAGACATGTGAGTGAGTGTAAGATCC
<b>5' RACE 1:</b>	CCAAAGCAAGAAGAAGGAACAACC
<b>5' RACE 2:</b>	CCTCTAGTAAACACGCTATCTCC
<b>5' RACE 3:</b>	GCTTGAAGTAAGCGAGGATACG
<b>5' RACE 4:</b>	CGACGAGCTACTCTCAGTAGC
<b>5' UTR + 51:</b>	CTCGACCTATGAAGCCTGAAGCTCC
<b>ACT For:</b>	GATCCTAACCGAGCGTGGTTAC
<b>ACT Rev:</b>	GACCTGACTCGTCATACTCTGC
<b>Adaptor:</b>	CTTATACGGATATCCTGGCAATTCGGACTT
<b>ATKO For1:</b>	GTTAGGAAGGCCTTATCTCGACCTATGAA
<b>ATKO Rev1:</b>	AATTCATGTGTCGTCCATGCTTCACTCTT
<b>ATKO Rev4:</b>	TCCTCGGTAAAGAATGATCCACTAGAATC
<b>Cds For:</b>	GATCCCTCGAGCCTCTCTCTC
<b>Con-1A:</b>	CGTCTAGGTGGTTCAGTACCTGTTGAATG
<b>Con-1B:</b>	TTTATCGAAGAAACATGTCGTTGAACCAG
<b>CTR For:</b>	CGCCAAACTTCTTCAACAATGGC
<b>CTR Rev:</b>	GAAGTCCGTAAAGCAGACTCGTCC
<b>GFP-RE2-F:</b>	CCCGGGAGAAGACGGAGGAGTTCTTAC
<b>GFP-RE2-R:</b>	CCCGGGCTTCCTCGGTAAAGAATGATCC
<b>GFP-GW2-F:</b>	GAATTCTACAATTTCCATTCGGCCGGT
<b>GFP-GW2-R:</b>	GAATTCTCATTCCCTCGGTAAAGAATGA
<b>HD Exon 1:</b>	GTTTCCTTCCGATTACCAAGC
<b>HD Exon 2:</b>	GAGGAGATTCAACGGGAGAGTG
<b>HD Exon 3:</b>	AAGACCGTTTGACGAGGCAACG
<b>HD Exon 4:</b>	GAATTTGGTGTAACAGAGGATGG

<b>HD Exon 4 Rev:</b>	GCAACCTATCTTTGAGGTCC
<b>HD Exon 5:</b>	GATAGCATTAGCTGATGCAACG
<b>JL-202:</b>	CATTTTATAATAACGCTGCGGACATCTAC
<b>KDEL (SacI):</b>	GAGCTCTTACAGCTCGTCCTTCT
<b>LBb1:</b>	GCGTGGACCGCTTGCTGCACCT
<b>M13F:</b>	GTAAAACGACGGCCAG
<b>M13R:</b>	GAGGAAACAGCTATGAC
<b>MHF:</b>	AGGGAGCCTCAAGCAAGAGTTCA
<b>MHRT:</b>	GCTTCCAATGCCGTTTCCTCTGG
<b>Oligo d(T)<sub>15</sub> adaptor:</b>	
	CTTATACGGATATCCTGGCAATTCGGACTTTTTTTTTTTTTTTTTT(A/G/C)
<b>pENTR3CF:</b>	CGTTTCTACAAACTCTTCCTG
<b>pENTR3CR:</b>	CTTGTGCAATGTAACATCAGAG
<b>Probe F:</b>	GTTTCCTTCCGATTACCAAGC
<b>Probe R:</b>	CATCATTCTTCGGATCTCC
<b>Promoter For:</b>	CCCAAGCTTGTGGCGCATCGCATGGATAACC
<b>Promoter Rev:</b>	GCTCTAGAGAACTCCTCCGTCTTCTAAATCG
<b>Prom Seq For:</b>	CTTTTTGGTTAAAGTGCTCG
<b>Prom Seq Rev:</b>	CCACTAAACTACACGCAAC
<b>RNAiF1(BglII):</b>	AGATCTGATGGAATGTACAATTTCCATTCCG
<b>RNAiF1(SpeI):</b>	ACTAGTGATGGAATGTACAATTTCCATTCCG
<b>RNAiF2(BglII):</b>	AGATCTGTTCTTCTTCTTGCTTTGG
<b>RNAiF2(SpeI):</b>	ACTAGTGTTCTTCTTCTTGCTTTGG
<b>RNAipromF:</b>	CCATGGGTGGCGCATCGCATGGATAACC
<b>RNAipromR:</b>	CCCGGGGAACTCCTCCGTCTTCTAAATCG
<b>RNAiR1(SphI):</b>	GCATGCCCTTTTGGCAATCGATGTAAGC
<b>RNAiR1(XbaI):</b>	TCTAGACCTTTTGGCAATCGATGTAAGC
<b>RNAiR2(SphI):</b>	GCATGCGTCTTCACATCTTTGTCTCC
<b>RNAiR2(XbaI):</b>	TCTAGAGTCTTCACATCTTTGTCTCC
<b>SALK_047931 For:</b>	CAACTTCTTTTGGTCAGATG
<b>SALK_047931 Rev1:</b>	AGACTCCAACAAGAACATGCAG
<b>SALK_047931 Rev2:</b>	CTTTACAGCTAACTCTTTCAGC
<b>TEVL (SmaI):</b>	CCCGGGCTCAACACAACATATACAA

### **Nested degenerate homeobox primers**

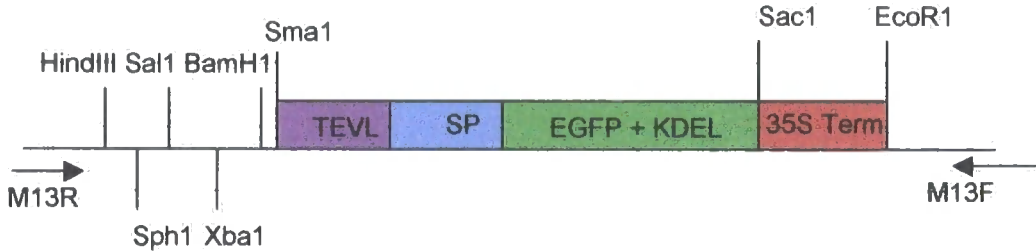
- KN1 1:** TGGTGGI(A/G)III(T/G)CA(T/C)(T/A)(C/A)IAA(A/G)  
**KN1 2:** (A/T)IAACA(A/G)AT(C/A)ACAATTGG  
**BEL 1:** GTIII(G/A)TICTI(C/A)GIICTTGG  
**BEL 2:** GIA(G/A)(C/T)CAGGTITCAAA(C/T)TGG  
**PHD 1:** TTT(G/C)(C/A)AGAGA(C/A)T(C/G)A(A/G)(T/C)(T/A)TCC  
**PHD 2:** GA(G/A)GGA(G/T)(A/C)G(C/T)(C/T)T(A/T)GC(C/A)AAAGAGC  
**GL2 1:** TT(T/C)AAIGA(G/A)(T/A)ITCCICATCC  
**GL2 2:** (C/A)CI(C/A)IICAAGTCAAGTT(T/C)TGG  
**ZIP I 1:** AICA(G/A)(G/A)TIA(G/A)IICI(T/C)TIGAG  
**ZIP I 2:** CA(A/G)(G/A)TIGCI(G/A)TITGGTTTTTC  
**ZIP II 1:** CIAAA(G/C)AICAA(G/T)CTI(T/C)IITTC  
**ZIP II 2:** AAAGAICA(C/T)A(G/A)(T/C)ACICT(C/T)AATCC  
**ZIP III 1:** GAACAAGT(T/G)GAAGCTCTIGAGAG  
**ZIP III 2:** CAGCTIATICGIGA(G/A)TGTCC

## Appendix 2

### pEGFPper vector

pUC19 based (high copy number). Ampicillin resistant

size ~3.87 kb

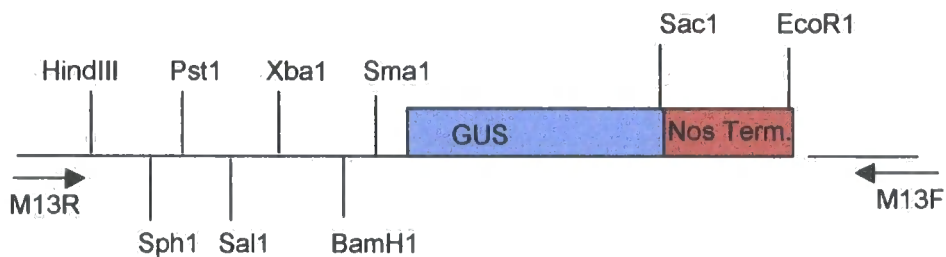


- TEVL is a translational enhancer from etch potivirus
- SP is the signal peptide from chitinase which allows the GFP to enter the ER
- EGFP encodes Enhanced Green Fluorescent Protein and includes a KDEL sequence at the 3' end for ER retention
- CaMV 35S terminator

### pGUS-1 vector

pUC19 based (high copy number). Ampicillin resistant

size ~3.87 kb



- GUS encodes the  $\beta$ -glucuronidase gene from *E. coli*
- Nos terminator

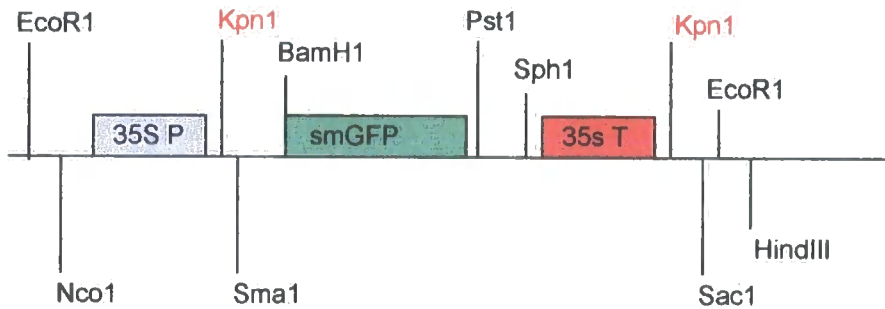
## Appendix 2

### p35S-GFP

pDH51 based vector (Ampicillin resistant), high copy number

Size is ~ 4.14 kb

Allows production of protein::GFP fusions with the GFP at the C terminal of the protein of interest (which is cloned in at the Sma1 and/or BamH1 sites).

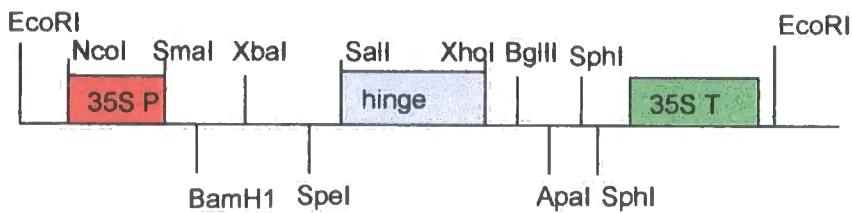


- CaMV 35S promoter
- smGFP - no ATG but has a stop codon
- CaMV 35S terminator

### pRNAi

pDH51 based vector (Ampicillin resistant), high copy number

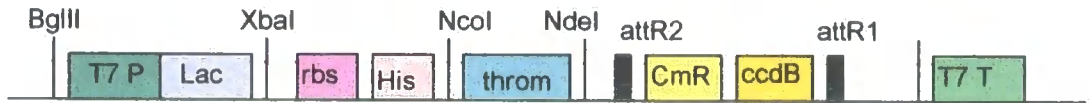
Size is ~ 4.14 kb



- CaMV 35S promoter
- Ampicillin-based hinge region
- CaMV 35S terminator

### pGAT4 cloning site

pET17b backbone with BglIII/XhoI fragment from pET28a(+). NdeI to HindIII site then replaced with Gateway™ cassette. pGAT4 carries an ampicillin resistance gene. Vector approx. 4.4 kb



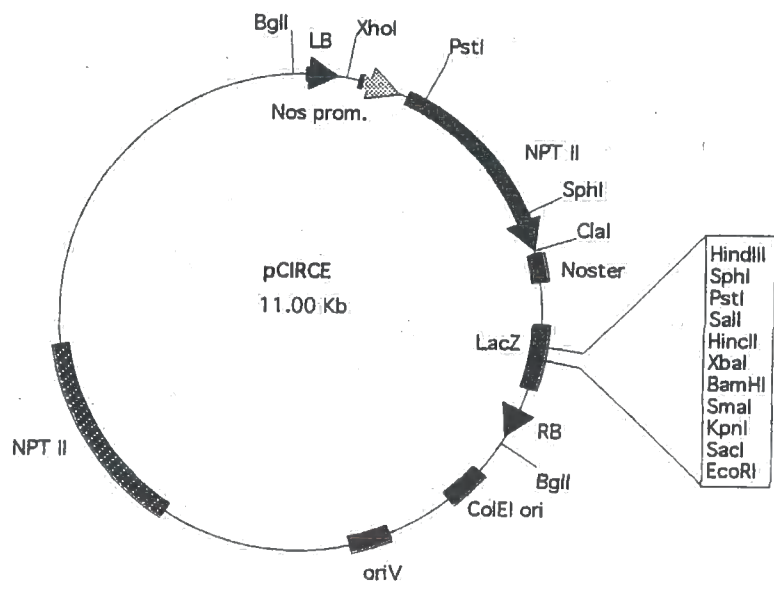
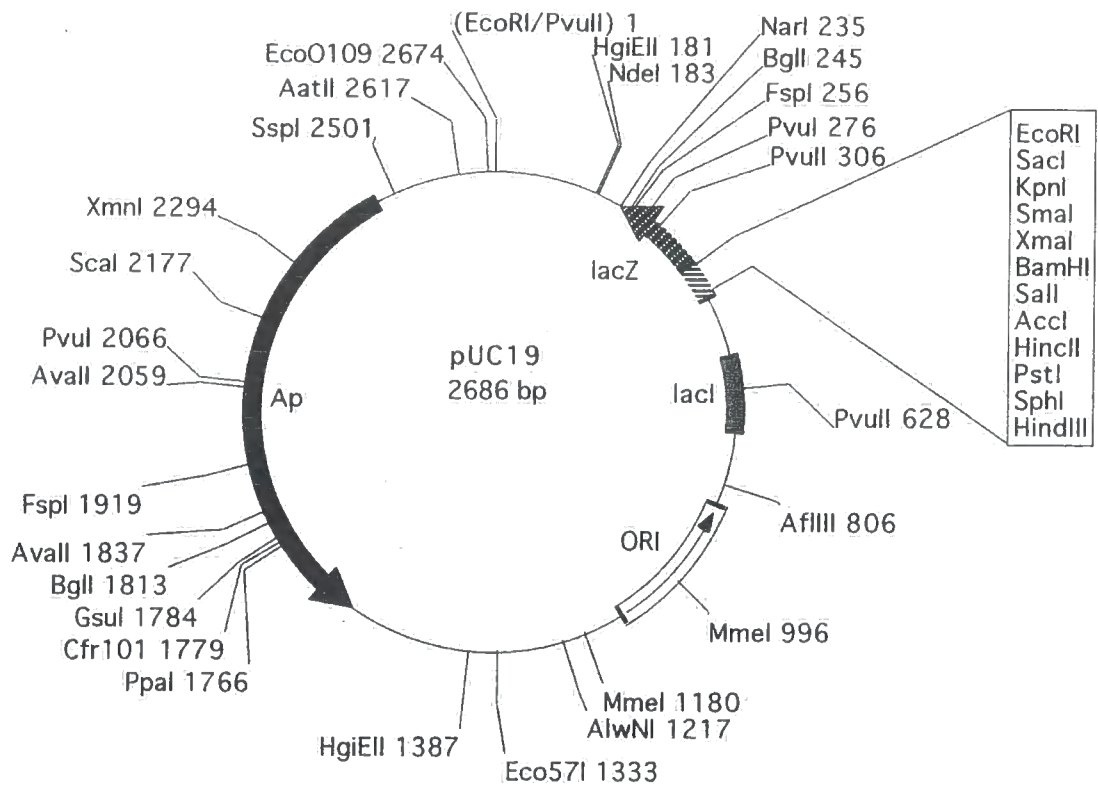
- T7 promoter
- LacZ
- Ribosome binding site
- His Tag
- Thrombin
- Chloramphenicol resistance gene
- ccdB cytotoxic gene
- T7 Terminator

### pBinAGRFAN T-DNA

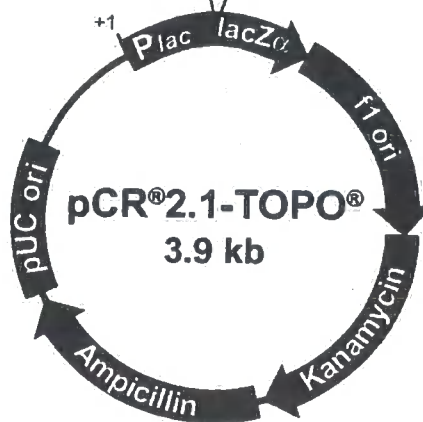
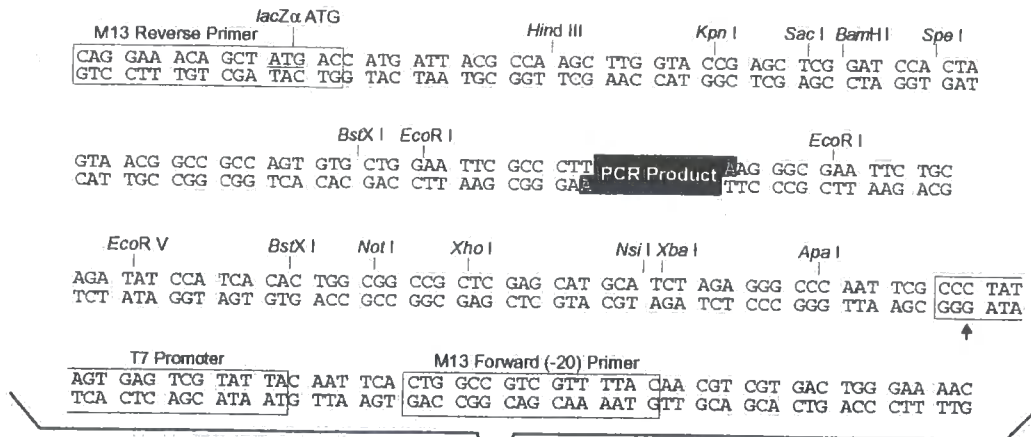
Gateway™ compatible binary vector based on pBIN19. The selectable marker is kanamycin. Vector approx 12 kb



- nptII gene confers kanamycin resistance to plants
- CaMV 35S promoter
- AlcR gene coding sequence
- Nos terminator
- Chloramphenicol resistance gene
- Cytotoxic ccdB gene
- smGFP coding sequence
- AlcA promoter

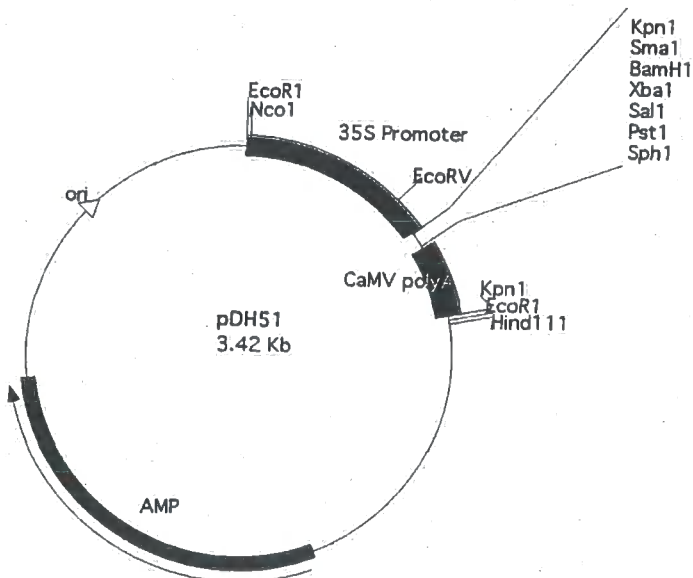


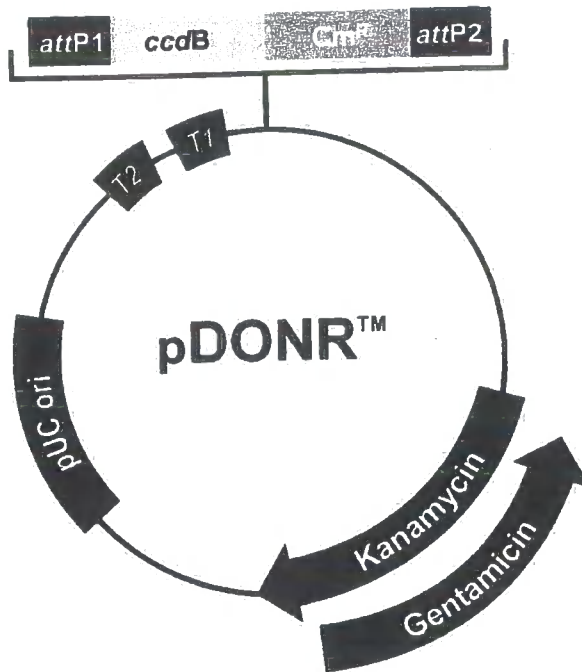
## Appendix 2 Plasmid maps



### Comments for pCR®2.1-TOPO® 3931 nucleotides

- LacZα fragment: bases 1-547
- M13 reverse priming site: bases 205-221
- Multiple cloning site: bases 234-357
- T7 promoter/priming site: bases 364-383
- M13 Forward (-20) priming site: bases 391-406
- f1 origin: bases 548-985
- Kanamycin resistance ORF: bases 1319-2113
- Ampicillin resistance ORF: bases 2131-2991
- pUC origin: bases 3136-3809





**Comments for:**

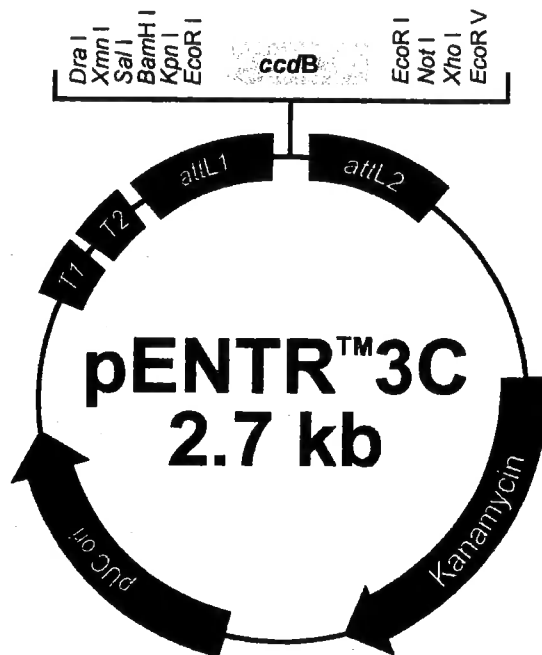
*rrnB* T2 transcription termination sequence (c):  
*rrnB* T1 transcription termination sequence (c):  
 Recommended forward priming site:  
*attP1*:  
*ccdB* gene (c):  
 Chloramphenicol resistance gene (c):  
*attP2* (c):  
 Recommended reverse priming site:  
 Kanamycin resistance gene:  
 Gentamicin resistance gene (c):  
 pUC origin:  
 (c) = complementary strand

**pDONR™201**  
 4470 nucleotides

**pDONR™207**  
 5584 nucleotides

73-100  
 232-275  
 300-324  
 332-563  
 959-1264  
 1606-2265  
 2513-2744  
 2769-2792  
 2868-3677  
 —  
 3794-4467

73-100  
 232-275  
 300-324  
 332-563  
 959-1264  
 1606-2265  
 2512-2743  
 2768-2791  
 —  
 3527-4060  
 4908-5581



**Comments for pENTR™3C**  
**2723 nucleotides**

*rrnB* T1 transcription termination sequence: bases 106-149

*rrnB* T2 transcription termination sequence: bases 281-308

*attL1*: bases 358-457 (complementary strand)

*ccdB* gene: bases 618-923

*attL2*: bases 952-1051

Kanamycin resistance gene: bases 1174-1983

pUC origin: bases 2047-2720

### Appendix 3 Kanamycin segregation data for transgenic lines

**Table 1 T2 pKNAT6::GUS lines**

Line	Kan <sup>R</sup>	Kan <sup>S</sup>	Line	Kan <sup>R</sup>	Kan <sup>S</sup>
1	449	4	9	221	81
2	410	135	10	158	19
3	174	63	11	169	41
4	311	112	12	197	60
5	165	43	13	167	48
6	395	150	14	159	14
7	314	84	15	151	8
8	218	75	-	-	-

**Table 2 T2 pKNAT6::GFP lines**

Line	Kan <sup>R</sup>	Kan <sup>S</sup>	Line	Kan <sup>R</sup>	Kan <sup>S</sup>
1	229	8	9	80	33
2	51	12	10	70	29
3	158	45	11	107	40
4	245	85	12	169	55
5	136	4	13	162	51
6	105	32	14	195	53
7	172	51	15	196	79
8	67	26	16	130	45

**Table 3 T2 35S::KNAT6 original splice sense (S) lines**

Line	Kan <sup>R</sup>	Kan <sup>S</sup>	Line	Kan <sup>R</sup>	Kan <sup>S</sup>
S1	129	16	S16	83	1
S2	195	47	S17	139	5
S3	219	7	S18	113	58
S4	123	28	S19	103	25
S5	196	11	S20	72	23
S6	342	122	S21	114	35
S7	163	57	S22	184	0
S8	237	19	S23	129	8
S9	145	52	S24	52	17
S10	245	83	S25	104	7
S11	171	15	S26	73	1
S12	162	43	S27	176	9
S13	164	66	S28	127	32
S14	170	5	S29	61	1
S15	263	0	S30	200	62

**Table 4 T2 35S::KNAT6 alternative splice sense (asS) lines**

Line	Kan <sup>R</sup>	Kan <sup>S</sup>	Line	Kan <sup>R</sup>	Kan <sup>S</sup>
asS6	154	43	asS22	184	5
asS7	134	47	asS23	224	71
asS8	90	11	asS24	135	172
asS9	263	79	asS25	343	12
asS11	93	30	asS26	184	4
asS12	197	44	asS27	246	80
asS13	237	4	asS28	261	5
asS14	283	18	asS29	229	84
asS15	194	52	asS30	303	102
asS16	379	23	asS31	229	63
asS17	186	59	asS32	255	6
asS18	2	172	asS33	199	73
asS19	266	16	asS34	235	72
asS20	360	46	asS35	156	60
asS21	149	41	asS36	245	83

**Table 5 T2 35S::KNAT6 original splice antisense (AS) lines**

Line	Kan <sup>R</sup>	Kan <sup>S</sup>	Line	Kan <sup>R</sup>	Kan <sup>S</sup>
AS1	128	11	AS16	102	47
AS2	217	30	AS17	74	37
AS3	198	70	AS18	195	75
AS4	333	101	AS19	219	68
AS5	216	62	AS20	95	31
AS6	286	80	AS21	176	4
AS7	152	10	AS22	145	47
AS8	222	85	AS23	76	1
AS9	406	24	AS24	105	49
AS10	249	22	AS25	110	3
AS11	136	7	AS26	182	68
AS12	56	16	AS27	203	34
AS13	197	61	AS28	201	41
AS14	121	13	AS29	210	76
AS15	248	1	AS30	49	22

**Table 6 T2 RNAi lines**

Line	Kan <sup>R</sup>	Kan <sup>S</sup>	Line	Kan <sup>R</sup>	Kan <sup>S</sup>
RNAi1 1	161	8	RNAi1+P 1	143	46
RNAi1 2	135	3	RNAi1+P 2	195	66
RNAi1 3	292	100	RNAi1+P 3	116	20
RNAi1 4	147	31	RNAi1+P 4	131	59
RNAi1 5	250	6	RNAi1+P 5	270	119
RNAi1 6	285	84	RNAi1+P 6	177	54
RNAi1 7	217	5	RNAi1+P 7	160	55
RNAi1 8	126	76	RNAi1+P 8	197	64
RNAi1 9	273	56	RNAi1+P 9	107	43
RNAi1 10	220	3	RNAi1+P 10	157	16
RNAi1 11	122	22	RNAi1+P 11	140	46
RNAi1 12	160	38	RNAi1+P 12	183	13
RNAi1 13	324	28	RNAi1+P 13	81	79
RNAi1 14	154	64	RNAi1+P 14	211	11
RNAi1 15	88	67	RNAi1+P 15	224	13
RNAi2 1	194	71	RNAi2+P 1	129	45
RNAi2 2	213	81	RNAi2+P 2	106	34
RNAi2 3	258	42	RNAi2+P 3	238	70
RNAi2 4	241	83	RNAi2+P 4	235	98
RNAi2 5	202	51	RNAi2+P 5	294	82
RNAi2 6	314	22	RNAi2+P 6	143	47
RNAi2 7	152	42	RNAi2+P 7	95	13
RNAi2 8	217	7	RNAi2+P 8	98	37
RNAi2 9	217	87	RNAi2+P 9	234	14
RNAi2 10	0	100%	RNAi2+P 10	255	1
RNAi2 11	195	54	RNAi2+P 11	185	43
RNAi2 12	181	51	RNAi2+P 12	351	118
RNAi2 13	164	51	RNAi2+P 13	250	64
RNAi2 14	150	54	RNAi2+P 14	77	9
RNAi2 15	253	75	RNAi2+P 15	220	52

## Appendix 4 Root measurements

### Sense S T3 Homozygotes – main root length (mm)

DAG	Length	S15.6	Col-0	S10.4	S2d	S9c	S7a	S14b
3	Mean	5.75	5.33	5.92	6.82	5.92	3.92	5.92
	Std. dev.	1.36	1.44	1.24	1.47	1.00	1.00	1.31
6	Mean	28.50	26.25	26.58	29.09	25.83	12.00	27.92
	Std. dev.	3.40	4.22	2.91	4.85	6.00	3.67	2.50
9	Mean	58.33	57.17	56.67	60.27	52.75	17.67	59.33
	Std. dev.	9.24	5.24	8.34	9.88	12.37	5.84	4.03
12	Mean	83.00	89.33	83.33	90.36	78.50	24.25	88.92
	Std. dev.	15.65	5.37	14.36	11.57	20.58	7.83	6.57

### Sense S T3 Homozygotes – root tip to last lateral to emerge (mm)

DAG	Tip to 1 <sup>st</sup> lateral	S15.6	Col-0	S10.4	S2d	S9c	S7a	S14b
6	Mean	20.58	19.23	19.67	22.50	20.30	10.00	20.00
	Std. dev.	3.12	3.11	3.28	5.11	5.93	3.10	2.83
9	Mean	22.17	24.75	22.67	25.27	20.33	7.67	24.25
	Std. dev.	2.41	2.22	4.14	4.05	5.02	3.03	3.08
12	Mean	21.42	24.75	21.08	20.18	20.67	9.75	22.33
	Std. dev.	3.73	3.36	6.22	3.74	6.41	10.53	5.02

**Sense S T3 Homozygotes – number of lateral roots**

DAG	No. of laterals	S15.6	Col-0	S10.4	S2d	S9c	S7a	S14b
6	Mean	3.08	3.08	1.42	1.36	1.42	0.75	2.00
	Std. dev.	1.00	1.56	1.08	1.21	0.90	0.87	1.65
9	Mean	19.58	17.92	15.08	17.27	14.58	6.67	17.83
	Std. dev.	3.58	2.19	6.60	6.62	4.14	2.93	5.24
12	Mean	35.92	35.67	32.67	37.64	30.75	14.08	36.33
	Std. dev.	7.93	3.94	7.05	7.78	9.19	5.71	6.04

**Sense S T3 Homozygotes – number of anchor roots**

DAG	No. of anchors	S15.6	Col-0	S10.4	S2d	S9c	S7a	S14b
6	Mean	0.08	0.17	0.17	0.73	0.08	0.08	0.17
9	Mean	0.83	0.83	0.42	1.00	0.33	0.17	0.83
12	Mean	1.75	1.33	1.17	1.36	0.75	0.25	1.25

**RNAi 1 – main root length (mm)**

DAG	Length	Col	RNAi 1D	RNAi 2B	RNAi 3D	RNAi 4C	RNAi 5B	RNAi 6D	RNAi 7D	RNAi 9B	RNAi 11C	RNAi 12B
3	Mean	3.5	4.8	4.3	4.5	4.8	4.1	6.3	4.9	4.7	4.6	4.6
	Std. dev.	0.85	1.14	1.06	0.97	1.23	1.10	1.25	0.99	0.95	1.51	1.17
6	Mean	19.4	21.5	25.9	23.6	25.1	26	23.2	24.6	24.7	23.3	26.7
	Std. dev.	1.51	6.02	3.28	5.36	4.79	3.62	5.57	3.63	4.06	4.95	2.71
9	Mean	42.9	41.9	55.2	48.9	54.5	54.4	48.2	51.4	56.3	42.7	52.8
	Std. dev.	4.28	12.16	5.41	12.49	12.15	10.63	11.18	6.93	9.97	14.00	6.70
12	Mean	72.1	58	85.5	77.9	81.8	87	71.4	78.7	87.6	65.6	76.8
	Std. dev.	11.18	18.21	7.59	21.42	20.51	18.51	23.68	12.91	18.02	24.03	16.31

**RNAi 2 – main root length (mm)**

DAG	Length	Col	RNAi 1A	RNAi 2A	RNAi 4C	RNAi 5A	RNAi 6C	RNAi 7A	RNAi 8B	RNAi 9A	RNAi 11D	RNAi 13D
3	Mean	3.5	4.3	4.1	6.3	5.4	4.8	3.7	4.7	4	4.1	4.6
	Std. dev.	0.85	0.82	0.88	1.06	1.51	1.48	0.82	1.16	0.94	0.74	0.84
6	Mean	19.4	21.7	19.5	27.4	25.8	24.7	22	25.6	24.2	21.1	25
	Std. dev.	1.51	5.33	4.65	6.15	2.82	4.79	4.74	5.48	4.69	5.22	5.83
9	Mean	42.9	46.5	39.6	57.1	50.6	52.9	45.5	51.1	49.7	42.5	48.7
	Std. dev.	4.28	12.42	10.35	11.10	6.06	11.50	8.82	9.23	10.32	9.92	11.98
12	Mean	72.1	74	60.7	83.3	73.7	81.3	70.7	77	78.6	65.5	76.1
	Std. dev.	11.18	21.45	18.37	17.71	13.38	15.87	16.00	16.22	18.46	19.08	16.93

**RNAi 1+P – main root length (mm)**

DAG	Length	Col	RNAi 1A	RNAi 2A	RNAi 4C	RNAi 5A	RNAi 6C	RNAi 7A	RNAi 8B	RNAi 9A	RNAi 11D	RNAi 13D
3	Mean	3.5	3.8	3.9	4.1	4	4.2	4.2	6.3	4.5	4.8	4.8
	Std. dev.	0.85	0.92	1.10	0.99	1.25	0.92	0.92	1.42	1.18	0.92	0.92
6	Mean	19.4	21.9	21.6	23.1	22.2	21.3	22.3	26.4	23.5	24	24.3
	Std. dev.	1.51	3.48	2.46	3.03	2.90	2.16	2.83	4.48	2.92	1.89	3.40
9	Mean	42.9	46	47.1	47.1	49.5	45.1	45.6	51.8	49.4	51.5	55.4
	Std. dev.	4.28	8.21	6.21	8.62	5.36	6.14	6.93	8.01	6.88	6.69	4.22
12	Mean	72.1	74.9	75	76.3	78.4	71.8	73.6	75.7	77.4	80.8	84.8
	Std. dev.	11.18	17.98	12.23	16.59	12.01	11.83	15.51	17.01	14.77	14.60	14.67

**RNAi 2+P – main root length (mm)**

DAG	Length	Col	RNAi 1A	RNAi 2A	RNAi 4C	RNAi 5A	RNAi 6C	RNAi 7A	RNAi 8B	RNAi 9A	RNAi 11D	RNAi 13D
3	Mean	3.5	4.6	4.3	4.8	5	4.2	4.2	5	4.3	4.2	5.1
	Std. dev.	0.85	0.97	0.48	1.40	1.33	0.63	0.79	0.47	0.82	0.63	0.99
6	Mean	19.4	23.3	20.6	23.2	23.1	20.5	22.1	24.5	21.6	21.9	24.9
	Std. dev.	1.51	3.50	1.58	3.77	3.14	2.12	2.69	3.37	1.84	2.51	4.04
9	Mean	42.9	49.2	45.1	50.5	45.8	43.4	47.2	50	48.9	47.8	53.5
	Std. dev.	4.28	8.12	2.96	9.83	6.05	5.68	4.87	7.79	4.01	5.79	6.04
12	Mean	72.1	80	73.4	80.5	72	72.7	79.8	76.8	82	67.8	89.5
	Std. dev.	11.18	16.10	11.48	17.27	15.16	14.84	9.48	17.84	6.29	14.81	12.79

**RNAi 1 – root tip to last lateral to emerge (mm)**

DAG	Tip to 1 <sup>st</sup> Lateral	Col	RNAi 1A	RNAi 2A	RNAi 4C	RNAi 5A	RNAi 6C	RNAi 7A	RNAi 8B	RNAi 9A	RNAi 11D	RNAi 13D
6	Mean	15.83	17.38	19.90	17.67	18.80	20.30	17.50	19.33	18.80	17.44	18.10
	Std. dev.	2.14	3.07	2.60	3.16	4.92	4.00	4.60	7.39	3.49	5.05	1.66
9	Mean	18.50	20.56	23.90	22.00	23.90	23.50	19.10	22.80	24.90	17.50	21.30
	Std. dev.	2.46	3.05	2.38	5.19	5.93	6.36	3.73	2.53	3.45	6.13	3.02
12	Mean	24.50	16.78	24.40	23.10	21.90	23.40	20.40	23.80	24.70	17.70	22.00
	Std. dev.	3.34	3.27	3.66	7.06	6.85	5.17	7.95	4.44	6.06	7.99	4.85

**RNAi 2 – root tip to last lateral to emerge (mm)**

DAG	Tip to 1 <sup>st</sup> Lateral	Col	RNAi 1A	RNAi 2A	RNAi 4C	RNAi 5A	RNAi 6C	RNAi 7A	RNAi 8B	RNAi 9A	RNAi 11D	RNAi 13D
6	Mean	15.83	16.11	14.43	19.40	18.50	18.90	16.38	17.56	16.44	16.80	17.30
	Std. dev.	2.14	4.83	5.35	4.17	3.21	4.46	2.92	4.28	3.09	3.12	3.86
9	Mean	18.50	21.20	16.90	22.90	19.80	22.00	20.80	23.40	21.60	18.70	21.20
	Std. dev.	2.46	3.94	4.53	5.24	3.85	5.44	3.26	3.57	3.86	3.65	3.85
12	Mean	24.50	22.30	17.50	19.90	20.00	20.70	21.50	21.40	22.20	20.00	21.00
	Std. dev.	3.34	7.85	5.38	4.31	5.56	6.18	5.64	5.21	6.73	6.77	4.24

**RNAi 1+P – root tip to last lateral to emerge (mm)**

DAG	Tip to 1 <sup>st</sup> Lateral	Col	RNAi 1A	RNAi 2A	RNAi 4C	RNAi 5A	RNAi 6C	RNAi 7A	RNAi 8B	RNAi 9A	RNAi 11D	RNAi 13D
6	Mean	15.83	15.22	16.8	16	15.75	15.44	16.2	19.4	16.6	16.3	16
	Std. dev.	2.14	1.79	2.10	3.23	1.16	2.35	2.35	2.12	2.59	1.83	1.41
9	Mean	18.5	19.6	20.9	20.3	21.7	20.1	20.3	21.5	21.3	22.6	23.5
	Std. dev.	2.46	3.47	3.07	3.56	3.92	3.41	2.21	5.15	3.16	4.65	3.87
12	Mean	24.5	23.6	24.9	24.5	23.6	23.8	22.1	22.6	24.8	23.4	25.9
	Std. dev.	3.34	6.67	6.84	6.98	6.06	4.59	5.92	5.68	6.48	6.70	5.28

**RNAi 2+P – root tip to last lateral to emerge (mm)**

DAG	Tip to 1 <sup>st</sup> Lateral	Col	RNAi 1A	RNAi 2A	RNAi 4C	RNAi 5A	RNAi 6C	RNAi 7A	RNAi 8B	RNAi 9A	RNAi 11D	RNAi 13D
6	Mean	15.83	17.6	16.78	17.2	15.6	15.11	15.75	17.22	16.875	15.44	19.8
	Std. dev.	2.14	3.10	1.20	2.49	2.01	2.71	1.28	3.07	2.17	4.13	3.46
9	Mean	18.5	20.4	18.5	20.9	19.7	21.2	19.8	21.5	19.8	18.2	22.2
	Std. dev.	2.46	3.53	2.76	3.90	4.22	3.74	2.25	3.47	2.39	3.33	2.57
12	Mean	24.5	21.6	26	22.6	22	23.3	23.9	23.9	26.2	21.4	28.2
	Std. dev.	3.34	5.15	5.87	4.93	5.10	6.17	3.60	7.43	2.70	8.49	4.37

**RNAi 1 – number of lateral roots**

DAG	No. of laterals	Col	RNAi 1A	RNAi 2A	RNAi 4C	RNAi 5A	RNAi 6C	RNAi 7A	RNAi 8B	RNAi 9A	RNAi 11D	RNAi 13D
6	Mean	0.9	1.5	2.4	2.9	2.7	3.1	3.2	1	2.6	2.2	3
	Std. dev.	0.88	1.27	0.97	1.73	1.25	1.20	0.42	1.05	0.84	1.32	1.33
9	Mean	11.9	10.4	17.2	13.8	16.7	16.3	16.4	10.9	16.6	13.2	16
	Std. dev.	2.13	4.33	3.33	3.58	2.54	2.63	2.80	1.66	2.91	5.39	3.27
12	Mean	24	25	35.9	29.2	33.7	33.2	30.4	28.4	34.1	26.6	31.8
	Std. dev.	4.76	3.81	5.34	7.02	3.80	6.09	5.38	3.06	4.77	9.18	4.64

**RNAi 2 – number of lateral roots**

DAG	No. of laterals	Col	RNAi 1A	RNAi 2A	RNAi 4C	RNAi 5A	RNAi 6C	RNAi 7A	RNAi 8B	RNAi 9A	RNAi 11D	RNAi 13D
6	Mean	0.9	1.4	1.6	4.4	2.8	3.7	2	3.6	2	2.4	3.1
	Std. dev.	0.88	0.97	1.58	1.35	1.14	1.25	1.41	1.78	1.49	1.26	1.37
9	Mean	11.9	15	11.5	17.9	15.4	17.1	11.5	15.8	14.4	12.9	12.7
	Std. dev.	2.13	3.37	3.24	2.69	2.37	2.51	6.13	3.01	3.50	3.51	4.76
12	Mean	24	32.1	25.8	37.3	30.7	33.2	28.9	33.1	31	31.1	27.7
	Std. dev.	4.76	4.36	5.49	8.98	4.99	5.09	5.40	4.56	6.02	5.04	8.08

**RNAi 1+P – number of lateral roots**

DAG	No. of laterals	Col	RNAi 1A	RNAi 2A	RNAi 4C	RNAi 5A	RNAi 6C	RNAi 7A	RNAi 8B	RNAi 9A	RNAi 11D	RNAi 13D
6	Mean	0.9	1.8	2.1	2.7	2.2	1.3	2	3.1	3.8	3	3.2
	Std. dev.	0.88	1.32	0.88	1.06	1.48	0.67	0.94	0.99	1.23	1.49	1.69
9	Mean	11.9	15	15.1	13.8	15.4	11.8	12.7	16.7	16.3	15.2	16
	Std. dev.	2.13	3.40	2.96	2.94	4.30	2.44	3.43	3.59	2.75	2.78	3.20
12	Mean	24	29	30.1	29.2	29.9	25.5	28.1	30.8	31.6	29.9	29.9
	Std. dev.	4.76	6.13	10.04	4.71	7.23	4.93	5.49	4.21	5.70	5.32	4.56

**RNAi 2+P – number of lateral roots**

DAG	No. of laterals	Col	RNAi 1A	RNAi 2A	RNAi 4C	RNAi 5A	RNAi 6C	RNAi 7A	RNAi 8B	RNAi 9A	RNAi 11D	RNAi 13D
6	Mean	0.9	2.3	1.5	3.2	3.3	2.3	2.11	2	1.7	1.6	2.7
	Std. dev.	0.88	0.95	0.71	1.14	0.82	1.16	1.17	1.05	1.16	0.97	1.34
9	Mean	11.9	13.1	12.3	15.8	15.7	13.3	13.4	14.6	14	14.4	17.3
	Std. dev.	2.13	3.18	2.00	2.62	2.71	2.21	2.88	3.27	2.26	3.10	2.87
12	Mean	24	27.8	27	31.3	29.7	30.2	27.5	30.6	28.5	27.2	32.6
	Std. dev.	4.76	5.61	4.81	4.92	6.07	5.51	4.14	6.93	3.34	3.85	5.04

**RNAi 1 – number of anchor roots**

DAG	No. of anchors	Col	RNAi 1A	RNAi 2A	RNAi 4C	RNAi 5A	RNAi 6C	RNAi 7A	RNAi 8B	RNAi 9A	RNAi 11D	RNAi 13D
6	Mean	0.67	0.3	0.2	0.3	0.3	0.7	0.2	0.4	0.1	0.4	0.3
9	Mean	0.6	0.2	0.5	0.9	0.6	0.9	0.6	1.1	0.8	0.8	0.67
12	Mean	1	0.9	1.7	1.4	1.4	1.5	1.3	1.3	1.6	1.2	1.6

**RNAi 2 – number of anchor roots**

DAG	No. of anchors	Col	RNAi 1A	RNAi 2A	RNAi 4C	RNAi 5A	RNAi 6C	RNAi 7A	RNAi 8B	RNAi 9A	RNAi 11D	RNAi 13D
6	Mean	0.67	0.3	0.5	0.6	0.3	1	0.8	0.3	0.5	0.8	0.9
9	Mean	0.6	0.6	0.9	0.9	0.5	0.5	1	0.4	0.8	1.1	1.4
12	Mean	1	1.2	1.7	1.6	1.3	1.6	1.8	1.2	1.4	1.8	1.5

**RNAi 1+P – number of anchor roots**

DAG	No. of anchors	Col	RNAi 1A	RNAi 2A	RNAi 4C	RNAi 5A	RNAi 6C	RNAi 7A	RNAi 8B	RNAi 9A	RNAi 11D	RNAi 13D
6	Mean	0.67	0.8	0.2	0.6	0.3	0	0.4	0.1	0.4	0.5	0.2
9	Mean	0.6	1.5	0.5	1	0.78	0.6	1.1	0.6	0.8	0.6	0.6
12	Mean	1	1.6	1.1	1.6	1.6	1.2	1.5	1.7	1.7	1.3	0.9

**RNAi 2+P – number of anchor roots**

DAG	No. of anchors	Col	RNAi 1A	RNAi 2A	RNAi 4C	RNAi 5A	RNAi 6C	RNAi 7A	RNAi 8B	RNAi 9A	RNAi 11D	RNAi 13D
6	Mean	0.67	0.7	0.1	0.8	0.7	0.4	0.6	0.4	0.7	0.3	0.6
9	Mean	0.6	1.1	0.6	1.1	1.2	0.5	0.9	0.8	0.8	0.8	0.9
12	Mean	1	1.8	1.4	1.7	1.3	1.3	1.6	1.3	1.6	1.6	1.4

